OCTOBER-DECEMBER 2018 VOL. 10 № 4 (39)

ISSN 2075-8251

ActaNaturae

The EIMB Hydrogel Microarray Technology: Thirty Years Later

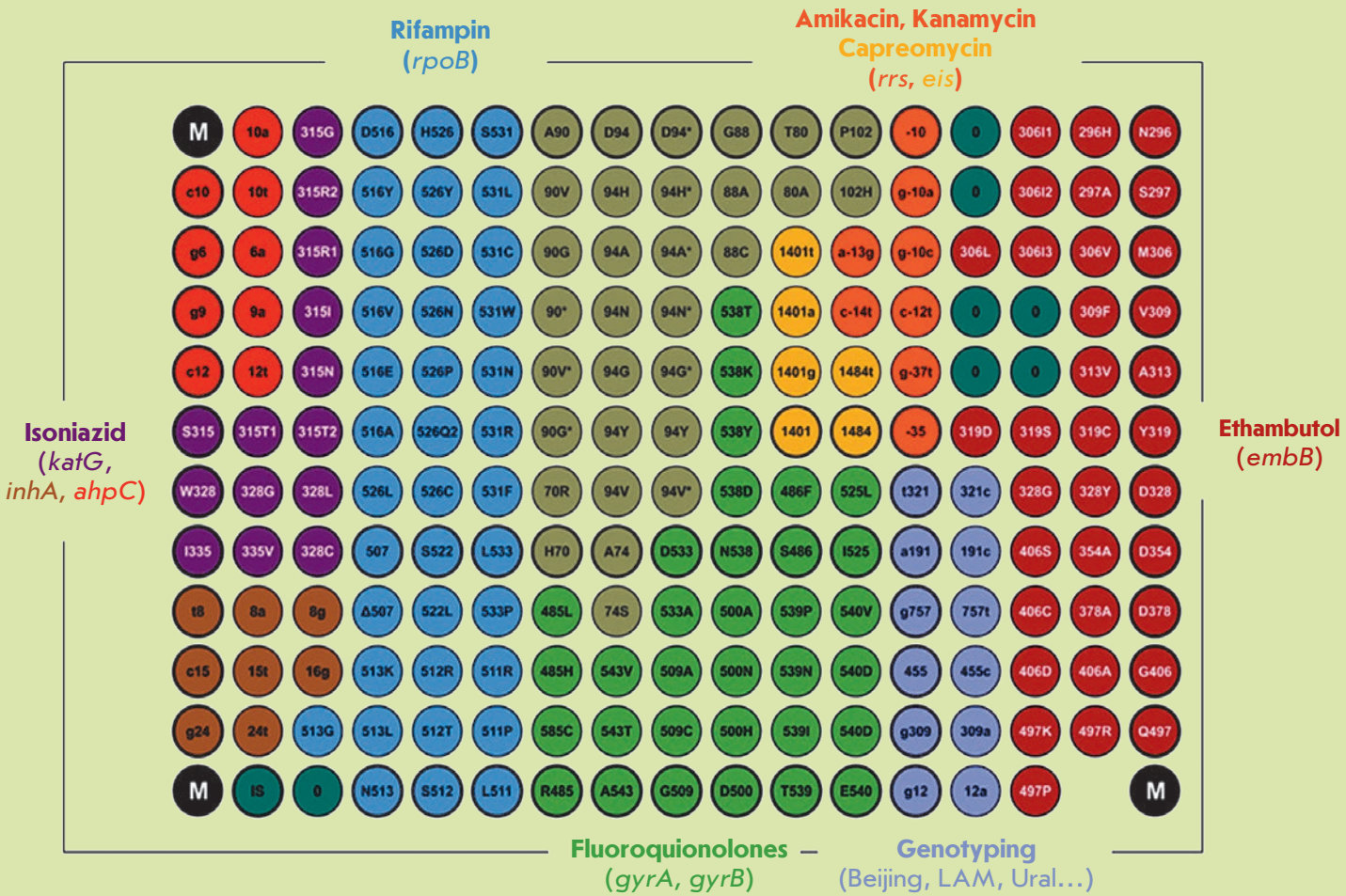

MERCK

Comprehensive solutions for cell analysis

- Cell lines and primary cells
- Traditional and specialized culture media
- Sterilizing filtration
- Biochemical reagents
- Water purification systems
- Cell counting and analysis
- Cryopreservation

An extensive range and top quality of cell lines from our partner, the European Collection of Authenticated Cell Cultures (ECACC):

- 4000 animal and human cell lines;
- Cells of 45 animal species and 50 tissue types;
- 370 B-lymphoblastoid cell lines for which human leukocyte antigen (HLA) typing data are available;
- 480 hybridoma cell lines secreting monoclonal antibodies;
- DNA, RNA, and cDNA extracted from the cell lines from our collection;

SIGMAaldrich.com/ECACC

LLC Merck
Valovaya Str., 35, Moscow, 115054, Russia;
Tel. +7 (495) 937-33-04
E-mail: mm.russia@merckgroup.com, ruorder@sial.com

SIGMAaldrich.com/cellculture
MERCKmillipore.com/cellculture

SIGMA-ALDRICH® is now MERCK

Multifaced Roles of the Urokinase System in the Regulation of Stem Cell Niches

K. V. Dergilev, V. V. Stepanova, I. B. Beloglazova, Z. I. Tsokolayev, E. V. Parfenova

One of the most important proteolytic systems involved in the regulation of cell migration and proliferation is the urokinase system represented by the urokinase plasminogen activator, its receptor, and inhibitors. This review addresses the issues of urokinase system involvement in the regulation of stem cell niches in various tissues and analyzes the possible effects of this system on the signaling pathways responsible for the proliferation, programmed cell death, phenotype modulation, and migration properties of stem cells.

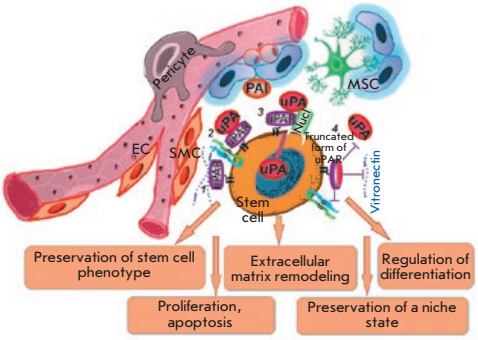

The urokinase system modulates the state of stem cells in cell niches

Bacterial Enzymes and Antibiotic Resistance

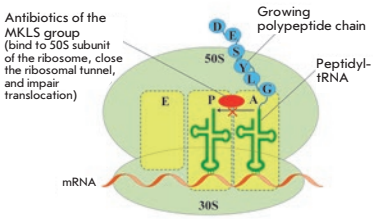

Binding of antibiotics of the MKLS group to the ribosome and their effect on protein synthesis

A. M. Egorov, M. M. Ulyashova, M. Yu. Rubtsova

The resistance of microorganisms to antibiotics has been developing for more than 2 billion years and is widely distributed among various representatives of the microbiological world. The main mechanisms of resistance development are associated with the evolution of superfamilies of bacterial enzymes due to the variability of the genes encoding them. The collection of all antibiotic resistance genes is known as the resistome. Tens of thousands of enzymes and their mutants that implement various mechanisms of resistance form a new community that is called "the enzystome." Analysis of the structure and functional characteristics of enzymes, which are the targets for different classes of antibiotics, will allow us to develop new strategies for overcoming the resistance.

Tag7-Mts1 Complex Induces Lymphocytes Migration via CCR5 and CXCR3 Receptors

T. N. Sharapova, E. A. Romanova, L. P. Sashchenko, D. V. Yashin

The discovery of new chemokines that induce the migration of lymphocytes to the infection site is important for the targeted search for therapeutic agents in immunotherapy. The study investigated the migration of human peripheral blood mononuclear cells under the action of the Tag7-Mts1complex. It has been established that the movement of peripheral blood mononuclear cells along the concentration gradient of the Tag7-Mts1 complex is induced by the classical chemotactic receptors CCR5 and CXCR3. It should be noted that the Tag7-Mts1 complex can be considered as a new ligand of the classical chemotactic receptors CCR5 and CXCR3.

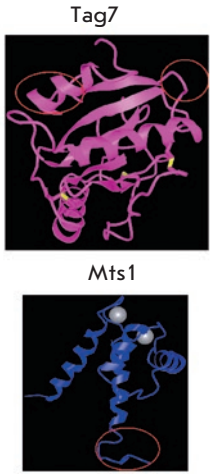

3D structures of the Mts1, Tag7 and MIP1α proteins

ActaNaturae
OCTOBER-DECEMBER 2018 VOL. 10 № 4 (39)

Founders
Ministry of Education and
Science of the Russian Federation,
Lomonosov Moscow State University,
Park Media Ltd

Phone/Fax: +7 (495) 727 38 60
E-mail: vera.knorre@gmail.com, actanaturae@gmail.com

Номер подписан в печать 27 декабря 2018 г.
Тираж 200 экз. Цена свободная.
Отпечатано в типографии «МИГ ПРИНТ»

Indexed in Pubmed, Web of Science, Scopus, and RISC

CONTENTS

REVIEWS

RESEARCH ARTICLES

SHORT REPORTS

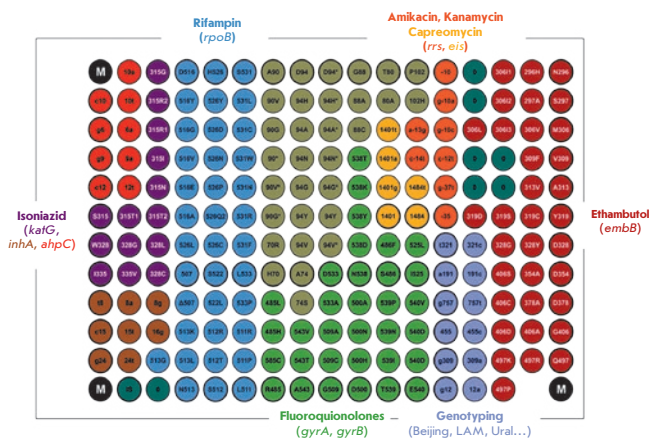

IMAGE ON THE COVER PAGE
(see the article by Gryadunov *et al.*)

The EIMB Hydrogel Microarray Technology: Thirty Years Later

D. A. Gryadunov*, B. L. Shaskolskiy, T. V. Nasedkina, A. Yu. Rubina, A. S. Zasedatelev
Engelhardt Institute of Molecular Biology, Russian Academy of Sciences, Vavilova Str., 32, Moscow, 119991, Russia
*E-mail: grad@biochip.ru
Received September 13, 2018; in final form September 24, 2018

ABSTRACT **Biological microarrays (biochips) are analytical tools that can be used to implement complex integrative genomic and proteomic approaches to the solution of problems of personalized medicine (e.g., patient examination in order to reveal the disease long before the manifestation of clinical symptoms, assess the severity of pathological or infectious processes, and choose a rational treatment). The efficiency of biochips is predicated on their ability to perform multiple parallel specific reactions and to allow one to study the interactions of biopolymer molecules, such as DNA, proteins, glycans, etc. One of the pioneers of microarray technology was the Engelhardt Institute of Molecular Biology of the Russian Academy of Sciences (EIMB), with its suggestion to immobilize molecular probes in the three-dimensional structure of a hydrophilic gel. Since the first experiments on sequencing by hybridization on oligonucleotide microarrays conducted some 30 years ago, the hydrogel microarrays designed at the EIMB have come a long and successful way from basic research to clinical laboratory diagnostics. This review discusses the key aspects of hydrogel microarray technology and a number of state-of-the-art approaches for a multiplex analysis of DNA and the protein biomarkers of socially significant diseases, including the molecular genetic, immunological, and epidemiological aspects of pathogenesis.**
KEYWORDS **hydrogel microarrays, nucleic acid hybridization, multiplex immunochemical assay, antimicrobial drug resistance, genotyping, tumor markers.**
ABBREVIATIONS **NAs – nucleic acids; NGS – next-generation sequencing; FDA – Food and Drug Administration (USA); MTB – *Mycobacterium tuberculosis*, causative agent of tuberculosis; NTM – non-tuberculous mycobacteria, causative agents of mycobacteriosis; HCV – hepatitis C virus; RMP – rifampin; INH – isoniazid; EMB – ethambutol; MDR – multidrug resistance; XDR – extensive drug resistance; RTIs – reproductive tract infections; AMD – antimicrobial drugs; CRC – colorectal carcinoma; CEA – carcinoembryonic antigen; CA – carbohydrate antigen.**

INTRODUCTION

Abundant knowledge on the molecular mechanisms of the biochemical processes that underlie the function of living systems has been accumulated over the past decade. This knowledge allows one to estimate the likelihood of someone developing a disease long before the manifestation of its clinical symptoms, to predict the severity of pathological or infectious processes, and to choose an effective and rational treatment. Solving the problems of personalized medicine should include both genome-wide analysis and the multiplex approaches used to quantify markers of pathological conditions.

Many approaches and techniques have been developed for the simultaneous, quantitative analysis of nucleic acid (NA) sequences. One such method, the microarray (biochip) technology, has proved efficient when used for transcription profiling, comparative genomic hybridization, and simultaneous identification of multiple targets in the genomes of humans, plants, microorganisms, and viruses [1]. The key component of a biochip platform is an array of spots, with each spot containing a probe whose nucleotide sequence is specific to a fragment of the analyzed genome. The reactions of NA hybridization and/or amplification performed simultaneously in each microarray element allow for parallel identification of different genomic targets, thus implementing the principle of multi-parameter analysis of a biological sample. Hence, DNA microarrays can be used as an efficient molecular tool to detect clinically significant markers of causative agents and the causes of socially consequential diseases.

Microarrays can also contain matrixes of elements with immobilized proteins or oligosaccharides. Depending on the experimental objectives, each microarray element can carry either an individual, immobilized probe or their combination. The interactions between

different classes of molecules involve a receptor–ligand, an antigen–antibody, an enzyme–substrate, and other types of interactions. When incubated with a specimen containing the molecules being analyzed, the immobilized ligand forms a specific complex. At this stage, a mixture of analyzed compounds is separated according to the ability of individual compounds to bind specifically to the immobilized ligands, making it possible to use a single microarray to simultaneously analyze different biological objects by implementing the principle of multiplex immunoassay. This test is required for proteomics research and for diagnosing diseases characterized by variations in many parameters in a patient's serum.

THE KEY ASPECTS OF A MICROARRAY ANALYSIS

A DNA microarray analysis is based on nucleic acid hybridization. The advantages of hybridization include its simplicity, multiplexity, and the reproducibility of results. Unlike enzymatic reactions, hybridization can be performed in a broad range of temperatures and buffer compositions. Meanwhile, nucleic acid hybridization does not allow for performing direct amplification of nucleic acids and must be used in combination with signal amplification methods or highly sensitive tools to detect nucleic acid duplexes. Therefore, microarrays are applied in direct quantification of RNA isolated from a large-volume specimen or for detecting the hybridization complexes formed by immobilized probes and the nucleic acid fragments obtained at the preliminary amplification stage. Hence, the sensitivity of a microarray assay depends on the initial amount of nucleic acids, amplification efficiency, and the method used to detect the complexes. The sensitivity of the most commonly used method - fluorescent detection of interactions in microarray elements - depends on the fluorescence analyzer.

In theory, DNA microarrays are supposed to ensure nucleic acid quantification [2]. However, real-world experiments show that there is significant quantitative bias in the gene expression data obtained using different microarray platforms and even different microarrays produced by the same manufacturer [3]. First, the hybridization kinetics nonlinearly depends on the density of the probes that reside on the microarray surface, since the oligonucleotides immobilized or synthesized on high-density microarray substrates are nonspecifically hybridized with each other, depending on their homology. Second, hybridization kinetics is affected by the length and nucleotide sequence of the target DNA molecules. Third, the quantum yield of a fluorophore used for detection depends both on the sequence of the adjacent nucleic acid and on proximity to other fluorophores. In this context, gene expression microarrays are used more often for reproducible analysis to evaluate the nucleic acid content rather than for an accurate determination of concentration [4].

One of the key parameters that characterize microarrays is the type of microarray substrate: substrates with hydrogel-based coatings (e.g., coatings made of polyacrylamide or agarose), as well as matrices carrying functional groups, such as aldehydes, epoxy or amino groups, etc. [5]. Due to their hydrophilic properties, polymeric hydrogels are high-priority substrate for biomolecule immobilization. The conventional approach to manufacturing microarrays consists in depositing a homogeneous hydrogel layer onto a substrate, followed by the immobilization of probes or *in situ* oligonucleotide synthesis. Both synthetic polymers (e.g., poly(2-hydroxyethyl methacrylate) and polyacrylamides) and non-synthetic polymer collagen are used as crosslinking agents to form hydrogel substrates [6]. As a result, the capacity of probe immobilization on microarrays increases by several orders of magnitude [7], making it possible to detect signals in microarray elements that are 10- to 100-fold more intense than the signals observed during immobilization on planar matrices.

A unique feature of microarray technology elaborated by researchers at the Engelhardt Institute of Molecular Biology, Russian Academy of Sciences, under the aegis of academician Andrey Darievich Mirzabekov (1937–2003), is the immobilization of molecular probes in 3D hydrogel elements anchored to a planar substrate [8, 9].

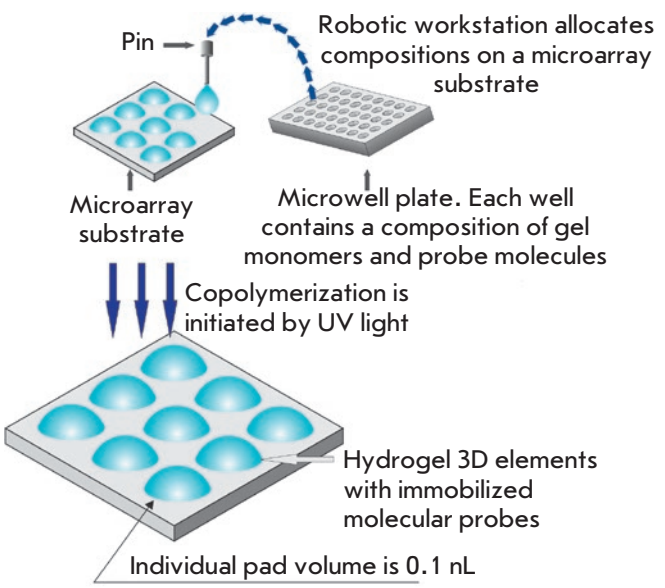

Fig. 1. Manufacture of a microarray with 3D elements containing compositions of hydrogel and molecular probes

Molecular probes, oligonucleotides or oligosaccharides are modified by attachment of amino- or sulfo groups that are subsequently used as covalent binding sites during chain propagation. Meanwhile, protein-based probes require no special modification, as they carry proper functional amino acid groups within their structure. The macroporous structure of hydrogel elements is formed via copolymerization of a methacrylic acid derivative monomer with an unsaturated derivative of O- or N-substituted saccharide, a bifunctional crosslinking agent, and a molecular probe. The polymerization mixture (0.1 nL) is applied onto a substrate by the pins of a robotic workstation (*Fig. 1*). Almost any carriers (glass, plastic, etc.) can be used as a substrate. Next, UV radiation-induced copolymerization of molecular probes with the main hydrogel components takes place and the compounds being immobilized are uniformly embedded into the growing polymer structure. It should be mentioned that optimal conditions for molecular probe polymerization have been selected, making it possible to maximally retain the original biological activity of the probes. After polymerization, hydrogel elements (pads) formed on the substrate are washed and prepared for experiments. The efficiency of this immobilization procedure is 50–80%, depending on the particular molecular probe.

Depending on the type of microarray, the diameter of the gel element varies from 50 to 300 μm; the distance between pads can range between 100 and 500 μm. The number of spots per microarray depends on the specific task that needs to be solved and varies from several dozens to several thousands. The application quality is controlled by a specialized hardware and software complex. Microarrays in which the discrepancy in the geometric parameters of the elements is $\leqslant$ 10% and the discrepancy in the parameters between different microarray batches is $\leqslant$ 20% are used for further experiments [10]. These characteristics comply with the criteria used for the best commercial microarrays, manufactured by ArrayIt (USA) and Schott AG (Germany).

Since the first experiments on sequencing by hybridization with oligonucleotide micromatrices conducted some 30 years ago [11], hydrogel microarrays have come a long way from basic research to clinical

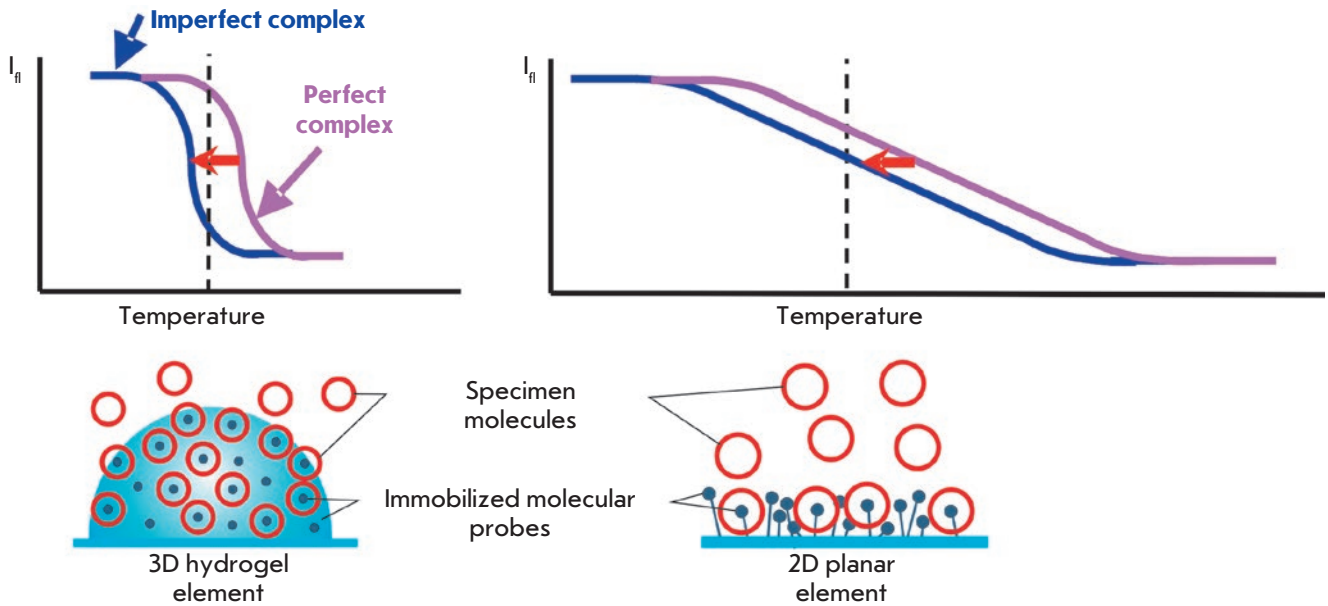

Fig. 2. Advantages of biochips with 3D elements in comparison with 2D elements residing on a planar surface. Molecular complexes formed in 3D elements and distributed uniformly throughout the volume are located in the water-like homogeneous environment of the hydrogel and have identical energies of formation. In this case, the temperature-induced dissociation of such complexes occurs in a narrow temperature range and it is always possible to select a temperature at which the perfect complex remains stable, while the imperfect complex will be substantially dissociated. Therefore, in the case of 3D elements, perfect complexes can be detected by signals exceeding the signals of imperfect complexes several times. In 2D elements, the energy of complex formation is superimposed with different energy interactions between the complexes and the substrate surface. As a result, the dissociation curves of molecular complexes have a gentle slope and the temperature shift (usually 3–4°C) between the curves characterizing the perfect and imperfect complexes is insufficient to provide a significant difference in the corresponding signals

laboratory diagnostics. Kinetic and thermodynamic studies of hybridization of DNA fragments have demonstrated that application of short probes (up to 25 nucleotides long) make it possible to efficiently discriminate between point nucleotide substitutions, while immobilization in 3D hydrogel elements significantly enhances the intensity of positive signals and reduces the statistical dispersion, as compared to 2D planar microarrays [12, 13] (*Fig. 2*).

Gryadunov *et al.* [14] experimentally selected the hybridization conditions and concentrations of immobilized probes; they also proposed algorithms for computing probe sequences that would ensure high positive signals and discrimination ratios. Substantial progress was made in the analytical sensitivity of the assay thanks to the elaboration of a multiplex PCR assay procedure that can simultaneously amplify several dozen genome fragments [15, 16], as well as thanks to the synthesis of novel dyes and the optimization of fluorescent labeling [17, 18].

Rubina *et al.* [19] have developed, for the first time, procedures for efficient immobilization of protein and glycan molecules in hydrogel and proposed methods for multiplex quantitation of different proteins in serum. Several generations of universal fluorescence analyzers have been designed. The most recent one can be used to measure the signal intensity of microarray elements at wavelengths ranging from 380 to 850 nm and perform qualitative and quantitative analyses with an accuracy of ± 5% [20].

The universal platform of hydrogel microarrays designed by EIMB researchers has made it possible to elaborate, validate, and implement a number of applications for multi-parameter analysis of the biomarkers of socially important diseases. These applications will be discussed below.

ANALYSIS OF SPECIFIC SEQUENCES OF BACTERIAL AND VIRAL GENOMES

The need to analyze bacterial and viral genomes is largely rooted in the social importance of pathogens, which often include the drug-resistant causative agents of tuberculosis (*Mycobacterium tuberculosis*, MTB) and mycobacteriosis (non-tuberculous mycobacteria, NTM), hepatitis C virus (HCV), and microorganisms belonging to the group responsible for infection and inflammation of the reproductive tract. With regard to these objects, the technology of hydrogel-based DNA microarrays has proved to be an efficient tool for determining the profile of antibiotic resistance determinants, as well as for intra- and interspecies genotyping of microorganisms and viruses in order to select an adequate therapy and perform epidemiological surveillance.

Application of microarrays in the laboratory diagnosis of tuberculosis

The TB-Biochip-1 diagnostic kit for identifying 48 mutations in the *Mycobacterium tuberculosis* genome, which are responsible for the resistance of this bacteria to rifampin (RMP) and isoniazide (INH), was the first microarray-based assay in the world to be designed and approved for *in vitro* clinical diagnostics [21]. The diagnostic characteristics of this method were evaluated using the results of a 10-year (2005–2015) application of the TB-Biochip-1 kit in medical anti-tuberculosis institutions in Russia, Kyrgyzstan, and Azerbaijan. A meta-analysis of 16 publications that reported data on an evaluation of > 5,000 clinical specimens and isolates using a TB-Biochip-1 diagnostic kit and microbiological assays demonstrated that the diagnostic sensitivity of this method, used to identify the RMP-resistant phenotype of MTB, lies in the 88.8–96.9% range and that its specificity is 90.3–99.4%. When this method is used to analyze INH-resistant strains, its sensitivity and specificity are 85.7–96.9% and 85.3–98.2%, respectively. There was an 80–90% match between the results obtained using the TB-Biochip-1 kit and molecular assays recommended by the WHO (Xpert MTB/RIF (Cepheid, USA) and Genotype MTBRD*plus* (Hain Lifescence, Germany)) [22, 23].

An important result is that the TB-Biochip-1 kit proved effective in the treatment of patients with destructive pulmonary tuberculosis, depending on the time when the treatment schedule was adjusted, as confirmed by the chief visiting Physiologist of the Ministry of Health of the Russian Federation [24]. When using microarrays for early diagnosis of multidrug-resistant (MDR) forms of tuberculosis, the number of cured patients increased at least threefold, as opposed to the case when the diagnosis was made using standard culture-based methods [14, 25]. Today, the TB-Biochip-1 kit is still actively used for laboratory diagnostics of tuberculosis. It promptly reveals multidrug-resistant isolates, so the patients can be switched to other treatment schedules.

Meanwhile, sequential accumulation of mutations associated with drug resistance not only increased the number of incident patients with MDR forms of tuberculosis (from ~15% in 2005 [21] to ~50% in 2015 [26]), but also resulted in the emergence of isolates with extensive drug resistance (XDR) and total drug resistance to all antituberculosis medication. In order to solve these problems, we have developed a method that allows one to detect MTB DNA and simultaneously identify the genotype of strains endemic to Russia and genetic determinants of MDR and XDR. The analysis procedure includes multiplex PCR assay with adapter primers and cyclic elongation to ensure simultaneous

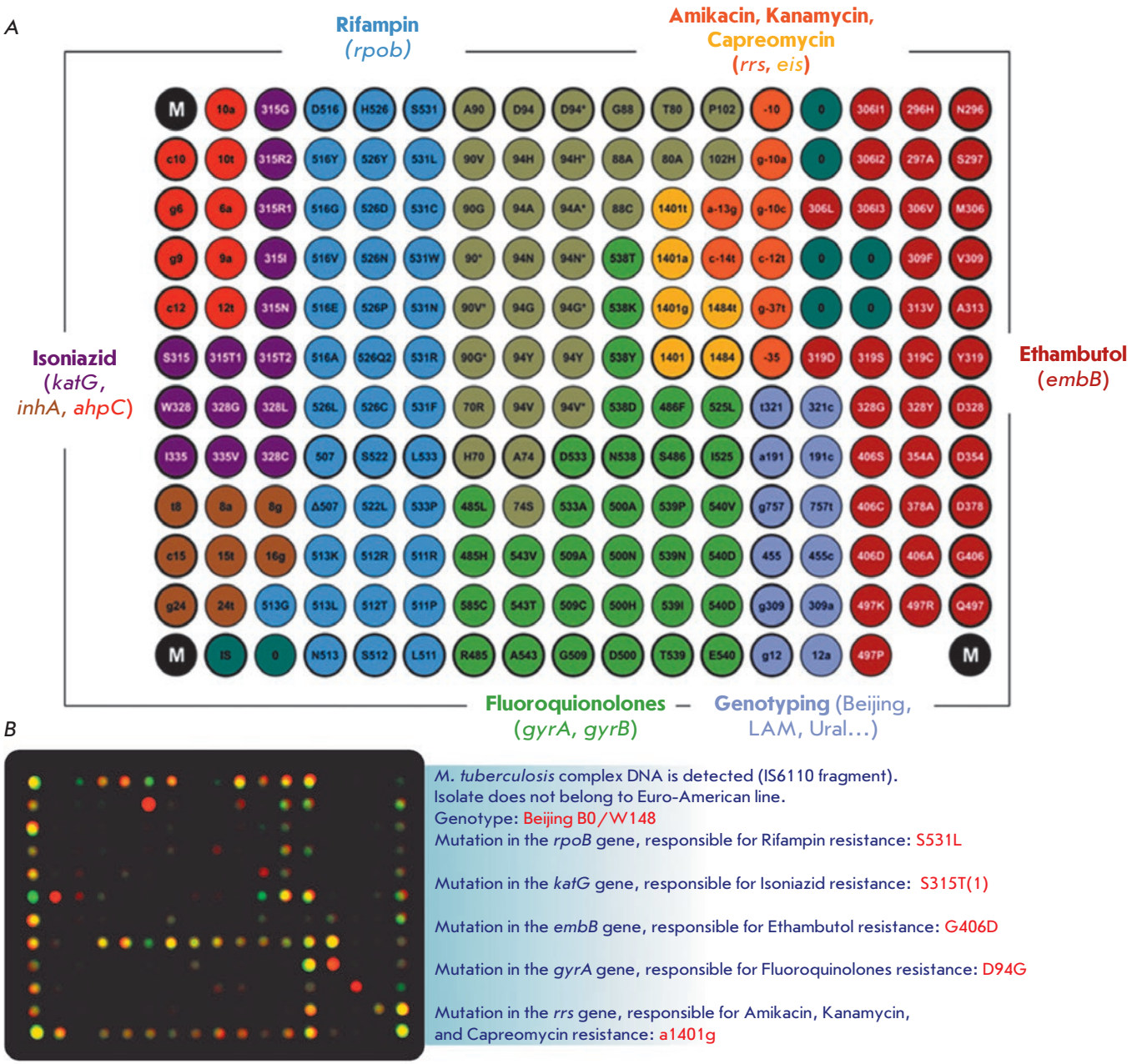

Fig. 3. (*A*) Microarray configuration for simultaneous determination of the MTB genotype and identification of the MDR and XDR genetic determinants. Various colors show groups of elements with immobilized probes specific to wild-type sequences and mutant variants of the genes associated with drug resistance to different anti-tuberculosis drugs. (*B*) An example of the biochip hybridization pattern and the result of interpretation upon analysis of *M. tuberculosis* DNA from an extensively drug-resistant isolate of the Beijing B0/W148 genotype

amplification and labeling of 17 loci of the *M. tuberculosis* genome, followed by hybridization. As the key component of this approach, the microarray allows one to identify MTB DNA, to determine the lineages of the causative agent endemic to Russia, and to detect a total of 116 genetic determinants of drug resistance to rifampin, isoniazid, fluoroquinolones, injectable drugs (amikacin, kanamycin, and capreomycin), and ethambutol (EMB) (*Fig. 3*).

A clinical trial of the method conducted at the St. Petersburg Research Institute of Phthisiopulmonology of the Ministry of Health of the Russian Federation dem-

onstrated that the diagnostic sensitivity and specificity of the elaborated procedure amounted to > 90% for all drugs, except for ethambutol [15]. Sensitivity for this drug was 89.9%, significantly higher than the value published earlier (58%) [27].

An analysis of MTB lineages revealed that strains with the Beijing genotype were predominant (73.1%). The LAM (12.1%) and Ural (~7%) families, as well as Euro-American strains (7.2%), were less frequent (*Fig. 4*). The B0/W148 cluster accounted for > 30% of all Beijing genotype isolates. If an isolate was found to belong to a certain genotype, this meant that the MDR or XDR phenotype was revealed with a 100% probability, thus confirming the clinical significance of the detection of this genotype. Contrariwise, isolates of the Euro-American lineage not belonging to the LAM and Ural families were mostly associated with the drug-susceptible phenotype [15].

Nosova *et al.*, in collaboration with the Moscow Research and Clinical Center for Tuberculosis Control of the Moscow Government Health Department, revealed correlations between the genetic determinants of drug resistance and minimal inhibitory concentrations that characterize the level of resistance to a certain anti-tuberculosis drug [28]. It is very important that the results of the analysis of the determinants associated with different resistance levels allow physicians to prescribe different doses of anti-tuberculosis drugs belonging to an extremely narrow range of specific therapeutic agents.

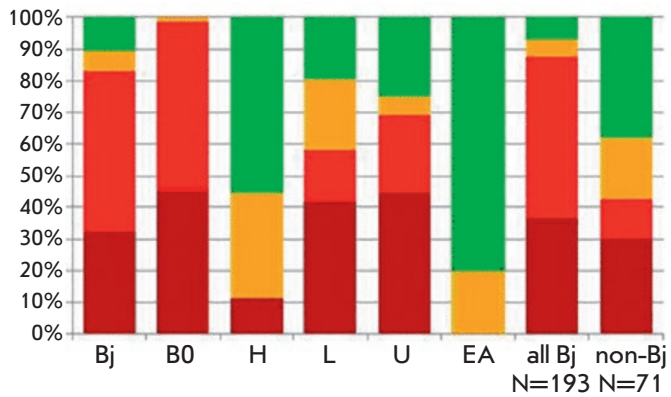

Fig. 4. Association of MTB lineages with drug resistance. The drug resistance profile is marked with colors: dark red – XDR, red – MDR, yellow – mono- or poly-drug-resistant, green – susceptible isolates. Designations of lineages: Bj – Beijing; B0 – Beijing B0/W148; H – Haarlem; L – LAM; U – Ural; EA – Euro-American lineage

The elaborated method has underlain the development of a TB-TEST diagnostic kit. The TB-TEST kit has undergone trials and has been approved for use by the Russian Federal Service for Surveillance in Healthcare and Social Development. The TB-Biochip diagnostic kits are giving way to the application of the TB-TEST kit. The range of genomic targets for first- and second-line drugs that can be analyzed using the TB-TEST kit includes at least chemotherapy schedules I–IV for tuberculosis patients in compliance with Order no. 951 of the Ministry of Health of the Russian Federation dated December 29, 2014. The speed and feasibility of the analysis of respiratory material allow clinicians to use this kit for rapid screening of patients' specimens and subsequent adjustment of therapy schedules and switching of patients to new anti-tuberculosis drugs [29].

The SPOLIGO-BIOCHIP kit has been developed for routine intraspecies genotyping of strains of the Mycobacterium tuberculosis complex. This kit provides information about the genetic profile of each MTB isolate by identifying its genotype [30]. The approach is also used to differentiate between MTB and the tuberculosis vaccine strain *M. bovis BCG* in contents of cold abscess in children with post-vaccination complications.

The species-specific polymorphism of the *gyrB* gene in microorganisms belonging to the *Mycobacterium* genus made it possible to design a microarray for identifying 35 different mycobacterial species [31]. An analysis of mycobacterial populations in the Central and Northwestern regions of the Russian Federation revealed that such NTM species as the *Mycobacterium avium* complex (39%), *M. fortuitum* (17%), and *M. xenopi* (13%) predominate in European Russia. The infection caused by these NTM species manifests itself in immunosuppressed patients, as well as patients with a chronic obstructive pulmonary disease and HIV [31].

Hence, the combination of diagnostic kits in the analysis of the causative agents of tuberculosis and mycobacteriosis allows one to thoroughly examine material collected from patients using a universal diagnostic microarray platform in a clinical laboratory. A unified assay that complies with all current requirements, automated analysis of the results, and their interpretation through the provision of specific recommendations allow one to improve the treatment schedules of tuberculosis caused by drug-resistant strains.

Analysis of the genetic determinants of antibiotic resistance of the causative agents of reproductive tract infections

There are significant challenges that are related to the diagnostics and selection of a personalized therapy strategy for reproductive tract infections (RTIs)

due to the wide variety of RTIs that often develop as mixed drug-resistant forms, including both sexually transmitted obligate pathogens and a number of causative agents of opportunistic infections. *Neisseria gonorrhoeae* holds a special place among the causative agents of RTIs. Similar to the causative agent of tuberculosis, gonococci possess an extraordinary ability to develop drug resistance. Unlike in MTB, chromosomal mutations are not the only mechanism through which *N. gonorrhoeae* acquires new resistant properties . It also actively employs various mobile genetic elements and horizontal gene transfer from other species. The mutations affecting membrane permeability and enhancing efflux pump activity are especially efficient in *Neisseria gonorrhoeae*, since these systems can help simultaneously develop resistance to many antimicrobials [32].

A microarray (*Fig. 5A*) and a procedure for its use have been developed to identify the DNAs of 12 different obligate and opportunistic microorganisms and simultaneously perform the differential analysis of 39 genetic determinants of resistance to β-lactam antibiotics, macrolides, aminoglycosides, tetracycline, spectinomycin, fluoroquinolones, and nitroimidazole [33].

An analysis of more than 500 clinical specimens and isolates obtained at the State Research Center of Dermatovenerology and Cosmetology of the Ministry of Health of the Russian Federation has demonstrated that the developed method exhibits high sensitivity and specificity in the identification of the DNA of the causative agents of RTIs. It also allowed clinicians to determine prognostic efficiency in identifying the markers of antibiotic resistance for these agents.

A study focused on tetracycline-resistant strains of *N. gonorrhoeae* isolated in Russia in 2015–2017 demonstrated that long-term interruption (since 2003) in the use of tetracycline for the treatment of gonorrhea led to a reduction in the percentage of resistant strains in Russia ranging from 70 to 42.6%. However, this does not provide grounds for recommending tetracyclines for the treatment of gonococcal infection. The type of *tetM* gene in plasmid DNA associated with a high level

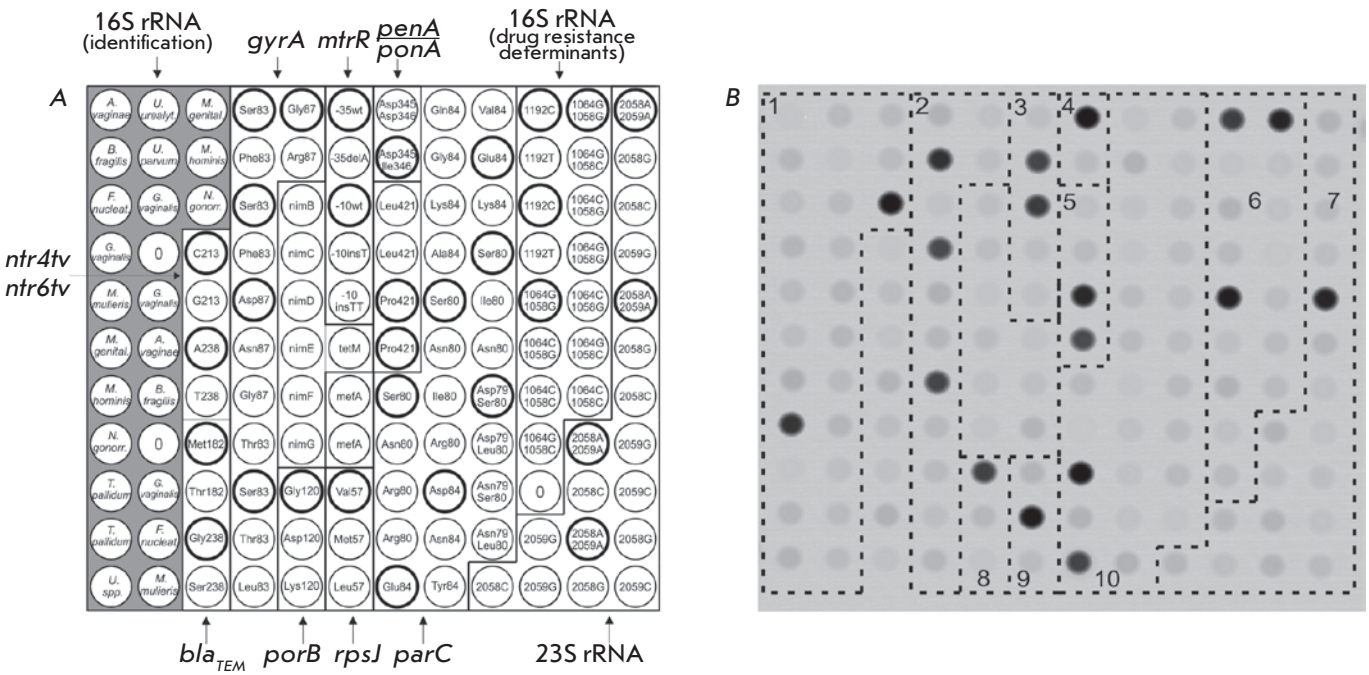

Fig. 5. (*A*) Microarray for the analysis of the drug resistance of RTI causative agents. The biochip contained immobilized probes corresponding to the species-specific polymorphism of the *16S rRNA* gene, which were used for the identification of microorganisms, and also probes specific to the *rrs*, *rrl*, *gyrA*, *parC*, *mefA*, *mtrR*, *nimB-G*, *penA*, *ponA*, *porB*, *rpsJ*, *ntr4tv*, *ntr6tv*, *blaSHV*, *blaTEM*, and *tetM* genes sequences, which act as determinants of resistance of RTI causative agents to different AMD. The elements containing wild-type oligonucleotides are circled in black. (*B*) The hybridization pattern obtained by analyzing *N. gonorrhoeae* DNA contained the following mutations: S91F+D95G in the *gyrA* gene (group 2), -35delA in the promoter of the *mtrR* gene (group 3), insD345 in the *penA* gene (group 4), and S87R in the *parC* gene (group 10)

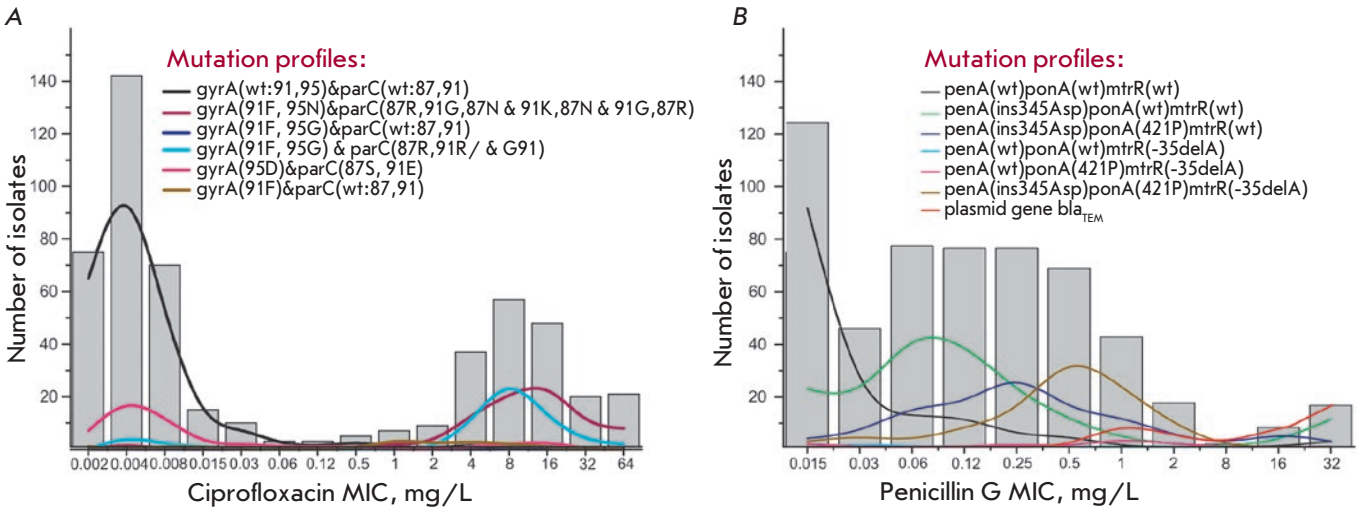

Fig. 6. The distribution of *N. gonorrhoeae* isolates with different mutation profiles for minimal inhibitory concentrations (MICs) of ciprofloxacin (*A*) and penicillin G (*B*). (*A*) Profiles include mutations in the *gyrA* and *parC* genes, leading to resistance to ciprofloxacin. (*B*) Profiles include mutations in the *penA*, *ponA*, and *mtrR* genes associated with resistance to penicillin G. The profile of isolates carrying the bla_{TEM} plasmid gene is shown separately. Designation: wt – wild type

of tetracycline resistance regardless of the presence of chromosomal resistance determinants was characterized for the first time in Russia [34].

The *N. gonorrhoeae* strains carried multiple mutations in the *penA*, *ponA*, *rpsJ*, *gyrA*, *parC*, *mtrR*, and other genes (*Fig. 5B*). The prognostic significance of these mutations with respect to phenotypic resistance substantially increased in the presence of combinations of genetic resistance determinants (*Fig. 6*) [35, 36].

This circumstance is in definite conflict with the fact that modern therapy for gonococcal infection is based on a preferential use of third-generation cephalosporins and technically does not exert "selection pressure" on the genetic determinants that regulate resistance to the drugs used earlier (penicillins or fluoroquinolones). Hence, it is reasonable to expect these mutations to be eliminated from the genome of the modern population of *N. gonorrhoeae*. The presence of these mutations could be attributed to the multifactorial nature of antibiotic resistance, where a number of earlier gene mutations underlie the next turn of the evolutionary spiral of *N. gonorrhoeae*. In particular, this is true for the *penA* and *ponA* genes, whose mutations currently appear to be significant for the developing resistance to cephalosporins. Hence, it is fair to anticipate an emergence of resistance to modern antibiotics (first of all, among the multidrug-resistant strains of *N. gonorrhoeae* as is happening in EU member states) [37]. This circumstance is an indication that continuous monitoring of antibiotic resistance by the causative agent of gonorrhea is a rather topical issue. The hydrogel microarray technology is currently one of the methods used for such monitoring.

Identification of the genotype and subtype of the hepatitis C virus by analyzing the NS5B region of the viral genome

According to existing classification, the hepatitis C virus (HCV) is subdivided into seven main genotypes and 67 subtypes [38]. The HCV genotype and subtype are the key determinants taken into account when choosing schedules of treatment with direct-acting antiviral agents (DAAs) affecting the key targets of the virus life cycle [39]. Accurate identification of the HCV genotype and subtype defines the choice of treatment schedule (particular DAA, treatment course duration, and whether or not ribavirin needs to be prescribed).

In collaboration with the Virology Laboratory of the University of Toulouse (France), researchers have proposed a method for identifying six genotypes and 36 subtypes of HCV by analyzing the genotype- and subtype-specific sequences in the HCV NS5B on a hydrogel microarray (*Fig. 7A*). The analysis procedure involves amplification and fluorescent labeling of the NS5B region, followed by hybridization on microarray, signal detection, and interpretation. An example of the assay for a HCV subtype 1b RNA sample and interpretation of the results are shown in *Fig. 7B*.

The developed method was used to analyze 345 HCV specimens as compared to the "gold standard" of genotyping, namely, sequencing of the NS5B region, followed by a phylogenetic analysis. The genotypes

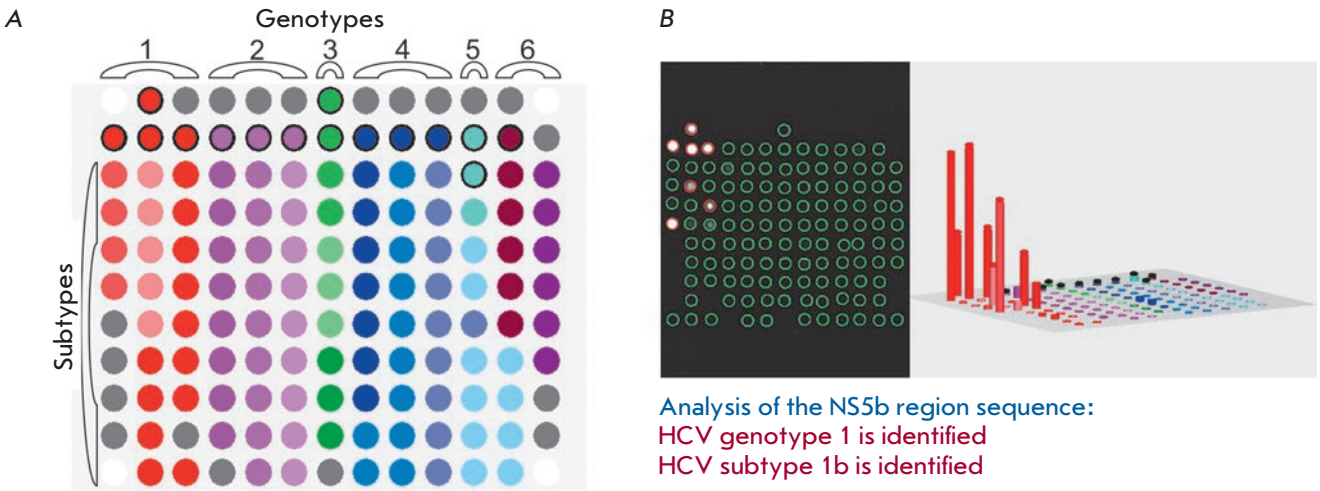

Fig. 7. (*A*) Configuration of microarray with 110 immobilized oligonucleotides for identifying the genotypes and subtypes of HCV. Elements containing genotype-specific probes in the upper rows are encircled in a thick black contour. (*B*) The hybridization pattern of HCV RNA subtype 1b, histogram of signal intensities of biochip elements, and results of interpretation

were identified for all RNA samples with 100% match. Matching results of subtype identification were obtained for 329 out of 330 specimens [40].

The characteristics of the designed HCV-Biochip kit render it as efficient as the sequencing technology. Being an efficient tool for routine genotyping, this method can be used to evaluate the response to treatment with DAAs, depending on the HCV subtype [41, 42].

MICROARRAYS FOR PERSONALIZED TREATMENT OF CANCER PATIENTS

Molecular genetic analysis of chimeric genes in leukemia

Detection of structural genomic rearrangements that give rise to chimeric genes in tumor cells in the bone marrow (especially in children) is used in most state-of-the-art protocols to divide patients into risk groups and to choose the proper therapy.

A LK-BIOCHIP kit has been developed and approved by the Russian Federal Service for Surveillance in Healthcare and Social Development for the analysis of the 13 most clinically significant chromosomal breakpoints in leukemia [43]. The LK-BIOCHIP was used to diagnose chromosomal translocations in children in multi-center trials aimed at treating acute lymphoblastic leukemia (ALL MB-2002 and ALL MB-2008) in the Russian Federation in 2005–2015 [44]. The new generation of microarrays for leukemia diagnosis is capable of detecting an extended range of chromosomal translocations, including nine additional clinically significant rearrangements t(1;11) MLL/MLLT11, t(1;11) MLL/EPS15, Del1 SIL/TAL1, t(2;5) NPM1/ALK, t(16;21) FUS/ERG, t(1;22) RBM15-MKL1, t(10;11) CALM/AF10, t(17;19) E2A/HLF, and t(6;9) DEK/CAN (*Fig. 8*). The diagnostic kit can detect one tumor cell among 1,000 normal ones in a clinical specimen, with a specificity ≥ 95% [45].

Microarrays for analyzing somatic mutations

Detection of somatic mutations in tumor tissue allows one to choose specific drugs that engage the desired molecular targets for treatment. The proportion of mutant DNA in the analyzed material is often negligible because of tumor heterogeneity or contamination of the specimen with normal tissue. Paraffin-embedded tumor tissue blocks are typically used as material for molecular genetic examination. When stored under these conditions, tumor DNA is partially degraded and fragmented; so, there are some limitations associated with the application of molecular genetic methods.

Emelyanova *et al.* [46] developed a method for analyzing somatic mutations using a microarray; the detection limit for revealing mutant DNA reached 0.5%. This approach was used to analyze somatic mutations in patients with melanoma. The recent breakthrough in the treatment of this disease is associated with the application of targeted drugs that specifically act on the molecular targets and immunotherapy, whose effectiveness largely depends on the tumor genotype. This

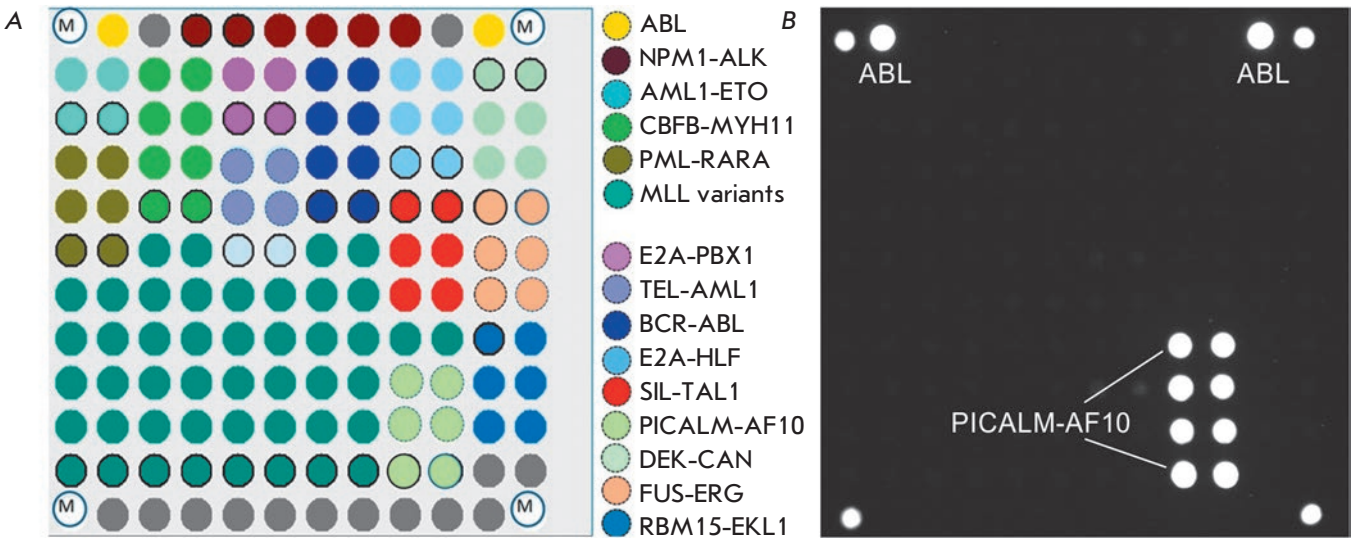

Fig. 8. (*A*) Microarray layout for the identification of the chromosomal rearrangements leading to different types of leukemia. Elements of the biochip with immobilized oligonucleotides specific to the sequences of different chimeric genes are marked in various colors. (*B*) The hybridization pattern obtained by analyzing an RNA sample containing the PICALM-AF10 fusion transcript that is associated with a poor prognosis. Such type of leukemia requires allogeneic transplantation of hematopoietic stem cells

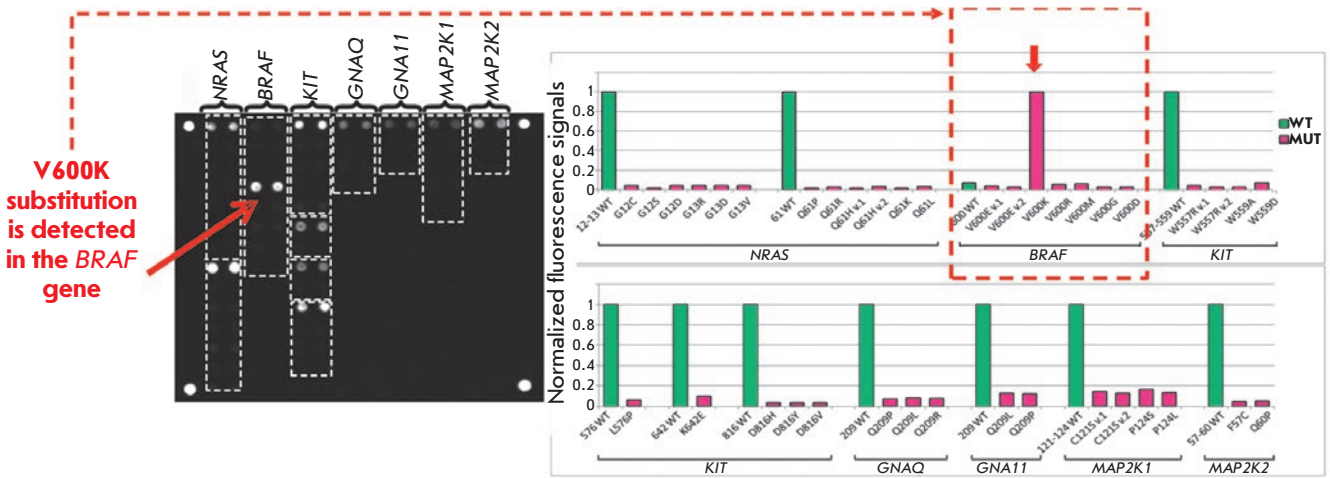

Fig. 9. Hybridization pattern and histograms of normalized signals of biochip elements for the determination of somatic mutations in DNA samples of skin melanoma. The V600K substitution in the *BRAF* gene is detected. Administration of the BRAF inhibitors vemurafenib and dabrafenib is recommended

method relies upon using a microarray to identify the 39 clinically relevant somatic mutations in the *BRAF*, *NRAS*, *KIT*, *GNAQ*, *GNA11*, *MAP2K1*, and *MAP2K2* genes (*Fig. 9*).

A total of 253 clinical specimens of melanoma were tested using this method. Various mutations in the *BRAF* (51.0%), *NRAS* (17.8%), *KIT* (2.4%), *GNAQ* (1.6%), *GNA11* (0.8%), and *MAP2K1* genes have been revealed (0.8%). The approach allows one to efficiently detect clinically relevant somatic mutations and choose the optimal target drug in 70% of melanoma patients [47].

MULTIPLEX IMMUNOASSAY USING MICROARRAYS

Depending on the specific clinical problem, there are two main types of multiplex immunoassays: (1) identification of various individual antigens in the specimen

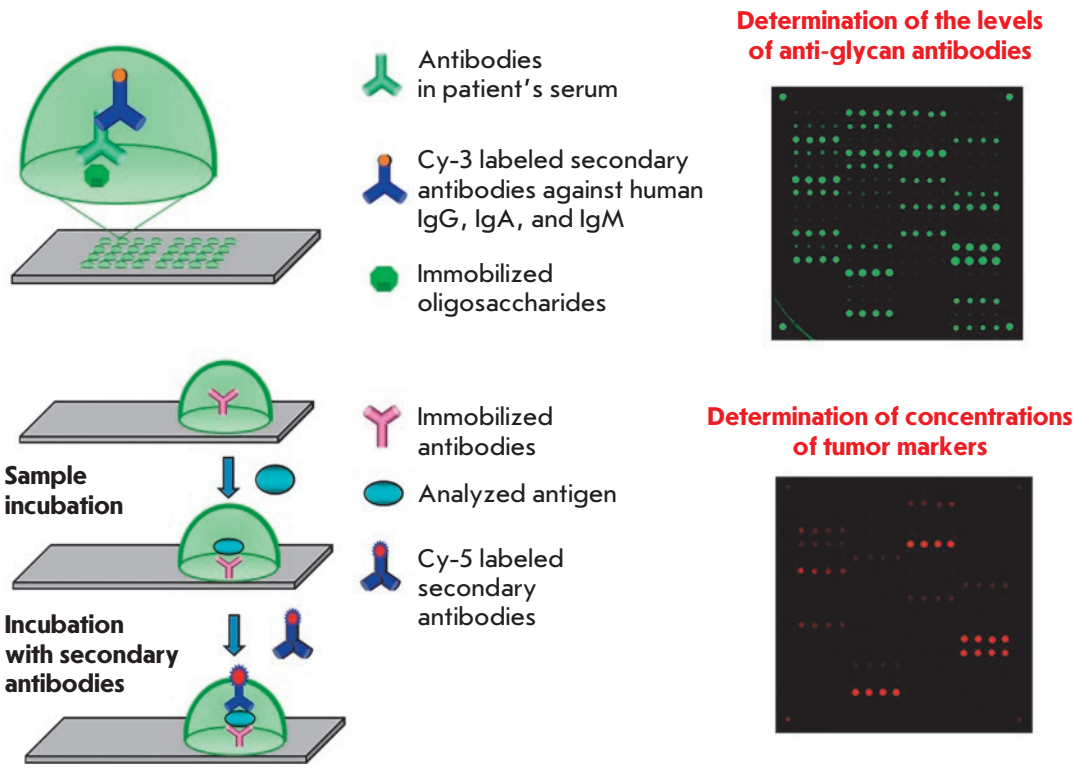

Fig. 10. Simultaneous determination of the levels of antibodies against tumor-associated glycans and concentrations of tumor markers. An immunoassay scheme and an example of fluorescence biochip images after analysis are shown

or (2) detection of antibodies circulating in the serum. In the former case, the microarray contains a panel of immobilized antibodies and each of these antibodies specifically binds to a certain antigen under analysis. In the latter case, the microarray contains immobilized ligands of protein or other nature, which specifically bind to immunoglobulins within the specimen. An example of the type 1 method is the kit for the quantitation of a number of biotoxins developed in collaboration with researchers from the M.M. Shemyakin–Yu.A. Ovchinnikov Institute of Bioorganic Chemistry of the Russian Academy of Sciences (IBCh RAS), under the aegis of academician E.V. Grishin [48].

Multiplex microarray analysis of tumor markers

A large number of studies have focused on a search for clinically significant biomarkers exhibiting high sensitivity and specificity with respect to certain tumors. The diagnostic efficiency can be enhanced by simultaneous detection of several tumor markers.

Meanwhile, some tumors cannot be timely detected using this approach. Hence, an analysis of the serum tumor markers CEA and CA 19-9 is recommended for *in vitro* diagnosis of colorectal cancer (CRC). The results of large-scale clinical trials demonstrate that these biomarkers mostly detect the disease at its late stages (III and IV) and are clinically relevant only for on-treatment monitoring [49]. Most CRC-associated markers are glycoproteins or carbohydrate antigens; they contain either O- or N-glycosites [50]. Modification of the glycosylation of these markers changes the levels of respective antigens, which can be detected by multiplex microarray assay.

An approach relying on a simultaneous analysis of serological protein-based tumor markers and antibodies belonging to different classes specific to tumor-associated glycans has been developed in collaboration with researchers at the Laboratory of Carbohydrates of the IBCh RAS. A combined microarray has been designed, with its elements containing glycans and antibodies specific to tumor markers for CRC. The serum levels of anti-glycan antibodies were determined by fluorescent microarray assay (*Fig. 10*).

Studies carried out in collaboration with the P.A. Hertzen Moscow Cancer Research Institute revealed combinations (signatures) consisting of levels of antibodies against some tumor-associated glycans and concentrations of the main tumor markers, which made it possible to reliably differentiate between CRC patients and healthy volunteers [51]. It has been demonstrated that combined use of protein and glycan signatures has a better predictive value for detecting CRC than the conventional pair of CEA + CA 19-9 tumor markers. The sensitivity and specificity of this method were 88%

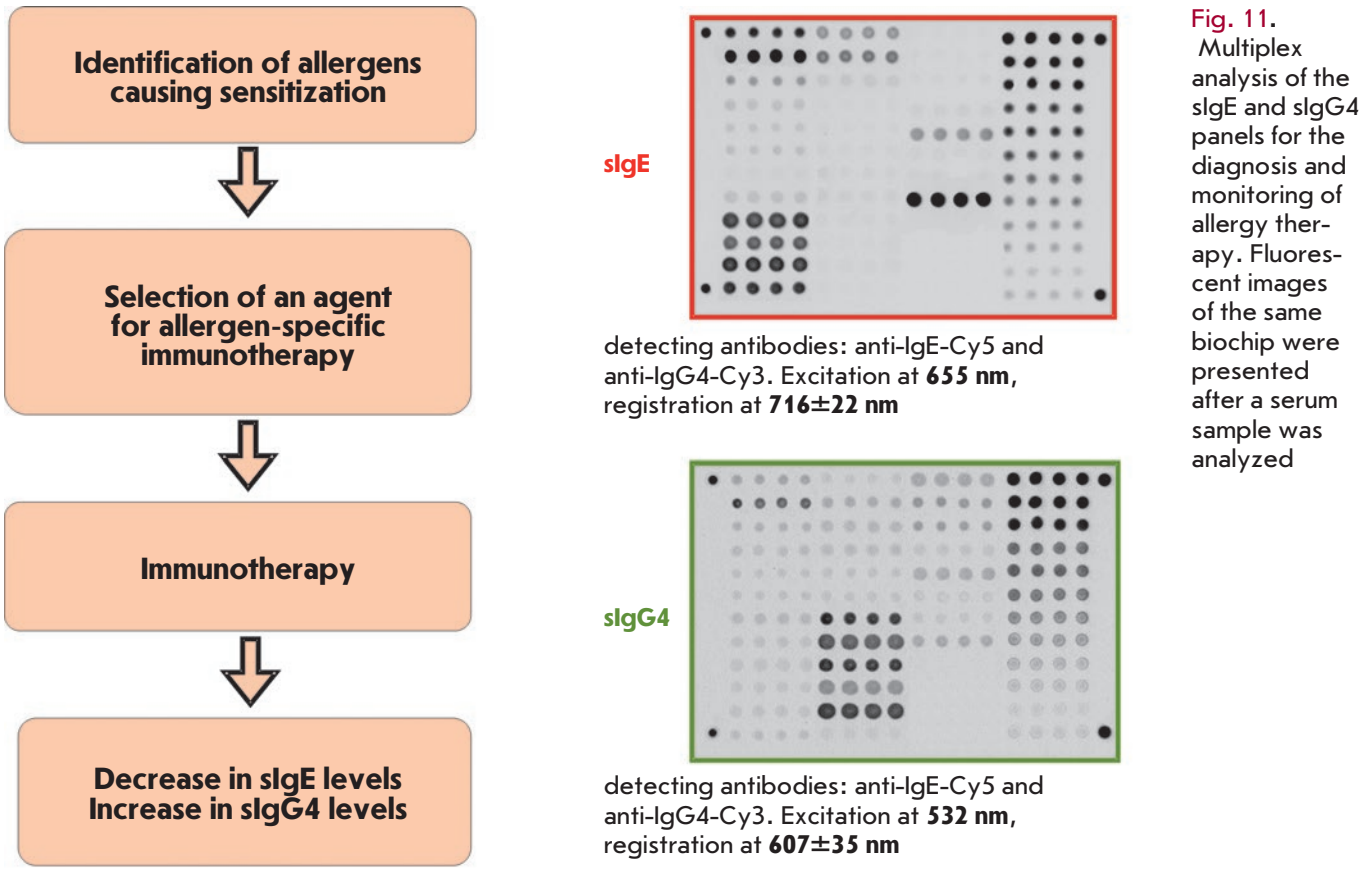

Fig. 11. Multiplex analysis of the sIgE and sIgG4 panels for the diagnosis and monitoring of allergy therapy. Fluorescent images of the same biochip were presented after a serum sample was analyzed

and 98, respectively, while the combination of CEA and CA 19-9 detected CRC in 80% of the cases with 21% sensitivity.

Microarray analysis of allergen-specific immunoglobulins (Igs)

Today, the key markers of allergy are immunoglobulins E, which mediate type I allergic reactions (anaphylaxis and Quincke's edema). Immunoglobulins belonging to the other classes can also be involved in allergic reactions. Thus, specific immunoglobulins belonging to the IgG4 class (sIgG4) play a role in the development of tolerance (i.e., the absence of clinical manifestations in response to certain allergens, following sensitization to these allergens). Although sIgG4 is not a diagnostic marker, identification of this parameter is important for evaluating the sIgE/sIgG4 ratio, which shows the effectiveness of a specific immunotherapy. sIgG4 act as blocking antibodies impeding the development of type I allergic reactions [52].

The Allergobiochip kit (*Fig. 11*) designed at the EIMB in collaboration with DR. FOOKE Laboratorien GmbH company (Germany) is intended for a parallel analysis of sIgE and sIgG4 panels specific against the following classes of allergens: pollen allergens (trees and shrubs; weeds and flowers; grasses and graminaceous plants), epidermal allergens, insect venom allergens, mite allergens, food, and fungal allergens. The diagnostic kit is a modification of solid-phase immunoassay involving fluorescent signal detection on the microarray platform. This method was tested using more than 2,000 serum specimens collected from allergic patients and healthy volunteers. The Allergobiochip kit has proved efficient in detecting type 1 hypersensitivity. Detection thresholds for sIgE and sIgG4, as well as sensitivity and specificity of the assay, were determined. The measurement range was 0.35–100 IU/mL for sIgE and 100–2500 ng/mL for sIgG4 [53, 54].

An epidemiological study involving a model pediatric population residing in central Russia (800 patients at the Filatov Moscow Pediatric Clinical Hospital aged 0–16 years and 50 healthy volunteers) was conducted to evaluate the occurrence of sensitization to various classes of allergens depending on patients' age [55]. Profiles of the levels of allergen-specific sIgE and sIgG4 in each specimen were obtained. Among inhaled allergens, sensitization was most frequently caused by birch pollen and cat dander, while the sIgE response

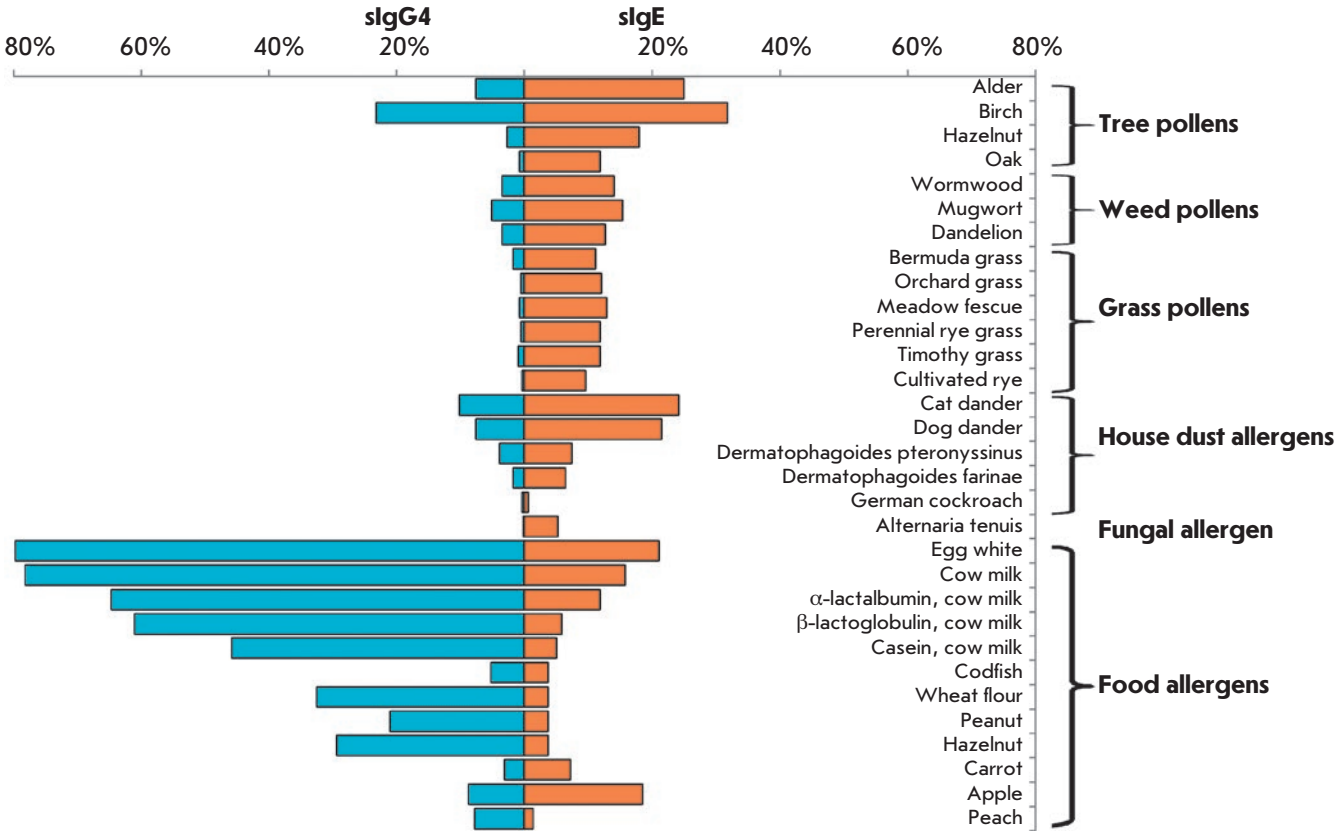

Fig. 12. Analysis of the frequency of allergic sensitization of different groups in allergic diseases. The percentages of patients (%) aged 0–16 years from the Moscow region with allergic symptoms and increased concentrations of sIgE (⩾ 0.35 IU/mL) and sIgG4 (≥100 ng/mL) to each of the 31 allergens

was typically related to egg and milk allergens, among food allergens (*Fig. 12*). The percentage of patients with elevated levels of sIgE specific to inhaled allergens increases with age, while the percentage of patients sensitized to most of the food allergens (except for carrot, apple, and peach allergens) decreases.

CONCLUSIONS

It has been 30 years since the first study focused on sequencing by hybridization with immobilized octanucleotide probes was published [56]. During this period, researchers at the EIMB Laboratory of Biological Microarrays have developed universal methods to be used for multi-parameter analysis of protein and DNA markers in statistical and clinical studies involving large series of biological specimens of differing nature. A production line to manufacture hydrogel-based microarrays, with an annual capacity of up to 1 million microarrays, has been established and certified as in compliance with the international standard ISO 13485. The Russian Federal Service for Surveillance in Healthcare and Social Development has granted 12 registration certificates to the EIMB for the developed medical devices (reagent kits and equipment for *in vitro* diagnostics using hydrogel-based microarrays).

With PCR technologies and next-generation sequencing platforms rapidly evolving, DNA microarrays have recently faced serious competition. Today, DNA microarrays occupy an intermediate niche between various nucleic acid amplification tests attempting to outcompete high-throughput sequencing technologies and exerting growing pressure. In our case, immobilization of any types of biomolecules in hydrogel and the feasibility of conducting enzymatic reactions in it [57], including isothermal ones [58], makes it possible to design portable next-generation biosensors. Hence, 3D hydrogel elements can be used as a platform for simultaneous immobilization of genome-editing agents (the nucleases Cas13 and Cas12a), together with guiding and detecting RNA/DNA molecules [59]. The "programmable" performance of nucleases (if needed, supplemented with isothermal amplification), in combination with the elaborated microfluidic systems for the isolation of nucleic acids [60], will allow the manu-

facture of highly sensitive CRISPR-biosensors. These biosensors could potentially be used under field conditions. These integrative autonomous systems containing the hydrogel-based microarray platform and the coordinated supporting modules will make it possible to obtain more informative and accurate results in a shorter time than is now the case. They will play a crucial role in the personalized medicine of the future.

Thus far, more than 2,000 patients of the Filatov Moscow Pediatric Clinical Hospital have been examined using the Allergo-biochip kit. In addition to the apparent economic benefit due to the "one specimen–one analysis" format, the proposed approach allows one to identify the allergen causing a severe allergic reaction in a child using only 100 μL of serum. Such a small specimen volume is a substantial advantage when examining children of a young age (several months old). It is rather promising to design protein microarrays for the differential diagnosis of rheumatologic diseases and other immune disorders. Extending the scope of microarray applications to the analysis of predictive markers for cancer also holds great promise. It is our hope that developing a new approach based on comprehensive signature analysis will allow clinicians to solve this challenging problem.

Hence, the hydrogel microarray technology has already proved an efficient tool in personalized medicine. It allows one to perform molecular profiling of a plethora of clinically significant markers of causative agents and reasons for socially important diseases, save the lives of hundreds of patients, and optimize the public funds allocated for healthcare. ●

This work was supported by the Russian Science Foundation (grants nos. 14-50-00060 and 17-75-20039).

REFERENCES

1. Marzancola M.G., Sedighi A., Li P.C. // Methods Mol. Biol. 2016. V. 1368. P. 161–178.
2. Rosenfeld S. // Gene Regul. Syst. Bio. 2010. V. 4. P. 61–73.
3. Eklund A.C., Szallasi Z. // Genome Biol. 2008. V. 9. № 2. P. R26.
4. Salazar R., Roepman P., Capella G., Moreno V., Simon I., Dreezen C., Lopez-Doriga A., Santos C., Marijnen C., Westerga J., et al. // J. Clin. Oncol. 2011. V. 29. № 1. P. 17–24.
5. Damin F., Galbiati S., Ferrari M., Chiari M. // Biosens. Bioelectron. 2016. V. 78. P. 367–733.
6. Le Goff G.C., Srinivas R.L., Hill W.A., Doyle P.S. // Eur. Polym. J. 2015. V. 72. P. 386–412.
7. Beyer A., Pollok S., Berg A., Weber K., Popp J. // Macromol. Biosci. 2014. V. 14. № 6. P. 889–898.
8. Yershov G., Barsky V., Belgovskiy A., Kirillov E., Kreindlin E., Ivanov I., Parinov S., Guschin D., Drobishev A., Dubiley S., et al. // Proc. Natl. Acad. Sci. USA. 1996. V. 93. № 10. P. 4913–4918.
9. Rubina A.Y., Pan'kov S.V., Dementieva E.I., Pen'kov D.N., Butygin A.V., Vasiliskov V.A., Chudinov A.V., Mikheikin A.L., Mikhailovich V.M., Mirzabekov A.D. // Anal. Biochem. 2004. V. 325. № 1. P. 92–106.
10. Rubina A.Y., Kolchinsky A., Makarov A.A., Zasedatelev A.S. // Proteomics. 2008. V. 8. № 4. P. 817–831.
11. Khrapko K.R., Lysov Yu P., Khorlyn A.A., Shick V.V., Florentiev V.L., Mirzabekov A.D. // FEBS Lett. 1989. V. 256. № 1–2. P. 118–122.
12. Sorokin N.V., Chechetkin V.R., Livshits M.A., Pan'kov S.V., Donnikov M.Y., Gryadunov D.A., Lapa S.A., Zasedatelev A.S. // J. Biomol. Struct. Dyn. 2005. V. 22. № 6. P. 725–734.
13. Pan'kov S.V., Chechetkin V.R., Somova O.G., Antonova O.V., Moiseeva O.V., Prokopenko D.V., Yurasov R.A., Gryadunov D.A., Chudinov A.V. // J. Biomol. Struct. Dyn. 2009. V. 27. № 2. P. 235–244.
14. Gryadunov D., Mikhailovich V., Lapa S., Roudinskii N., Donnikov M., Pan'kov S., Markova O., Kuz'min A., Chernousova L., Skotnikova O., et al. // Clin. Microbiol. Infect. 2005. V. 11. № 7. P. 531–539.
15. Zimenkov D.V., Kulagina E.V., Antonova O.V., Zhuravlev V.Y., Gryadunov D.A. // J. Antimicrob. Chemother. 2016. V. 71. № 6. P. 1520–1531.
16. Zimenkov D.V., Antonova O.V., Kuz'min A.V., Isaeva Y.D., Krylova L.Y., Popov S.A., Zasedatelev A.S., Mikhailovich V.M., Gryadunov D.A. // BMC Infect. Dis. 2013. V. 13. P. 240.
17. Shershov V.E., Lapa S.A., Kuznetsova V.E., Spitsyn M.A., Guseinov T.O., Polyakov S.A., Stomahin A.A., Zasedatelev A.S., Chudinov A.V. // J. Fluoresc. 2017. V. 27. № 6. P. 2001–2016.
18. Zasedateleva O.A., Vasiliskov V.A., Surzhikov S.A., Kuznetsova V.E., Shershov V.E., Guseinov T.O., Smirnov I.P., Yurasov R.A., Spitsyn M.A., Chudinov A.V. // Nucl. Acids Res. 2018. V. 46. № 12. P. e73.
19. Rubina A.Y., Dementieva E.I., Stomakhin A.A., Darii E.L., Pan'kov S.V., Barsky V.E., Ivanov S.M., Konovalova E.V., Mirzabekov A.D. // Biotechniques. 2003. V. 34. № 5. P. 1008–1022.
20. Lysov Y., Barsky V., Urasov D., Urasov R., Cherepanov A., Mamaev D., Yegorov Y., Chudinov A., Surzhikov S., Rubina A., et al. // Biomed. Opt. Express. 2017. V. 8. № 11. P. 4798–4810.
21. Gryadunov D., Mikhailovich V., Lapa S., Roudinskii N., Donnikov M., Pan'kov S., Markova O., Kuz'min A., Chernousova L., Skotnikova O., et al. // Clin. Microbiol. Infect. 2005. V. 11. № 7. P. 531–539.
22. Kurbatova E.V., Kaminski D.A., Erokhin V.V., Volchenkov G.V., Andreevskaya S.N., Chernousova L.N., Demikhova O.V., Ershova J.V., Kaunetis N.V., Kuznetsova T.A., et al. // Eur. J. Clin. Microbiol. Infect. Dis. 2013. V. 32. № 6. P. 735–743.
23. Nosova E., Krasnova M.A., Galkina K., Makarova M.V., Litvinov V.I., Moroz A.M. // Mol. Biol. (Mosk.). 2013. V. 47. № 2. P. 267–274.
24. Vasil'eva I.A., Samoilova A.G., Ergeshov A.E., Bagdasarian T.R., Chernousova L.N. // Vestn. Ross. Akad. Med. Nauk. 2012. V. 67. № 11. P. 9–14.
25. Daurov R.B., Vasilyeva I.A., Perfilyev A.V., Chernousova L.N., Kuzmin A.V., Glazkova N.A. // Tuberk. Bolezni Leg-

kih. 2010. V. 87. № 4. P. 10–13.
26. Mokrousov I., Vyazovaya A., Solovieva N., Sunchalina T., Markelov Y., Chernyaeva E., Melnikova N., Dogonadze M., Starkova D., Vasilieva N., et al. // BMC Microbiol. 2015. V. 15. P. 279.
27. Koser C.U., Bryant J.M., Comas I., Feuerriegel S., Niemann S., Gagneux S., Parkhill J., Peacock S.J. // J. Antimicrob. Chemother. 2014. V. 69. № 8. P. 2298–2299.
28. Nosova E.Y., Zimenkov D.V., Khakhalina A.A., Isakova A.I., Krylova L.Y., Makarova M.V., Galkina K.Y., Krasnova M.A., Safonova S.G., Litvinov V.I., et al. // PLoS One. 2016. V. 11. № 11. P. e0167093.
29. Zimenkov D.V., Nosova E.Y., Kulagina E.V., Antonova O.V., Arslanbaeva L.R., Isakova A.I., Krylova L.Y., Peretokina I.V., Makarova M.V., Safonova S.G., et al. // J. Antimicrob. Chemother. 2017. V. 72. № 7. P. 1901–1906.
30. Bespyatykh J.A., Zimenkov D.V., Shitikov E.A., Kulagina E.V., Lapa S.A., Gryadunov D.A., Ilina E.N., Govorun V.M. // Infect. Genet. Evol. 2014. V. 26. P. 41–46.
31. Zimenkov D.V., Kulagina E.V., Antonova O.V., Krasnova M.A., Chernyaeva E.N., Zhuravlev V.Y., Kuz'min A.V., Popov S.A., Zasedatelev A.S., Gryadunov D.A. // J. Clin. Microbiol. 2015. V. 53. № 4. P. 1103–1114.
32. Shaskolskiy B., Dementieva E., Leinsoo A., Runina A., Vorobyev D., Plakhova X., Kubanov A., Deryabin D., Gryadunov D. // Front. Microbiol. 2016. V. 7. P. 747.
33. Leinsoo A.T., Shaskol'skii B.L., Dement'eva E.I., Gryadunov D.A., Kubanov A.A., Chestkov A.V., Obraztsova O.A., Shpilevaya M.V., Deryabin D.G. // Bull. Exp. Biol. Med. 2017. V. 164. № 1. P. 54–60.
34. Shaskolskiy B., Dementieva E., Leinsoo A., Petrova N., Chestkov A., Kubanov A., Deryabin D., Gryadunov D. // Infect. Genet. Evol. 2018. V. 63. P. 236–242.
35. Kubanov A., Vorobyev D., Chestkov A., Leinsoo A., Shaskolskiy B., Dementieva E., Solomka V., Plakhova X., Gryadunov D., Deryabin D. // BMC Infect. Dis. 2016. V. 16. P. 389.
36. Kubanov A.A., Leinsoo A.T., Chestkov A.V., Dementieva E.I., Shaskolskiy B.L., Solomka V.S., Gryadunov D.A., Deryabin D.G. // Mol. Biol. (Mosk.). 2017. V. 51. № 3. P. 431–441.
37. Harris S.R., Cole M.J., Spiteri G., Sanchez-Buso L., Golparian D., Jacobsson S., Goater R., Abudahab K., Yeats C.A., Bercot B., et al. // Lancet. Infect. Dis. 2018. V. 18. № 7. P. 758–768.
38. Welzel T.M., Bhardwaj N., Hedskog C., Chodavarapu K., Camus G., McNally J., Brainard D., Miller M.D., Mo H., Svarovskaia E., et al. // J. Hepatol. 2017. V. 67. № 2. P. 224–236.
39. Manns M.P., Buti M., Gane E., Pawlotsky J.M., Razavi H., Terrault N., Younossi Z. // Nat. Rev. Dis. Primers. 2017. V. 3. P. 17006.
40. Gryadunov D., Nicot F., Dubois M., Mikhailovich V., Zasedatelev A., Izopet J. // J. Clin. Microbiol. 2010. V. 48. № 11. P. 3910–3917.
41. Rodriguez-Frias F., Nieto-Aponte L., Gregori J., Garcia-Cehic D., Casillas R., Tabernero D., Homs M., Blasi M., Vila M., Chen Q., et al. // Clin. Microbiol. Infect. 2017. V. 23. № 10. doi: 10.1016/j.cmi.2017.02.007
42. Soria M.E., Gregori J., Chen Q., Garcia-Cehic D., Llorens M., de Avila A.I., Beach N.M., Domingo E., Rodriguez-Frias F., Buti M., et al. // BMC Infect. Dis. 2018. V. 18. № 1. P. 446.
43. Nasedkina T.V., Guseva N.A., Gra O.A., Mityaeva O.N., Chudinov A.V., Zasedatelev A.S. // Mol. Diagn. Ther. 2009. V. 13. № 2. P. 91–102.
44. Nasedkina T.V., Ikonnikova A.Y., Tsaur G.A., Karateeva A.V., Ammour Y.I., Avdonina M.A., Karachunskii A.I., Zasedatelev A.S. // Mol. Biol. (Mosk.). 2016. V. 50. № 6. P. 968–977.
45. Ikonnikova A.Yu., Fesenko D.O., Karateeva A.V., Zasedatelev A.S., Nasedkina T.V. Patent 2639513. Russia. C12N 15/00. 2017.
46. Emelyanova M., Arkhipova K., Mazurenko N., Chudinov A., Demidova I., Zborovskaya I., Lyubchenko L., Zasedatelev A., Nasedkina T. // Appl. Immunohistochem. Mol. Morphol. 2015. V. 23. № 4. P. 255–265.
47. Emelyanova M., Ghukasyan L., Abramov I., Ryabaya O., Stepanova E., Kudryavtseva A., Sadritdinova A., Dzhumakova C., Belysheva T., Surzhikov S., et al. // Oncotarget. 2017. V. 8. № 32. P. 52304–52320.
48. Rubina A.Y., Filippova M.A., Feizkhanova G.U., Shepeliakovskaya A.O., Sidina E.I., Boziev Kh.M., Laman A.G., Brovko F.A., Vertiev Y.V., Zasedatelev A.S., et al. // Anal. Chem. 2010. V. 82. № 21. P. 8881–8889.
49. Duffy M.J., Lamerz R., Haglund C., Nicolini A., Kalousova M., Holubec L., Sturgeon C. // Int. J. Cancer. 2014. V. 134. № 11. P. 2513–2522.
50. Kufe D.W. // Nat. Rev. Cancer. 2009. V. 9. № 12. P. 874–885.
51. Butvilovskaya V.I., Popletaeva S.B., Chechetkin V.R., Zubtsova Z.I., Tsybulskaya M.V., Samokhina L.O., Vinnitskii L.I., Ragimov A.A., Pozharitskaya E.I., Grigoreva G.A., et al. // Cancer. Med. 2016. V. 5. № 7. P. 1361–1372.
52. Vazquez-Ortiz M., Pascal M., Jimenez-Feijoo R., Lozano J., Giner M.T., Alsina L., Martin-Mateos M.A., Plaza A.M. // Clin. Exp. Allergy. 2014. V. 44. № 4. P. 579–588.
53. Feyzkhanova G.U., Filippova M.A., Talibov V.O., Dementieva E.I., Maslennikov V.V., Reznikov Y.P., Offermann N., Zasedatelev A.S., Rubina A.Y., Fooke-Achterrath M. // J. Immunol. Methods. 2014. V. 406. P. 51–57.
54. Feyzkhanova G., Voloshin S., Smoldovskaya O., Arefieva A., Filippova M., Barsky V., Pavlushkina L., Butvilovskaya V., Tikhonov A., Reznikov Y., et al. // Clin. Proteomics. 2017. V. 14. P. 1.
55. Voloshin S., Smoldovskaya O., Feyzkhanova G., Arefieva A., Pavlushkina L., Filatova T., Butvilovskaya V., Filippova M., Lysov Y., Shcherbo S., et al. // PLoS One. 2018. V. 13. № 3. P. e0194775.
56. Lysov Iu P., Florent'ev V.L., Khorlin A.A., Khrapko K.R., Shik V.V. // Dokl. Akad. Nauk SSSR. 1988. V. 303. № 6. P. 1508–1511.
57. Khodakov D.A., Zakharova N.V., Gryadunov D.A., Filatov F.P., Zasedatelev A.S., Mikhailovich V.M. // Biotechniques. 2008. V. 44. № 2. P. 241–248.
58. Kashkin K.N., Strizhkov B.N., Griadunov D.A., Surzhikov S.A., Grechishnikova I.V., Kreindlin E., Chupeeva V.V., Evseev K.B., Turygin A., Mirzabekov A.D. // Mol. Biol. (Mosk.). 2005. V. 39. № 1. P. 30–39.
59. Gootenberg J.S., Abudayyeh O.O., Kellner M.J., Joung J., Collins J.J., Zhang F. // Science. 2018. V. 360. № 6387. P. 439–444.
60. Mamaev D., Shaskolskiy B., Dementieva E., Khodakov D., Yurasov D., Yurasov R., Zimenkov D., Mikhailovich V., Zasedatelev A., Gryadunov D. // Biomed. Microdevices. 2015. V. 17. P. 18.

Multifaced Roles of the Urokinase System in the Regulation of Stem Cell Niches

K. V. Dergilev[1*], V. V. Stepanova[2], I. B. Beloglazova[1,3], Z. I. Tsokolayev[1], E. V. Parfenova[1,3]
[1]Laboratory of Angiogenesis, National Medical Research Center of Cardiology, 3rd Cherepkovskaya Str., 15a, Moscow, 121552, Russia
[2]Department of Pathology and Laboratory Medicine, University of Pennsylvania Perelman School of Medicine, Philadelphia, USA
[3]Laboratory of Post-Genomic Technologies in Medicine, Faculty of Fundamental Medicine, Moscow State University, Lomonosovsky Ave., 27-1, Moscow, 119991, Russia
*E-mail: doctorkote@gmail.com
Received April 20, 2018; in final form November 06, 2018

ABSTRACT **Proliferation, subsequent migration to the damaged area, differentiation into appropriate cell types, and/or secretion of biologically active molecules and extracellular vesicles are important processes that underlie the involvement of stem/progenitor cells in the repair and regeneration of tissues and organs. All these functions are regulated through the interaction between stem cells and the microenvironment in the tissue cell niches that control these processes through direct cell-cell interactions, production of the extracellular matrix, release of extracellular vesicles, and secretion of growth factors, cytokines, chemokines, and proteases. One of the most important proteolytic systems involved in the regulation of cell migration and proliferation is the urokinase system represented by the urokinase plasminogen activator (uPA, urokinase), its receptor (uPAR), and inhibitors. This review addresses the issues of urokinase system involvement in the regulation of stem cell niches in various tissues and analyzes the possible effects of this system on the signaling pathways responsible for the proliferation, programmed cell death, phenotype modulation, and migration properties of stem cells.**
KEYWORDS **urokinase, urokinase receptor, plasminogen activator inhibitors, regeneration, stem cells, cell niches.**

INTRODUCTION

Currently, stem cells (SCs) are considered as an important regulator of cellular homeostasis and a component of the regeneration/repair of all body tissues. SCs have already been used in medical practice; however, production of biomedical products with certain properties remains an unsolved problem due to the complex, not fully understood pathways of regulation which underlie their unique properties. Regulation of SC functions in tissues involves a certain microenvironment that forms specific structures called "cell niches" [1, 2]. This microenvironment originates from interactions between stem cells and neighboring differentiated cells, as well as components of the extracellular matrix (ECM) due to the activation/inhibition of various signaling pathways (Notch, Wnt, TGF-β, Sonic Hedgehog, etc.) through direct cell-cell interactions, release of extracellular vesicles, and secretion of growth factors, cytokines, chemokines, and various proteases [3]. An important component of this complex regulation is the urokinase system represented by urokinase (also known as urokinase-type plasminogen activator (uPA), its receptor (uPAR/CD87), and two of its inhibitors (PAI-1 and PAI-2). The uniqueness of this system is related to the urokinase receptor anchored to the cell membrane by glycosylphosphatidylinositol, which enables the receptor to move in the membrane bilayer and locally concentrate the proteolytic activity of urokinase in the direction of cell movement. The urokinase-triggered cascade of proteolytic reactions, including the local formation of plasmin and activation of matrix metalloproteinases, promotes degradation of the ECM along a path of a moving cell, activation of growth factors, and release

of the growth factors sequestered in the matrix [4–7]. However, in addition to the activation of extracellular proteolysis, most cellular responses modulated by the urokinase system require transmembrane signaling. This signaling is mediated by the interaction between components of this system and a variety of extracellular and intracellular proteins and membrane receptors that transmit signals to the intracellular pathways that regulate various cellular functions. The urokinase system components are present in the niches of bone marrow stem cell [8], striated muscles [9], neural cells [10], and tumor cells [11]. They are involved in the regulation of important biological processes, such as inflammation, angiogenesis, myogenesis, remodeling of extracellular matrix proteins, metastasis, and tumor growth. This review discusses potential ways for regulating stem cell functions by the urokinase system through extracellular matrix remodeling and interaction with the signaling pathways responsible for the regulation of division, programmed cell death, and modulation of the phenotype and cell motility, which is important in the development of approaches to directed influence on their properties.

UROKINASE SYSTEM: STRUCTURE AND FUNCTIONS

Urokinase is an extracellular serine protease with narrow substrate specificity which is involved in the conversion of plasminogen to plasmin. In humans, urokinase is secreted by various cell types: monocytes/macrophages [12, 13], tumor cells [14–16], fibroblasts [17, 18], smooth muscle cells [19, 20], and endothelial cells [21, 22]. Urokinase consists of 411 amino acid residues (molecular weight of 53 kDa) [23] and is secreted by cells as a single-chain protein (sc-uPA) comprising three domains: a N-terminal growth factor-like domain (GFD) structurally homologous to the epidermal growth factor (residues 9–45), a kringle domain (KD, residues 45–134), and a C-terminal proteolytic domain (PD, residues 144–411). The growth factor-like domain function is high affinity interaction with the urokinase receptor on the cell surface [24]. The proteolytic domain converts plasminogen into plasmin and activates some growth factors and matrix metalloproteinases [25]. The function of the kringle domain is not yet fully understood; however, the domain is believed to be involved in the stimulation of cell migration under the action of urokinase [26], stabilize the interaction between urokinase and the receptor [27], and participate in the transport of urokinase into the nucleus [28] (*Fig. 1*).

The urokinase receptor uPAR/CD87 was first identified as a urokinase-type plasminogen activator receptor on the surface of human monocytes [29]. uPAR was also detected on endothelial cells [30], neutrophils [31], smooth muscle cells [32], placental trophoblast cells [33], and also on the cells of various tumor lines [34–37]. uPAR/CD87 is overexpressed by blood cells during inflammation [38, 39]. uPAR belongs to the Ly-6 family [40] and is a single-chain, highly glycosylated protein [41] anchored to the cell membrane by glycosylphosphatidylinositol covalently bound to the third, C-terminal domain of the receptor [42]. uPAR has a molecular weight of 55–60 kDa and consists of

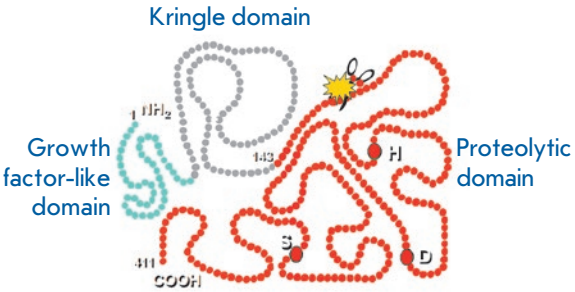

Fig. 1. Schematic representation of the urokinase structure

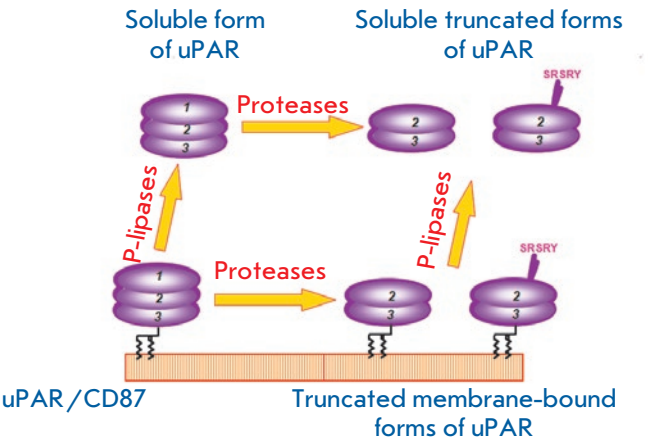

Fig. 2. Action of proteases and phospholipases leads to formation of truncated membrane-bound and soluble forms of the urokinase receptor

313 amino acid residues that form three structurally homologous domains [43]. The first domain of the receptor plays a major role in the binding to urokinase and interacts with its growth factor-like domain. According to crystallography data, the ligand-bound urokinase receptor occurs in a more compact state, because the first and third domains of the receptor come in close proximity during its interaction with urokinase. One of the important processes regulating the uPAR function is proteolytic cleavage between the first and second domains (*Fig. 2*) by proteases such as plasmin, matrix metalloproteinases, and urokinase itself [44, 45]. After cleavage, uPAR loses its ability to bind urokinase, but it acquires the ability to regulate cell migration independently of urokinase [46]. Both the full-length and cleaved (c-uPAR) forms of the urokinase receptor can be removed from the membrane surface by proteases or phospholipase C specific to glycosylphosphatidylinositol [47–52]. This process results in soluble full-length (su-uPAR) and cleaved (su-c-uPAR) forms of the receptor, which circulate in the blood plasma and serve as markers of some inflammatory or immunological diseases. It is important to note that the soluble cleaved urokinase receptor is a strong chemoattractant for cells (neutrophils, monocytes, macrophages) expressing receptors for the bacterial N-formyl-methionyl-leucyl-phenylanilanne (fMLP) peptide [53, 54].

A high level of urokinase proteolytic activity may be detrimental to cells. To regulate the level of extracellular proteolysis, cells synthesize specific protein inhibitors of plasminogen activators – PAI-1, PAI-2, protease nexin-1, and protein C inhibitor [55–58]. They belong to a group of arginine-serpin inhibitors. They mimic the substrate during interaction with a double-chain form of the enzyme, which results in a 1 : 1 stable covalent enzyme–inhibitor complex and enzyme inactivation [59]. The interaction with single-chain urokinase does not lead to a covalent complex. PAI-1 is a 45–50 kDa single-chain glycoprotein. After secretion, PAI-1 is rapidly inactivated due to conformational rearrangements and becomes unable to bind to urokinase. Activation of the inhibitor requires the interaction of an inactive PAI-1 molecule with physiological cofactors – the extracellular matrix protein vitronectin or heparin [60]. Matrix-bound PAI-1, unlike its free form, can remain active for a long time [61]. Active PAI-1 interacts with both free and receptor-bound urokinase, inhibiting the pericellular proteolysis process [62]. Single-chain urokinase has low proteolytic activity and can also bind PAI-1, but at a much lower rate [63]. The PAI-1 activity can be regulated in several ways. Urokinase is able to cleave and inactivate PAI-1 [64]. In addition, binding of PAI-1 to uPA/uPAR leads to a ternary complex that is immediately internalized by cells [65, 66]. This process is triggered by the interaction between the ternary complex and endocytic receptors from the low-density lipoprotein receptor family. Urokinase and PAI-1 are degraded in the lysosomes, and the uPAR and endocytic receptor return to the cell surface, thereby initiating intracellular signaling and cytoskeleton rearrangement. Therefore, along with the ability to regulate proteolytic activity, PAI-1 is involved in the regulation of cell migration and adhesion.

The PAI-2 urokinase inhibitor is a 47 kDa single-chain glycoprotein [67]. Its ability to inhibit urokinase is much lower than that of PAI-1. For example, the constant for association of receptor-bound urokinase with PAI-1 is 15-fold greater than that with PAI-2 [63]. For a long time, inhibition of urokinase had been believed to be the main function of PAI-2. However, only a small fraction of the newly synthesized inhibitor is found to be secreted as a glycosylated polypeptide into the extracellular space [68]. The main fraction remains inside cells and protects them from the apoptosis induced by the tumor necrosis factor-α (TNF-α) [69, 70], as well as regulates the level of interferon-α/β secretion [71]. The secreted form of PAI-2 is involved in the regulation of fibrinolysis and tissue remodeling. The cytosolic form of PAI-2 plays an important role in the intracellular proteolysis involved in the regulation of apoptosis and inflammation.

UROKINASE SYSTEM AND HEMATOPOIETIC BONE MARROW STEM CELLS

The bone marrow contains a population of hematopoietic stem cells (HSCs) capable of self-renewal and differentiation into all blood cells and some other cell types. In the bone marrow, HSCs express uPAR on their surface and are localized in cell niches that are mainly represented by osteoblasts, endothelial cells, and mesenchymal stem cells [72, 73]. These cells are poorly differentiated and characterized by a low level of proliferation/apoptosis due to cell cycle arrest in the G0/G1 phase. However, in *uPAR*-deficient mice ($Plaur^{-/-}$ mice), HSCs actively enter the cell cycle, differentiate, and enter the systemic circulation, which reduces their poorly differentiated pool and indicates the role of the urokinase receptor in maintaining the low-differentiated state of HSCs [74]. In addition, uPAR controls post-transplant survival of HSCs and the efficiency of hematopoietic recovery [74]. HSCs obtained from transgenic $uPAR^{-/-}$ mice and transplanted to wild-type splenectomized mice after radiation exposure (9.5 Gy) had reduced indicators of bone marrow integration and survival for

a 2-week follow-up period compared to those of wild-type mouse HSCs. One of the potential molecular mechanisms of these effects may be the interaction of uPAR with integrins, in particular with α4β1-integrin that regulates migration and adhesion of HSCs to fibronectin and VCAM-1 during their homing and engraftment in the bone marrow [74–78]. The function of α4β1-integrin is known to depend on intact uPAR, because only the intact urokinase receptor interacts with integrins [79, 80]. Proteolytic cleavage of uPAR with removal of the D1 domain reduces α4β1-mediated cell adhesion [81]. Transgenic mice deficient in the urokinase receptor are characterized by impaired α4β1-integrin-mediated adhesion of HSCs in the bone marrow, which probably leads to disruption of their integration into the bone marrow tissue. Soluble forms of the urokinase receptor (s-uPAR) may play some role in HSC release from the bone marrow; the level of receptors significantly increases in blood plasma during mobilization of HSCs with the granulocyte colony-stimulating factor (G-CSF) [82, 83]. s-uPAR may facilitate migration of HSCs into the bloodstream, either directly or indirectly, by suppressing the activity of the CXCR4 receptor that is responsible for keeping cells in the bone marrow niche. *In vivo* experiments demonstrated that peptides developed on the basis of a cleaved s-c-uPAR form were able to induce the release of mouse CD34+ HSCs from bone marrow depots as efficiently as G-CSF [82].

Therefore, the urokinase receptor both maintains HSCs at rest in the bone marrow niche and regulates their release from the niche, probably, through several mechanisms, including interaction with integrins and direct chemotactic action.

UROKINASE SYSTEM AND ENDOTHELIAL PROGENITOR CELLS

Pathogenesis of many cardiovascular diseases is associated with dysfunction and damage to the vascular wall endothelial layer that plays an important role in the regulation of the cardiovascular system function. Circulating endothelial progenitor cells (EPCs) released from bone marrow niches provide endothelial layer repair and postnatal vasculogenesis [84].

Damage to the vessel activates synthesis and secretion of a wide range of cytokines and chemokines (VEGF, IGF2, MCP-1, IL-8, bradykinin, MIF, SDF-1, etc.) that create a gradient inside the vascular wall and promote EPC homing to the damaged area via the adhesion and transendothelial migration mechanisms. The urokinase system is known to be involved in the regulation of angioarteriogenesis in ischemia and inflammation [85–87], in particular via regulation of directed migration of EPCs [88, 89] expressing high levels of uPA and uPAR [90]. In this case, in non-stimulated EPCs, the urokinase receptor is localized in lipid rafts and absent in caveolae; however, stimulation by VEGF causes increased expression of caveolin-1 and uPAR, assembly of caveolae, and uPAR internalization in EPCs [91]. Impairment of caveolae assembly in EPCs caused by methyl beta-cyclodextrin (β-MCD) or inhibition of caveolin-1 does not cause redistribution of uPAR on the cell membrane, while suppression of uPAR expression disrupts the normal organization of caveolae. These data suggest that uPAR may be an organizer of the assembly of caveolar rafts in EPCs, which underlies the behavior of these cells in the vascular wall [92]. For example, caveolin-dependent ERK1/2 phosphorylation stimulated by VEGF is the initiating event in migration/differentiation of EPCs, and the caveolae integrity affects the angiogenic properties of EPCs [93]. VEGF increases expression of caveolin-1 and uPAR in EPCs and triggers redistribution of uPAR in caveolae, which increases invasion of EPCs and promotes capillary morphogenesis. Suppression of uPAR expression by antisense oligonucleotides disrupts caveolae formation and inhibits EPC invasion and capillary genesis. [93]. Thus, the formation of caveolar uPAR is considered a critical step in implementation of the angiogenic properties of EPCs. Secretion of uPA and the precursor of matrix metalloproteinase-2 (pro-MMP-2) is also increased in EPCs stimulated with VEGF or TNF-α [93], and inhibition of uPA or uPAR by monoclonal antibodies significantly reduces proliferation, migration, and formation of capillary-like structures by these cells *in vitro* [93, 94]. Recently, autophagy was shown to play a certain role in the regulation of EPC migration [95], which regulates, via the mTOR-P70S6K signaling pathway, expression of uPA and matrix metalloproteinases that degrade extracellular matrix proteins, which is necessary for migration of EPCs to the damaged area. Therefore, the existing data indicate the crucial role of urokinase and its receptor in providing homing into the injured vessel and the angiogenic properties of circulating endothelial progenitor cells.

UROKINASE SYSTEM AND PROGENITOR CELLS OF STRIATED MUSCLE TISSUE

Satellite cells (SCs) form a stable self-renewing pool in the skeletal muscles of an adult organism. As revealed by electron microscopy more than four decades ago, striated muscle stem cells are mononuclear cells located between the muscle fiber sarcolemma and the basal lamina surrounding the fiber [96]. This anatomical location acts as the basis of a cell niche where satellite cells can be maintained at rest or activated,

divide, and differentiate in response to external stimuli associated with muscle growth and recovery. Activated SCs undergo division and give rise to myogenic progenitor cells – skeletal myoblasts [97]. Myoblasts begin to express myogenic transcription factors, such as MyoD, Myf5, MRF4, myogenin, and other muscle proteins, secrete uPA and PAI-1, express uPAR on the surface, and fuse to form muscle tubes that are the future muscle fibers [98, 99]. The urokinase system is involved in the regeneration of striated muscles through regulation of the functions of SCs and skeletal myoblasts. Binding of uPA to the receptor was shown to be necessary to initiate migration of SCs, their differentiation, and fusion with pre-existing myotubes. Blockade of this binding with antibodies inhibits migration of cultured G8-1 myoblasts and suppresses their ability for myogenic differentiation [100]. The latter may be due to suppressed expression of myogenin and MyoD, which occurs when binding of uPA to uPAR is inhibited [101].

Skeletal muscle regeneration is regulated by a balance between uPA and PAI-1, which may affect regeneration through several mechanisms, including triggering of intracellular signaling upon binding of urokinase to the receptor [99] and modulation of the effects of growth factors, in particular, FGF-2 [102]. Also, uPA is necessary for myoblast fusion when uPA expression in these cells increases manifold. Antibodies blocking the catalytic activity of uPA or the interaction between uPA and uPAR completely inhibit fusion and muscle tube formation [103, 104]. Therefore, uPA regulates proliferation, migration, and fusion of myoblasts. The mechanisms underlying this regulation cannot be explained solely by the proteolytic function of uPA and require further investigation.

UROKINASE SYSTEM AND MESENCHYMAL STEM CELLS

Mesenchymal stem cells (MSCs) are found in almost all organs and tissues. Together with extracellular matrix proteins, MSCs form the microenvironment of resident stem cells in tissue cell niches [105]. They regulate tissue repair, modulating the properties of stem and immune cells and their homing due to secretion of a wide range of biologically active factors and release of the extracellular vesicles that transfer not only protein factors, but also regulatory miRNAs to recipient cells [106]. One of the most important properties of MSCs is their ability to stimulate the angiogenic behavior of endothelial cells (ECs) both through paracrine effects and through direct contacts in the vascular cell niche [107, 108]. In most tissues, MSCs are located in the vascular wall in the peri-endothelial and supra-adventitial compartments [109]. Peri-endothelial MSCs are able, through the basement membrane pores, to interact directly with endothelial cells, regulating their functions through direct contacts and secretory mechanisms. A definite role in this regulation is played by the urokinase system. MSCs isolated from the bone marrow and adipose tissue express and secrete all urokinase system components: uPA, uPAR, and PAI-1 [110, 111]. However, depending on the tissue origin of MSCs, their role in ECM remodeling during vascularization is different. A number of studies, including ours, have demonstrated that bone marrow and adipose tissue MSCs co-cultured with endothelial cells stimulate them to form tubular structures [111, 112], through different proteolytic systems. Bone marrow MSCs remodel the matrix through membrane-bound metalloproteinases during angiogenesis, and adipose tissue MSCs (AT-MSCs) remodel the matrix through activation of plasminogen by urokinase [111, 112]. Our *in vitro* experiments demonstrated that in the absence of exogenous ECM ECs need direct contact with MSCs to stimulate the formation of vascular structures. We also found a significant increase in the expression of the urokinase receptor on the surface of ECs co-cultured with AT-MSCs. The latter was found to be crucial for MSC-stimulated angiogenesis, because uPAR inhibitory antibodies dose-dependently inhibited formation of the capillary structures [111]. Other components of the urokinase system also played a significant role in the regulation of the angiogenic behavior of endothelial cells by mesenchymal stem cells, because inhibitors of urokinase system components (amiloride, LRP antagonist RAP protein) also inhibited MSC-stimulated angiogenesis [113]. These results suggest that in the vascular cell niche of adipose tissue the urokinase system plays an important role in the regulation of the angiogenic behavior of endothelial cells AT-MSCs. In addition, an important role in the formation of the vascular network, especially during its stabilization, is played by pericytes that are considered as vascular MSCs [114]. The urokinase system regulates directional migration of vascular mural cells [115, 116] and MSCs. In model *in vitro* experiments, uPA enhanced spontaneous migration of MSCs through induction of secretion of matrix metalloproteinase 9 by MSCs, and also mediated migration in response to PDGF-BB, because blockade of the interaction between uPA and uPAR antibodies completely inhibited PDGF-BB-induced MSC migration [117]. In addition, the uPA/uPAR system is absolutely necessary for intracellular signaling triggered by PDGF-AB to induce bone marrow and adipose tissue MSC migration [118], which indicates the important role of this system in the regulation of the directional

movement of MSCs necessary for their participation both in vessel growth and in other physiological and pathological processes [109]. Another important effect of urokinase system activation is regulation of MSC differentiation. Intracellular signals from uPAR were shown to regulate adipogenic differentiation of MSC [119] through PI3K/Akt pathway activation, and their osteogenic differentiation [120] through the NF-kB-mediated mechanisms.

An important mechanism that regulates the properties of cells in tissue niches is their interaction with extracellular matrix proteins. Synthesizing and remodeling the matrix through proteolytic mechanisms, MSCs are able to regulate cell functions in the tissue niche and their own functions. These effects are explained by a change in the matrix density due to matrix remodeling by MSCs, which is important in determining the direction of differentiation [121]. It may be supposed that by remodeling the extracellular matrix in tissue niches, MSCs can regulate the differentiation properties of resident stem cells and that this regulation is mediated by signals that affect urokinase receptor expression in MSCs [73]. In addition, MSCs secrete urokinase that triggers a proteolytic cascade on the cell surface, which promotes the release of growth factors sequestered in the matrix surrounding cells and contributing to the regulation of the functions of both MSCs and other cells of the microenvironment. Therefore, the urokinase system is involved, through different mechanisms, in the regulation of the functions of MSCs and other cells in tissue cell niches and may be considered as a promising target for effects on these cells.

UROKINASE SYSTEM AND TUMOR STEM CELLS

Studies in recent years have demonstrated that a population of tumor stem cells (TSCs) residing in the tumor tissue are responsible for initiation, spread (metastasis), and recurrence of tumors. TSCs were first found in the bone marrow in acute myeloid leukemia [122] and later in most solid malignant tumors of the ovaries [123], prostate [124], pancreas [125], large intestine [126], brain [127], etc. TSCs possess the main features of stem cells: resistance to radiotherapy and chemotherapy, the ability to quickly form the main populations of tumor cells and restore the cellular microenvironment, even after treatment. The role of the urokinase system in the development and metastasis of tumors has been explored for several decades, but there are only a few studies on tumor stem cells. According to the available data, the urokinase system may be considered as an important regulator of the state and development of TSCs. For example, plasmid overexpression of uPAR in human breast cancer MCF-7 and MDA-MB-468 cell lines caused the formation of TSCs with a characteristic immunophenotype $CD24^{low}/CD44^{high}$ and containing stem phenotype markers – integrin β1/CD29 and α6/CD49f [128]. A suspension of these cells transplanted into adipose tissue of the mammary gland of immunodeficient SCID mice resulted in pronounced integration of the graft into the tissues of the recipient animal and promoted a higher rate of primary tumor foci with a larger size than upon transplantation of cells transfected with control "empty" plasmids [128]. This indicates involvement of uPAR in the formation of the stem phenotype of tumor cells. Another mechanism for the regulation of TSC plasticity, which involves uPAR, is activation of the epithelial-mesenchymal transition (EMT). The results of numerous studies have confirmed that triggering of the EMT program in epithelial TSCs facilitates the mesenchymal phenotype in TSCs and increased expression of the stem phenotype markers contributing to the initiation of tumor development and metastasis [129–131]. Under hypoxic conditions, uPAR contributes to the initiation of EMT in a culture of human breast cancer MDA-MB-468 cells with an epithelial phenotype due to activation of different signaling mechanisms, including ERK1/2, PI3K/Akt, Src, and Rac1 [132, 133] . Preservation of the acquired mesenchymal phenotype of TSCs requires a high level of uPAR expression and is completely reversible upon suppression of uPAR expression, inhibition of the uPA–uPAR interaction, and blockade of PI3K, Src, and ERK1/2 signaling [132, 133]. Formed TSCs expressing uPAR can occur in tissues at rest (in the G0/G1 phase) for a long time, and proliferation/growth of the dormant tumor can happen after many years. Another mechanism for the involvement of the urokinase system in the development of tumors is direct or plasmin-mediated activation of mitogens. For example, urokinase activates HGF that is secreted by fibroblasts as a single-chain biologically inactive precursor and accumulates in the extracellular matrix. Cleavage of HGF by urokinase produces an active protein heterodimer [134] that is a mitogen activating the proliferation of many cells, including TSCs. Other pro-mitogenic factors released from the matrix and activated by urokinase are FGF-2, VEGF189, IGF-1, and TGF-β [135–138]. The activity of uPA/uPAR in TSCs is regulated by plasminogen activator inhibitors – PAI-1/PAI-2 [139, 140]. However, their effect on TSCs is associated not only with the ability to inhibit the urokinase activity, but also with the ability to interact with vitronectin responsible for keeping cells in tumor niches. Vitronectin-bound PAI-1 reduces the interaction of vitronectin with integrins on the

surface of TSCs and, thereby, promotes the release of TSCs from tumor niches, regulating their adhesion and migration.

Several years ago, we found a fundamentally new signaling pathway by which urokinase regulates acquisition of the stem phenotype by tumor cells and their resistance to cytotoxic agents. In particular, we demonstrated for the first time that urokinase is transported to the nucleus [28], where it binds to the transcription factors (HOXA5, HHEX, Lhx-2) involved in the regulation of the stem phenotype and survival of tumor [141] and endothelial [28] cells. Using fluorescent immunohistochemistry, we identified the localization of urokinase in the nuclei of tumor cells and in endothelial cells associated with the tumor [142]. The mechanism of uPA transport to the nucleus has not been fully studied, but we have demonstrated that the kringle domain of urokinase is necessary for the transport of urokinase to the nucleus, and we have also identified the nucleolin protein (Nuc1) that, binding to the kringle domain, is involved in the transport of urokinase to the nucleus [28]. Nucleolin, despite its preferential localization in the nucleus and nucleoli, is able to circulate between the cell membrane, cytoplasm, and nucleus and bind to different classes of proteins. In particular, it is involved in the transport of several secreted proteins, such as FGF-1, FGF-2, midkine, and laminin [143]. Nucleolin is recognized as one of the promising targets for anticancer therapy [144], and inhibition of urokinase transport into the nucleus may be one of the mechanisms of this effect [28]. Our data indicate that the urokinase receptor inhibits urokinase transport to the nucleus, retaining urokinase on the cell surface (V. Stepanova, unpublished data). We suppose that in tumor stem cells, where the urokinase level is significantly increased [142], urokinase is transported mainly to the nucleus, which is facilitated by removal of the first domain or the full-length urokinase receptor from the surface of tumor cells by proteases or shedding of the full-length uPAR by PI-PLC [47–52].

Further studies should provide answers to the following questions: 1) what form of the urokinase receptor (full-length or cleaved between the first and second domains) prevails on the surface of tumor cells that have a predominantly stem phenotype; 2) whether the rate of urokinase receptor removal from the surface of TSCs is increased; 3) whether the cells that have a predominantly stem phenotype have increased nuclear acummulation of uPA? These studies, in our opinion, will expand our understanding of the role of the urokinase system in the regulation of tumor stem cell functioning and define targets and ways to reduce their resistance and induce apoptosis.

THE ROLE OF FIBRINOLYTIC SYSTEM COMPONENTS IN REGULATION OF HEART STEM/PROGENITOR CELL FUNCTIONS

The role of urokinase in the regulation of heart stem/progenitor cell functions has been studied only in the most recent years. This system, as in tumor stem cells, was shown to be capable of controlling the epithelial–mesenchymal transition [145, 146] that produces the multipotent epicardial progenitor cells that represent some of the subtypes of the resident heart progenitor cells involved in regenerative processes through differentiation into blood vessel and myocardial cells and paracrine secretion of growth factors, cytokines, and exosomes [147–150]. There are only a few publications devoted to the role of the urokinase system in the reparative processes in the myocardium. Earlier, we demonstrated that urokinase expression significantly increased immediately after simulation of myocardial infarction in rats, but after a few days, it dropped below the baseline level in an unaffected myocardium (unpublished data). This suggested that an increase in urokinase expression in the heart following myocardial infarction may stimulate reparative processes through activation of growth factors. To test this suggestion, we used plasmid expression of urokinase in the peri-infarction area of the rat's heart, which promoted significant stimulation of the reparative/regenerative processes in the heart: neovascularization and a decrease in the size of infarction and post-infarction fibrosis [151]. These results indirectly indicate the involvement of urokinase in heart recovery after myocardial infarction; however, the mechanisms of this involvement have not yet been identified.

The main trigger initiating post-infarction remodeling is known to be death of cardiomyocytes, which is accompanied by the development of an aseptic inflammatory reaction, redistribution of extracellular matrix proteins, and recruitment of stem/progenitor cells to the damaged area. Along with other components of the extracellular matrix, vitronectin is involved in this process. However, unlike most of these proteins synthesized by heart cells, vitronectin is formed mainly in the liver, where from it enters gets into the systemic circulation and then accumulates in the damaged area. We demonstrated that vitronectin was almost completely absent in the intact myocardium, but its level increased significantly after the experimental myocardial infarction, and the dynamics of its accumulation correlated with accumulation of heart progenitor cells (HPCs) in the infarction and peri-infarction areas. Earlier, using immunohistochemical staining, we showed that the urokinase receptor was present on the surface of HPCs in the myocardium; the receptor remained during cultiva-

tion of HPCs *in vitro* and was able to specifically bind vitronectin [152, 153]. Furthermore, HPCs isolated from the myocardium of *uPAR* knockout mice much poorly adhered to vitronectin than HPCs derived from the heart of wild-type mice ($HPCs^{WT}$). In addition, inhibition of the urokinase receptor by specific antibodies on the surface of $HPCs^{WT}$ led to a decrease in the ability of cells to adhere and spread on the vitronectin matrix [152]. Therefore, we suggested that uPAR may act as a regulator of the adhesive properties of HPCs, which may become a determining factor in their accumulation and integration within the damaged area. The interaction between uPAR and vitronectin can be either independent of integrins or be due to the activation of various integrins [154], thereby modulating the choice of the matrix for interaction [155–157]. Elucidating the role of uPAR and other components of the urokinase system in the regulation of the epithelial-mesenchymal transition of epicardial cells and the mechanisms of their participation in the regulation of the interaction of HPCs with various extracellular matrix proteins, their migration, and proliferative and differentiating properties is the object of our further research.

CONCLUSION

The stem cells of an adult organism exist in a set microenvironment, the so-called cell niches, that controls their ability to self-renew and the level of proliferation and differentiation. In niches, stem cells occur in close connection with committed progenitor cells, stromal cells, and extracellular matrix proteins the interaction with which regulates maintenance of the resting state, optimal metabolic profile, and low differentiated state, as well as processes of differentiation and release of stem cells from the niche after reception of an appropriate stimulus. Numerous studies suggest that the urokinase system coordinates specific signals from the components of the extracellular matrix and surrounding cells (*Fig. 3*). Its main components (uPAR and uPA) are abundant in the cells that form tissue cell niches, including stem cells and microenvironment cells, and their suppression in most cases leads to decreased proliferation, transition of stem cells to the resting state, induction of apoptosis, and inhibition of invasion, migration, and differentiation. Inhibitors of plasminogen activators regulate the functions of stem/progenitor cells by limiting extracellular proteolysis to ensure specialized functions for progenitor cells, as well as maintaining the competitive interaction of vitronectin with integrins and uPAR and recirculation of uPAR on the cell surface. The influence of urokinase system components on stem cell functions is associated with both differential regulation of the activity of a big variety of signaling molecules (*Fig. 4*) and direct action of urokinase in the nucleus, which may induce a unique program of stem cell self-maintenance or, conversely, lead to reduced adhesion, escape of cells from the niche, and activation of their migration to the damaged area (*Fig.*

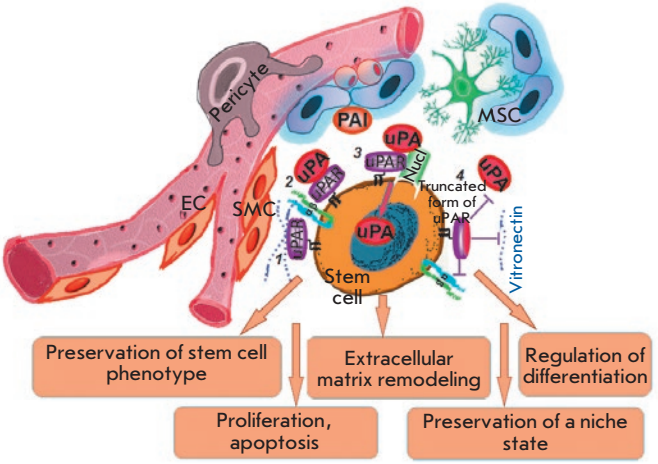

Fig. 3. The urokinase system modulates the state of stem cells in cell niches. The interaction between urokinase and the urokinase receptor promotes localization of the proteolytic activity on the cell surface, which, in turn, leads to the extracellular matrix remodeling necessary for maintaining the microenvironment of the cell niche. In addition to active participation in proteolysis, the urokinase–receptor complex (*1, 2*) interacts with vitronectin, an important extracellular matrix protein, and is able to co-localize with integrins, growth factor receptors, and other molecules inside the signaling complex, which leads to activation of intracellular signaling and, as a result, to preservation of the stem cell phenotype, as well as to regulation of proliferation/apoptosis and differentiation. Urokinase proteolytic activity is regulated by inhibitors of plasminogen activators, PAI-1 and PAI-2. With participation of nucleolin, urokinase can be transported into the nucleus (*3*), which can lead to activation of a unique self-sustaining program or, conversely, to reduced adhesion, escape of cells from the niche, and migration to the damaged area. The urokinase receptor can be proteolytically cleaved by various molecules (*4*), which inhibits its ability to bind ligands (uPA and vitronectin), interact with integrins, and activate the appropriate signaling mechanisms. SMC is a smooth muscle cell

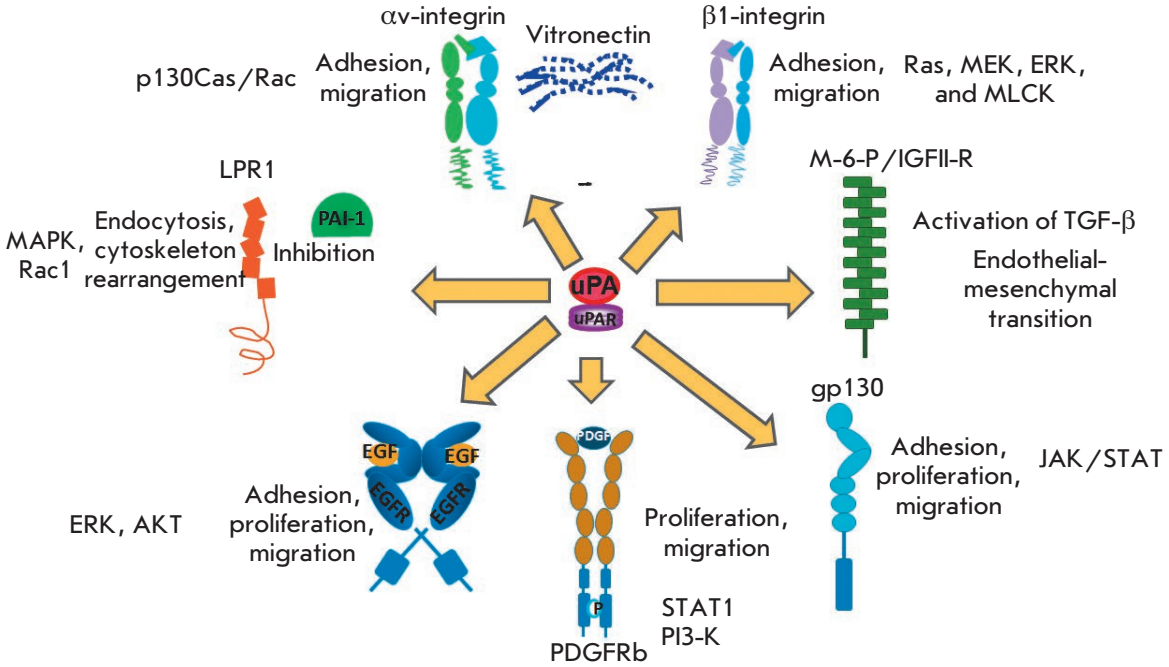

Fig. 4. Main signaling molecules involved in urokinase system activity

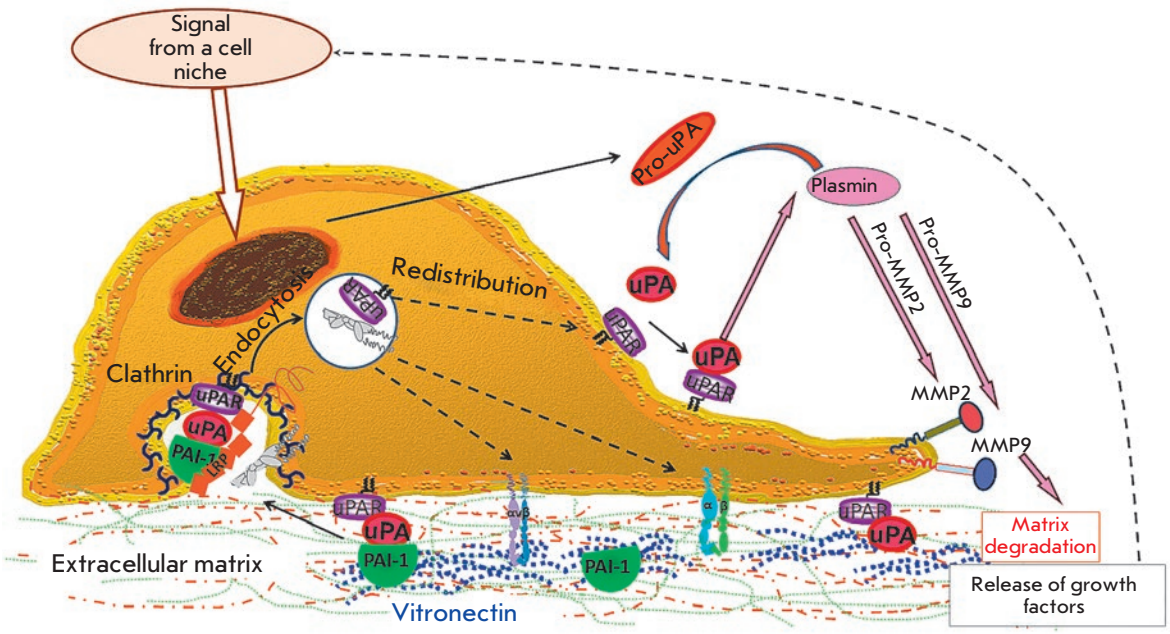

Fig. 5. Involvement of the urokinase system in the regulation of stem/progenitor cell migration. Specific signals arising in the cell niche promote the formation of a promigratory phenotype of the stem/progenitor cell and an increase in the production of urokinase, its receptor, and other factors necessary for cell migration. Urokinase activates a proteolytic cascade involving plasminogen and matrix metalloproteinases (MMPs). This leads to cleavage of the extracellular matrix and release of latent growth factors and PAI-1. PAI-1 inactivates urokinase, and a newly formed complex acquires high affinity for LRP-1 that mediates clathrin-dependent endocytosis. This triggers intracellular signaling, cytoskeleton rearrangement, and redistribution of the urokinase receptor at the leading edge of the cell, which promotes directional migration

5). The main role in this process is apparently played by the urokinase receptor that represents a part of a large signaling complex consisting of a variety of proteins, both outside and inside the cell, which triggers intracellular signaling. One can suggest that the uPAR composition and its interaction with various partners represents an evolutionarily conservative key that determines the molecular features and retention of stem cells in the cell niche. To this end, uPAR functions are modulated by proteolytic cleavage, which leads to the formation of truncated membrane-bound forms of uPAR (c-uPAR), as well as soluble forms of the urokinase receptor (su-uPAR). c-uPAR lacking the D1 domain cannot bind ligands (uPA and vitronectin), interact with integrins, and activate the appropriate signaling mechanisms. In addition, the soluble form su-uPAR can compete with the membrane-bound form uPAR for binding to ligands, thereby limiting signal transduction into the cell, extracellular proteolysis, and adhesion. This highly controlled system which regulates location and functions of stem cells in cell niches opens up new opportunities for the development of approaches to specifically regulate their differentiation and other functions. Elucidation of the mechanisms maintaining the balance of proliferation/apoptosis, migration, and differentiation of the stem cells controlled by urokinase system components is an important biological and medical problem that should be resolved as soon as possible. Targeting the uPA/PAI/uPAR system alone or in combination with other signaling pathways may hold promise in improving the therapeutic potential of stem/progenitor cells or helping eliminate tumor stem cells during treatment of cancer diseases. ●

This work was supported by the Russian Science Foundation (grant No. 17-15-01368) and Russian Foundation for Basic Research (grant No. 18-015-00430) (participation of MSCs in formation of cell niches and regulation of their properties by urokinase system components).

REFERENCES

1. Tay J., Levesque J.P., Winkler I.G. // Internat. J. Hematol. 2017. V. 105. № 2. P. 129–140.
2. Dergilev K.V., Rubina K.A., Parfenova E.V. // Kardiologiia. 2011. V. 51. № 4. P. 84–92.
3. Méndez-Ferrer S., Michurina T.V., Ferraro F., Mazloom A.R., MacArthur B.D., Lira S.A., Scadden D.T., Ma'ayan A., Enikolopov G.N., Frenette P.S. // Nature. 2010. V. 466 № 7308. P. 829–834.
4. Stepanova V.V., Tkachuk V.A. // Biochemistry (Moscow). 2002. V. 67. № 1. P. 109–118.
5. Parfenova E.V., Plekhanova V.V., Stepanova V.V., Men'shikov M.I., Tsokaleva Z.I., Talitskiĭ K.A., Rakhmatzade T.M., Traktuev D.O., Torosian N.A., Rogunova N.I., et al. // Ross. Fiziol. Zh. Im. I.M. Sechenova. 2004. V. 90. № 5. P. 547–568.
6. Blasi F. // Bioessays. 1993. V. 15. № 2. P. 105–111.
7. Tkachuk V.A., Stepanova V.V., Volynskaia E.A. // Vestn. Ross. Akad. Med. Nauk. 1998. V. 8. P. 36–41.
8. Heissig B., Lund L.R., Akiyama H., Ohki M., Morita Y., Rømer J., Nakauchi H., Okumura K., Ogawa H., Werb Z. // Cell Stem Cell. 2007. V. 1. № 6. P. 658–670.
9. Philippou A., Maridaki M., Koutsilieris M. // In Vivo. 2008. V. 22. № 6. P. 735–750.
10. Gutova M., Najbauer J., Frank R.T., Kendall S.E., Gevorgyan A., Metz M.Z., Guevorkian M., Edmiston M., Zhao D., Glackin C.A., et al. // Cell Stem Cells. 2008 V. 26. № 6. P. 1406–1413.
11. Breznik B., Motaln H., Lah Turnšek T. // J. Biol. Chem. 2017. V. 398. № 7. P. 709–719.
12. Saksela O., Hovi T., Vaheri A. // J. Cell. Physiol. 1985. V. 122. № 1. P. 125–132.
13. Arefi'eva T.I., Mukhina S.A., Poliakov A.A., Stepanova V.V., Minashkin M.M., Gurskiĭ Ia.G., Domogatskiĭ S.P., Krasnikova T.L. // Ross. Fiziol. Zh. Im. I.M. Sechenova. 1998. V. 84. № 12. P. 1432–1437.
14. Stump D.C., Thienpont M., Collen D. // J. Biol. Chem. 1986. V. 261. № 27. P. 12759–12766.
15. Stepanova V., Dergilev K.V., Holman K.R., Parfyonova Y.V., Tsokolaeva Z.I., Teter M., Atochina-Vasserman E.N., Volgina A., Zaitsev S.V., Lewis S.P., et al. // J. Biol. Chem. 2017. V. 292. № 50. P. 20528–20543.
16. Asuthkar S., Stepanova V., Lebedeva T., Holterman A.L., Estes N., Cines D.B., Rao J.S., Gondi C.S. // Mol. Biol. Cell. 2013. V. 24. № 17. P. 2620–2632.
17. Eaton D.L., Scott R.W., Baker J.B. // J. Biol. Chem. 1984. V. 259. № 10. P. 6241–6247.
18. Plekhanova O.S., Stepanova V.V., Ratner E.I., Bobik A., Tkachuk V.A., Parfyonova Y.V. // J. Vasc. Res. 2006. V. 43. № 5. P. 437–446.

19. Clowes A.W., Clowes M.M., Au Y.P., Reidy M.A., Belin D. // Circ. Res. 1990. V. 67. № 1. P. 61–67.
20. Goncharova E.A., Vorotnikov A.V., Gracheva E.O., Wang C.L., Panettieri R.A. Jr, Stepanova V.V., Tkachuk V.A. // Biol. Chem. 2002. V. 383. № 1. P. 115–126.
21. Pepper M.S., Vassalli J.D., Montesano R., Orci L. // J. Cell Biol. 1987. V. 105. № 1. 2535–2541.
22. Parfenova E.V., Plekhanova O.S., Men'shikov M.Iu., Stepanova V.V., Tkachuk V.A. // Ross. Fiziol. Zh. Im. I.M. Sechenova. 2009. V. 95. № 5. P. 442–464.
23. Günzler W.A., Steffens G.J., Otting F., Buse G., Flohé L. // Hoppe-Seyler's Zeitschrift Fur Physiol. Chemie. 1982. V. 363. № 2. P. 133–141.
24. Apella E., Robinson E.A., Ullrich S.J., Stoppelli M.P., Corti A., Cassani G., Blasi F. // J. Biol. Chem. 1987. V. 262. № 10. P. 4437–4440.
25. Blasi F., Sidenius N. // FEBS Lett. 2010. V. 584. № 9. P. 1923–1930.
26. Mukhina S., Stepanova V., Traktouev D., Poliakov A., Beabealashvilly R., Gursky Y., Minashkin M., Shevelev A., Tkachuk V. // J. Biol. Chem. 2000. V. 275. № 22. P. 16450–16458.
27. Bdeir K., Kuo A., Sachais B.S., Rux A.H., Bdeir Y., Mazar A., Higazi A.A., Cines D.B. // Blood. 2003. V. 102. № 10. P. 3600–3608.
28. Stepanova V., Lebedeva T., Kuo A., Yarovoi S., Tkachuk S., Zaitsev S., Bdeir K., Dumler I., Marks M.S., Parfyonova Y., et al. // Blood. 2008. V. 112. № 1. P. 100–110.
29. Vassalli J.D., Baccino D., Belin D. // J. Cell Biol. 1985. V. 100. № 1. P. 86–92.
30. Barnathan E.S., Kuo A., Kariko K., Rosenfeld L., Murray S.C., Behrendt N., Ronne E., Weiner D., Henkin J., Cines D.B. // Blood. 1990. V. 76. № 9. P. 1795–1806.
31. Cao D., Mizukami I.F., Garni-Wagner B.A., Kindzelskii A.L., Todd R.F. 3rd, Boxer L.A., Petty H.R. // J. Immunol. 1995. V. 154. № 4. P. 1817–1829.
32. Okada S.S., Tomaszewski J.E., Barnathan E.S. // Exp. Cell Res. 1995. V. 217. № 3. P. 180–187.
33. Zini J.M., Murray S.C., Graham C.H., Lala P.K., Kariko K., Barnathan E.S., Mazar A., Henkin J., Cines D.B., McCrae K.R. // Blood. 1992. V. 79. № 11. P. 2917–2929.
34. Cubellis M.V., Nolli M.L., Cassani G., Blasi F. // J. Biol. Chem. 1986. V. 261. № 34. P. 15819–15822.
35. Estreicher A., Wohlwend A., Belin D., Schleuning W.D., Vassalli J.D. // J. Biol. Chem. 1989. V. 264. № 2. P. 1180–1189.
36. Stoppelli M.P., Corti A., Soffientini A., Cassani G., Blasi F., Assoian R.K. // Proc. Natl. Acad. Sci. USA. 1985. V. 82. № 15. P. 4939–4943.
37. Hoyer-Hansen G., Ronne E., Solberg H., Behrendt N., Ploug M., Lund L.R., Ellis V., Danø K. // J. Biol. Chem. 1992. V. 267. № 25. P. 18224–18229.
38. Danø K., Behrendt N., Brunner N., Ellis V., Ploug M., Pyke C. // Fibrinolysis. 1994. V. 8. P. 189–203.
39. Todd R.F. 3rd, Mizukami I.F., Vinjamuri S.D., Trochelman R.D., Hancock W.W., Liu D.Y. // Blood Cells. 1990. V. 16. № 1. P. 167–179.
40. Wang Y., Dang J., Johnson L.K., Selhamer J.J., Doe W.F. // Eur. J. Biochem. 1995. V. 227. № 1–2. P. 116–122.
41. Roldan A.L., Cubellis M.V., Masucci M.T., Behrendt N., Lund L.R., Danø K., Appella E., Blasi F. // EMBO J. 1990. V. 9. № 2. P. 467–474.
42. Ploug M., Rønne E., Behrendt N., Jensen A.L., Blasi F., Danø K. // J. Biol. Chem. 1991. V. 266. № 3. P. 1926–1933.
43. Behrendt N., Ronne E., Ploug M., Petri T., Lober D., Nielsen L.S. // J. Biol. Chem. 1990. V. 265. № 11. P. 6453–6460.
44. Montuori N., Visconte V., Rossi G., Ragno P. // Thromb. Haemost. 2005. V. 93. P. 192–198.
45. Leduc D., Beaufort N., de Bentzmann S., Rousselle J.C., Namane A., Chignard M., Pidard D. // Infect. Immun. 2007. V. 75. P. 3848–3858.
46. Resnati M., Guttinger M., Valcamonica S., Sidenius N., Blasi F., Fazioli F. // EMBO J. 1996. V. 15. P. 1572–1582.
47. Høyer-Hansen G., Rønne E., Solberg H., Behrendt N., Ploug M., Lund L.R., Ellis V., Danø K. // J. Biol. Chem. 1992. V. 267. P. 18224–18229.
48. Beaufort N., Leduc D., Rousselle J.C., Magdolen V., Luther T., Namane A., Chignard M., Pidard D. // J. Immunol. 2004. V. 172. P. 540–549.
49. Montuori N., Rossi G., Ragno P. // FEBS Lett. 1999. V. 460. P. 32–36.
50. Andolfo A., English W.R., Resnati M., Murphy G., Blasi F., Sidenius N. // Thromb. Haemost. 2002. V. 88. P. 298–306.
51. Ragno P., Montuori N., Covelli B., Hoyer-Hansen G., Rossi G. // Cancer Res. 1998. V. 58. № 6. P. 1315–1319.
52. Mustjoki S., Sidenius N., Sier C.F., Blasi F., Elonen E., Alitalo R., Vaheri A. // Cancer Res. 2000. V. 60. P. 7126–7132.
53. Montuori N., Bifulco K., Carriero M.V., La Penna C., Visconte V., Alfano D., Pesapane A., Rossi F.W., Salzano S., Rossi G., Ragno P. // Cell Mol. Life Sci. 2011. V. 68. № 14. P. 2453–2467.
54. Barinka C., Parry G., Callahan J., Shaw D.E., Kuo A., Bdeir K., Cines D.B., Mazar A. Lubkowski J. // J. Mol. Biol. 2006. V. 363. № 2. P. 482–495.
55. Manchanda N., Schwartz B.S. // J. Biol. Chem. 1995. V. 270. № 34. P. 20032–20035.
56. Reinartz J., Schaefer B., Bechtel M.J., Kramer M.D. // Exp. Cell Res. 1996. V. 223. № 1. P. 91–101.
57. Baker J.B., Low D.A., Simmer R.L., Cunningham D.D. // Cell. 1980. V. 21. № 1. P. 37–45.
58. Geiger M., Huber K., Wojta J., Stingl L., Espana F., Griffin J.H., Binder B.R. // Blood. 1989. V. 74. № 2. P. 722–728.
59. Potempa J., Korzus E., Travis J. // J. Biol. Chem. 1994. V. 269. № 3. P. 15957–15960.
60. Ehrlich H.J., Keijer J., Preissner K.T., Gebbink R.K., Pannekoek H. // Biochemistry. 1991. V. 30. № 4. P. 1021–1028.
61. Deng G., Royle G., Seiffert D., Loskutoff D.J. // Thromb. Haemost. 1995. V. 74. № 1. P. 66–70.
62. Cubellis M.V., Nolli M.L., Cassani G., Blasi F. // J. Biol. Chem. 1986. V. 261. № 34. P. 15819–15822.
63. Ellis V., Wun T.C., Behrendt N., Ronne E., Dano K. // J. Biol. Chem. 1990. V. 265. № 17. P. 9904–9908.
64. Laiho M., Saksela O., Keski-Oja J. // J. Biol. Chem. 1987. V. 262. № 36. P. 17467–17474.

65. Planus E., Barlovatz-Meimon G., Rogers R.A., Bonavaud S., Ingber D.E., Wang N. // J. Cell Sci. 1997. V. 110. № 9. P. 1091–1098.
66. Nykjaer A., Conese M., Christensen E.I., Olson D., Cremona O., Gliemann J., Blasi F. // EMBO J. 1997. V. 16. № 10. P. 2610–2620.
67. Antalis T.M., Clark M.A., Barnes T., Lehrbach P.R., Devine P.L., Schevzov G., Goss N.H., Stephens R.W., Tolstoshev P. // Proc. Natl. Acad. Sci. USA. 1988. V. 85. № 4. P. 985–989.
68. Kruithof E.K., Baker M.S., Bunn C.L. // Blood. 1995. V. 86. № 11. P. 4007–4024.
69. Kumar S., Baglioni C. // J. Biol. Chem. 1991. V. 266. № 31. P. 20960–20964.
70. Dickinson J.L., Bates E.J., Ferrante A., Antalis T.M. // J. Biol. Chem. 1995. V. 270. № 46. P. 27894–27904.
71. Antalis T.M., La Linn M., Donnan K., Mateo L., Gardner J., Dickinson J.L., Buttigieg K., Suhrbier A. // J. Exp. Med. 1998. V. 187. № 11. P. 1799–1811.
72. Taichman R.S., Emerson S.G. // J. Exp. Med. 1994. V. 179. № 5. P. 1677–1682.
73. Gao X., Xu C., Asada N., Frenette P.S. // Development. 2018. V. 145. № 2. P. 1391–1432.
74. Tjwa M., Sidenius N., Moura R., Jansen S., Theunissen K., Andolfo A., De Mol M., Dewerchin M., Moons L., Blasi F., et al // J. Clin. Invest. 2009. V. 119. № 4. P. 1008–1018.
75. Selleri C., Montuori N., Salvati A., Serio B., Pesapane A., Ricci P., Gorrasi A., Li Santi A., Hoyer-Hansen G., Ragno P. // Oncotarget. 2016. V. 7. № 37. P. 60206–60217.
76. Theien B.E., Vanderlugt C.L., Nickerson-Nutter C., Cornebise M., Scott D.M., Perper S.J., Whalley E.T., Miller S.D. // Blood. 2003. V. 102. № 13. P. 4464–4471.
77. Wright N., Hidalgo A., Rodríguez-Frade J.M., Soriano S.F., Mellado M., Parmo-Cabañas M., Briskin M.J., Teixidó J. // J. Immunol: Official J. Am. Assoc. Immunol. 2002. V. 168. № 10. P. 5268–5277.
78. Sidenius N., Blasi F. // FEBS Lett. 2000. V. 470. № 1. P. 40–46.
79. Blasi F., Carmeliet P. // Nat. Rev. Mol. Cell Biol. 2002. V. 3. № 12. P. 932–943.
80. Tarui T., Mazar A.P., Cines D.B., Takada Y. // J. Biol. Chem. 2001. V. 276. № 6. P. 3983–3990.
81. Montuori N., Ragno P. // Front. Biosci. 2009. V. 14. P. 2494–2503.
82. Selleri C., Montuori N., Ricci P., Visconte V., Baiano A., Carriero M.V., Rotoli B., Rossi G., Ragno P. // Cancer Res. 2006. V. 66. P. 10885–10890.
83. Montuori N., Carriero M.V., Salzano S., Rossi G., Ragno P. // J. Biol. Chem. 2002. V. 277. № 49. P. 46932–46939.
84. Lu W., Li X. // Cell. Mol. Life Sc.: CMLS. 2018. V. 75. № 5. P. 859–869.
85. Tkachuk V.A., Plekhanova O.S., Parfyonova Y.V. // Can. J. Physiol. Pharmacol. 2009. V. 87. № 4. P. 231–251.
86. Kapustin A., Stepanova V., Aniol N., Cines D.B., Poliakov A., Yarovoi S., Lebedeva T., Wait R., Ryzhakov G., Parfyonova Y., et al. // Biochem. J. 2012. V. 443. № 2. P. 491–503.
87. Stepanova V., Jayaraman P.S., Zaitsev S.V., Lebedeva T., Bdeir K., Kershaw R., Holman K.R., Parfyonova Y.V., Semina E.V., Beloglazova I.B., Tkachuk V.A., Cines D.B. // J. Biol. Chem. 2016. V. 291. № 29. P. 15029–15045.
88. Loscalzo J. // Semin. Thromb. Hemost. 1996. V. 22. № 6. P. 503–506.
89. Binder B.R., Mihaly J., Prager G.W. // Thromb. Haemost. 2007. V. 97. № 3. P. 336–342.
90. Basire A., Sabatier F., Ravet S., Lamy E., Mialhe A., Zabouo G., Paul P., Gurewich V., Sampol J., Dignat-George F. // Thromb. Haemost. 2006. V. 95. № 4. P. 678–688.
91. Margheri F., Chillà A., Laurenzana A., Serratì S., Mazzanti B., Saccardi R., Santosuosso M., Danza G., Sturli N., Rosati F., et al. // Blood. 2011. V. 118. № 13. P. 3743–3755.
92. Burgermeister E., Liscovitch M., Röcken C., Schmid R.M., Ebert M.P. // Cancer Lett. 2008. V. 268. № 2. P. 187–201.
93. Basire A., Sabatier F., Ravet S., Lamy E., Mialhe A., Zabouo G., Paul P., Gurewich V., Sampol J., Dignat-George F. // Thromb. Haemost. 2006. V. 95. № 4. P. 678–688.
94. van Beem R.T., Verloop R.E., Kleijer M., Noort W.A., Loof N., Koolwijk P., van der Schoot C.E., van Hinsbergh V.W., Zwaginga J.J. // J. Thromb. Haemost.: JTH. 2009. V. 7. № 1. P. 217–226.
95. Li W.D., Hu N., Lei F.R., Wei S., Rong J.J., Zhuang H., Li X.Q. // Biochem. Biophys. Res. Commun. 2015. V. 466. № 3. P. 376–380.
96. Mauro A. // J. Biophys. Biochem. Cytol. 1961. V. 9. P. 493–495.
97. Baghdadi M.B., Tajbakhsh S. // Dev. Biol. 2018. V. 433. № 2. P. 200–209.
98. Guthridge M., Wilson M., Cowling J., Bertolini J., Hearn M.T. // Growth Factors. 1992. V. 6. № 1. P. 53–63.
99. Fibbi G., Barletta E., Dini G., Del Rosso A., Pucci M., Cerletti M., Del Rosso M. // Lab. Invest.; J. Tech. Meth. Pathol. 2001. V. 81. № 1. P. 27–39.
100. Wells J.M., Strickland S. // J. Cell. Physiol. 1997. V. 171. № 2. P. 217–225.
101. Lluís F., Roma J., Suelves M., Parra M., Aniorte G., Gallardo E., Illa I., Rodríguez L., Hughes S.M., Carmeliet P., et al. // Blood. 2001. V. 97. № 6. P. 1703–1711.
102. Fibbi G., D'Alessio S., Pucci M., Cerletti M., Del Rosso M. // Biol. Chem. 2002. V. 383. № 1. P. 127–136.
103. Muñoz-Cánoves P., Miralles F., Baiget M., Félez J. // Thromb. Haemost. 1997. V. 77. № 3. P. 526–534.
104. Bonavaud S., Charrière-Bertrand C., Rey C., Leibovitch M.P., Pedersen N., Frisdal E., Planus E., Blasi F., Gherardi R., Barlovatz-Meimon G. // J. Cell Sci. 1997. V. 110. № 9. P. 1083–1089.
105. Ferraro F., Celso C.L., Scadden D. // Adv. Exp. Med. Biol. 2010. V. 695. P. 155–168.
106. Roura S., Gálvez-Montón C., Mirabel C., Vives J., Bayes-Genis A. // Stem Cell Res. Therapy. 2017. V. 8. № 1. P. 238.
107. Sun K., Zhou Z., Ju X., Zhou Y., Lan J., Chen D., Chen H., Liu M., Pang L. // Stem Cell Res. Therapy. 2016. V. 7. № 1. P. 151.
108. Kfoury Y., Scadden D.T. // Cell Stem Cell. 2015. V. 16. № 3. P. 239–253.
109. Gu W., Hong X., Potter C., Qu A., Xu Q. // Microcircula-

tion: Official J. Microcirculatory Soc., Inc. 2017. V. 24. № 1.
110. Chiellini C., Cochet O., Negroni L., Samson M., Poggi M., Ailhaud G., Alessi M.C., Dani C., Amri E.Z. // BMC Mol. Biol. 2008. V. 26. № 9. P. 26.
111. Koptelova N.V., Beloglazova I.B., Zubkova E.S., Sukhareva O.Yu., Dyikanov D.T., Ratner, E.I., Akopyan Zh.A., Shestakova M.V., Parfenova E.V. // Tekhnologii Zhivykh Sistem. 2016. V. 13. № 8. P. 4–13.
112. Ghajar C.M., Kachgal S., Kniazeva E., Mori H., Costes S.V., George S.C., Putnam A.J. // Exp. Cell Res. 2010. V. 316. № 5. P. 813–825.
113. Meirelles Lda.S., Fontes A.M., Covas D.T., Caplan A.I. // Cytokine Growth Factor Rev. 2009. V. 20. № 5. P. 419–427.
114. Plekhanova O.S., Stepanova V.V., Ratner E.I., Bobik A., Tkachuk V.A., Parfyonova Y.V. // J. Vasc. Res. 2006. V. 43. № 5. P. 437–446.
115. Mukhina S., Stepanova V., Traktouev D., Poliakov A., Beabealashvilly R., Gursky Y., Minashkin M., Shevelev A., Tkachuk V. // J. Biol. Chem. 2000. V. 275. № 22. P. 16450–16458.
116. Beloglazova I., Dergilev K., Zubkova E., Ratner E., Molokotina Y., Tsokolaeva Z., Dyikanov D., Parfyonova Y. // FEBS J. 2017. V. 284. № 1. P. 275.
117. Beloglazova I.B., Zubkova E.S., Tsokolaeva Z.I., Stafeev Y.S., Dergilev K.V., Ratner E.I., Shestakova M.V., Sukhareva O.Y., Parfenova E.V., Men'shikov M.Y. // Bull. Exp. Biol. Med. 2016. V. 161. № 6. P. 775–778.
118. Chabot V., Dromard C., Rico A., Langonné A., Gaillard J., Guilloton F., Casteilla L., Sensebé L. // Stem Cell Res. Therapy. 2015. V. 6. P. 188.
119. Kanno Y., Matsuno H., Kawashita E., Okada K., Suga H., Ueshima S., Matsuo O. // Thromb. Haemost. 2010. V. 104. № 6. P. 1124–1132.
120. Kalbasi Anaraki P., Patecki M., Larmann J., Tkachuk S., Jurk K., Haller H., Theilmeier G., Dumler I. // Stem Cells Dev. 2014. V. 23. № 4. P. 352–362.
121. Gilbert P.M., Havenstrite K.L., Magnusson K.E., Sacco A., Leonardi N.A., Kraft P., Nguyen N.K., Thrun S., Lutolf M.P., Blau H.M. // Science. 2010. V. 329. № 5995. P. 1078–1081.
122. Bonnet D., Dick J.E. // Nat. Med. 1997. V. 3. № 7. P. 730–737.
123. Zhang S., Balch C., Chan M.W., Lai H.C., Matei D., Schilder J.M., Yan P.S., Huang T.H., Nephew K.P. // Cancer Res. 2008. V. 68. № 11. P. 4311–4320.
124. Maitland N.J., Collins A.T. // J. Clin. Oncol.: Official J. Am. Soc. Clin. Oncol. 2008. V. 26. № 17. P. 2862–2870.
125. Li C., Heidt D.G., Dalerba P., Burant C.F., Zhang L., Adsay V., Wicha M., Clarke M.F., Simeone D.M. // Cancer Res. 2007. V. 67. № 3. P. 1030–1037.
126. O'Brien C.A., Pollett A., Gallinger S., Dick J.E. // Nature. 2007. V. 445. № 7123. P. 106–110.
127. Singh S.K., Clarke I.D., Terasaki M., Bonn V.E., Hawkins C., Squire J., Dirks P.B. // Cancer Res. 2003. V. 63. № 18. P. 5821–5828.
128. Jo M., Eastman B.M., Webb D.L., Stoletov K., Klemke R., Gonias S.L. // Cancer Res. 2010. V. 70. № 21. P. 8948–8958.
129. Morel A.P., Lièvre M., Thomas C., Hinkal G., Ansieau S., Puisieux A. // PLoS One. 2008. V. 3. № 8. P. e2888.
130. Mani S.A., Guo W., Liao M.J., Eaton E.N., Ayyanan A., Zhou A.Y., Brooks M., Reinhard F., Zhang C.C., Shipitsin M., et al. // Cell. 2008. V. 133. № 4. P. 704–715.
131. Puisieux A., Brabletz T., Caramel J. // Nat. Cell Biol. 2014. V. 16. № 6. P. 488–494.
132. Jo M., Lester R.D., Montel V., Eastman B., Takimoto S., Gonias S.L. // J. Biol. Chem. 2009. V. 284. № 34. P. 22825–22833.
133. Lester R.D., Jo M., Montel V., Takimoto S., Gonias S.L. // J. Cell Biol. 2007. V. 178. № 3. P. 425–436.
134. Naldini L., Tamagnone L., Vigna E., Sachs M., Hartmann G., Birchmeier W., Daikuhara Y., Tsubouchi H., Blasi F., Comoglio P.M. // EMBO J. 1992. V. 11. P. 4825–4833.
135. Duffy M.J. // Curr. Pharmaceut. Design. 2004. V. 10. № 1. P. 39–49.
136. Rifkin DB. // Fibrinol. Proteolysis. 1997. V. 1. № 11. P. 3–9.
137. Plouët J., Moro F., Bertagnolli S., Coldeboeuf N., Mazarguil H., Clamens S., Bayard F. // J. Biol. Chem. 1997. V. 272. № 20. P. 13390–13396.
138. Mars W.M., Zarnegar R., Michalopoulos G.K. // Am. J. Pathol.1993. V. 143. № 3. P. 949–958.
139. Czekay R.P., Aertgeerts K., Curriden S.A., Loskutoff D.J. // J. Cell Biol. 2003. V. 160. № 5. P. 781–791.
140. Cubellis M.V., Wun T.C., Blasi F. // EMBO J. 1990. V. 9. № 4. P. 1079–1085.
141. Asuthkar S., Stepanova V., Lebedeva T., Holterman A.L., Estes N., Cines D.B., Rao J.S., Gondi C.S. // Mol. Biol. Cell. 2013. V. 24. № 17. P. 2620–2632.
142. Stepanova V., Jayaraman P.S., Zaitsev S.V., Lebedeva T., Bdeir K., Kershaw R., Holman K.R., Parfyonova Y.V., Semina E.V., Beloglazova I.B., Tkachuk V.A., Cines D.B. // J. Biol. Chem. 2016. V. 291. № 29. P. 15029–15045.
143. Jia W., Yao Z., Zhao J., Guan Q., Gao L. // Life Sci. 2017. V. 186. P. 1–10.
144. Chen Z., Xu X. // Saudi Med. J. 2016. V. 37. № 12. P. 1312–1318.
145. Blom J.N., Feng Q. // Pharmacol. Ther. 2018. V. 186. P. 114–129.
146. Pavón M.A., Arroyo-Solera I., Céspedes M.V., Casanova I., León X., Mangues R. // Oncotarget. 2016. V. 7. № 35. P. 57351–57366.
147. Dergilev K.V., Rubina K.A., Tsokolaeva Z.I., Sysoeva V.Iu., Gmyzina A.I., Kalinina N.I., Beliavskaia T.M., Akchurin R.S., Parfenova Ye.V., Tkachuk V.A. // Tsitologiia. 2010. V. 52. № 11. P. 921–930.
148. Dergilev K.V., Tsokolaeva Z.I., Rubina K.A., Sysoeva V.Yu., Makarevich P.I., Boldyreva M.A., Beloglazova I.B., Zubkova E.S., Sharonov G.V., Akchurin R.S., Parfyonova Ye.V. // Tsitologiia. 2016. V. 58. № 5. P. 340–348.
149. Dergilev K.V., Rubina K.A., Parfenova E.V. // Kardiologiia. 2011. V. 51. № 4. P. 84–92.
150. Dergilev K.V., Tsokolaeva Z.I., Beloglazova I.B., Zubkova E.S., Boldyreva M.A., Ratner E.I., Dykanov D.T., Menshikov M.Yu., Parfyonova Ye.V. // Genes Cells. 2018. V. 13. № 1.

P. 75–81.
151. Traktuev D.O., Tsokolaeva Z.I., Shevelev A.A., Talitskiy K.A., Stepanova V.V., Johnstone B.H., Rahmat-Zade T.M., Kapustin A.N., Tkachuk V.A., March K.L., Parfyonova Ye.V. // Mol. Ther. 2007. V. 15. № 11. P. 1939–1946.
152. Dergilev K., Tsokolaeva Z., Beloglazova I., Zubkova E., Parfyonova Ye. // FEBS Open Bio. 2018. V. 8. Suppl. S1. P. 156–157.
153. Dergilev K., Tsokolaeva Z., Makarevich P., Beloglazova I., Zubkova E., Boldyreva M., Ratner E., Dyikanov D., Menshikov M., Ovchinnikov A., et al. // Biomed. Res. Int. 2018. V. 18. P. 3536854.
154. Kugler M.C., Wei Y., Chapman H.A. // Curr. Pharm. Des. 2003. V. 9. № 19. P. 1565–1574.
155. Simon D.I., Wei Y., Zhang L., Rao N.K., Xu H., Chen Z., Liu Q., Rosenberg S., Chapman H.A. // J. Biol. Chem. 2000. V. 275. № 14. P. 10228–10234.
156. Wei Y., Lukashev M., Simon D.I., Bodary S.C., Rosenberg S., Doyle M.V., Chapman H.A. // Science. 1996. V. 273. № 5281. P. 1551–1555.
157. Wei Y., Eble J.A., Wang Z., Kreidberg J.A., Chapman H.A. // Mol. Biol. Cell. 2001. V. 12. № 10. P. 2975–2986.

Bacterial Enzymes and Antibiotic Resistance

A. M. Egorov, M. M. Ulyashova, M. Yu. Rubtsova*
Chemistry Faculty, M.V. Lomonosov Moscow State University, Leninskie gori, 1, bldg. 3, Moscow, 119991, Russia
*E-mail: mrubtsova@gmail.com
Received July 28, 2018; in final form August 29, 2018

ABSTRACT **The resistance of microorganisms to antibiotics has been developing for more than 2 billion years and is widely distributed among various representatives of the microbiological world. Bacterial enzymes play a key role in the emergence of resistance. Classification of these enzymes is based on their participation in various biochemical mechanisms: modification of the enzymes that act as antibiotic targets, enzymatic modification of intracellular targets, enzymatic transformation of antibiotics, and the implementation of cellular metabolism reactions. The main mechanisms of resistance development are associated with the evolution of superfamilies of bacterial enzymes due to the variability of the genes encoding them. The collection of all antibiotic resistance genes is known as the resistome. Tens of thousands of enzymes and their mutants that implement various mechanisms of resistance form a new community that is called "the enzystome." Analysis of the structure and functional characteristics of enzymes, which are the targets for different classes of antibiotics, will allow us to develop new strategies for overcoming the resistance.**
KEYWORDS **antibiotic resistance, enzymes, mutant forms, antibiotics.**
ABBREVIATIONS **AMD – antimicrobial drugs; AME – aminoglycoside modifying enzymes; ESBL – extended spectrum β-lactamases; MBL – metallo-β-lactamases; MKLS – macrolides, ketolides, lincosamides and streptogramins; PBP – penicillin-binding proteins; AAC – aminoglycoside-N-acetyltransferases; ANT – aminoglycoside-O-adenylyltransferases; APH – aminoglycoside-O-phosphotransferases; CAT – chloramphenicol acetyltransferase; MPH – macrolide phosphotransferases; NAG – N-acetylglucosamine; NAM – N-acetylmuramic acid; QRDR – quinolone resistance determining region; SAM – S-adenosyl-L-methionine.**

INTRODUCTION

Antibiotic resistance of the causative agents of infectious diseases is a global problem in biology and medicine [1, 2]. Modern antimicrobial drugs (AMDs) represent the largest group of pharmaceutical drugs, including 16 classes of natural and synthetic compounds (*Fig. 1*).

Synthesis of antibiotics has existed in nature for more than 2 billion years. During all this time, bacteria have been developing mechanisms of resistance to their toxic action. Resistance may occur as an adaptive process unrelated to the structure of an antibiotic or develop as a result of the selection of resistant strains of microorganisms under the influence of antibiotics. The anthropogenic factors associated with the application of antibiotics in medicine and, especially, in agriculture since the mid-20th century have led to a significant evolution of resistance mechanisms; the time it takes to develop resistance to new drugs has significantly reduced [3, 4].

The role of bacterial enzymes in resistance development is rather versatile and involves several key mechanisms (*Fig. 2*) [5]. The enzymes involved in cell wall biosynthesis, as well as the synthesis of nucleic acids and metabolites, serve as a direct target for antibiotics. The resistance mechanism is associated with structural changes in these enzymes. Another mechanism is associated with the enzymatic modification of the structural elements affected by antibiotics: for example, modification of ribosomes by methyltransferases. A large group of enzymes modify or destroy the structure of antibiotics by inactivating them. Enzymes catalyzing metabolic processes and modifying AMDs in the form of prodrugs are also involved in resistance development.

The bacterial enzymes that determine resistance usually belong to large superfamilies; many of them originated from enzymes that originally had other functions [6]. The genes responsible for the synthesis of these enzymes and their mutational variability are of-

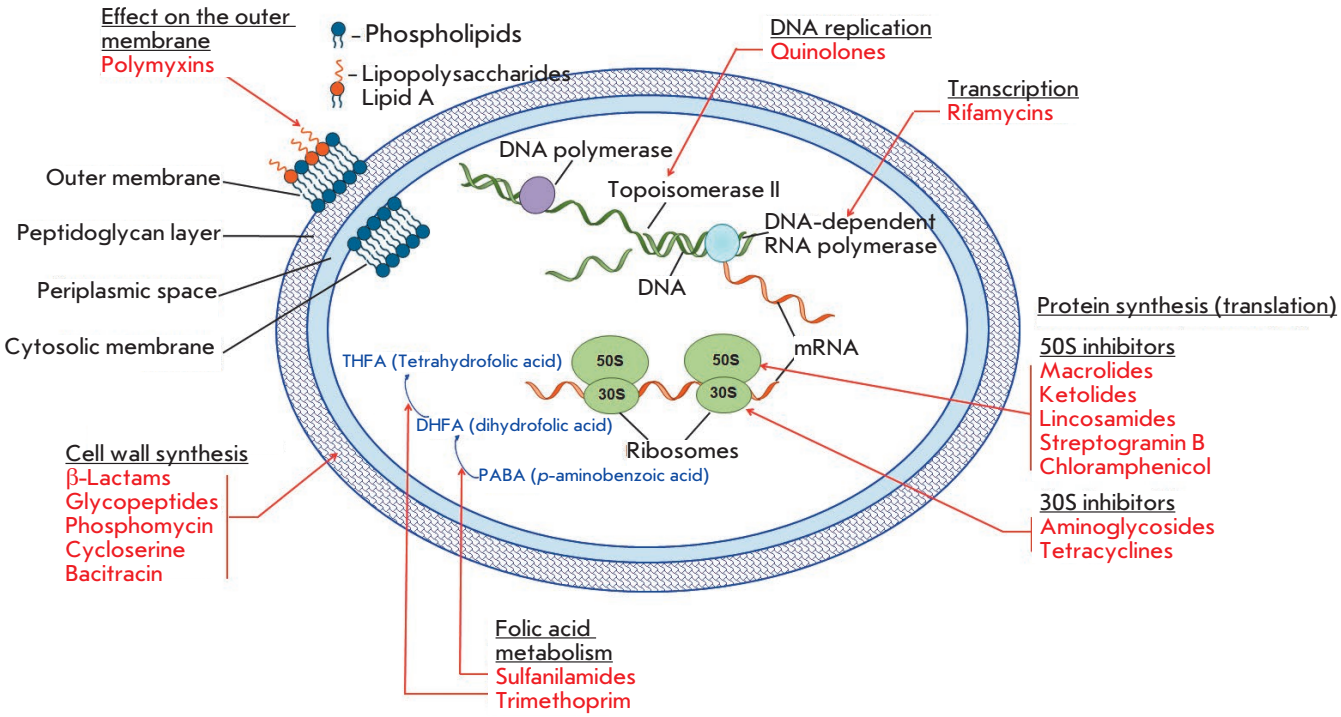

Fig. 1. The main classes of antimicrobial drugs, their targets, and their effect on the main processes of vital activity of a bacterial cell

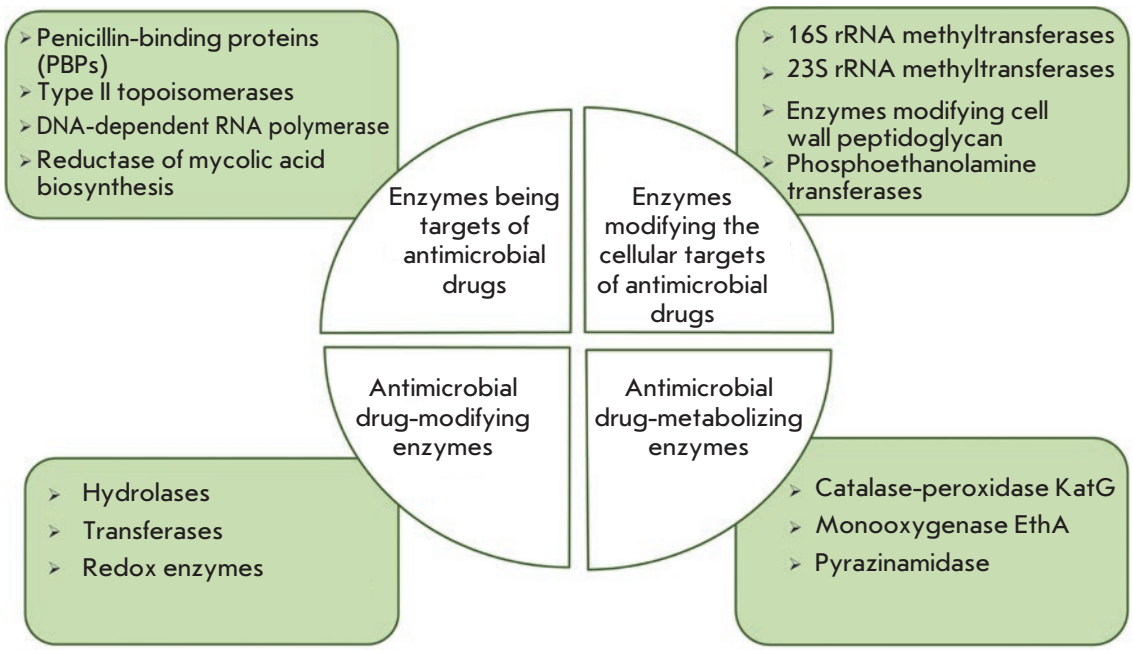

Fig. 2. Classes of enzymes involved in various mechanisms of resistance to antimicrobial drugs

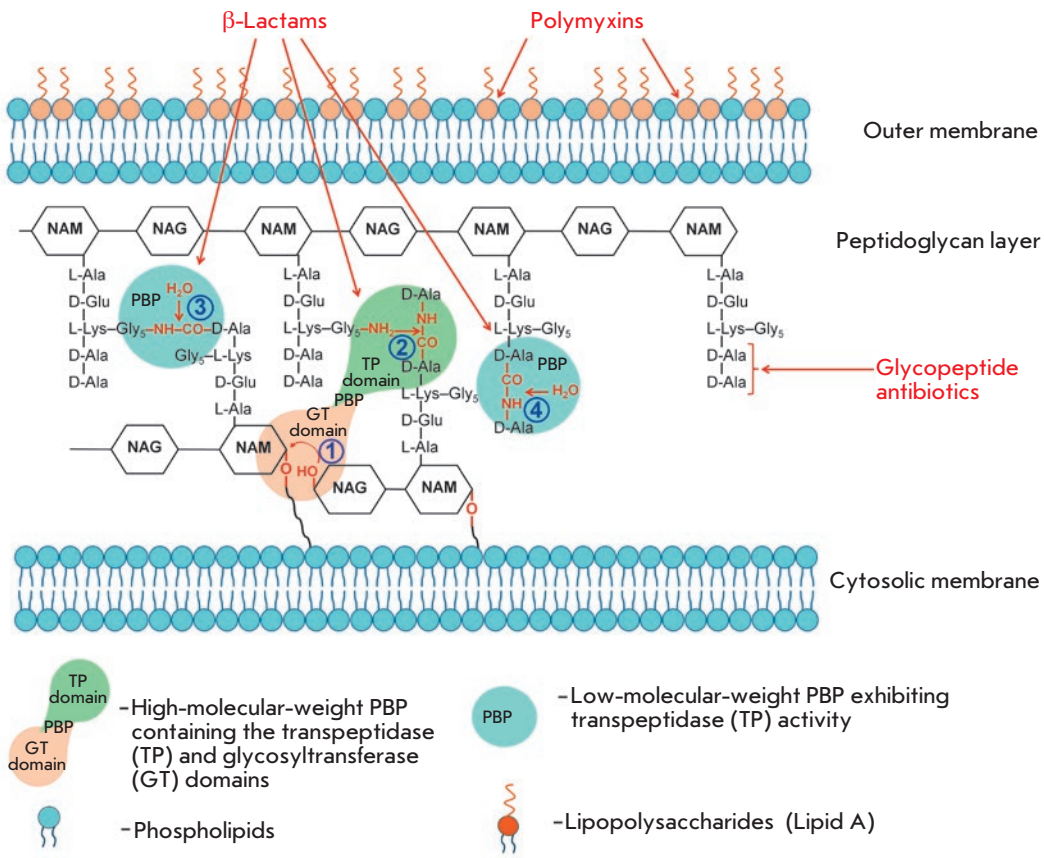

Fig. 3. The structure of bacterial cell wall peptidoglycan and involvement of penicillin-binding proteins in different reactions of its synthesis: 1 – transglycosylation reaction, 2 – transpeptidation reaction, 3 – endopeptidation reaction, and 4 – carboxypeptidation reaction

ten localized on mobile genetic elements, thus ensuring the rapid spread of resistance between microorganisms.

This review presents data on the functional features of the main classes and groups of the bacterial enzymes involved in the implementation of the mechanisms of bacterial resistance to AMDs.

BACTERIAL ENZYMES AS THE TARGETS OF AMDs

Penicillin-binding proteins

Penicillin-binding proteins (PBPs) play a key role in the synthesis of peptidoglycan, the main component of bacterial cell walls. PBPs are the targets of β-lactam antibiotics. Peptidoglycan is a polymer consisting of alternating N-acetylglucosamine (NAG) and N-acetylmuramic acid (NAM) residues (*Fig. 3*). Peptides containing *L*-Ala, *D*-Glu, meso-diaminopimelic acid or *L*-Lys, and two *D*-Ala residues are attached to all NAM residues [7]. PBPs are bound to the inner cell membrane or found in free form in the cytosol [8, 9]. PBPs are divided into high-molecular-weight (> 50 kDa) proteins consisting of two domains and low-molecular-weight proteins (< 50 kDa).

The N-terminal domain of high-molecular-weight PBP catalyzes transglycosylation reactions (sequential elongation of glycan chains by the addition of NAG-NAM-pentapeptide to the glycan backbone, 1 in *Fig. 3*). The C-terminal domain catalyzes transpeptidase reactions (cross-linking of peptide residues in two glycan chains, 2 in *Fig. 3*). Low-molecular-weight PBPs prevent cross-linking in peptidoglycan; they catalyze endopeptidase (hydrolysis of the peptide bond connecting two glycan chains, 3 in *Fig. 3*) and carboxypeptidase (hydrolysis of the bond in *D*-Ala-*D*-Ala dipeptide, 4 in *Fig. 3*) reactions.

The C-terminal domains of all PBPs are the targets of β-lactam antibiotics, which constitute more than half of all currently used AMDs [10]. These antibiotics contain a β-lactam ring, a structural analogue of *D*-Ala-*D*-Ala dipeptide, and, therefore, act as competitive inhibitors of PBPs. The interaction between the carbonyl group in the β-lactam ring and the hydroxyl group of serine in the active center of a PBP gives rise to an inactive acylated form of the enzyme. Irreversible inhibition disrupts the synthesis of the bacterial cell wall [9, 10].

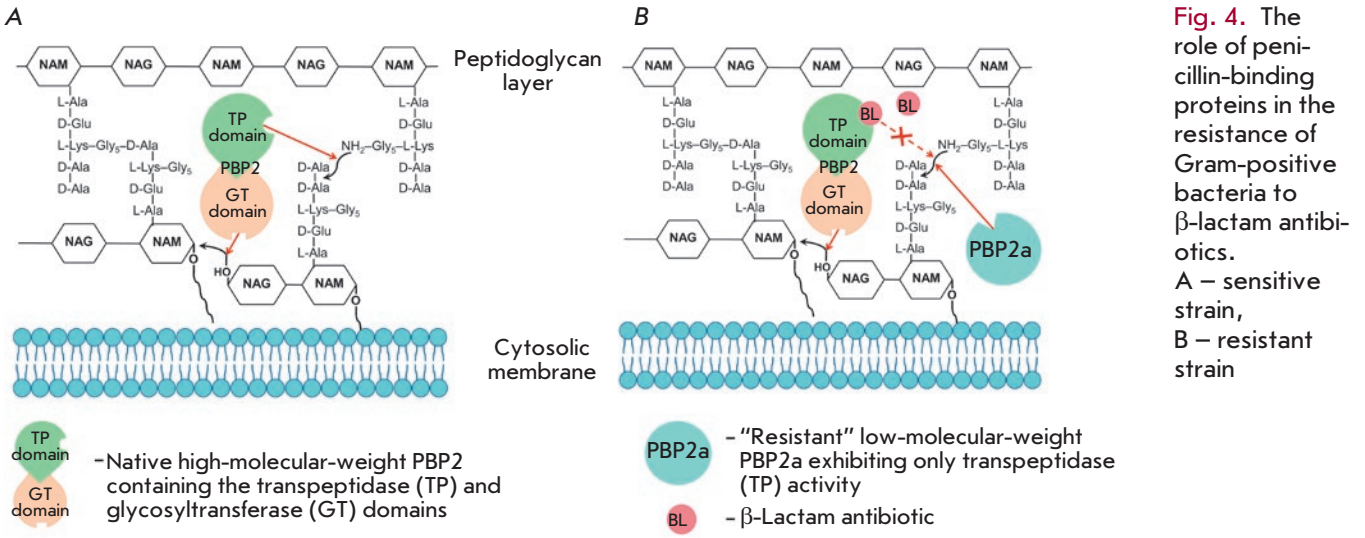

Fig. 4. The role of penicillin-binding proteins in the resistance of Gram-positive bacteria to β-lactam antibiotics. A – sensitive strain, B – resistant strain

The main reasons why Gram-positive bacteria develop resistance to β-lactam antibiotics include mutations in native PBPs, their hyperproduction, and the synthesis of new PBPs that are insensitive to inhibition by β-lactams [11]. Today, the spread of *Staphylococcus aureus* strains resistant to methicillin and other semisynthetic penicillins and cephalosporins poses a threat [12]. Resistance is determined by expression of the fifth enzyme, PBP2a (in addition to the four native PBPs), which has low affinity for β-lactam antibiotics and exhibits transpeptidase activity only. *Figure 4* shows the resistance mechanism: without an antibiotic, both domains of a high-molecular-weight PBP are involved in peptidoglycan biosynthesis (*A*); only the glycosyltransferase domain remains active in a high-molecular-weight PBP in the presence of an antibiotic, while the transpeptidase domain is acylated and does not form crosslinks. It is the acquired low-molecular-weight PBP2a (B) that exhibits transpeptidase activity in the resistant strain. As a result, cell viability is restored.

PBP2a enzymes are encoded by the genes mecA [13] or mecC [14]. The *mecA* and *mecC* genes, together with the genes regulating their expression (*mecI*, *mecR1* and *mecR2*), are the components of the mobile genetic element of the staphylococcal cassette chromosome *mec* [15].

Proteins belonging to the PBP family play a crucial role in the formation of the bacterial cell wall and are precursors of the resistance caused by β-lactamase production (see Section "β-Lactamases").

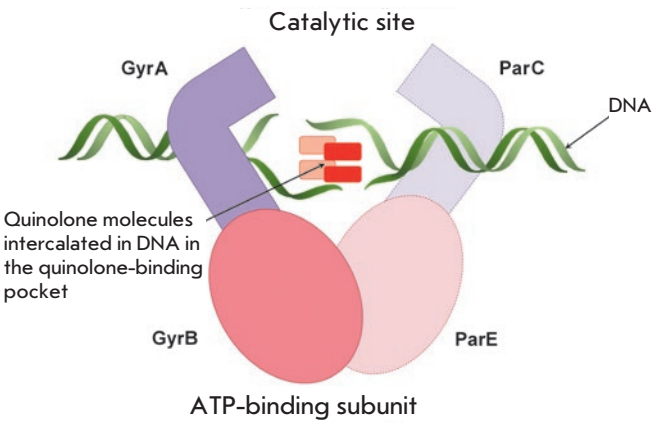

Fig. 5. The schematic structure of a ternary complex between type II topoisomerases, DNA, and quinolones. (Gyr A, Gyr B – gyrase subunits, Par C, Par E – topoisomerase IV subunits)

Type II topoisomerases: DNA gyrase and topoisomerase IV

Type II topoisomerases include DNA gyrase and topoisomerase IV, which catalyze changes in the spatial configuration of the DNA molecule during replication, transcription, and cell division [16, 17]. DNA gyrase and topoisomerase IV are heterotetrameric enzymes: DNA gyrase consists of two GyrA subunits (97 kDa) and two GyrB subunits (90 kDa); topoisomerase IV consists of

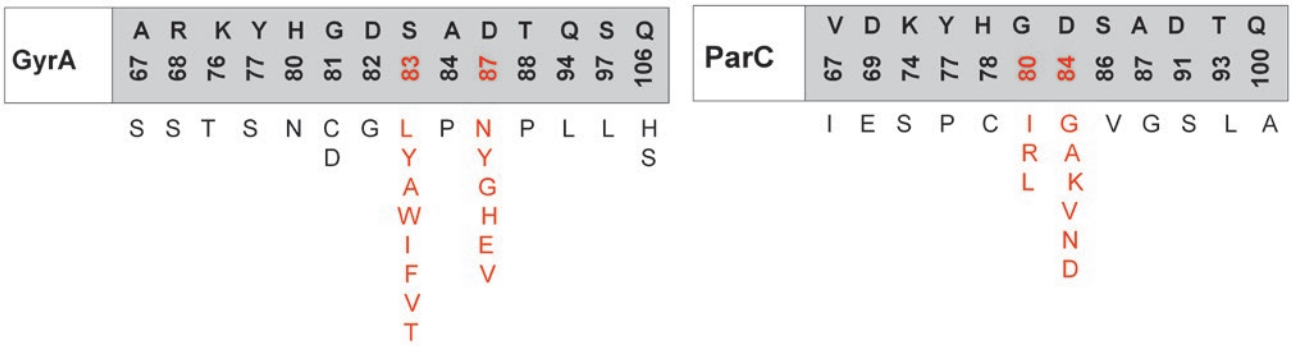

Fig. 6. Amino acid mutations in the QRDR region of the GyrA and ParC subunits of type II topoisomerases from *E. coli*, which are responsible for the resistance to quinolones. The color indicates the positions of the mutations whose combination causes a synergistic effect

two ParC subunits (84 kDa) and two ParE subunits (70 kDa). The GyrA and ParC subunits form the catalytic domains involved in the formation of complexes with the DNA molecule for its break/ligation; the GyrB and ParE subunits exhibit ATPase activity to supply energy to the process.

DNA gyrase and topoisomerase IV serve as targets for quinolones and their derivatives, fluoroquinolones. Formation of the DNA–type II topoisomerase complex is a necessary condition for inhibition (*Fig. 5*). The site of antibiotic binding to the enzyme in the ternary complex is known as the quinolone-binding pocket [17, 18].

The antibiotic binds non-covalently to the active site of the enzyme, so the motion of the enzyme and the replication fork along the DNA molecule is stopped [19]. The formation of the tertiary quinolone–topoisomerase type II–DNA complex stops not only replication, but also transcription, since the motion of RNA polymerase along the DNA template is inhibited [20]. Therein, breaks are formed in the double-stranded DNA molecule, which also determines the bactericidal action of quinolones [21]. Quinolones do not affect mammalian type II topoisomerases, because they differ significantly from bacterial topoisomerases.

The development of quinolone resistance is mainly associated with a reduction in the efficiency of their interaction with the DNA-type II topoisomerase complex due to mutations in the genes, leading to amino acid substitutions in the quinolone-binding pocket. The region of the genes where mutations occur is called QRDR (the quinolone resistance-determining region). These mutations mainly localize to the N-terminal part of the GyrA subunit (the region between residues 67–106 according to the *E. coli* numbering system) and/or ParC subunit (amino acid residues 63–102) (*Fig. 6*) but can also affect the GyrB and ParE subunits [18].

The degree of reduction in sensitivity to an antibiotic depends on the mutation type and develops gradually. First, mutations occur in one enzyme and, only later, in another one. A single amino acid substitution at position 67 of the GyrA subunit in *E. coli* increases the MIC of all fluoroquinolones fourfold; at position 81 of the same subunit, eightfold; at position 87, 16-fold; and at position 83, 32-fold [22]. The genes of both subunits carry several mutations, and a synergistic effect is often observed in microorganism strains with a high level of quinolone resistance. Thus, a combination of mutations at GyrA positions 83 and 87 and at ParC position 80 increases the MIC of fluoroquinolones over 4,000-fold [22].

DNA-dependent RNA polymerase

The bactericidal effect of rifamycins (rifampin, rifabutin) consists in inhibiting DNA-dependent RNA polymerase [23]. This enzyme consists of five subunits: two α- (molecular weight of each subunit is 35 kDa), β- (155 kDa), β'- (165 kDa), and σ-subunits (70 kDa). The four subunits ββ'αα form the so-called apoenzyme, which exhibits catalytic activity and performs all the main stages of transcription. Transcription initiation and recognition of bacterial gene promoters require the formation of a holoenzyme, which occurs when the regulatory σ-subunit binds to the apoenzyme [24].

Rifamycins selectively bind to the β-subunit of the enzyme near the main channel and inhibit elongation of the originating RNA strand. The emergence of resistance to rifamycins in most cases is associated with mutations in a relatively small fragment of the *rpoB* gene (codons 507–533) encoding the β-subunit of RNA polymerase. Mutations in amino acid residues at positions 513, 516, 526, and 531 (*Fig. 7*) are characterized by the highest degree of polymorphism [25].

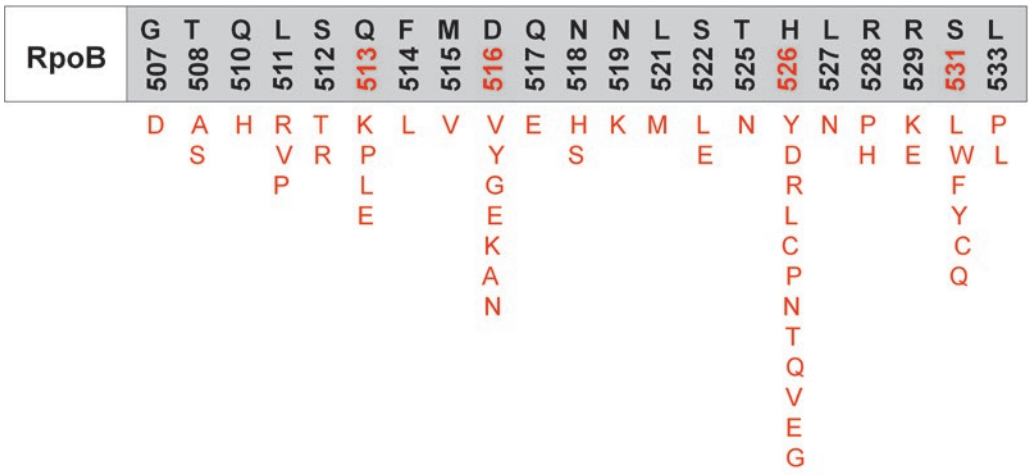

Fig. 7. Amino acid mutations in the RpoB fragment of the β-subunit of RNA polymerase, which are responsible for the resistance to rifamycins

Enzymes catalyzing the biosynthesis of mycolic acids

The term "mycolic acids" is a generic name for a group of long-chain branched fatty acids, components of the mycobacterial cell wall. Some antituberculosis drugs, derivatives of isonicotinic acid (isoniazid, ethionamide and prothionamide), suppress the synthesis of mycolic acids [25, 26]. These drugs are targeted at enoyl-acyl carrier protein reductase (known as InhA), which is a component of FAS-II fatty acid synthase. It catalyzes the reduction of D_2-unsaturated fatty acids to saturated ones using the NADPH cofactor as a hydrogen donor [27]. Disrupted synthesis of mycolic acids suppresses the synthesis of the mycobacterial cell wall.

Resistance to these drugs is caused by mutations in the *inhA* gene, which affect either both the promoter region of the *mabA–inhA* operon and cause hyperproduction of the enzyme, or the sequence encoding the enzyme, thus reducing its affinity for the complex between the isonicotinic acid radical and NAD^+ [28, 29].

BACTERIAL ENZYMES MODIFYING THE CELL TARGETS OF AMDs

rRNA methyltransferases

Bacterial ribosomes act as targets for many AMDs [30]. The small 30S subunit consists of 16S rRNA and 21 proteins. Aminoglycosides bind to the 30S subunit to yield hydrogen bonds with the nitrogenous bases of several nucleotides of 16S rRNA, which prevents proper binding of aminoacyl-tRNA to the anticodon and leads to protein synthesis errors and subsequent cell death (*Fig. 8A*). Some aminoglycosides can directly inhibit the initiation or block the elongation of the polypeptide chain [30, 31].

One of the mechanisms of resistance to aminoglycosides is methylation of the A-site of 16S rRNA by bacterial 16S rRNA methyltransferases that results in a loss of the ability to bind to the ribosome by antibiotics [32, 33]. S-adenosyl-*L*-methionine (SAM) donates the methyl group for these enzymes. Eleven different 16S rRNA methyltransferases, which can be divided into two groups according to the type of modified nucleotide in the A-site, have been described. Enzymes classified into the first group (ArmA, RmtA, RmtB, RmtC, RmtD1, RmtD2, RmtE, RmtF, RmtG and RmtH) catalyze the methylation of 16S rRNA at position N7 of nucleotide G1405 and render bacteria resistant only to 4,6-disubstituted aminoglycosides. The second group includes NmpA methyltransferase, which methylates nucleotide A1408 at the N1 position and confers resistance to all known aminoglycosides, except for streptomycin and spectinomycin [31, 32].

The genes encoding these enzymes mainly localize to conjugative plasmids and/or are associated with transposons; they are often linked to other antibiotic resistance genes [34]. The RmtB and ArmA enzymes are the most common. RmtB producers have been isolated not only from clinical specimens of human pathogens, but also from domestic animals, which indicates that resistance determinants can probably be transmitted from animals to humans [33].

Macrolides, ketolides, lincosamides, and streptogramin B (MKLS group according to the name of its components) are targeted at the large 50S subunit of the ribosome containing 5S and 23S rRNA and 33 ribosomal proteins. Despite the differences in their structure, these antibiotics have a common binding site with the 50S subunit in close proximity to the peptidyl transferase center. Meanwhile, they close the ribosomal tunnel, the structural element located in the large ribosomal subunit. This interaction results in dissociation of peptidyl-tRNA from the ribosome, which leads to

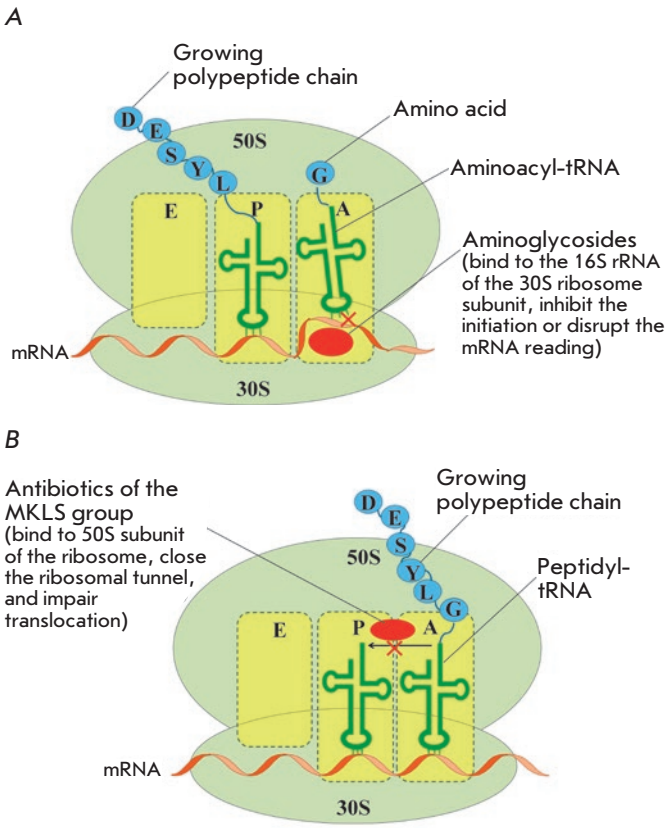

Fig. 8. Binding of aminoglycosides (A) and antibiotics of the MKLS group (B) to the ribosome and their effect on protein synthesis

translocation disruption and termination of protein synthesis (*Fig. 8B*).

One of the mechanisms of resistance to MKLS drugs is the production of 23S rRNA methyltransferases, which catalyze the post-transcriptional modification of 23S rRNA that consists in methylation of A2058 located in the site of antibiotic binding to the ribosome [35]. Like in 16S rRNA methyltransferase, SAM is the donor of the methyl group. Transfer of the methyl group from SAM to A2058 consists of two stages, including the intermediate methylation of the conserved cysteine residue in the C-terminal domain of methyltransferase [36]. Thirty-nine genes encoding 23S rRNA methyltransferase have been described, mainly in Gram-positive microorganisms. In *Enterobacteriaceae*, both chromosomal genes (e.g., *rlmAI*) and the ones localized on mobile genetic elements and encoding ErmB, ErmC, ErmD, ErmE, ErmF, and Erm42 methylases are known. Expression of Erm methyltransferases can be constitutive and inducible. In the constitutive type of expression, synthesis of methyltransferase occurs continuously and does not depend on external conditions. Phenotypically, it manifests itself in resistance to macrolides, lincosamides, and streptogramins B, while ketolides remain active. In the inducible type, methyltransferase is synthesized only in the presence of MKLS. In the absence of an inducer, the regulatory leader sequence of mRNA methyltransferase located in front of the coding sequence has a hairpin conformation and prohibits synthesis of the enzyme. The interaction between the inducer and the mRNA regulatory sequence leads to its rearrangement, which causes the synthesis of methyltransferase.

An active search for efficient inhibitors of rRNA methyltransferase is currently under way. Inhibitors of the SAM-binding center of enzymes mimicking the molecule – donor of the methyl group have been proposed as inhibitors of rRNA methyltransferase but turned out to be non-selective [37]. Compounds inhibiting both the SAM-binding and substrate-binding centers of the enzymes were also proposed [38].

Enzymes involved in the modification of peptidoglycan in the bacterial cell wall

Resistance of Gram-positive bacteria to glycopeptide antibiotics (vancomycin and teicoplanin) is caused by the production of enzymes (dihydrogenase, serine racemase, ligase) catalyzing peptidoglycan modification [11]. These antibiotics are high-molecular-weight compounds consisting of glycosylated cyclic or polycyclic peptides. They form a complex with *D*-Ala–*D*-Ala peptidoglycan terminal dipeptide, which is stable thanks to the formation of five hydrogen bonds. Furthermore, these antibiotics prevent the transglycosylation and transpeptidation reactions in the cell membrane (*Fig. 3*) [39]. Resistance to them is caused by substitution of the last amino acid residue *D*-Ala of peptidoglycan for *D*-Lac or *D*-Ser, which reduces the affinity of the terminal dipeptide for the antibiotic (by three orders of magnitude for *D*-Ala-*D*-Lac and by two orders of magnitude for *D*-Ala-*D*-Ser) [40]. Nine operons responsible for the resistance of enterococci to glycopeptide antibiotics have been detected [41, 42]. The *vanA*, *vanB*, *vanD*, and *vanM* operons ensure synthesis of peptidoglycan precursors with the *D*-Ala-*D*-Lac C-terminal dipeptide; the *vanC*, *vanE*, *vanG*, *vanL*, and *vanN* operons ensure synthesis of peptidoglycan precursors with the *D*-Ala-*D*-Ser C-terminal dipeptide [42]. Expression of the products of the aforementioned operons is inducible [43]. The determinants of resistance to glycopeptide antibiotics often localize in plasmids but can also be found in the chromosome.

Phosphoethanolamine transferases

Polymyxins (colistin) are targeted at the lipopolysaccharides of the outer membrane of Gram-negative bacteria. The main constituent of these AMDs is the positively charged cyclic polypeptide, whose mechanism of action is similar to that of cationic detergents. Interaction between polymyxin molecules and the negatively charged phosphate groups of lipopolysaccharides neutralizes the membrane charge and changes membrane permeability for the intra- and extracellular components. The main mechanism of resistance to polymyxins is associated with closure of the channel of antibiotic penetration into the cell. This channel is closed via the modification of lipid A (the component of lipopolysaccharides) with phosphoethanolamine, which is catalyzed by phosphoethanol amine transferase (*Fig. 9*) [44]. The gene encoding this enzyme has chromosomal localization. The *mcr-1* gene has recently been detected on plasmids [45]. The development of this type of resistance is associated with mutations in phosphoethanolamine transferase genes [46].

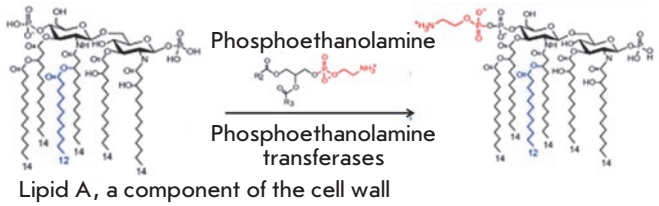

Fig. 9. Scheme of modification of lipid A, a component of lipopolysaccharides of the outer cell membrane, by phosphoethanolamine transferase

BACTERIAL ENZYMES MODIFYING AMDS

Destruction or modification of the antibiotic structure is one of the most common mechanisms of resistance involving enzymes. Depending on the type of reactions they catalyze, the enzymes involved in this resistance mechanism are subdivided into hydrolases, transferases, and oxidoreductases (*Fig. 10*). The structures of the main AMD classes and positions of their enzymatic modification are shown in *Fig. 11*.

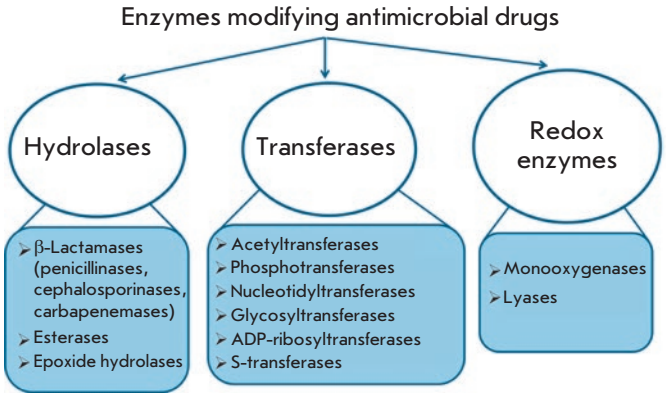

Fig. 10. The main classes of enzymes modifying antimicrobial drugs

Hydrolases

β-Lactamase and macrolide esterases destroying β-lactams and macrolides, respectively, are the most common enzymes catalyzing antibiotic hydrolysis. The same mechanism is responsible for the resistance to phosphomycin and chloramphenicol [5, 47].

β-Lactamases

β-Lactamases hydrolyze the amide bond in the β-lactam ring, the common structural element of all β-lactam antibiotics (penicillins, cephalosporins, carbapenems, and monobactams). They form an enzyme superfamily that currently consists of more than 2,000 members [47]. According to the homology of amino acid sequences, β-lactamases are subdivided into four molecular classes [48]. The enzymes of classes A, C, and D are serine hydrolases, the enzymes of class B are metalloenzymes.

Serine β-lactamases have structural elements similar to those of the C-domain of PBPs, which indicates that they are evolutionarily related [49]. The evolution of β-lactamase develops via two main mechanisms: the emergence of new mutations in the genes of known enzymes and the emergence of enzymes with a new structure. The high mutation rate of β-lactamases and the localization of their genes on mobile genetic elements contribute to the rapid spread of resistant bacteria, which poses a global threat [50]. Bacteria simultaneously carrying up to eight β-lactamase genes have been detected [51].

Class A β-lactamases (CTX-M, TEM, SHV, and KPC lactamases) are the most common ones [51]. Mutational variability is a feature of TEM and SHV β-lactamases. The key mutations in the active site increase the enzyme volume and make it capable of hydrolyzing the bulk molecules of cephalosporins of the second-to-fourth generations [52]. These mutant forms are known as extended-spectrum β-lactamases (ESBLs). Certain mutations in amino acid residues located at a distance from the active site are compensating and may have multidirectional effects on stability [53, 54].

Class C β-Lactamases efficiently hydrolyze cephalosporins. Initially, this class was represented by the

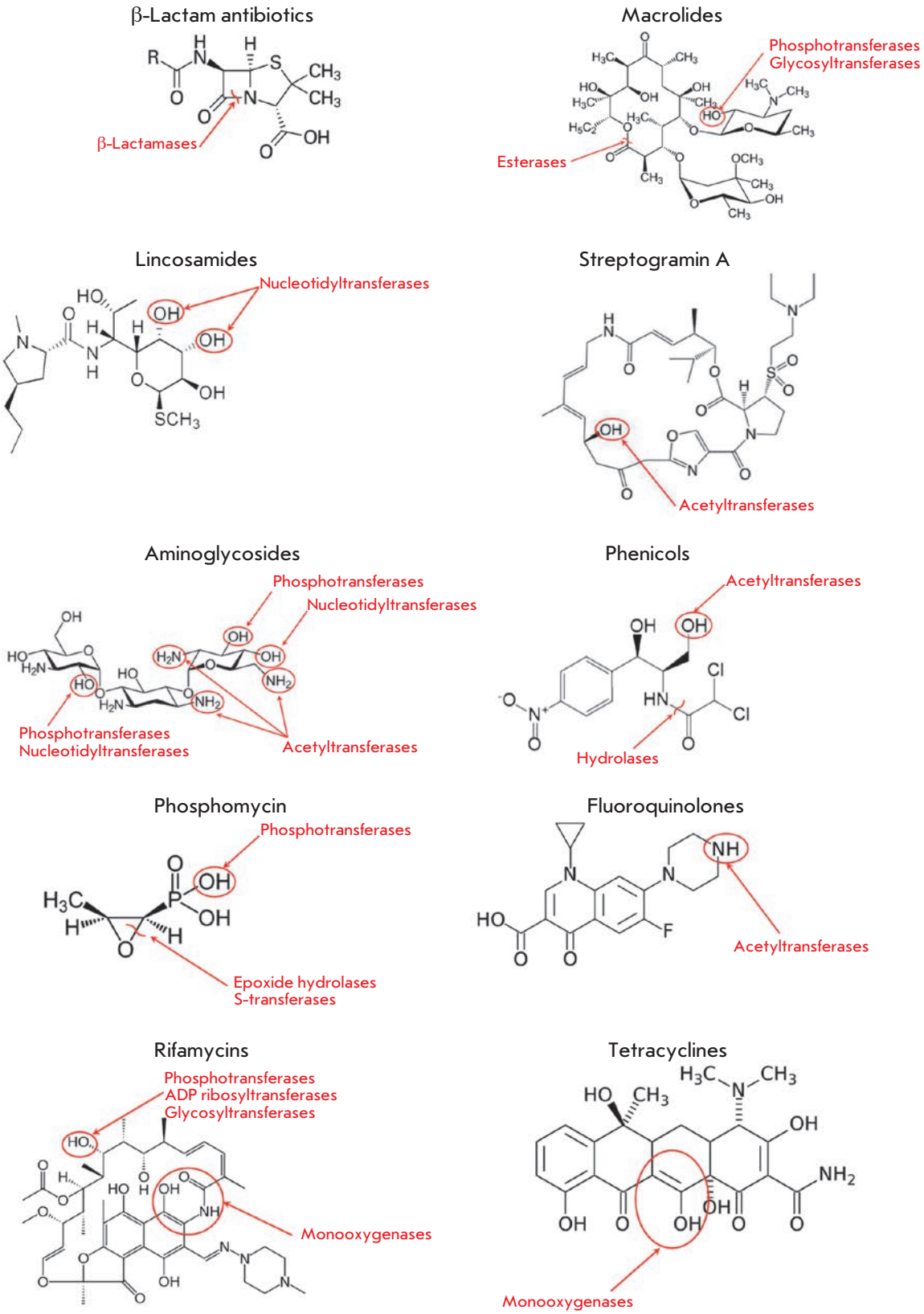

Fig. 11. Structures of the main classes of antimicrobial drugs and the enzymes modifying them

enzymes encoded by chromosomal genes and having an inducible type of expression. Then, enzymes encoded by the genes located on mobile elements were discovered [55].

Class D β-lactamases include OXA-type β-lactamases and are the most structurally diverse enzymes among serine β-lactamases.

The molecular class B is a heterogeneous family of metallo-β-lactamases (MBL) [56]. They contain one or two zinc ions in their active site, hydrolyze almost all β-lactam antibiotics except for monobactams, and are inhibited by chelating agents (EDTA, dipicolinic acid and *o*-phenanthroline). The emergence of new MBL variants (e.g., NDM-type carbapenemases) and their co-expression with serine β-lactamases result in the emergence of bacteria resistant to all β-lactam antibiotics [57].

In order to overcome the resistance caused by production of β-lactamases, an active search for inhibitors of these enzymes is currently under way [58, 59]. In clinical practice, combinations of β-lactams with clavulanic acid, sulbactam, and tazobactam (which contain a β-lactam ring, form a more stable acyl-enzyme complex and have a low deacylation rate) are intensively used to inhibit class A enzymes. The newest inhibitors that are structurally similar to β-lactams but contain no β-lactam ring include diazabicyclooctanes (avibactam and MK-7655). They form carbamyl–enzyme complexes with involvement of catalytic serine, which are then subjected to slow reversible recyclization, accompanied by the release of an inhibitor molecule. These inhibitors have proved effective against A, C, and partly D class β-lactamases. Boronic acid derivatives capable of inhibiting class A carbapenemases are being extensively studied. Particular attention is paid to the search for inhibitors of MBL, but none of them has been used in practice yet [60].

Macrolide esterases

Resistance to 14- and 15-membered macrolides (erythromycin, azithromycin, etc.) is caused by the production of esterases catalyzing hydrolysis of the lactone ring [35, 61]. Macrolides containing 16-membered rings are not substrates of these enzymes. Erythromycin esterases EreA and EreB are of the greatest clinical significance. EreA has a more limited substrate specificity profile. It does not hydrolyze azithromycin and telithromycin. It is a metal-dependent enzyme whose activity is inhibited by chelating agents. EreB confers resistance to almost all 14- and 15-membered macrolides, except for telithromycin. The genes encoding these esterases localize in plasmids and are often linked to other antibiotic resistance genes [62].

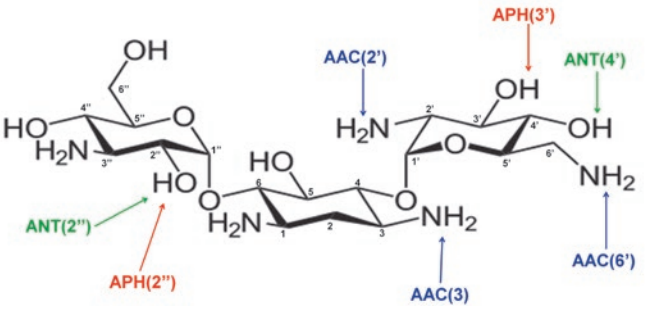

Fig. 12. The structure of kanamycin B and positions of its modification by aminoglycoside-modifying enzymes

Transferases

Transferases modifying AMD molecules by covalently binding various chemical groups represent a large superfamily of enzymes [5, 6, 63]. Their main groups, differing in terms of substrate specificity, type of modification and mechanism of action, are discussed below.

Aminoglycoside-modifying enzymes

Enzymatic modification of aminoglycoside antibiotics is the most common resistance mechanism that is implemented by aminoglycoside-modifying enzymes (AMEs). Several hundred different AME are known; almost each enzyme is represented by several isoenzymes that possess unique substrate specificity and modify aminoglycosides at certain positions [31]. AME genes localize in mobile genetic elements; that is why they rapidly spread.

Three AME families are distinguished according to the reaction type: N-acetyltransferases (AAC), O-phosphotransferases (ANT), and O-adenylyltransferases (ANT) (*Fig. 12*). AAC enzymes use acetyl-CoA as a cofactor; ATP or GTP acts as a donor of phosphate groups and adenine for APH and ANT [23]. AAC enzymes are the most common and clinically significant enzymes; 48 AAC variants acetylating aminoglycosides at one of the positions (1, 3, 2 'or 6') have been isolated. The unique Eis enzyme, which is able to simultaneously acetylate aminoglycosides at several positions, is also known.

APH is the second largest family of AME that includes seven types of enzymes catalyzing phosphate group transfer at positions 4, 6, 9, 3', 2'', 3'' or 7" of aminoglycosides. ANT enzymes are divided into five classes modifying aminoglycosides at position 6, 9, 4', 2'' or 3'' [64, 65].

Several approaches have been proposed in order to overcome resistance to aminoglycosides: regulat-

ing gene expression by antisense oligonucleotides [66], designing novel aminoglycosides [67, 68], and searching for AME inhibitors [64, 69]. Bisubstrates consisting of aminoglycoside and acetyl-CoA were the first to be proposed as inhibitors of AAC. However, this compound poorly penetrates through the cell membrane and exhibits low effectiveness in *in vivo* experiments because of its considerable size and negative charge [70]. A number of recent studies have shown that AAC and Eis activities are inhibited by the cations of different metals, which increases the effectiveness of aminoglycosides [71]. Various inhibitors of APH possessing kinase activity have been investigated [72]. The natural inhibitor quercetin was found to be among the most effective: it suppresses the activity of several APHs both *in vitro* and *in vivo*. Inhibitors targeted at various AMEs are considered promising: for example, compounds based on 3-(dimethylamino)propylamine inhibit both ANT and APH with sufficient effectiveness [73]. Cationic peptides were bound to the negatively charged active site of AME and exhibited high affinity for different AAC and APH but did not affect resistant bacterial strains, probably due to poor permeability across their cell membrane [74]. The neomycin A dimer inhibited the activity of both monofunctional AAC(6′)-Ii and APH(3′)-IIIa enzymes and the bifunctional AAC(6')-APH(2") enzyme, including *in vivo* inhibition using the clinical *Pseudomonas aeruginosa* strain [69, 75].

Enzymes modifying chloramphenicol and its analogues

Production of chloramphenicol acetyltransferases (CATs) is the main mechanism of bacterial resistance to chloramphenicol. These enzymes catalyze the addition of the acetyl group of acetyl-CoA to the 3-hydroxyl group of chloramphenicol or its synthetic analogues (thiamphenicol, azidamphenicol), thereby preventing the binding of the antibiotic molecule to ribosomes [5]. CATs do not inactivate fluorophenicol, since the 3-hydroxyl group in its molecule is replaced with a fluorine atom [63]. CATs of different types have extremely low homology of amino acid sequences, which does not exceed 10%. The *cat* genes can be located on chromosomes [76] but are more typically localized on plasmids as components of transposons in association with genes encoding resistance to other AMDs. Expression of the *cat* genes is induced by chloramphenicol [63].

In addition to acetylation, inactivation of chloramphenicol can be ensured by O-phosphorylation. This mechanism of antibiotic resistance was described for *S. venezuelae*, a chloramphenicol producer [77].

Enzymes modifying MKLS antibiotics

Macrolide phosphotransferases (MPHs) are enzymes that modify the structure of macrolides by adding a phosphate group to the 2'-OH group [5]. The phosphate group is donated by nucleoside triphosphates, most typically by GTP. Seven different enzymes of this group have been described so far. MPHA preferably catalyzes the phosphorylation of 14- and 15-membered macrolides, while MPHB modifies 14- and 16-membered macrolides [35, 62]. The genes encoding MPH are located on mobile genetic elements containing other genes encoding resistance to macrolides and other antibiotic classes [78, 79]. Expression of the genes coding for macrolide phosphotransferases can be either inducible (*mphA*) or constitutive (*mphB*) [35].

Macrolide glycosyltransferases are enzymes that inactivate macrolides by glycosylating the 2'-OH group of the macrolide ring [6]. They use UDP glucose as a cofactor.

Streptogramin acetyltransferases inactivate only streptogramins A by acetylation of an unbound hydroxyl group; their mechanism of action is similar to that of CAT [5]. The genes encoding these enzymes have been identified in a number of Gram-positive pathogens, including staphylococci and enterococci [63].

Phosphomycin-modifying enzymes

FosA, FosB, and FosX epoxidases, as well as FomA and FomB kinases, are metalloenzymes that inactivate phosphomycin [11, 23, 80]. Epoxidases open the epoxy group of phosphomycin (the oxirane ring) by adding various substrates. FosA is glutathione-S-transferase that uses Mn^{2+} and K^{+} metal ions as cofactors, besides glutathione. Bacillithiol or *L*-Cys acts as a source of the thiol group in FosB; additionally, these enzymes use Mg^{2+} as a cofactor [11, 81]. The FosX enzyme is a Mn^{2+}-dependent hydrolase. Most of the genes encoding these enzymes localize on the plasmid, although FosA in *P. aeruginosa* and FosB in *S. aureus* are encoded by chromosomal genes.

FomA and FomB kinases add one or two phosphate groups to the phosphomycin molecule, using ATP and Mg^{2+} ions as cofactors. These enzymes are isolated from phosphomycin producer *S. wedriensis* [11].

Rifamycin-modifying enzymes

Several groups of enzymes inactivate rifamycins by modifying the hydroxyl group, the key group involved in the binding of an antibiotic molecule to the β-subunit of RNA polymerase. NAD^{+}-dependent enzymes belonging to the Arr group catalyze ADP-ribosylation, RPH kinases catalyze phosphorylation, and glycosyltransferases catalyze glycosylation [23, 82, 83].

Monooxygenases

The flavin-dependent monooxygenase TetX confers resistance to all tetracyclines, including the broad-spectrum antibiotic tigecycline [5]. TetX catalyzes monohydroxylation of tetracyclines in the presence of NADPH, O_2, and Mg^{2+}, leading to intramolecular cyclization and decomposition of the molecule. Flavin-dependent monooxygenases Rox inactivate rifamycins by oxidating the naphthyl group at position 2, leading to ring opening and linearization of the antibiotic molecule [84].

Enzymes of metabolic processes modifying AMD in the prodrug form

Antibiotics can also be modified by the enzymes that protect cells against toxic molecules. In most cases, prodrug forms of AMDs are modified to the active forms.

Isoniazid is activated by KatG catalase-peroxidase, giving rise to free radicals of isonicotinic acid, which block the enzymes involved in the synthesis of mycolic acids [85]. Resistance is caused by mutations in the *katG* gene, which are most often localized in codon 315 and cause conformational changes in the isoniazid-binding pocket.

Structural analogues of isoniazid, ethionamide and prothionamide, are activated by NADPH-dependent FAD-containing monooxygenase encoded by the *ethA* gene [85]. The oxidized forms of ethionamide and prothionamide in a complex with NAD^+ inhibit the enzymes responsible for the synthesis of mycolic acids (primarily InhA), similar to the case of isoniazid. Expression of the *ethA* gene is regulated by the transcriptional repressor EthR. Resistance is caused by mutations in the *ethA* and *ethR* genes.

BIFUNCTIONAL ENZYMES: A NEW EVOLUTIONARY TREND

Mutations in bacterial genomes and selection of new resistant phenotypes are the main mechanisms in bacteria responsible for antibiotic resistance. As a result, there is a wide variety of forms causing resistance for a number of enzymes: thus, over 2,000 β-lactamases have been described. However, single amino acid substitutions cause limited changes in the activity and specificity of a particular enzyme. The emergence of bifunctional enzymes encoded by two linked genes is a new trend in the evolutionary development of resistance. This phenomenon significantly increases substrate specificity and provides evolutionary advantage for extremely broad resistance to various AMDs [86].

Bifunctional β-lactamases

The first bifunctional enzyme Tp47 was isolated from the causative agent of syphilis *Treponema palladium* [87]. It has two active sites: one exhibiting PBP activity; and the second one, β-lactamase activity. Since Tr47 has a very low β-lactamase activity, it does not really provide resistance to β-lactams.

Another bifunctional β-lactamase, blaLRA-13, was found in β-lactam-resistant *E. coli* strains isolated from Alaskan soils [88]. This enzyme consists of 609 amino acids, which is almost twice greater than the length of the typical monofunctional β-lactamase. The C-domain of this enzyme (356 amino acids) is highly homologous to class C β-lactamases and ensures resistance to amoxicillin, ampicillin, and carbenicillin, while the N-domain (253 amino acids) is highly homologous to class D β-lactamases and ensures resistance to cephalexin. In addition to blaLRA-13, the isolated strains also produced several monofunctional β-lactamases belonging to different classes. Although this bifunctional β-lactamase has not yet been found in clinical bacterial strains, one cannot rule out the possibility that it will be distributed among infectious human diseases in the future. Moreover, the discovery of this enzyme confirms the evolutionary hypothesis that soil microorganisms, as well as microorganisms of other ecological niches, have a wide range of resistance mechanisms that can be transferred over time to clinically significant pathogens.

Enzyme bifunctionality could have occurred during the evolutionary changes in high-molecular-weight dual-domain PBP, whose transpeptidase domain can form a stable complex with β-lactam antibiotics. During mutation emergence, the binding site became able to hydrolyze the β-lactam ring; i.e., a new group of antibiotic-hydrolyzing enzymes was formed.

Bifunctional aminoglycoside-modifying enzymes

Gram-positive bacteria were found to have a bifunctional AAC(6')-Ie/APH(2")-Ia enzyme. The N-terminal domain of this enzyme possesses acetyltransferase activity, while the C-domain exhibits phosphotransferase activity [89]. The AAC domain of the enzyme can acylate only one type of aminoglycoside rings, while the APH domain has broader specificity and catalyzes the O-phosphorylation of four different aminoglycoside rings [90]. A bifunctional enzyme ensures resistance to almost all known, clinically significant aminoglycosides, except for streptomycin and spectinomycin.

The bifunctional ANT(3'')-Ii/AAC(6')-IId enzyme is characterized by a combination of nucleotidyltransferase activity against streptomycin and spectinomycin and acetyltransferase activity with broad substrate specificity [91].

The first domain of the bifunctional AAC(3)-Ib/AAC(6')-Ib' enzyme is specific only to gentamicin and fortimicin; the second domain exhibits broad substrate

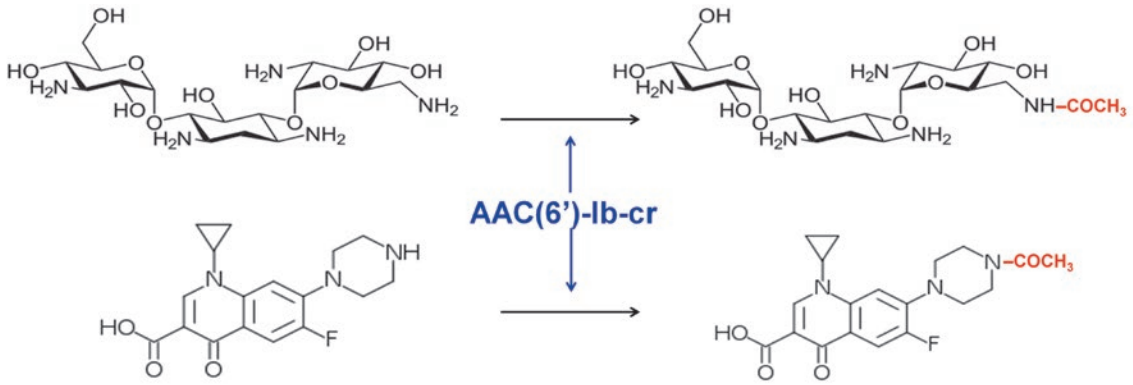

Fig. 13. Acylation of kanamycin B and ciprofloxacin catalyzed by the bifunctional enzyme AAC(6')-Ib-cr

specificity, including amikacin, dibekacin, gentamicin, isepamicin, kanamycin A, and neomycin [92].

A novel bifunctional enzyme, AAC(6')-30/AAC(6')-Ib', providing resistance to many aminoglycosides other than isepamicin and exhibiting higher activity than monofunctional enzymes, has recently been isolated from *P. aeruginosa* [93].

Bifunctional aminoglycoside- and fluoroquinolone-modifying enzyme

A novel variant of AAC(6')-Ib-cr acetyltransferase is the first enzyme that can simultaneously inactivate aminoglycosides and fluoroquinolones (*Fig. 13*) [94]. Two mutations encoding the W102R and D179Y substitutions ensure ciprofloxacin resistance [95]. The gene coding for this enzyme has both plasmid and chromosomal localization. It was found on a multi-resistant plasmid, together with other resistance genes.

CONCLUSIONS

The question regarding the origin of the bacterial enzymes responsible for resistance development during evolution remains controversial. The genes encoding these enzymes are located on chromosomes and mobile elements. The enzymes encoded by chromosomal genes protect microorganisms producing antibiotics against modification of their potential targets. Resistance occurs when the genes coding for these enzymes are transferred to other bacteria.

Another group of enzymes encoded by chromosomal genes has evolved from enzymes belonging to superfamilies with isolation of subgroups with altered substrate specificity. Enzymes that perform vital functions and are responsible for the biosynthesis of cell wall polysaccharides, proteins, nucleic acids, and metabolites serve as targets for antibiotics. Modification of the active sites of target enzymes contributed to their ability to use antibiotics as substrates. The presence of proto-resistance genes causing the evolutionary relationship between β-lactamases and PBP, kinases and acetyltransferases, with aminoglycoside-modifying enzymes, has been established.

Many enzymes have originated from bacterial pro-enzymes that used to have other functions. Mutations in the genes encoding enzymes emerged due to exogenous and endogenous factors (in particular, antibiotics and products of their metabolism). These mutations changed the structure, catalytic properties, and substrate specificity of these products. The multiplicity of mutations indicates that both the key and accompanying amino acid residues undergo mutations. The key amino acid residues are important for catalytic processes, while changes in the accompanying residues compensate for structural changes and function as allosteric sites of activity regulation.

The multidirectionality of the processes is a feature typical of bacterial resistance. Combination of several resistance mechanisms in a single cell (e.g., modification of structural cellular elements, changes in the expression level of proteins, including porins, and activation of efflux systems) complicates the development of methods for suppressing resistance. The scientific concept of combining objects related to the most important biological processes into certain groups has emerged in recent years. Thus, the concept of "microbiome" as a combination of microorganisms of a certain species and humans appeared. Non-pathogenic microorganisms, and soil bacteria in particular, represent a huge reservoir and source of resistance genes. Their wide distribution among microorganisms is associated with localization on plasmids and other mobile genetic elements and a high rate of exchange and transmission between bacterial cells, including pathogenic strains.

The combination of the genes responsible for the resistance of pathogenic clinical strains and non-pathogenic bacteria in the environment and microbiota is known as the "resistome." Its important feature is that the genome of a single bacterium carries several

resistance genes that ensure multiresistance. Bacterial cells can rapidly reproduce, change their gene structure, and undergo selection; so, they have developed new mechanisms ensuring cell survival. Enzymes with various functions play the most important role in these processes. The term "enzystome" can be used to refer to the enzyme-based defense system that has developed throughout the long-term evolution of bacteria.

The presented classification of bacterial enzymes of the "enzystome" will be further developed and supplemented. Having summarized the results of analyzing the contribution of enzymes to the development of antibiotic resistance in bacteria, one should acknowledge the fundamental biological significance of this process as it ensures the survivability of microorganisms and their adaptability. The adaptability of microorganisms to new environmental conditions largely depends on "biocatalytic functionality." We believe that microbiologists, molecular biologists, and biotechnologists should focus closely on changes in this functionality at the genetic level. The growing industrial-scale production of AMDs and their uncontrolled use in medicine and veterinary medicine has become a powerful anthropogenic factor which has significantly contributed to the acceleration of resistance development. Research into the structures of the enzymes that compose the "enzystome" and the analysis of evolutionary variability and the conservative sites of the "resistome" will allow us to understand the mechanisms of regulation in bacterial cells and to find new targets for developing rational approaches to the production of selective and effective AMDs in order to overcome resistance. It is of particular interest to use enzymes capable of destroying and metabolizing antibiotics as medications to protect the beneficial microbiota and prevent side effects during antibiotics therapy. ●

This study was supported by the Russian Science Foundation.

REFERENCES

1. Antimicrobial Resistance Global Report on surveillance. // 2014.http://www.who.int/ drugresistance/en
2. Roca I., Akova M., Baquero F., Carlet J., Cavaleri M., Coenen S., Cohen J., Findlay D., Gyssens I., Heure O.E., et al. // New Microbes New Infect. 2015. V. 6. P. 22–29.
3. Chang Q., Wang W., Regev-Yochay G., Lipsitch M., Hanage W.P. // Evol. Appl. 2015. V. 8. № 3. P. 240–247.
4. Holmes A.H., Moore L.S.P., Sundsfjord A., Steinbakk M., Regmi S., Karkey A., Guerin P.J., Piddock L.J.V. // Lancet. 2016. V. 387. P. 176–187.
5. Wright G.D. // Adv. Drug Deliv. Rev. 2005. V. 57. № 10. P. 1451–1470.
6. Morar M., Wright G.D. // Annu. Rev. Genet. 2010. V. 44. № 1. P. 25–51.
7. Vollmer W., Blanot D., De Pedro M.A. // FEMS Microbiol. Rev. 2008. V. 32. № 2. P. 149–167.
8. Sauvage E., Kerff F., Terrak M., Ayala J.A., Charlier P. // FEMS Microbiol. Rev. 2008. V. 32. № 2. P. 234–258.
9. Sauvage E., Terrak M. // Antibiotics. 2016. V. 5. № 1. P. 12.
10. Bush K., Bradford P.A. // Cold Spring Harb. Perspect. Med. 2016. V. 6. № 8. P. 1–22.
11. Nikolaidis I., Favini-Stabile S., Dessen A. // Protein Sci. 2014. V. 23. № 3. P. 243–259.
12. Chambers H.F., Deleo F.R. // Nat. Rev. Microbiol. 2009. V. 7. № 9. P. 629–641.
13. Fuda C., Suvorov M., Vakulenko S.B., Mobashery S. // J. Biol. Chem. 2004. V. 279. № 39. P. 40802–40806.
14. Diaz R., Ramalheira E., Afreixo V., Gago B. // Diagn. Microbiol. Infect. Dis. 2016. V. 84. № 2. P. 135–140.
15. Liu J., Chen D., Peters B.M., Li L., Li B., Xu Z., Shirliff M.E. // Microb. Pathog. 2016. V. 101. P. 56–67.
16. Correia S., Poeta P., Hébraud M., Capelo J.L., Igrejas G. // J. Med. Microbiol. 2017. V. 66. № 5. P. 551–559.
17. Aldred K.J., Kerns R.J., Osheroff N. // Biochemistry. 2014. V. 53. № 10. P. 1565–1574.
18. Hooper D.C., Jacoby G.A. // Cold Spring Harb. Perspect. Med. 2016. V. 6. № 9. P. 1–21.
19. Wentzell L.M., Maxwell A. // J. Mol. Biol. 2000. V. 304. № 5. P. 779–791.
20. Willmott C.J., Critchlow S.E., Eperon I.C., Maxwell A. // J. Mol. Biol. 1994. V. 242. P. 351–363.
21. Drlica K., Malik M., Kerns R.J., Zhao X. // Antimicrob. Agents Chemother. 2008. V. 52. № 2. P. 385–392.
22. Drlica K., Hiasa H., Kerns R., Malik M., Mustaev A., Zhao X. // Curr. Top. Med. Chem. 2009. V. 9. № 11. P. 981–998.
23. Costa V.D., Wright G.D. // Antimicrobial Drug Resistance / Ed. Mayers D.L. New York: Humana Press, 2009. P. 81–95.
24. Borukhov S., Nudler E. // Curr. Opin. Microbiol. 2003. V. 6. № 2. P. 93–100.
25. Dookie N., Rambaran S., Padayatchi N., Mahomed S., Naidoo K. // J. Antimicrob. Chemother. 2018. V. 73. № 5. P. 1138–1151.
26. Palomino J.C., Martin A. // Antibiot. 2014. V. 3. № 3. P. 317–340.
27. Vilchèze C., Morbidoni H.R., Weisbrod T.R., Iwamoto H., Kuo M., Sacchettini J.C., Jacobs W.R. // J. Bacteriol. 2000. V. 182. № 14. P. 4059–4067.
28. Larsen M.H., Vilchèze C., Kremer L., Besra G.S., Parsons L., Salfinger M., Heifets L., Hazbon M.H., Alland D., Sacchettini J.C., et al. // Mol. Microbiol. 2002. V. 46. № 2. P. 453–466.
29. Machado D., Perdigão J., Ramos J., Couto I., Portugal I., Ritter C., Boettger E.C., Viveiros M. // J. Antimicrob. Chemother. 2013. V. 68. № 8. P. 1728–1732.
30. Wilson D.N. // Nat. Rev. Microbiol. 2014. V. 12. № 1. P. 35–48.
31. Krause K.M., Serio A.W., Kane T.R., Connolly L.E. // Cold Spring Harb. Perspect. Med. 2016. V. 6. № 6. P. 1–18.
32. Doi Y., Wachino J., Arakawa Y. // Infect. Dis. Clin. North Am. 2016. V. 30. № 2. P. 523–537.

33. Wachino J.I., Arakawa Y. // Drug Resist. Updat. 2012. V. 15. № 3. P. 133–148.
34. Hidalgo L., Hopkins K.L., Gutierrez B., Ovejero C.M., Shukla S., Douthwaite S., Prasad K.N., Woodford N., Gonzalez-Zorn B. // J. Antimicrob. Chemother. 2013. V. 68. № 7. P. 1543–1550.
35. Fyfe C., Grossman T.H., Kerstein K., Sutcliffe J. // Cold Spring Harb. Perspect. Med. 2016. V. 6. № 10. P. 1–38.
36. Boal A.K., Grove T.L., McLaughlin M.I., Yennawar N.H., Booker S.J., Rosenzweig A.C. // Science. 2011. V. 332. № 6033. P. 1089–1092.
37. Hajduk P.J., Dinges J., Schkeryantz J.M., Janowick D., Kaminski M., Tufano M., Augeri D.J., Petros A., Nienaber V., Zhong P., et al. // J. Med. Chem. 1999. V. 42. № 19. P. 3852–3859.
38. Feder M., Purta E., Koscinski L., Čubrilo S., Vlahovicek G.M., Bujnicki J.M. // ChemMedChem. 2008. V. 3. № 2. P. 316–322.
39. Périchon B., Courvalin P. // Antibiotic Discovery and Development / Eds Dougherty T.J., Pucci M.J. Boston: Springer US, 2012. P. 515–542.
40. Courvalin P. // Clin. Infect. Dis. 2006. V. 42. P. 25–34.
41. Hegstad K., Mikalsen T., Coque T.M., Werner G., Sundsfjord A. // Clin. Microbiol. Infect. 2010. V. 16. № 6. P. 541–554.
42. Cattoir V., Leclercq R. // J. Antimicrob. Chemother. 2013. V. 68. № 4. P. 731–742.
43. Sidorenko S.V., Tishkov V.I. // Uspehi biologicheskoy khimii. 2004. V. 44. P. 263–306 (In Russian).
44. Poirel L., Jayol A., Nordmanna P. // Clin. Microbiol. Rev. 2017. V. 30. № 2. P. 557–596.
45. Liu Y.Y., Wang Y., Walsh T.R., Yi L.X., Zhang R., Spencer J., Doi Y., Tian G., Dong B., Huang X., et al. // Lancet Infect. Dis. 2016. V. 16. № 2. P. 161–168.
46. Sun J., Zhang H., Liu Y.H., Feng Y. // Trends Microbiol. 2018. V. 26. № 9. P. 794–808.
47. Bonomo R.A. // Cold Spring Harb. Perspect. Med. 2017. V. 7. № 1. P. 1–16.
48. Hall B.G., Barlow M. // J. Antimicrob. Chemother. 2005. V. 55. № 6. P. 1050–1051.
49. Ghuysen J.-M. // Trends Microbiol. 1994. V. 2. № 10. P. 372–380.
50. Bush K., Jacoby G.A. // Antimicrob. Agents Chemother. 2010. V. 54. № 3. P. 969–976.
51. Bush K. // Ann. N. Y. Acad. Sci. 2013. V. 1277. № 1. P. 84–90.
52. Orencia M.C., Yoon J.S., Ness J.E., Stemmer W.P.C., Stevens R.C. // Nat. Struct. Biol. 2001. V. 8. № 3. P. 238–242.
53. Brown N.G., Pennington J.M., Huang W., Ayvaz T., Palzkill T. // J. Mol. Biol. 2010. V. 404. № 5. P. 832–846.
54. Grigorenko V., Uporov I., Rubtsova M., Andreeva I., Shcherbinin D., Veselovsky A., Serova O., Ulyashova M., Ishtubaev I., Egorov A. // FEBS Open Bio. 2018. V. 8. № 1. P. 117–129.
55. Philippon A., Arlet G., Jacoby G.A. // Antimicrob. Agents Chemother. 2002. V. 46. № 1. P. 1–11.
56. Bebrone C. // Biochem. Pharmacol. 2007. V. 74. № 12. P. 1686–1701.
57. Nordmann P., Poirel L., Walsh T.R., Livermore D.M. // Trends Microbiol. 2011. V. 19. № 12. P. 588–595.
58. Docquier J.D., Mangani S. // Drug Resist. Updat. 2018. V. 36. № November 2017. P. 13–29.
59. King D.T., Sobhanifar S., Strynadka N.C.J. // Protein Sci. 2016. V. 25. № 4. P. 787–803.
60. Rotondo C.M., Wright G.D. // Curr. Opin. Microbiol. 2017. V. 39. P. 96–105.
61. Morar M., Pengelly K., Koteva K., Wright G.D. // Biochemistry. 2012. V. 51. № 8. P. 1740–1751.
62. Gomes C., Martínez-Puchol S., Palma N., Horna G., Ruiz-Roldán L., Pons M.J., Ruiz J. // Crit. Rev. Microbiol. 2017. V. 43. № 1. P. 1–30.
63. Schwarz S., Shen J., Kadlec K., Wang Y., Michael G.B., Feßler A.T., Vester B. // Cold Spring Harb. Perspect. Med. 2016. V. 6. № 11. P. 1–30.
64. Zárate S., De la Cruz Claure M., Benito-Arenas R., Revuelta J., Santana A., Bastida A. // Molecules. 2018. V. 23. № 2. P. 284.
65. Garneau-Tsodikova S., Labby K.J. // Med. Chem. Comm. 2016. V. 7. № 1. P. 11–27.
66. Soler Bistué A.J.C., Martín F.A, Vozza N., Ha H., Joaquín J.C., Zorreguieta A., Tolmasky M.E. // Proc. Natl. Acad. Sci. USA. 2009. V. 106. P. 13230–13235.
67. Fair R.J., McCoy L.S., Hensler M.E., Aguilar B., Nizet V., Tor Y. // ChemMedChem. 2014. V. 9. № 9. P. 2164–2171.
68. Santana A.G., Zárate S.G., Asensio J.L., Revuelta J., Bastida A. // Org. Biomol. Chem. 2016. V. 14. № 2. P. 516–525.
69. Labby K.J., Garneau-Tsodikova S. // Future Med. Chem. 2013. V. 5. № 11. P. 1285–1309.
70. Gao F., Yan X., Auclair K. // Chem. Eur. J. 2009. V. 15. № 9. P. 2064–2070.
71. Li Y., Green K.D., Johnson B.R., Garneau-Tsodikova S. // Antimicrob. Agents Chemother. 2015. V. 59. № 7. P. 4148–4156.
72. Shakya T., Stogios P.J., Waglechner N., Evdokimova E., Ejim L., Blanchard J.E., McArthur A.G., Savchenko A., Wright G.D. // Chem. Biol. 2011. V. 18. № 12. P. 1591–1601.
73. Welch K.T., Virga K.G., Whittemore N.A., Özen C., Wright E., Brown C.L., Lee R.E., Serpersu E.H. // Bioorganic Med. Chem. 2005. V. 13. № 22. P. 6252–6263.
74. Boehr D.D., Draker K., Koteva K., Bains M., Hancock R.E., Wright G.D. // Chem. Biol. 2003. V. 10. P. 189–196.
75. Berkov-Zrihen Y., Green K.D., Labby K.J., Feldman M., Garneau-Tsodikova S., Fridman M. // J. Med. Chem. 2013. V. 56. № 13. P. 5613–5625.
76. Galopin S., Cattoir V., Leclercq R. // FEMS Microbiol. Lett. 2009. V. 296. № 2. P. 185–189.
77. Mosher R.H., Camp D.J., Yang K., Brown M.P., Shaw W. V, Vining L.C., Mosher M., Microbiol G. // J. Biol. Chem. 1995. V. 270. № 45. P. 27000–27006.
78. Woodford N., Carattoli A., Karisik E., Underwood A., Ellington M.J., Livermore D.M. // Antimicrob. Agents Chemother. 2009. V. 53. № 10. P. 4472–4482.
79. Lee Y., Kim B.-S., Chun J., Yong J.H., Lee Y.S., Yoo J.S., Yong D., Hong S.G., D'Souza R., Thomson K.S., et al. // Biomed. Res. Int. 2014. V. 2014. P. 1–6.
80. Silver L.L. // Cold Spring Harb. Perspect. Med. 2017. V. 7. № 2. P. 1–12.
81. Roberts A.A., Sharma S. V., Strankman A.W., Duran S.R., Rawat M., Hamilton C.J. // Biochem. J. 2013. V. 451. № 1. P. 69–79.
82. De Pascale G., Wright G.D. // ChemBioChem. 2010. V. 11. № 10. P. 1325–1334.
83. Spanogiannopoulos P., Waglechner N., Koteva K., Wright G.D. // Proc. Natl. Acad. Sci. USA. 2014. V. 111. № 19. P. 7102–7107.
84. Koteva K., Cox G., Kelso J.K., Surette M.D., Zubyk H.L., Ejim L., Stogios P., Savchenko A., Sørensen D., Wright G.D. // Cell Chem. Biol. 2018. V. 25. № 4. P. 403–412.
85. Laborde J., Deraeve C., Bernardes-Génisson V. // ChemMedChem. 2017. V. 12. № 20. P. 1657–1676.

86. Zhang W., Fisher J.F., Mobashery S. // Curr. Opin. Microbiol. 2009. V. 12. № 5. P. 505–511.
87. Cha J.Y., Ishiwata A., Mobashery S. // J. Biol. Chem. 2004. V. 279. № 15. P. 14917–14921.
88. Allen H.K., Moe L.A., Rodbumrer J., Gaarder A., Handelsman J. // ISME J. 2009. V. 3. № 2. P. 243–251.
89. Boehr D.D., Daigle D.M., Wright G.D. // Biochemistry. 2004. V. 43. № 30. P. 9846–9855.
90. Daigle D.M., Hughes D.W., Wright G.D. // Chem. Biol. 1999. V. 6. № 2. P. 99–110.
91. Green K.D., Garneau-Tsodikova S. // Biochimie. 2013. V. 95. № 6. P. 1319–1325.
92. Green K.D., Chen W., Garneau-Tsodikova S. // Antimicrob. Agents Chemother. 2011. V. 55. № 7. P. 3207–3213.
93. Mendes R.E., Toleman M. A., Ribeiro J., Sader H.S., Jones R.N., Walsh T.R. // Antimicrob. Agents Chemother. 2004. V. 48. № 12. P. 4693–4702.
94. Robicsek A., Strahilevitz J., Jacoby G.A., Macielag M., Abbanat D., Chi H.P., Bush K., Hooper D.C. // Nat. Med. 2006. V. 12. № 1. P. 83–88.
95. Vetting M.W., Park C.H., Hegde S.S., Jacoby G.A., Hooper D.C., Blanchard J.S. // Biochemistry. 2008. V. 47. № 37. P. 9825–9835.

"Noah's Ark" Project: Interim Results and Outlook for Classic Collection Development

M. V. Kalyakin#, A. P. Seregin#, A. E. Solovchenko#, P. A. Kamenski*, V. A. Sadovnichiy
M.V. Lomonosov Moscow State University, Leninskie Gory, 1, Moscow, 119991, Russia
#These authors contributed equally to the work
*E-mail: peter@protein.bio.msu.ru
Received March 20, 2018; in final form November 09, 2018

ABSTRACT **The "Noah's Ark" project, afoot at M.V. Lomonosov Moscow State University since 2015 and aimed at studying biodiversity, is the largest ongoing Russian project in life sciences. During its implementation, several hundred new species have been described; a comprehensive genetic and biochemical characterization of these species, as well as that of the pre-existing specimens in Moscow University's collections, has been performed. A consolidated IT system intended to house the knowledge generated by the project has been developed. Here, we summarize the investigations around the Moscow University classical biocollections which have taken place within the framework of the project and discuss future promise and the outlook for these collections.**
KEYWORDS **Animals, biobank, depository, microorganisms, plants.**

INTRODUCTION

There is little doubt that, in the near future, our existence will be largely governed by so-called "big data": huge arrays of information whose effective use is already revolutionizing many aspects of human life. In the field of life sciences, the term "big data" is traditionally associated with genomic information; i.e., the results of sequencing of many genomes. However, genomic data is just one example of real "big data" generated by life sciences; namely, by profound studies of biological collections. A biological collection is defined as an organized repository of biological specimens of any kind – from dried plants to living human cells, and even sequenced genomes.

It is becoming increasingly clear that the potential of biological collections is significantly higher than has been commonly accepted. However, to harness this potential, one must treat biological collections as sources of "big data" – vast amounts of information about living systems. Combining this information with the modern techniques of life sciences would allow us to obtain invaluable insights into the origin and evolution of life on Earth. This is expected to arise from comparative studies of numerous biological samples. The resulting knowledge could be implemented in practice for the preservation of the biodiversity of our planet.

This was the guiding principle behind Noah's Ark, a project dedicated to the conservation, investigation, and profitable use of biological diversity. The most important prerequisite for successful implementation of the project was the creation of a unified virtual space for biocollections with the potential to harvest diverse data on a virtually unlimited number of biological samples. Such a space has already been created, so far on the scale of Moscow State University, but there are plans to make it nationwide. It is already obvious that a global approach to the study of biodiversity significantly increases the quality of scientific results, allowing us to identify more general, and more complex, patterns in the organization of life on our planet.

Here, we review the interim results of Noah's Ark project for classical biological (animal, plant, and microbiological) collections.

ANIMALS

The purpose of a biobank is to accumulate collections that adequately reflect the multidimensional structure of biodiversity (BD), making it possible to explore its various manifestations. An analysis of the scientific status of zoological collections was carried out [1], and it was shown that the collections perform the function of a research sample in BD studies. Their main characteristics are their representativeness, which is further detailed by their informational value, reliability, systemic character, scope, structure, etc.

The studies in the "Animals" section are aimed at analyzing key aspects of BD on the basis of an integrated approach combining phylogenomic and phylo-

morphological analyses of data resulted from electron microscopic and 3D reconstructions data.

The macrotaxonomic analysis of the main Animalia groups included taxa ranging from order to phylum. One fundamentally new finding is the reliable substantiation of the monophiletic status of the Lophophorata clade including Phoronida, Brachiopoda, and Bryozoa: it is supported by the architecture of the coelomic system and innervation of lophophore tentacles [2–9]. This conclusion is of crucial importance for elucidating the structure of the phylogeny of animals at the level of the Metazoan basal radiation. The study of phylogenetic relationships in the Ophiuroidea class was also one of the breakthroughs achieved. It is divided into the Euryophiurida and Ophintegrida superorders, and four new orders and 11 families have been recognized [10]. Essentially new results were obtained for the classification of the Nudibranchia (Mollusca) order, in which three new families were described [11]. The importance of pedomorphosis in the formation of new taxa of high rank and the need to study the diversity of ontogenetic patterns for their identification has been demonstrated within the framework of the ontogenetic systematics concept [12–15]. The molecular phylogenetic analysis demonstrated the monophily of eight genera of the Acrothoracica (Copepoda) superorder [16]. The analysis of the generic composition revealed 24 new taxa of this rank in the Gastropoda, Maxillopoda, and Mammalia classes [11, 17–22]. It is obvious that a sole phylogenomic approach to the analysis of the structure of macrotaxonomic diversity is insufficient: it should be supplemented by a study of morphological diversity at the level of ontogenetic patterns. This is consistent with the most recent ideas about the evo-devo concept according to which the historical development of multicellular organisms is mainly an evolution of their ontogeny; in macrotaxonomic studies, these ideas are developed through the concept of ontogenetic systematics.

The microtaxonomic analysis of species and subspecies was carried out on the basis of the concept of integrative taxonomy: species were identified using genetic material, then the results were clarified using morphological and epiphenotypic (including acoustic) characters.

New species and subspecies of animals were identified (their number is indicated in brackets) in Cercozoa (4) [23, 24], Cnidaria (1) [25], Kamptozoa (6) [21, 26], Phoronida (5) [3, 27], Nematoda (13) [28, 29], Annelida (9) [30–33], Chaetognatha (1) [34], Mollusca (27) [11, 17, 18, 35–41]; Maxillopoda (23) [42–46], Arachnida (2) [47, 48], Insecta (48) [49–60], Osteichthyes (7) [61–63], Amphibia (16) [64–67], Reptilia (14) [68], Aves (4) [69], and Mammalia (4) [22, 70]. The possibility of a reliable identification of the related species and subspecies of a number of Asian Insecta, Amphibia, Reptilia, Aves, and Mammalia by acoustic parameters was demonstrated for the first time [71–76]. A method has been developed for determining the genetic identity of jellyfish and polyps in the laboratory lines of some Cercozoa, which makes it possible to adequately assess the diversity of these species [77]. The specific and subspecific levels of taxonomic differentiation of the Asterocheridae and Ascothoracida groups have been marked [43, 45]: correct differentiation of these levels is one of the key challenges of microsystematics.

The combination of genomic phylogeography and genetic barcoding provided new data on the structure of species diversity in a number of animal groups. In the Nothybidae (Insecta) family [78], several economically important species of Salmonidae and Cyprinidae (Osteichthyes) [79–84] and species-level taxa from 10 families of terrestrial vertebrates in Eurasia have been studied in this respect [64, 85–95]. The high efficiency of *COI* gene analysis in revealing the diversity of phylogenetic lineages in a number of *Amphibia* genera has been demonstrated [96].

A preliminary study of the molecular genetic and morphological diversity of representatives of the Megophryidae, Dicroglossidae, Microhylidae, Rhacophoridae (Amphibia), and Gekkonidae (Reptilia) families revealed a high level of "hidden" species diversity, which requires a more detailed study. Comparative analysis of the geographic variability of some model Palaearctic bird species (Aegithalidae, Sylviidae, Corvidae families etc) indicates a group-specific nature of their intraspecific differentiation. [97]. Active reticular microevolution has been shown to occur in the genus *Darevskia* (Reptilia) [98]. Revealing the complex of sympatric forms of the genus *Salvelinus* (Osteichthies) suggests their sympatric speciation [81, 82]. It was found that local populations of *Hypomesus olidus* and *Salvelinus malma* (Osteichthies) are being formed as independent units in isolation on the Commander Islands [99, 100]. On the basis of a comprehensive analysis of fish from several families, weak agreement of divergence of population and species units in morphogenetic characteristics and the presence of a large number of cryptic species have been demonstrated; the species diversity of the studied groups of animals is significantly underestimated. Therefore, the key task is to translate the "hidden" diversity into an "obvious" one through collection and storage, including those of new forms of collection material, and the development of new methods for analyzing species differentiation.

Within the results of a study of the meronomic diversity of animals, the most impressive is the demonstration that the miniaturization of insects of

the Coleoptera (fam. Ptiliidae), Psocoptera (fam. Liposcelididae), and Thysanoptera orders, which are comparable in size to unicellulars (about 1 mm), has almost no effect on the anatomy of the most important organs of the head section [101, 102]. The result is of fundamental importance for understanding the mechanisms that ensure conservation of the structure of multicellular animals. A new type of oogenesis, autoheterosynthesis, has been described in Phoronida [103], which expands our comprehension of the diversity of ontogenetic patterns. A mechanism for the emission of sound signals has been, for the first time, discovered in representatives of a number of Orthopteran and Homopteran families, suggesting repeated formation of a similar stridulation signal during their evolution [71]. The results of the analysis of vibration and sound signals in the species of a number of Orthoptera and Homoptera families [71–73, 77] confirm the hypothesis that they serve as an effective reproductive barrier. Cranial differences in isolated populations of Arctic fox *Vulpes lagopus* on the Commander Islands were shown to result from selection, rather than genetic drift [104].

In the studies of the biochorological section, the faunistic complexes of invertebrates and vertebrates of the seas of the Arctic Basin, the Russian Far East, the North Atlantic, the Australasian tropical seas, and the Red Sea were examined. An analysis of the diversity of representatives of five Nematoda groups of hydrothermal sites of the Mid-Atlantic Ridge at depths of 1,200–1,500 m [105, 106] was conducted. In terms of taxonomic composition and biological characteristics, hydrothermal nematodes differ from deep-water bathyal and abyssal nematodes, but they are similar to shelf and sublittoral species and communities. It has been shown that the faunistic diversity of marine benthic heterotrophic representatives of Flagellata in the World Ocean is more consistent with the predictions of the "cosmopolitanism" model rather than "moderate endemism" [107]. It is shown that the Harpacticoida fauna at low latitudes is much richer and has a significantly higher degree of endemism compared to the fauna of high latitudes; the populations of shallow (up to 50 m) and deeper zones differ in species composition. A significant difference between the harpacticoid faunas of the Eastern and Western parts of the Arctic seas has been revealed [108]. The composition of the Laptev Sea macrobenthos and its diversity revealed the presence of a general bathymetric trend: one set of factors affects both the composition and functioning of benthic communities [109]. It has been established that differences in the composition of the Cladocera freshwater fauna of the Arctic and Subarctic zones are determined primarily by modern climatic factors, which makes it possible to use these faunistic complexes as bioindicators [110]. Large-scale studies of the invertebrate species composition of the Arctic and Far Eastern seas have been carried out, and new data on representatives of Ciliophora and Kamptozoa have been obtained [109, 111–113]. A relationship between genetic, morphological, and taxonomic diversity in the four Annelida families from the fauna of the northern seas has been revealed [109]. The species composition of the Cladocera of the freshwater lakes and shallow seas of Asia was clarified [114, 115]; it has been found that the Cladocera fauna of the coastal waters of Borneo is significantly poorer than the mainland one [116]. Four types of communities of shell amoebas (Testacea) were identified in the basin of the Belaya River [117].

The development of an integrated approach to long-term monitoring of the spatial dynamics of species and faunistic diversity based on the regular collection and analysis of monitoring collections in the focal regions of northern Eurasia is of fundamental importance [118]. It allows for the identification of regions with potentially increased vulnerability for biodiversity and proposing measures for its conservation.

The study of the ecological aspect of BD mainly centers on the analysis of the spatial dynamics of the energetics of birds inhabiting different environments. A significant specificity of the energy of Old World tropical birds was confirmed. In particular, it was demonstrated that the absence of a phylogenetic signal in basal metabolism is independent of body weight [119].

PLANTS

Reconstruction of the origin, spread, and kinship of various groups of plants in the project is achieved through a wide use of molecular methods in classical science.

In the Fabaceae family, the results of a long-term molecular-genetic and morphological analysis of wild bird-foots made it possible to reconstruct not only the evolution of the *Lotus* genus, but also the key points of the historical biogeography of the group [120]. The independence of families close to the bird-foots *Hammatolobium*, *Tripodion,* and *Cytisopsis* was also demonstrated [121]. The history of the *Lagochilus* genus from the Lamiaceae family was also reconstructed [122]. It was shown that the diversification of this Central Asian genus is directly related to recent geological history and subsequent climatic shifts. In the Apiaceae family, the scope of intrageneric divisions in the *Prangos* genus has been revised based on a DNA analysis and a new *Koelzella* subgenus has been established [123]. In turn, the "forgotten" Afghan endemic *Prangos akymatodes* [124] was restored as a separate species within. In addition, in order to ensure monophyletism, the monotypic

Alococarpum genus was transferred to the *Prangos* genus [125].

The integrative molecular-morphological approach allows not only to establish the origin and relationship of taxa, but also to restore the most probable course of evolution of individual features. For example, the presence of single-seeded fruits from a common ancestor of the Caryophyllales order, numbering 12,000 species, has been established [126]. A detailed description of the seeds of the polyphyletic *Mollugo* genus was provided, which made it possible to draw important conclusions for the classification and taxonomy of groups [127]. A consistency of seeds structure features with the latest molecular data has also been demonstrated for Caucasian species of the *Minuartia* genus [128].

Molecular phylogenetic analysis was used to demonstrate the need to revise many groups of moss. The most illustrative example is the polyphilia of the Ditrichaceae family: a detailed analysis convincingly demonstrated that characteristics that were considered to be taxonomically significant appeared independently in different groups [129]. Based on this relationship, a new order and three new moss families have been described [130]. Further revision of individual groups of mosses led to a significant revision of relations in the Grimmiales order [131].

Attempts to solve the particular problem of describing a new species of *Bryoerythrophyllum duellii*, using molecular data not only for this genus, but also for its immediate relatives, made it possible to completely revise the scope of the *Bryoerythrophyllum* genus [132].

An in-depth study of the genomes of flowering plants and mosses has been performed. The full plastomas of three types of *Dryopteris*, *Adianthum hispidulum* [133], *Seseli montanum* [134], and some others, has been deciphered and annotated. The structure of the intergenic spacer IGS1 of the ribosomal operon in moss of the *Schistidium* genus was studied in detail [135].

An example of a monographic study that combines both the classical morphological approach and the latest molecular methods is the processing of herbarium specimens of wild onions from the *Allium saxatile* group [136]. Of the 15 species, five were new to science. Geographic isolation was the main cause of previously underestimated speciation: researchers were able to describe new species from Romania, Bulgaria, Russia, Kazakhstan, and China. Later, another type of onion from Uzbekistan [137] and another one from Turkey [138] were described.

A monographic revision of the recently described *Paramollugo* (Molluginaceae) genus, which, as expected, consists of only three species, has doubled the number of known species [139]. Two new species are described for Madagascar (*Paramollugo simulans* and *P. elliotii*), and another "forgotten" species was found in collections from New Caledonia.

Another successful example of monographic processing is the revision of the African *Corbichonia* (Lophiocarpaceae) genus, which included only two species [140]. A third species, *C. exellii*, which is spread over several countries of Southern Africa at once, has been discovered and certified.

The results of the revision of the *Rhabdosciadium* genus from the Apiaceae family have been published, which includes seven species distributed in the mountainous areas of Turkey and Iran. It was possible to analyze the DNA of all members of the genus, including several narrow-local endemics. The monophyletism of this genus has been demonstrated, and a new species, *R. anatolyi,* common in Turkish Kurdistan [141], has been described. A new species of endemic umbellate from Laos has been found: *Xyloselinum laoticum* [142].

The traditional study of the systemic structure and taxonomy of the Chenopodiaceae family has been extended. A new species, *Dysphania geoffreyi*, has been described for areas hard-to-reach for European researchers, such as Lhasa and Bhutan [143]. Subsequently, *Atriplex congolensis* orach from the Democratic Republic of the Congo [144] and the *Arthrocnemum franzii* saltwater from the Cape Verde Islands [145] have been described.

According to the results of an extensive revision of the genus *Atraphaxis*, several new taxa of the Polygonaceae family have emerged: *Atraphaxis kamelinii* species from Mongloia [146], *Bactria* genus with *B. lazkovii*species from Kygryzstan [147], and the *Persepolium* genus [148].

For reasons of nomenclature, *Calciphilopteris wallichii,* a new species of fern from the Philippines, had to be re-described [149]. We would also like to note the description of a new species of moss *Schistidium relictum* [150], widespread in Canada and Russia.

Refining of our knowledge of the geographical distribution of organisms follows two paths: studying existing collections that had not previously been described accurately and field studies. As a result of this work, a whole layer of new data has been acquired, which is referred to as "floristic finds" [151].

One of the most remarkable discoveries is that of *Scapania aspera* earwort. It was possible to find in nature, correctly recognize, and subsequently perform a DNA analysis of the plant found on the Anabarsky plateau, 3,000 km from the nearest known habitats of this earwort in Europe [152].

Floristic finds are merely at the top of a huge reservoir of information that accumulates as a result of a floristic survey of any territory. The results of such work are reflected in the "Floras" and checklists. For

example, the results of studying the flora of Sevastopol were summarized. It has been shown that the western extremity of Mountainous Crimea is one of the most floristically rich corners of Russia, with 1,859 species of vascular plants recorded in an area of about 600 km^2 [153].

Important results were obtained in the field of palelinology during the course of the project. Mass pollination of plants can be considered not only as a biological process, but also as a special natural phenomenon that can be studied from the standpoint of botany, meteorology, paleogeography, and allergology.

A group of palynologists analyzed long-term data on birch pollination in the Moscow region and identified the main meteorological factors affecting the concentration of pollen during its season [154]. A comparative study of urban and suburban pollen spectra showed that pollen monitoring station data collected in large cities can be extrapolated to the surrounding countryside [155].

Traditional studies of the morphology and anatomy of pollen and spores were extended: heterosulcate pollen grains of the swamp forget-me-not *Myosotis scorpioides* and their development were described in detail [156], as well as the structure of sphagnum moss spores at different stages of germination [157].

Herbarium samples are an important and easily accessible source for the selection of DNA samples, but DNA molecules are gradually destroyed during storage. Therefore, the method developed for extracting DNA from old herbarium specimens deserves special attention [158].

Translating these collections into electronic form or, in other words, virtualization of the collection space was conceived as a mainstream development in the study of plants. The large project on the digitization of the Herbarium of Moscow State University was used as the basis for this work [159].

MICROORGANISMS AND FUNGI

Within the "Microorganisms and fungi" section, a comprehensive depository of bacteria, fungi, fungi-like organisms (myxomycetes and oomycetes), and algae has been created. A unique array of information about the microorganisms has been compiled, along with extensive collections important for scientific research as well as for practice. The uniqueness of the biomaterial collections and knowledge accumulated within the framework of the Project rests in its complexity and the scope of the biodiversity captured in the collections and in the diversity of the habitats screened. Microbial communities of soils of different natural zones, urbanized biotopes, habitats with extreme conditions have been characterized [160]. An important aspect was the study of the soil microbial communities of Antarctica [161–165]. The dominant fungi in moss-covered Antarctic soil were those from the genera *Phoma, Thelebolus, Penicillium, Rhodotorula*, in "cobblestone pavement", *Cadophora, Cladosporium, Cladophialophora*, in aquatic habitats, *Antarctomyces, Hyphozyma, Goffeauzyma, Phoma, Thelebolus, and Geotrichum.*

Another group of fungi, macromycetes, was the focus of research on diversity, ecology, and potential practical use. This group encompasses major decomposers closing the nutrient loop in ecosystems. Rare species were found [166], and a number of new species of macromycete fungi have been described [167–169]. The study of urbanized ecosystems was equally important, as was the inventory and quantification of potentially pathogenic fungal species in the soil [170, 171] and plant pollen [172]. Micromycete complexes enriched with species potentially hazardous to health and causing bio-damage are forming in urban soils [171]. On the other hand, parks and botanical gardens created in cities are refugia for rare and interesting species of mushrooms and myxomycetes. The previously unexplored and poorly described features of yeasts from diverse soil types and biocenoses have been studied: soils in the temperate zone of Russia [173], soils under the thickets of invasive plants (such as *Heracleum sosnowskyi*) [174–176], soils under the vineyards of Dagestan [177, 178], and plantations in South Vietnam [179]. Overall, the soils turned out to be a natural reservoir of yeast biodiversity.

Fungi and fungi-like organisms (myxomycetes and oomycetes) are extremely important both for the functioning of ecosystems and for human practice. Their ubiquity obviates the need for collections encompassing many different regions for studying these organisms. It is important to cover both reference habitats in natural reserves and anthropogenically impacted areas. The Project made it possible to carry out unprecedentedly broad studies of the diversity of soil microscopic fungi and myxomycetes of nature reserves (the Central Forest Biosphere Reserve, the Kaluga Zaseki Reserve, the Volga-Akhtubinskaya Floodplain Natural Park) [180]. Extensive data on the diversity and distribution of microscopic fungi in the protected forests of Vietnam were collected both for cultivated and uncultivable species, as well for myxomycetes [181].

The collections created within the framework of the Project became a unique database for studies of practically important microorganisms. Strains–producers of broad-spectrum antibiotics from the peptaibol family [182], the anticancer metabolite Brefeldin-A, as well as potential steroid producers, have been identified [183]. The study of phytopathogenic fungi in both natural habitats, which are reservoirs of phytopathogens, and

in agrocenoses is of great interest and practical importance [184]. Extensive collections were created and used as the basis for population studies of the most dangerous potato pathogens, *Phytophthora infestans* [185] and *Alternaria* [186]. Their population features and mechanisms of fungicide resistance have been identified [187, 188]. Among the huge diversity of microorganisms inhabiting different soil horizons, yeast fungi deserve special attention as one of the most biotechnologically significant groups of microorganisms [189].

Identification of the most resilient microorganisms in the extreme natural habitats of the Earth is among the most important tasks of microbiology, largely unsolvable without the study of ancient rock sediments. Gamma-ray resistance of the microbial communities from permafrost sedimentary rocks of the Arctic was studied by exposure to gamma radiation (100 kGy) in low temperature (−50 °C) and low pressure (1 mmHg) conditions. These results can be considered as terrestrial models of the conditions encountered by microorganisms in the regolith habitats on Mars. Microbial communities of permafrost showed high resistance to the simulated harsh extraterrestrial conditions, retaining ample cultured, metabolically active prokaryotes [190]. The results obtained indicate the possibility of long-term cryopreservation of viable microorganisms in the Martian regolith. Taking into account the intensity of radiation on the surface of Mars, our data suggest the possibility of conservation of hypothetical Mars ecosystems in the regolith layer (e.g. protected from UV rays) for at least 1.3–2 mln years. At a depth of 2 m (the estimated sampling depth of the ExoMars 2020 mission), the viability expectance is at least 3.3 mln years, and at a depth of 5 m–at least 20 mln years. Of particular interest are microscopic fungi naturally adapted to extreme salinities and alkalinities. Therefore, a collection of isolates from the White Sea marshy habitats [191] and soda solonchaks [192] was a focus of the project, generating a plethora of physiological and biochemical studies. Important stress tolerance mechanisms associated with the structure of membranes were deciphered using these collections [193].

CONCLUSIONS AND OUTLOOK

The abovementioned studies convincingly demonstrate the scientific potential in approaching biocollection studies globally. Such an approach presumes, for example,, comprehensive analyses of large numbers of samples regardless of their (zoological, botanical or microbiological) nature. Moreover, the depth of the insight from comparative studies seems to linearly or even exponentially depend on the number of specimens involved. Therefore, the number of biological specimens available should be maximized by every means for further progress in comprehensive biological studies. We believe that the natural way to achieve this is to embrace as many biological collections as possible in a consolidated data environment. The prototype of such an environment has already been created in the form of the IT-system of the Noah's Ark project (https://depo.msu.ru/). As of March 2018, the IT -system contained information on more than a million biological specimens. Making this system nationwide will provide a powerful impetus to the development of life sciences in Russia and to the translation of the fundamental research results into practice. We envision the extension of the IT-system of the Noah's Ark project towards the main directions of its development.

The success of the Noah's Ark project is largely due to its interdisciplinary character. Implementation of the project was the main driver behind fulfilling the long-held dream of classical biocollection owners at MSU–creating genetic and biochemical service labs focused on maintenance of these collections. Of course, specimens of these collections had been studied before, but that activity was of secondary importance to other laboratories in the project, naturally affecting their efficiency. At present, any specimen newly deposited in a MSU collection is subjected to thorough genetic and, in many cases, biochemical characterization. It also became possible to analyze DNA extracted from museum samples. Of special importance is the possibility of comprehensive microscopic studies. It is clear that such an integrated approach will be much more insightful. There is also little doubt that the synthesis of the classical and modern research methods implemented in the project must be fully endorsed and further developed in other research areas.

Collectively, we envision (i) the extension of the project IT nationwide and, later, internationally as well as (ii) the elaboration of new advanced genetic, biochemical, and physico-chemical tools that would be used to analyze specimens from biocollections as the main avenues for further development of the Noah's Ark project. ●

The authors express their deep gratitude to the team participating in the grant, the Noah's Ark project team. M.V. Kalyakin is especially grateful to I.Ya. Pavlinov for his assistance in work on the manuscript.

This work was supported by the Russian Science Foundation (Grant No. 14-50-00029).

REFERENCES

1. Pavlinov I.Ya., Kalyakin M.V., Sysoev A.V. // Arch. Zool. Mus. MSU. 2016. V. 54. P. 733–786.
2. Temereva E.N. // Evol. Dev. 2017. V. 19. P. 171–189.
3. Temereva E.N., Chichvarkhin A. // Invertebr. Syst. 2017. V. 31. № 1. P. 65–84.
4. Temereva E.N., Kosevich I.A. // BMC Evol. Biol. 2016. V. 16. № 181. P. 1–24.
5. Temereva E.N., Neretina T.V., Stupnikova A.N. // Russ. J. Mar. Biol. 2016. V. 42. № 2. P. 128–138.
6. Temereva E.N., Malakhov V.V. // BMC Evol. Biol. 2015. V. 15. № 229. P. 1–28.
7. Temereva E.N. // J. Zool. 2015. V. 296. № 2. P. 79–94.
8. Temereva E.N., Tsitrin E.B. // PLoS One. 2015. V. 10. № 4. P. e0123040.
9. Temereva E.N., Gebruk A.A., Malakhov V.V. // Zool. Anz. 2015. V. 256. P. 22–27.
10. O'Hara T.D., Hugall A.F., Thuy B., Stohr S., Martynov A.V. // Mol. Phylogenet. Evol. 2017. V. 107. P. 415–430.
11. Korshunova T., Martynov A., Bakken T., Evertsen J., Fletcher K., Mudianta I.W., Saito H., Lundin K., Schrodl M., Picton B. // Zookeys. 2017. № 717. P. 1–139.
12. Stohr S., Martynov A. // PLoS One. 2016. V. 11. № 11. P. e0164562.
13. Ezhova O.V., Malakhov V.V., Martynov A.V. // Zoomorphology. 2016. V. 135. № 3. P. 333–350.
14. Zhadan A., Vortsepneva E., Tzetlin A. // Zoomorphology. 2015. V. 134. № 4. P. 509–521.
15. Martynov A., Ishida Y., Irimura S., Tajiri R., O'Hara T., Fujita T. // PLoS One. 2015. V. 10. № 10. P. e0139463.
16. Lin H.C., Kolbasov G.A., Chan B.K.K. // Mol. Phylogenet. Evol. 2016. V. 100. P. 292–302.
17. Korshunova T., Zimina O., Martynov A. // J. Mollus. Stud. 2017. V. 83. P. 409–421.
18. Korshunova T., Martynov A., Picton B. // Zootaxa. 2017. V. 4324. № 1. P. 1–22.
19. Sinev A.Y., Tiang-Nga S., Sanoamuang L. // Zootaxa. 2017. V. 4276. № 3. P. 416–426.
20. Martynov A., Korshunova T. // J. Mollus. Stud. 2015. V. 81. P. 365–379.
21. Borisanova A.O. // Zootaxa. 2016. V. 4084. № 1. P. 135–142.
22. Shenbrot G., Bannikova A., Giraudoux P., Quere J.P., Raoul F., Lebedev V. // J. Zool. Syst. Evol. Res. 2017. V. 55. № 4. P. 356–368.
23. Bobrov A., Mazei Y. // Zootaxa. 2017. V. 4294. № 5. P. 600–600.
24. Bobrov A., Mazei Y. // Zootaxa. 2017. V. 4282. № 2. P. 292–308.
25. Kolbasova G.D., Zalevsky A.O., Gafurov A.R., Gusev P.O., Ezhova M.A., Zheludkevich A.A., Konovalova O.P., Kosobokova K.N., Kotlov N.U., Lanina N.O., et al. // Polar Biol. 2015. V. 38. № 9. P. 1439–1451.
26. Borisanova A.O., Potanina D.M. // Zootaxa. 2016. V. 4184. № 2. P. 376–382.
27. Temereva E.N., Stupnikova A.N., Neretina T.V. // Syst. Biodivirs. 2016. V. 14. № 5. P. 509–523.
28. Tchesunov A.V. // Zootaxa. 2017. V. 4306. № 4. P. 478–500.
29. Fedyaeva M.A., Neretina T.V., Konovalova O.P., Tchesunov A.V. // Zootaxa. 2016. V. 4121. № 4. P. 382–411.
30. Zhadan A.E., Tzetlin A.B., Salazar-Vallejo S.I. // Zootaxa. 2017. V. 4226. № 1. P. 75–92.
31. Jirkov I.A. // Zootaxa. 2016. V. 4117. № 1. P. 125–134.
32. Schiaparelli S., Jirkov I.A. // Ital. J. Zool. 2016. V. 83. № 4. P. 531–542.
33. Zhadan A. // Rec. Aust. Mus. 2015. V. 67. № 1. P. 1–24.
34. Kulagin D.N., Neretina T.V. // ICES J. Mar. Sci. 2017. V. 74. № 7. P. 1875–1884.
35. Korshunova T., Martynov A., Bakken T., Picton B. // Zool. Scr. 2017. V. 46. № 6. P. 683–692.
36. Martynov A., Korshunova T. // Zootaxa. 2017. V. 4299. № 3. P. 391–404.
37. Furfaro G., Picton B., Martynov A., Mariottini P. // Zootaxa. 2016. V. 4193. № 2. P. 304–316.
38. Shipway J.R., O'Connor R., Stein D., Cragg S.M., Korshunova T., Martynov A., Haga T., Distel D.L. // PLoS One. 2016. V. 11. № 5. P. e0155269.
39. Korshunova T.A., Sanamyan N.P., Martynov A.V. // Zookeys. 2016. № 634. P. 15–28.
40. Korshunova T., Sanamyan N., Zimina O., Fletcher K., Martynov A. // Zookeys. 2016. № 630. P. 19–42.
41. Ekimova I., Korshunova T., Schepetov D., Neretina T., Sanamyan N., Martynov A. // Zool. J. Linn. Soc.-Lond. 2015. V. 173. № 4. P. 841–886.
42. Kolbasov G.A., Chan B.K.K., Cheng Y.R. // Zootaxa. 2017. V. 4290. № 3. P. 591–599.
43. Yu M.C., Kolbasov G.A., Hosie A.M., Lee T.M., Chan B.K.K. // Zootaxa. 2017. V. 4277. № 2. P. 151–198.
44. Maran B.A.V., Kim I.H., Bratova O.A., Ivanenko V.N. // Syst. Parasitol. 2017. V. 94. № 2. P. 227–241.
45. Kolbasov G.A., Chan B.K.K., Molodtsova T.N., Achituv Y. // Zootaxa. 2016. V. 4178. № 2. P. 182–208.
46. Kolbasov G.A., Chan B.K.K., Petrunina A.S. // Zootaxa. 2015. V. 3972. № 3. P. 328–342.
47. Mikhailov K.G., Otto S., Japoshvili G. // Zool. Middle East. 2017. V. 63. № 4. P. 362–368.
48. Mikhailov K.G. // Zookeys. 2016. № 558. P. 153–169.
49. Tishechkin D.Y. // Zootaxa. 2017. V. 4216. № 6. P. 537–558.
50. Galinskaya T.V., Shatalkin A.I. // Orient. Insects. 2017. V. 51. № 1. P. 6–10.
51. Gorbunov O.G., Krupitsky A.V., Marusov A.A. // Zootaxa. 2017. V. 4273. № 4. P. 559–575.
52. Prosvirov A.S. // Zootaxa. 2017. V. 4323. № 2. P. 269–276.
53. Prosvirov A.S. // Zootaxa. 2017. V. 4232. № 3. P. 376–384.
54. Prosvirov A.S. // Zootaxa. 2016. V. 4168. № 2. P. 279–296.
55. Galinskaya T.V. // Zookeys. 2016. № 615. P. 119–141.
56. Galinskaya T.V., Shatalkin A.I. // Zootaxa. 2015. V. 4012. № 3. P. 581–592.
57. Ozerov A.L., Krivosheina M.G. // Zootaxa. 2015. V. 4012. № 2. P. 201–257.
58. Tishechkin D.Y. // Zootaxa. 2015. V. 3985. № 1. P. 31–52.
59. Prosvirov A.S. // Zootaxa. 2015. V. 3980. № 3. P. 442–446.
60. Krivosheina M.G., Ozerov A.L. // Zootaxa. 2015. V. 3974. № 4. P. 595–598.
61. Markevich G.N., Esin E.V., Saltykova E.A., Busarova O.Y., Anisimova L.A., Kuzishchin K.V. // Russ. J. Mar. Biol. 2017. V. 43. № 3. P. 216–223.
62. Vasil'eva E.D., Kim D., Vasil'ev V.P., Ko M.H., Won Y.J. // Zootaxa. 2016. V. 4208. № 6. P. 577–591.
63. Vasil'eva E.D., Mousavi-Sabet H., Vasil'ev V.P. // Acta Ichthyol. Piscat. 2015. V. 45. № 2. P. 189–197.
64. Chen J.M., Zhou W.W., Poyarkov N.A., Stuart B.L., Brown R.M., Lathrop A., Wang Y.Y., Yuan Z.Y., Jiang K., Hou M., et al. // Mol. Phylogenet. Evol. 2017. V. 106. P. 28–43.
65. Min M.S., Baek H.J., Song J.Y., Chang M.H., Poyarkov N.A. // Zootaxa. 2016. V. 4169. № 3. P. 475–503.
66. Orlov N.L., Poyarkov N.A., Nguyen T.T. // Russ. J. Herpetol. 2015. V. 22. № 3. P. 206–218.
67. Poyarkov N.A., Rowley J.J.L., Gogoleva S.I., Vassilieva

A.B., Galoyan E.A., Orlov N.L. // Zootaxa. 2015. V. 3931. № 2. P. 221–252.
68. Faizi H., Rastegar-Pouyani N., Rastegar-Pouyani E., Nazarov R., Heidari N., Zangi B., Orlova V., Poyarkov N. // Zootaxa. 2017. V. 4320. № 2. P. 289–304.
69. Alstrom P., Rasmussen P.C., Zhao C., Xu J.Z., Dalvi S., Cai T.L., Guan Y.Y., Zhang R.Y., Kalyakin M.V., Lei F.M., Olsson U. // Avian Res. 2016. V. 7. P. 1–39.
70. Kruskop S.V. // Acta Chiropterol. 2015. V. 17. № 1. P. 49–57.
71. Tishechkin D.Y. // Zootaxa. 2017. V. 4318. № 3. P. 531–547.
72. Tishechkin D.Y. // Zootaxa. 2017. V. 4318. № 1. P. 167–176.
73. Tishechkin D.Y. // Zootaxa. 2015. V. 3999. № 4. P. 537–548.
74. Poyarkov N.A., Duong T.V., Orlov N.L., Gogoleva S.S., Vassilieva A.B., Nguyen L.T., Nguyen V.D.H., Nguyen S.N., Che J., Mahony S. // Zookeys. 2017. № 672. P. 49–120.
75. Vassilieva A.B., Gogoleva S.S., Poyarkov N.A. // Zootaxa. 2016. V. 4127. № 3. P. 515–536.
76. Samotskaya V., Marova I., Kvartalnov P., Arkhipov V.Y., Ivanitskii V. // Bird Study. 2016. V. 63. № 4. P. 479–489.
77. Zhantiev R., Korsunovskaya O., Benediktov A. // Eur. J. Entomol. 2017. V. 114. P. 301–311.
78. Prudkovsky A.A., Neretina T.V. // Polar Biol. 2016. V. 39. № 3. P. 533–542.
79. Galinskaya T.V., Oyun N.Y., Teterina A.A., Shatalkin A.I. // Oriental Insects. 2016. V. 50. № 2. P. 69–83.
80. Soshina V.A., Pavlov S.D., Zelenina D.A. // Russ. J. Genet. 2016. V. 52. № 11. P. 1208–1213.
81. Pavlov S.D., Ponomareva E.V., Kholodova M.V., Melnikova M.N., Mineeva T.V. // Biol. Bull. 2016. V. 43. № 1. P. 12–20.
82. Stierandova S., Vukic J., Vasil'eva E.D., Zogaris S., Shumka S., Halacka K., Vetesnik L., Svatora M., Nowak M., Stefanov T., et al. // Mol. Phylogenet. Evol. 2016. V. 94. P. 479–491.
83. Gruzdeva M.A., Pichugin M.Y., Kuzishchin K.V., Pavlov S.D., Melnikova M.N. // Russ. J. Mar. Biol. 2015. V. 41. № 6. P. 432–447.
84. Osinov A.G., Senchukova A.L., Mugue N.S., Pavlov S.D., Chereshnev I.A. // Biol. J. Linn. Soc. 2015. V. 116. № 1. P. 63–85.
85. Poyarkov N.A., Orlov N.L., Moiseeva A.V., Pawangkhanant P., Ruangsuwan T., Vassilieva A.B., Galoyan E.A., Nguyen T.T., Gogoleva S.S. // Russ. J. Herpetol. 2015. V. 22. № 4. P. 241–280.
86. Orlova V.F., Poyarkov N.A., Chirikova M.A., Nazarov R.A., Munkhbaatar M., Munkhbayar K., Terbish K. // Zootaxa. 2017. V. 4282. № 1. P. 1–42.
87. Spiridonova L.N., Valchuk O.P., Red'kin Y.A., Saitoh T., Kryukov A.P. // Russ. J. Genet. 2017. V. 53. № 8. P. 885–902.
88. Conklin J.R., Reneerkens J., Verkuil Y.I., Tomkovich P.S., Palsboll P.J., Piersma T. // J. Ornithol. 2016. V. 157. № 1. P. 325–332.
89. Abramov A.V., Bannikova A.A., Lebedev V.S., Rozhnov V.V. // Zootaxa. 2017. V. 4232. № 2. P. 216–230.
90. Bannikova A.A., Zemlemerova E.D., Colangelo P., Sozen M., Sevindik M., Kidov A.A., Dzuev R.I., Krystufek B., Lebedev V.S. // Zool. J. Linn. Soc.-Lond. 2015. V. 175. № 4. P. 930–948.
91. Bogdanov A.S., Lebedev V.S., Zykov A.E., Bakloushinskaya I.Y. // Russ. J. Genet. 2015. V. 51. № 12. P. 1243–1248.
92. Poplavskaya N.S., Romanenko S.A., Serdyukova N.A., Trifonov V.A., Yang F.T., Nie W.H., Wang J.H., Bannikova A.A., Surov A.V., Lebedev V.S. // Cytogenet. Genome Res. 2017. V. 152. № 2. P. 65–72.
93. Poplavskaya N.S., Lebedev V.S., Bannikova A.A., Belokon M.M., Belokon Y.S., Pavlenko M.V., Korablev V.P., Kartavtseva I.V., Bazhenov Y.A., Surov A.V. // Russ. J. Genet. 2017. V. 53. № 1. P. 76–90.
94. Lissovsky A.A., Obolenskaya E.V., Ge D.Y., Yang Q.S. // Hystrix. 2017. V. 28. № 1. P. 107–109.
95. Lissovsky A.A., Yatsentyuk S.P., Ge D.Y. // Zool. Scr. 2016. V. 45. № 6. P. 583–594.
96. Yuan Z.-Y., Zhou W.-W., Chen X., Poyarkov N.A., Chen H.-M., Jang-Liaw N.-L., Chou W.-H., Matzke N.J., Iizuka K., et al. // Syst. Biol. 2016. V. 65. № 5. P. 824–842.
97. Red'kin Ya.A., Arkhipov V.Yu., Volkov S.V., Mosalov A.A., Koblik E.A. // XIV International ornithological conf. Northern Eurasia. 2015. V. 2. P. 104–138.
98. Spangenberg V., Arakelyan M., Galoyan E., Matveevsky S., Petrosyan R., Bogdanov Y., Danielyan F., Kolomiets O. // Genes. 2017. V. 8. № 6. e149. doi: 10.3390/genes8060149
99. Melnikova M.N., Senchukova A.L., Pavlov S.D., Malyutina A.M. // Izv. Acad. Nauk. Ser. Biol. 2018. № 1. P. 16–21.
100. Soshnina V.A., Pavlov S.D., Zelenina D.A. // Russ. J. Genet. 2016. V. 52. № 11. P. 1336–1341.
101. Anton E., Yavorskaya M.I., Beutel R.G. // J. Morphol. 2016. V. 277. № 5. P. 615–633.
102. Polilov A.A., Shmakov A.S. // Arthropod Struct. Dev. 2016. V. 45. № 5. P. 496–507.
103. Temereva E.N. // J. Morphol. 2018. V. 279 № 2. P. 199–215.
104. Nanova O., Proa M. // Polar Res. 2017. V. 36. doi: 10.1080/17518369.2017.1310976
105. Tchesunov A.V. // Helgoland Mar. Res. 2015. V. 69. № 4. P. 343–384.
106. Geisen S., Mitchell E.A.D, Wilkinson D., Adl S., Bonkowski M., Brown M., Fiore-Donne A.M., Heger Th., Jassey V., Krashevska V., et al. // Soil Biol. Biochem. 2017. V. 111. P. 94–103.
107. Azovsky A.I., Garlitska L.A., Chertoprud E.S. // Mar. Biol. 2016. V. 163. № 5. P. 1–12.
108. Novichkova A.A., Azovsky A.I.// Polar Biol. 2017. V. 40. № 1. P. 185–198.
109. Kokarev V.N., Vedenin A.A., Basin A.B., Azovsky A.I.// J. Sea Res. 2017. V. 129. P. 61–69.
110. Ratcliffe J., Creevy A., Andersen R., Zarov E., Gaffney P., Taggart M., Mazei Yu, Tsyganov A., Rowson J., Lapshina E.D., et al. // Sci. Total Environ. 2017. V. 607–608. P. 816–828.
111. Novichkova A.A., Chertoprud E.S. // J. Nat. Hist. 2017. V. 51. № 29–30. P. 1781–1793.
112. Alalykina I.L., Dnestrovskaya N.Y., Jirkov I.A. // Zookeys. 2017. № 684. P. 1–18.
113. Garlitska L.A., Azovsky A.I. // J. Nat. Hist. 2016. V. 50. № 47–48. P. 2941–2959.
114. Chertoprud E.S., Sinev A.Y., Dimante-Deimantovica I. // Zootaxa. 2017. V. 4258. № 6. P. 561–573.
115. Sinev A.Y. // Zootaxa. 2016. V. 4200. № 4. P. 451–486.
116. Sinev A.Y., Yusoff F.M. // Zootaxa. 2015. V. 4000. № 5. P. 581–591.
117. Malysheva E., Mazei N., Shapovalov M., Saprykin M., Mazei Yu. // Inland Water Biol. 2017. V. 10. № 1. P. 92–96.
118. Romanov A.A., Koroleva E.G., Dikareva T.V. // Nat. Conservation-Bulgaria. 2017. № 22. P. 191–218.
119. Bushuev A., Tolstenkov O., Zubkova E., Solovyeva E., Kerimov A. // Curr. Zool. 2018. V. 64. № 1. P. 33–43.
120. Kramina T.E., Degtjareva G.V., Samigullin T.H., Valiejo-Roman C.M., Kirkbride J.H., Volis S., Deng T., Sokoloff D.D. // Taxon. 2016. V. 65. № 5. P. 997–1018.
121. Sokoloff D.D., Kramina T.E. // Phytotaxa. 2016. V. 245.

№ 1. P. 75–78.
122. Zhang M.L., Zeng X.Q., Sanderson S.C., Byalt V.V., Sukhorukov A.P. // PLoS One. 2017. V. 12. № 9. P. e0178389.
123. Lyskov D.F., Degtjareva G.V., Samigullin T.H., Pimenov M.G. // Plant Systematics Evol. 2017. V. 303. № 7. P. 815–826.
124. Lyskov D., Samigullin T. // Phytotaxa. 2017. V. 326. № 3. P. 202–210.
125. Lyskov D.F., Samigullin T.H., Pimenov M.G. // Phytotaxa. 2017. V. 299. № 2. P. 223–233.
126. Sukhorukov A.P., Mavrodiev E.V., Struwig M., Nilova M.V., Dzhalilova K.K., Balandin S.A., Erst A., Krinitsyna A.A. // PLoS One. 2015. V. 10. № 2. P. e0117974.
127. Sukhorukov A.P., Kushunina M. // Israel J. Plant Sci. 2017. V. 64. № 1–2. P. 31–47.
128. Zaychenko S.G., Zernov A.S. // Wulfenia. 2017. V. 24. P. 205–220.
129. Fedosov V.E., Fedorova A.V., Ignatova E.A., Bobrova V.K., Troitsky A.V. // Mol. Biol. 2015. V. 49. № 6. P. 890–894.
130. Fedosov V.E., Fedorova A.V., Fedosov A.E., Ignatov M.S. // Bot. J. Linnean Soc. 2016. V. 181. № 2. P. 139–155.
131. Fedosov V., Fedorova A., Ignatova E. // J. Bryology. 2017. V. 39. № 2. P. 161–170.
132. Blockeel T.L., Kucera J., Fedosov V.E. // J. Bryology. 2017. V. 39. № 3. P. 247–254.
133. Logacheva M.D., Krinitsina A.A., Belenikin M.S., Khafizov K., Konorov E.A., Kuptsov S.V., Speranskaya A.S. // BMC Plant Biology. 2017. V. 17. № S2. P. 255.
134. Samigullin T.H., Logacheva M.D., Terenteva E.I., Degtjareva G.V., Vallejo-Roman C.M. // Biochemistry (Moscow). 2016. V. 81. № 9. P. 981–985.
135. Milyutina I.A., Ignatova E.A., Ignatov M.S., Goryunov D.V., Troitsky A.V. // Biochemistry (Moscow). 2015. V. 80. № 11. P. 1485–1491.
136. Seregin A.P., Anackov G., Friesen N. // Bot. J. Linnean Soc. 2015. V. 178. № 1. P. 67–101.
137. Seregin A.P. // Phytotaxa. 2015. V. 205. № 3. P. 211–214.
138. Koçyiğit M., Seregin A.P., Ozhatay N., Friesen N. // Phytotaxa. 2016. V. 275. № 3. P. 228–242.
139. Sukhorukov A.P., Kushunina M. // Phytokeys. 2016. № 73. P. 93–116.
140. Sukhorukov A.P., Kushunina M. // Phytotaxa. 2015. V. 218. № 3. P. 227–240.
141. Lyskov D., Kljuykov E., Guner E.D., Samigullin T. // Phytotaxa. 2017. V. 331. № 2. P. 253–262.
142. Pimenov M.G., Degtjareva G.V., Ostroumova T.A., Samigullin T.H., Averyanov L.V. // Phytotaxa. 2016. V. 244. № 3. P. 248–262.
143. Sukhorukov A.P., Zhang M.L., Kushunina M. // Phytotaxa. 2015. V. 203. № 2. P. 138–146.
144. Sukhorukov A.P., Kushunina M., Verloove F. // Plant Ecol. Evol. 2016. V. 149. № 2. P. 249–256.
145. Sukhorukov A.P., Nilova M.V. // Botany Lett. 2016. V. 163. № 3. P. 237–250.
146. Yurtseva O.V., Kuznetsova O.I., Mavrodiev E.V. // Phytotaxa. 2016. V. 268. № 1. P. 1–24.
147. Yurtseva O.V., Kuznetsova O.I., Mavrodieva M.E., Mavrodiev E.V. // Peer J. 2016. V. 4. P. e1977.
148. Yurtseva O.V., Severova E.E., Mavrodiev E.V. // Phytotaxa. 2017. V. 314. № 2. P. 151–194.
149. Seregin A.P. // Phytotaxa. 2017. V. 303. № 1. P. 89–92.
150. McIntosh T.T., Blom H.H., Kuznetsova O.I., Ignatova E.A. // Phytotaxa. 2017. V. 299. № 2. P. 234–242.
151. Nobis M., Nowak A., Piwowarczyk R., Ebel A.L., Kiraly G., Kushunina M., Sukhorukov A.P., Chernova O.D., Kipriyanova L.M., Paszko B., et al. // Botany Lett. 2016. V. 163. № 2. P. 159–174.
152. Borovichev E., Fedosov V., Vilnet A. // Cryptogamie Bryol. 2016. V. 37. № 4. P. 445–454.
153. Seregin A.P., Yevseyenkov P.E., Svirin S.A., Fateryga A.V. // Wulfenia. 2015. V. 22. P. 33–82.
154. Severova E., Volkova O. // Aerobiologia. 2017. V. 33. № 2. P. 253–264.
155. Volkova O., Severova E., Nosova M. // Grana. 2016. V. 55. № 4. P. 311–318.
156. Volkova O., Severova E., Polevova S. // Grana. 2017. V. 56. № 5. P. 368–376.
157. Polevova S., Krinitsina A. // Wulfenia. 2017. V. 24. P. 125–133.
158. Krinitsina A.A., Sizova T.V., Zaika M.A., Speranskaya A.S., Sukhorukov A.P. // Biochemistry (Moscow). 2015. V. 80. № 11. P. 1478–1484.
159. Seregin A.P. // Taxon. 2016. V. 65. № 1. P. 206–208.
160. Dobrovol'skaya T., Zvyagintsev D., Chernov I.Y., Golovchenko A., Zenova G., Lysak L., Manucharova N., Marfenina O., Polyanskaya L., Stepanov A. // Eurasian Soil Sci. 2015. V. 48. № 9. P. 959–967.
161. Kudinova A., Lysak L., Soina V., Mergelov N., Dolgikh A., Shorkunov I. // Eurasian Soil Sci. 2015. V. 48. № 3. P. 276–287.
162. Manucharova N., Trosheva E., Kol'tsova E., Demkina E., Karaevskaya E., Rivkina E., Mardanov A. // Microbiology. 2016. V. 85. № 1. P. 102–108.
163. Marfenina O., Nikitin D., Ivanova A. // Eurasian Soil Sci. 2016. V. 49. № 8. P. 934–941.
164. Nikitin D., Marfenina O., Kudinova A., Lysak L., Mergelov N., Dolgikh A., Lupachev A. // Eurasian Soil Sci. 2017. V. 50. № 9. P. 1086–1097.
165. Pankratov T., Kachalkin A., Korchikov E., Dobrovol'skaya T. // Microbiology. 2017. V. 86. № 3. P. 293–309.
166. Viner I.A., Kokaeva L.Y. // Folia Cryptogamica Estonica. 2017. V. 54. P. 43.
167. Crous P., Wingfield M., Guarro J., Hernández-Restrepo M., Sutton D., Acharya K., Barber P., Boekhout T., Dimitrov R., Dueñas M. // Persoonia: Mol. Phylogeny Evol. Fungi. 2015. V. 34. P. 167.
168. Crous P., Wingfield M.J., Burgess T., Carnegie A., Hardy G.S.J., Smith D., Summerell B.A., Cano-Lira J., Guarro J., Houbraken J., et al. // Persoonia. 2017. V. 39. P. 270–467.
169. Morozova O., Noordeloos M., Popov E., Alexandrova A. // Mycol. Progress. 2018. V. 17. P. 381–392.
170. Ivanova A., Nikolaeva V., Marfenina O. // Eurasian Soil Sci. 2015. V. 48. № 5. P. 501–508.
171. Marfenina O.E., Danilogorskaya A.A. // Pedobiologia. 2017. V. 60. P. 11–19.
172. Glushakova A., Kachalkin A., Zheltikova T., Chernov I.Y. // Microbiology. 2015. V. 84. № 5. P. 722–725.
173. Glushakova A., Kachalkin A., Tiunov A., Chernov I.Y. // Eurasian Soil Sci. 2017. V. 50. № 7. P. 820–825.
174. Glushakova A., Kachalkin A., Chernov I.Y. // Eurasian Soil Sci. 2015. V. 48. № 2. P. 201–207.
175. Glushakova A., Kachalkin A., Chernov I.Y. // Microbiology. 2015. V. 84. № 5. P. 717–721.
176. Glushakova A., Kachalkin A., Chernov I.Y. // Eurasian Soil Sci. 2016. V. 49. № 7. P. 792–795.
177. Abdullabekova D., Magomedova E., Magomedov G., Aliverdieva D., Kachalkin A. // Eurasian Soil Sci. 2017. V. 50. № 12. P. 1463–1467.
178. Kachalkin A., Abdullabekova D., Magomedova E., Magomedov G., Chernov I.Y. // Microbiology. 2015. V. 84. № 3. P. 425–432.

179. Glushakova A., Kachalkin A., Maksimova I., Chernov I.Y. // Microbiology. 2016. V. 85. № 4. P. 488–492.
180. Gmoshinskiy V.I., Buchtoyarova N.Y., Matveev A.V. // Botanica Lithuanica. 2017. V. 23. № 2. P. 107–110.
181. Novozhilov Y.K., Erastova D.A., Shchepin O.N., Schnittler M., Alexandrova A.V., Popov E.S., Kuznetov A.N. // Nova Hedwigia. 2017. V. 104. № 1–2. P. 143–182.
182. Sadykova V., Kurakov A., Korshun V., Rogozhin E., Gromovykh T., Kuvarina A., Baranova A. // Antibiotiki i khimioterapiia. 2015. V. 60. № 11–12. P. 3–8.
183. Karpova N., Andryushina V., Stytsenko T., Druzhinina A., Feofanova T., Kurakov A. // Appl. Biochem. Microbiol. 2016. V. 52. № 3. P. 316–323.
184. Blagoveshchenskaya E.Y., Popkova E. // Moscow University Biol. Sci. Bull. 2016. V. 71. № 2. P. 80–81.
185. Elansky S., Pobedinskaya M., Kokaeva L., Statsyuk N., Dyakov Y.T. // J. Plant Pathol. 2015. V. 97. № 3. P. 449–456.
186. Kokaeva L.Y., Belosokhov A.F., Doeva L.Y., Skolotneva E.S., Elansky S.N. // J. Plant Dis. Protection. 2017. V. 125. P. 205–212.
187. Krutyakov Y.A., Kudrinskiy A.A., Zherebin P.M., Yapryntsev A.D., Pobedinskaya M.A., Elansky S.N., Denisov A.N., Mikhaylov D.M., Lisichkin G.V. // Materials Res. Express. 2016. V. 3. № 7. P. 075403.
188. Kutuzova I., Kokaeva L.Y., Pobendinskaya M., Krutyakov Y.A., Skolotneva E., Chudinova E., Elansky S. // J. Plant Pathol. 2017. V. 99. № 3. P. 635–642.
189. Yurkov A.M. // Yeast. 2018. V. 35. P. 369–378.
190. Cheptsov V.S., Vorobyova E.A., Manucharova N.A., Gorlenko M.V., Pavlov A.K., Vdovina M.A., Lomasov V.N., Bulat S.A. // Extremophiles. 2017. V. 21. № 6. P. 1057–1067.
191. Grum-Grzhimaylo O.A., Debets A.J., Bilanenko E.N. // Mycologia. 2016. V. 108. № 2. P. 233–254.
192. Grum-Grzhimaylo A.A., Georgieva M.L., Bondarenko S.A., Debets A.J., Bilanenko E.N. // Fungal Diversity. 2016. V. 76. № 1. P. 27–74.
193. Bondarenko S.A., Ianutsevich E.A., Danilova O.A., Grum-Grzhimaylo A.A., Kotlova E.R., Kamzolkina O.V., Bilanenko E.N., Tereshina V.M. // Extremophiles. 2017. V. 21. № 4. P. 743–754.

Gamma-Carbolines Derivatives As Promising Agents for the Development of Pathogenic Therapy for Proteinopathy

V. I. Skvortsova[1], S. O. Bachurin[2], A. A. Ustyugov[2*], M. S. Kukharsky[1,2], A. V. Deikin[3], V. L. Buchman[2,4], N. N. Ninkina[2,4]

[1]Pirogov Russian National Research Medical University, Ostrovitianov Str., 1, Moscow, 117997, Russia

[2]Institute of Physiologically Active Compounds of the Russian Academy of Sciences, Severny Dr., Chernogolovka, 1142432, Russia

[3]Institute of Gene Biology of the Russian Academy of Sciences, Vavilova Str., 34/5, Moscow, 119334, Russia

[4]Cardiff University, School of Biosciences, Sir Martin Evans Building, Museum Ave., Cardiff, CF10 3AX

*E-mail: alexey@ipac.ac.ru

Received July 04, 2018; in final form September 21, 2018

ABSTRACT **Uncontrolled protein aggregation, accompanied by the formation of specific inclusions, is a major component of the pathogenesis of many common neurodegenerative diseases known as proteinopathies. The intermediate products of this aggregation are toxic to neurons and may be lethal. The development strategy of pathogenic therapy for proteinopathy is based on the design of drugs capable of both inhibiting proteinopathy progression and increasing the survival of affected neurons. The results of a decade-long research effort at leading Russian and international laboratories have demonstrated that Dimebon (Latrepirdine), as well as a number of its derivatives from a gamma-carboline group, show a strong neuroprotective effect and can modulate the course of a neurodegenerative process in both *in vitro* and *in vivo* model systems. The accumulated data indicate that gamma-carbolines are promising compounds for the development of pathogenic therapy for proteinopathies.**

KEYWORDS **ALS, Dimebon, gamma-carbolines, proteinopathy, transgenic animals.**

ABBREVIATIONS **ALS – amyotrophic lateral sclerosis; FUS – fused in sarcoma; NDD – neurodegenerative disease; TDP-43 – transactive response DNA binding protein 43 kDa.**

INTRODUCTION

Uncontrolled aggregation of certain proteins, with the formation of histopathological inclusions (proteinopathy), is a major aspect of the pathogenesis of many neurodegenerative diseases (NDDs), including amyotrophic lateral sclerosis (ALS). Hence, the development of drugs capable of inhibiting proteinopathy progression is considered as an important direction in the development of pathogenic therapy for NDDs. Data from recent studies, which have been independently obtained at various laboratories in different countries, have convincingly proved the ability of a drug that belongs to a gamma-carboline group – Dimebon (Latrepirdine) – to effectively inhibit the progression of model proteinopathies in various transgenic animals. Our findings demonstrate the efficacy of Dimebon and its derivatives in inhibiting proteinopathy progression in model transgenic systems with a ALS phenotype.

Amyotrophic lateral sclerosis is a serious condition of the nervous system, with specific loss of motor neurons, and it is a type of proteinopathy caused by the aggregation of certain proteins. The association between pathogenic aggregation of these proteins and the development of a ALS phenotype has been demonstrated in numerous experimental studies on the modeling of the main mechanisms of a neurodegenerative process affecting motor neurons [1–3]. In a histopathological analysis of idiopathic ALS, the autopsy material of most patients contains intracellular protein inclusions. Of particular interest are deposits formed by TDP-43 and FUS DNA/RNA-binding proteins [4–6]. The direct mechanisms underlying the pathogenic aggregation of these proteins, leading to dysfunction and death of motor neurons, may be a specific trait of a given protein. There is little doubt that the process of pathogenic protein aggregation plays an important role in the

pathogenesis of all ALS forms and might be an obvious target for therapeutic interventions.

NEUROPROTECTIVE PROPERTIES OF GAMMA-CARBOLINES

Data from independent studies at several laboratories have demonstrated that compounds belonging to the gamma-carboline class are potential neuroprotective agents leading to reduced levels of pathogenic aggregation and/or activating the intracellular defense mechanisms of controlled degradation of aggregated proteins [7, 8]. Initial findings for these gamma-carbolines properties were obtained in Dimebon studies showing a correction of the cognitive function in patients with Alzheimer's disease (AD), which is the most common neurodegenerative disease in the proteinopathy group [9, 10]. Furthermore, clinical trials conducted at several centers have revealed a positive effect from Dimebon on the cognitive function of patients with Huntington's disease [11]. Yet, phase III clinical trials have indicated that Dimebon treatment is not considered effective compared to other developed drugs for the pathogenic therapy of AD [12], which is most likely due to the extremely high heterogeneity of nosological forms of Alzheimer's disease. However, the mechanisms of action of the drug and its derivatives on proteinopathy progression have remained the object of intense research at several laboratories [13]. For example, the results of a recent meta-analysis revealed a positive effect from Dimebon on neuropsychiatric status indicators in AD patients [14] and provided an additional incentive to continue research in this direction. In addition, in a homogeneous model system of transgenic animals, Dimebon was shown to inhibit the development of tau proteinopathy, which is one of the key components of AD pathology [15]. Another key proteinopathy in the pathogenesis of AD is cerebral amyloidosis, which was also inhibited by Dimebon in TgCRND8 [16–18] and 3xTg-AD [19] mice, but not in a 5xFAD model characterized by a more aggressive course of amyloidosis [20]. These data served as grounds for expanding the range of research areas of gamma-carbolines effects on the progression of other proteinopathies that play an important role in the pathogenesis of neurodegenerative diseases.

EFFECT OF GAMMA-CARBOLINES ON THE PROGRESSION OF PROTEINOPATHIES ASSOCIATED WITH THE SPECIFIC INVOLVEMENT OF MOTOR NEURONS

Chronic administration of Dimebon to a transgenic mouse model with the *pan*-neuronal expression of gamma-synuclein which reproduced the main features of ALS pathogenesis [21, 22] delayed the progression of proteinopathy [23, 24]. In this case, there was a significant decrease in the level of aggregated detergent-insoluble gamma-synuclein isoforms in affected areas of the nervous system in transgenic mice [25] and a decrease in gamma-synuclein-reactive inclusions in the affected spinal cord parts of the experimental animals [21, 22]. This effect was more pronounced if administration was begun at the pre-symptomatic stage, long before the first manifestations of the pathological process, according to both clinical symptoms and histological analysis. The same feature of Dimebon was observed in $SOD1^{G93A}$ transgenic mice: if Dimebon was administered long before the expected age of manifestations of ALS phenotype-associated symptoms, then the onset of model disease symptoms occurred later, leading to an increased lifespan for the animals [26]. However, if Dimebon administration was started at an age closer to the expected onset of model disease symptoms, then the drug effects were much less pronounced [27]. We confirmed the ability of Dimebon and its derivatives to inhibit proteinopathy progression in a FUS^{1-359} transgenic mouse line [28, 29] which was recently generated and represents an adequate model of specific involvement of motor neurons with the ALS phenotype. In the nervous system of these mice, similarly to patients with FUS-associated forms of ALS, the histopathological analysis reveals an accumulation of aberrant FUS isoforms in characteristic cytoplasmic protein aggregates. Both Dimebon and its derivatives could modify, albeit with different efficacies, the progression of FUS proteinopathy in the nervous system of the FUS^{1-359} mice [30]. For example, the lifespan of model animals treated with Dimebon increased statistically significantly. Furthermore, transfer of the FUS^{1-359} mouse line from the C57Bl/6J genetic background, which was initially used in most studies in various laboratories, to the CD-1 genetic background did not affect the proteinopathy-inhibiting effect of gamma-carbolines and may not be explained by increased sensitivity of the C57Bl/6J line to gamma-carbolines [30]. In addition to an increased lifespan, the FUS^{1-359} mice treated with Dimebon or its derivative were characterized by a delayed onset of model disease symptoms with the development of a pronounced ALS phenotype if administration of the compounds was initiated at early latent stages of FUS proteinopathy [31]. However, the exact mechanism of Dimebon action remains unclear. The existing data from biochemical studies, as well as experiments on cell cultures and animals, suggest that Dimebon is a multitarget drug capable of affecting many intracellular processes and various pathogenic pathways in neurons and other cells affected by neurodegenerative changes [7].

Particularly, Dimebon can modulate the functioning of receptors and channels, change the kinetics of sig-

naling enzymes [9, 32–35], as well as stabilize mitochondrial activity [36, 37]. But perhaps, the most significant property of Dimebon, which makes it a basic compound in the development of approaches for the treatment of proteinopathy, lies in its ability to inhibit the accumulation of cellular pathogenic protein aggregates.

GAMMA-CARBOLINE-BASED INHIBITION OF ACCUMULATION OF PATHOHISTOLOGICAL PROTEIN INCLUSIONS IN NEURONAL CYTOPLASM

The ability of Dimebon to prevent an accumulation of pathogenic protein inclusions in neuronal bodies was first demonstrated in our joint research with M. Hasegawa's and M. Goedert's laboratories on cell cultures producing the aberrant and highly aggregating RNA-binding protein TDP-43 [38, 39]. The effect was confirmed using another cell model with the aggregation of the RNA-binding protein FUS. We demonstrated that addition of Dimebon and/or its derivatives to cultured human neuroblastoma cells with FUS proteinopathy reduces both the amount of insoluble protein forms in the cytoplasmic fraction and the amount of protein inclusions formed in the cytoplasm (unpublished data). Subsequent studies performed on various model proteinopathy systems confirmed these effects, and in our view they are associated with the activation of the autophagosome system in Dimebon-treated groups [16, 40–42].

CONCLUSION

The results of a decade-long research effort conducted at leading Russian and international laboratories have demonstrated that compounds from the gamma-carboline series are indeed capable of suppressing the progression of certain types of proteinopathies and, as in the case of ALS models, slow down the development of the model phenotype of neurodegenerative processes *in vivo*. It is the modulation of aggregation of the proteins involved in proteinopathy mechanisms that is considered as the major element behind the concept of developing pathogenic therapy for neurodegenerative diseases [43]. At present, there is enough supporting evidence for considering Dimebon and its derivatives as promising compounds for the development of new therapeutic agents with improved pharmacokinetics and efficacy, which may be used as part of a complex pathogenic therapy for socially significant neurodegenerative diseases. ●

The study of neurodegenerative processes in model systems was supported by a grant of the Russian Science Foundation (No. 18-15-00357); maintenance of the animals was funded by the program for the support of bioresource collections of the Institute of Physiologically Active Compounds (IPAC) (Federal Agency for Scientific Organizations No. 0090-2017-0016) and conducted on the equipment of the Center for Scientific and Technical Studies of IPAC RAS and IGB RAS, in the framework of the State Assignment of IPAC RAS (topic of the State registration number 0090-2017-0019) and the basic research program of the Presidium of the Russian Academy of Sciences "Fundamental research for biomedical technologies."

REFERENCES

1. Skvortsova V.I., Bachurin S.O., Razinskaia O.D., Smirnov A.P., Kovrazhkina E.A., Pochigaeva K.I., Ninkina N.N., Shelkovnikova T.A., Ustiugov A.A. // Zh. Nevrol. Psikhiatr. im. S.S. Korsakova. 2011. V. 111. № 2. P. 4–9.
2. Bachurin S., Ninkina N., Tarasova T., Shelkovnikova T., Kovrazhkina E., Smirnov A., Razinskaia O. Skvortsova V. // Zh. Nevrol. Psikhiatr. im. S.S. Korsakova. 2013. V. 113. № 10. P. 74.
3. Bachurin S., Ninkina N., Tarasova T., Shelkovnikova T., Kovrazhkina E., Smirnov A., Razinskaya O. Skvortsova V. // Zh. Nevrol. Psikhiatr. im. S.S. Korsakova. 2013. V. 113. № 9. P. 86.
4. Mackenzie I.R., Bigio E.H., Ince P.G., Geser F., Neumann M., Cairns N.J., Kwong L.K., Forman M.S., Ravits J., Stewart H., et al. // Ann. Neurol. 2007. V. 61. № 5. P. 427–434.
5. Neumann M., Sampathu D.M., Kwong L.K., Truax A.C., Micsenyi M.C., Chou T.T., Bruce J., Schuck T., Grossman M., Clark C.M., et al. // Science. 2006. V. 314. № 5796. P. 130–133.
6. Scotter E.L., Chen H.J., Shaw C.E. // Neurotherapeutics. 2015. V. 12. № 2. P. 352–363.
7. Ustyugov A., Shevtsova E., Bachurin S. // Mol. Neurobiol. 2015. V. 52. № 2. P. 970–978.
8. Ustyugov A., Shevtsova E., Barreto G.E., Ashraf G.M., Bachurin S.O., Aliev G. // Curr. Med. Chem. 2016. doi: 10.2174/0929867323666160804122746.
9. Bachurin S., Bukatina E., Lermontova N., Tkachenko S., Afanasiev A., Grigoriev V., Grigorieva I., Ivanov Y., Sablin S., Zefirov N. // Ann. N.Y. Acad. Sci. 2001. V. 939. P. 425–435.
10. Doody R.S., Gavrilova S.I., Sano M., Thomas R.G., Aisen P.S., Bachurin S.O., Seely L., Hung D. Dimebon I. // Lancet. 2008. V. 372. № 9634. P. 207–215.
11. Kieburtz K., McDermott M.P., Voss T.S., Corey-Bloom J., Deue L.M., Dorsey E.R., Factor S., Geschwind M.D., Hodgeman K., Kayson E., et al. // Arch. Neurol. 2010. V. 67. № 2. P. 154–160.
12. Bharadwaj P.R., Bates K.A., Porter T., Teimouri E., Perry G., Steele J.W., Gandy S., Groth D., Martins R.N., Verdile G. // Transl. Psychiatry. 2013. V. 3. e332.
13. Bachurin S.O., Bovina E.V., Ustyugov A.A. // Med. Res. Rev. 2017. V. 37. № 5. P. 1186–1225.
14. Cano-Cuenca N., Solis-Garcia del Pozo J.E., Jordan J. // J. Alzheimers Dis. 2014. V. 38. № 1. P. 155–164.
15. Peters O.M., Connor-Robson N., Sokolov V.B., Aksinenko A.Y., Kukharsky M.S., Bachurin S.O., Ninkina N., Buchman V.L. // J. Alzheimers Dis. 2013. V. 33. № 4. P. 1041–1049.

16. Steele J.W., Gandy S. // Autophagy. 2013. V. 9. № 4. P. 617–618.
17. Steele J.W., Lachenmayer M.L., Ju S., Stock A., Liken J., Kim S.H., Delgado L.M., Alfaro I.E., Bernales S., Verdile G., et al. // Mol. Psychiatry. 2013. V. 18. № 8. P. 889–897.
18. Wang J., Ferruzzi M.G., Varghese M., Qian X., Cheng A., Xie M., Zhao W., Ho L., Pasinetti G.M. // Mol. Neurodegener. 2011. V. 6. № 1. P. 7.
19. Perez S.E., Nadeem M., Sadleir K.R., Matras J., Kelley C.M., Counts S.E., Vassar R., Mufson E.J. // Int. J. Physiol. Pathophysiol. Pharmacol. 2012. V. 4. № 3. P. 115–127.
20. Peters O.M., Shelkovnikova T., Tarasova T., Springe S., Kukharsky M.S., Smith G.A., Brooks S., Kozin S.A., Kotelevtsev Y., Bachurin S.O., et al. // J. Alzheimers Dis. 2013. V. 36. № 3. P. 589–596.
21. Ninkina N., Peters O., Millership S., Salem H., van der Putten H., Buchman V.L. // Hum. Mol. Genet. 2009. V. 18. № 10. P. 1779–1794.
22. Peters O.M., Millership S., Shelkovnikova T.A., Soto I., Keeling L., Hann A., Marsh-Armstrong N., Buchman V.L., Ninkina N. // Neurobiol. Dis. 2012. V. 48. № 1. P. 124-131.
23. Bachurin S.O., Shelkovnikova T.A., Ustyugov A.A., Peters O., Khritankova I., Afanasieva M.A., Tarasova T.V., Alentov I.I., Buchman V.L., Ninkina N.N. // Neurotox. Res. 2012. V. 22. № 1. P. 33–42.
24. Bachurin S.O., Ustyugov A.A., Peters O., Shelkovnikova T.A., Buchman V.L., Ninkina N.N. // Dokl. Biochem. Biophys. 2009. V. 428. P. 235–238.
25. Ustyugov A.A., Shelkovnikova T.A., Kokhan V.S., Khritankova I.V., Peters O., Buchman V.L., Bachurin S.O., Ninkina N.N. // Bull. Exp. Biol. Med. 2012. V. 152. № 6. P. 731–733.
26. Coughlan K.S., Mitchem M.R., Hogg M.C., Prehn J.H. // Neurobiol. Aging. 2015. V. 36. № 2. P. 1140–1150.
27. Tesla R., Wolf H.P., Xu P., Drawbridge J., Estill S.J., Huntington P., McDaniel L., Knobbe W., Burket A., Tran S., et al. // Proc. Natl. Acad. Sci. USA. 2012. V. 109. № 42. P. 17016–17021.
28. Shelkovnikova T.A., Peters O.M., Deykin A.V., Connor-Robson N., Robinson H., Ustyugov A.A., Bachurin S.O., Ermolkevich T.G., Goldman I.L., Sadchikova E.R., et al. // J. Biol. Chem. 2013. V. 288. № 35. P. 25266–25274.
29. Deikin A.V., Kovrazhkina E.A., Ovchinnikov R.K., Bronovitskii E.V., Razinskaia O.D., Smirnov A.P., Ermolkevich T.G., Eliakov A.B., Popov A.N., Fedorov E.N., et al. // Zh. Nevrol. Psikhiatr. im. S.S. Korsakova. 2014. V. 114. № 8. P. 62–69.
30. Bronovitsky E.V., Deikin A.V., Ermolkevich T.G., Elyakov A.B., Fedorov E.N., Sadchikova E.R., Goldman I.L., Ovchinnikov R.K., Roman A.Y., Khritankova I.V., et al. // Dokl. Biochem. Biophys. 2015. V. 462. P. 189–192.
31. Maltsev A.V., Deykin A.V., Ovchinnikov R.K., Chicheva M.M., Kovrazhkina E.A., Razinskaya O.D., Bronovitsky E.V., Budevich A.I., Kirikovich Y.K., Bachurin S.O., et al. // Zh. Nevrol. Psikhiatr. im. S.S. Korsakova. 2017. V. 117. № 4. P. 64–67.
32. Schaffhauser H., Mathiasen J.R., Dicamillo A., Huffman M.J., Lu L.D., McKenna B.A., Qian J., Marino M.J. // Biochem. Pharmacol. 2009. V. 78. № 8. P. 1035–1042.
33. Wu J., Li Q., Bezprozvanny I. // Mol. Neurodegener. 2008. V. 3. P. 15.
34. Wang C.C., Kuo J.R.,Wang S.J. // Eur. J. Pharmacol. 2014. V. 734. P. 67–76.
35. Weisova P., Alvarez S.P., Kilbride S.M., Anilkumar U., Baumann B., Jordan J., Bernas T., Huber H.J., Dussmann H., Prehn J.H. // Transl. Psychiatry. 2013. V. 3. e317.
36. Zhang S., Hedskog L., Petersen C.A., Winblad B., Ankarcrona M. // J. Alzheimers Dis. 2010. V. 21. № 2. P. 389–402.
37. Eckert S.H., Eckmann J., Renner K., Eckert G.P., Leuner K., Muller W.E. // J. Alzheimers Dis. 2012. V. 31. № 1. P. 21–32.
38. Yamashita M., Nonaka T., Arai T., Kametani F., Buchman V.L., Ninkina N., Bachurin S.O., Akiyama H., Goedert M., Hasegawa M. // FEBS Lett. 2009. V. 583. № 14. P. 2419–2424.
39. Kukharsky M.S., Khritankova I.V., Lytkina O.A., Ovchinnikov R.K., Ustyugov A.A., Shelkovnikova T.A., Bronovitsky E.V., Kokhan V.S., Ninkina N.N., Bachurin S.O. // Pathogenesis. 2013. V. 11. № 1. P. 53–60. (in Russ.).
40. Khritankova I.V., Kukharskiy M.S., Lytkina O.A., Bachurin S.O., Shorning B.Y. // Dokl. Biochem. Biophys. 2012. V. 446. P. 251–253.
41. Steele J.W., Ju S., Lachenmayer M.L., Liken J., Stock A., Kim S.H., Delgado L.M., Alfaro I.E., Bernales S., Verdile G., et al. // Mol. Psychiatry. 2013. V. 18. № 8. P. 882–888.
42. Bharadwaj P.R., Verdile G., Barr R.K., Gupta V., Steele J.W., Lachenmayer M.L., Yue Z., Ehrlich M.E., Petsko G., Ju S., et al. // J. Alzheimers Dis. 2012. V. 32. № 4. P. 949–967.
43. Kumar V., Sami N., Kashav T., Islam A., Ahmad F., Hassan M.I. // Eur. J. Med. Chem. 2016. V. 124. P. 1105–1120.

Assessment of the Parameters of Adaptive Cell-Mediated Immunity in Naïve Common Marmosets (*Callithrix jacchus*)

I. V. Gordeychuk[1,2,3], A. I. Tukhvatulin[2], S. P. Petkov[4], M. A. Abakumov [5,6], S. A. Gulyaev[1], N. M. Tukhvatulina[2], T. V. Gulyaeva[1], M. I. Mikhaylov[7,8], D. Y. Logunov[2], M. G. Isaguliants[1,2,9]

[1]Chumakov Federal Scientific Center for Research and Development of Immune-and-Biological Products of Russian Academy of Sciences, premises 8, bldg. 1, Village of Institute of Poliomyelitis, Settlement "Moskovskiy", Moscow, 108819, Russia

[2]N.F. Gamaleya National Research Center for Epidemiology and Microbiology, Gamaleya Str., 18, Moscow, 123098, Russia

[3]Sechenov First Moscow State Medical University, Bolshaya Pirogovskaya Str., 19, bldg. 1, Moscow, 119146, Russia

[4]MTC, Karolinska Institutet, 171 77, Stockholm, Sweden

[5]Pirogov Russian National Research Medical University, Ostovitjanova Str. 1, Moscow, 117997, Russia

[6]National University of Science and Technology MISiS, Leninsky Ave., 4, Moscow, 119049, Russia

[7]Russian Medical Academy of Continuous Professional Education, Barrikadnaja Str., 2/1, bldg. 1, Moscow, 125993, Russia

[8]Mechnikov Research Institute for Vaccines and Sera, Maliy Kazenniy Lane, 5a, Moscow, 105064, Russia

[9]Rīga Stradiņš University, LV-1007, Riga, Lativa

*E-mail: lab.gord@gmail.com

Received December 13, 2017; in final form August 28, 2018

ABSTRACT **Common marmosets are small New World primates that have been increasingly used in biomedical research. This report presents efficient protocols for assessment of the parameters of adaptive cell-mediated immunity in common marmosets, including the major subpopulations of lymphocytes and main markers of T- and B-cell maturation and activation using flow cytometry with a multicolor panel of fluorescently labelled antibodies. Blood samples from eight common marmosets were stained with fluorescently labeled monoclonal antibodies against their population markers (CD45, CD3, CD20, CD4, CD8) and lymphocyte maturation and activation markers (CD69, CD62L, CD45RO, CD107a and CD27) and analyzed by flow cytometry. Within the $CD45^+$ population, 22.7±5.5% cells were $CD3^-CD20^+$ and 67.6±6.3% were $CD3^+CD20^-$. The CD3+ subpopulation included 55.7±5.5% $CD3^+CD4^+CD8^-$ and 34.3±3.7% $CD3^+CD4^-CD8^+$ cells. Activation and maturation markers were expressed in the following lymphocyte proportions: CD62L on 54.0±10.7% of $CD3^+CD4^+$ cells and 74.4±12.1% of $CD3^+CD8^+$ cells; CD69 on 2.7±1.2% of $CD3^+CD4^+$ cells and 1.2±0.5% of $CD3^+CD8^+$ cells; CD45RO on 1.6±0.6% of $CD3^+CD4^+$ cells and 1.8±0.7% of $CD3^+CD8^+$ cells; CD107a on 0.7±0.5% of $CD3^+CD4^+$ cells and 0.5±0.3% of $CD3^+CD8^+$ cells; CD27 on 94.6±2.1% of $CD3^+$ cells and 8.9±3.9% $CD20^+$ cells. Female and male subjects differed in the percentage of $CD3^+CD4^+CD45RO^+$ cells (1.9±0.5 in females vs 1.1±0.2 in males; $p<0.05$). The percentage of $CD20^+CD27^+$ cells was found to highly correlate with animals' age ($r = 0.923$, $p < 0.005$). The basal parameters of adaptive cell-mediated immunity in naïve healthy marmosets without markers of systemic immune activation were obtained. These parameters and the described procedures are crucial in documenting the changes induced in common marmosets by prophylactic and therapeutic immune interventions.**

KEYWORDS **adaptive cell-mediated immunity, common marmoset, flow cytometry, *Callithrix jacchus*.**

ABBREVIATIONS **CD – cluster of differentiation; FMO – fluorescence minus one control; FSC – forward-scattered light; HEPA – high-efficiency particulate air; HLA – human leukocyte antigen; M±σ – mean value ± standard deviation; IU – International Unit; MHC – major histocompatibility complex; SSC – side-scattered light.**

INTRODUCTION

Common marmosets (CMs; *Callithrix jacchus*) are small New World primates that have been increasingly used in the modeling of human morbidities, including infectious diseases, neuropathological disorders, and cancer [1, 2]. With regard to the susceptibility of this species to infectious diseases, it represents an exquisite non-human primate model for viral, protozoan and bacterial agents, as well as prions [3], and, hence, an ideal platform for preclinical studies of the safety and effectiveness of novel immunotherapies and vaccines [4]. Substantial advantages of using CMs in biomedical research are their small size, evolutionary closeness to humans, relative ease of maintenance, and compressed lifespan, due to which the number of animals can be scaled up quickly when the need arises and then naturally reduced when the animals are not needed [3].

The evolutionary closeness to humans makes it possible to apply the well-established research methods commonly used in human studies to CMs. However, these primates significantly differ from other non-human primate species in many biological aspects [5]. Immunologically, marmosets (and other Callitrichids) are exceptions to the generalized stability in MHC Class I loci [6,7]. Each Callitrichid genus exhibits its own unique set of MHC Class I genes and expresses no loci comparable to the classical MHC Class I HLA-A, -B, and -C. MHC Class I loci also appear to have limited variability and a relatively accelerated turnover between generations, resulting in a low/no inter-individual variation in the immune responses to pathogens or tumor antigens [5]. The polymorphisms in their MHC class II loci are also quite limited [8]. This makes CMs particularly sensitive to viral infections [9–11], especially to infections with oncogenic viruses, which frequently result in induction of spontaneous tumors [12–15]. Early observations of this sensitivity were confirmed by experimental infection of CMs with sarcoma viruses and lymphotropic herpes viruses [16–18]. Such spontaneously and experimentally induced tumors are directly relevant to Burkitt's lymphoma and nasopharyngeal carcinoma in humans, making CMs a powerful model with which to test the corresponding antiviral treatments and immune interventions, including prophylactic and therapeutic vaccines against these oncogenic human viruses. Despite the outbred study groups, such studies are destined to generate coherent harmonious results due to the low variations in the immune response of individual animals.

Characterization of the effects of immune interventions, vaccine-induced responses, as well as the safety aspects of the aforementioned tests, requires a careful description of the immune status of the experimental animals in the naïve state and post-activation. One of the main methods to achieve this is flow cytometric analysis using monoclonal antibodies against cell surface and intracellular antigens. While many commercially available monoclonal antibodies used for analyzing human and non-human primate cells cross-react with the marmoset antigens, some work suboptimally and some do not to work at all [19–21].

This report presents an efficient protocol to characterize the immune status of common marmosets using flow cytometry with a multicolor panel of fluorescently labelled antibodies and its application for assessing the immune status parameters and markers of immune activation in these non-human primates.

MATERIALS AND METHODS

Animal care and housing conditions complied with the regulations of the European Parliament and the European Council Directive on the protection of animals used for scientific purposes (2010/63/EU) and also with the National Institutes of Health Guide for Care and Use of Laboratory Animals. The animals were housed in pairs in wire mesh cages (cage size 80×55×130 cm) with wooden sleeping boxes and branches for climbing. Urine and feces were removed daily by changing the trays. Room temperature was maintained at 27±2°C, and the relative humidity was kept between 60 and 80%. Light cycle was set to a 12-hour day/night switch. The HEPA-filtered air exchange rate was set to 8 times per hour. CMs received water *ad libitum* and custom marmoset feed that was unchanged during the experiment. Water and food quality were controlled on a regular basis.

The study protocol was approved by the Ethical Committee of the Chumakov Federal Scientific Center for Research and Development of Immune-and-Biological Products of the Russian Academy of Sciences (Chumakov FSC R&D IBP RAS, Moscow, Russia). The study included 8 animals, 3 males and 5 females, aged 23 to 48 months and weighing 360–400 grams, bred and maintained in the Experimental Clinic of Callitrichidae at the Chumakov FSC R&D IBP, RAS. All the experiments were performed by personnel certified for working with non-human primates by the Karolinska Institute (Stockholm, Sweden). The conditions of housing and maintenance of the animals remained unchanged throughout the experiment. No adverse events were detected in the subject animals during the experiment and in the two-week follow-up period after the procedure. All animals were identified using subcutaneous radio-frequency chips with unique 15-digit codes (Globalvet, Moscow, Russia). The IDs in tables and figures represent the last four digits of the code.

Venous blood samples (2 ml) were obtained from eight CMs by femoral vein puncture using a 2.5 ml

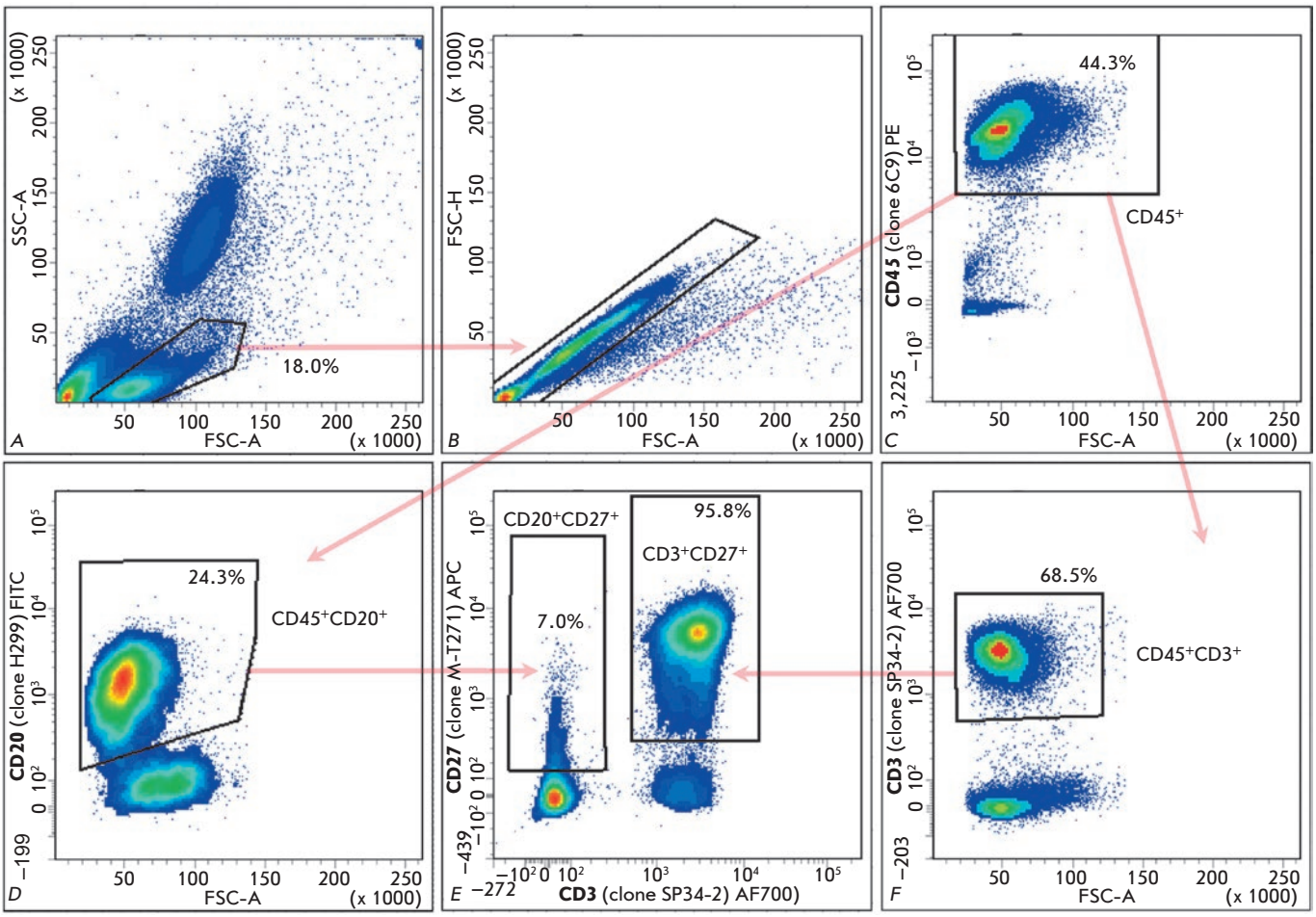

Fig. 1. Gating and cell staining patterns for the T- and B-cell populations of a naïve CM (ID 4540). FSC-A/SSC-A population separation plot (a) and exclusion of non-single cells (b) were used for CM CD45$^+$ leukocytes gating (c). The proportions of stained CD45$^+$CD20$^+$ (d) and CD45$^+$CD3$^+$ (f) cells are shown in respective gates as fractions of CD45$^+$. The proportions of stained CD3$^+$CD27$^+$ and CD20$^+$CD27$^+$ cells (e) are shown in respective gates as fractions of CD3$^+$ cells and CD20$^+$ cells. The reactivity of each monoclonal antibody was defined as the percentage of positively stained cells relative to cells stained with all other antibodies except for the one tested (FMO control). A total of 150,000 events were processed in each measurement

syringe with a 25G needle pre-filled with 25 IU of sodium-heparin (Belmedpreparaty, Minsk, Belarus) per ml. Aliquots of 50 µl of whole blood per test were incubated for 30 min at 22°C with pre-titrated amounts of the following antibodies: PE mouse anti-marmoset CD45 (BioLegend, San Diego, USA, clone 6C9, cat. 250204); Alexa Fluor 700 mouse anti-human CD3 (BD, New Jersey, USA, clone SP34-2, cat. 557917); FITC mouse anti-human CD20 (Beckman Coulter, Brea, USA, clone H299, cat. 6602381); PerCP-Cy5.5 mouse anti-human CD4 (BD, clone L200, cat. 552838); PE anti-marmoset CD8 (BioLegend, clone 6F10, 250304); APC mouse anti-human CD69 (BD, clone L78, cat. 654663); BV421 mouse anti-human CD62L (BD, clone SK11, cat. 743207); PE/Cy7 anti-human CD45RO (BioLegend, clone UCHL1, cat. 304230); BV421 mouse anti-human CD107a (BD, clone H4A3, cat. 562623); and APC anti-human CD27 (BioLegend, clone M-T271, cat. 356409). After incubation with the given antibodies, samples were treated with 1 ml of RBC lysis buffer (BioLegend, cat. 420301) for 15 min at RT and washed once with 1 ml PBS at 2000G. Samples were analyzed on a BD FACS Aria III flow-cytometer (BD) within 30 min after staining. The reactivity of each monoclonal antibody was defined as the percentage of positively stained cells relative to cells stained with all other antibodies except for the one tested (FMO control).

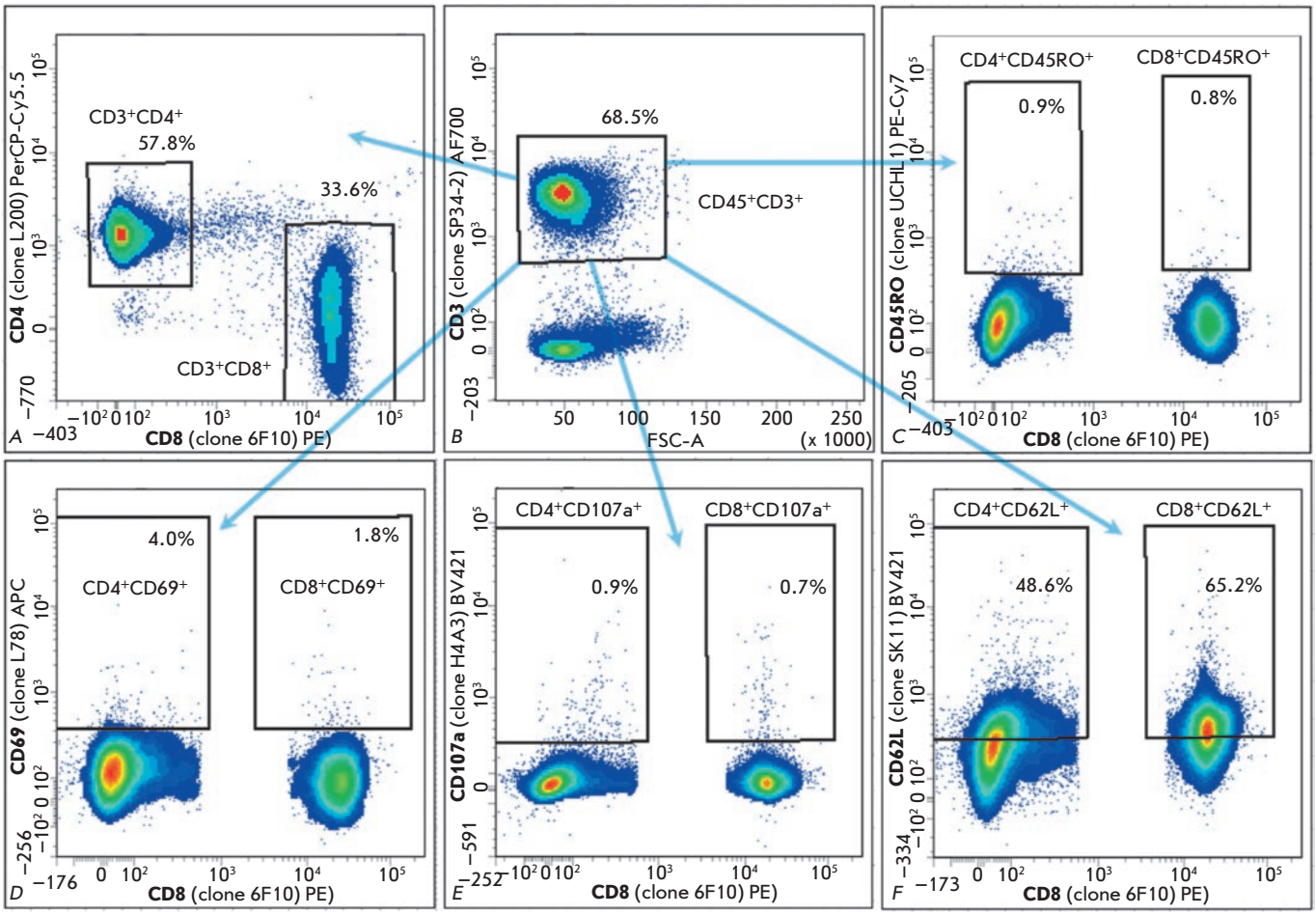

Fig. 2. Staining patterns of cell maturation and activation markers of a naïve CM (ID 4540). The proportions of stained $CD3^+CD4^+$ and $CD3^+CD8^+$ (a) cells are shown in respective gates as fractions of $CD45^+CD3^+$ (b) cells. The proportions of stained $CD45RO^+$ (c), $CD69^+$ (d), $CD107a^+$ (e), and $CD62L^+$ (f) cells are shown in respective gates as fractions of $CD3^+CD4^+$ and $CD3^+CD8^+$ cell populations. The reactivity of each monoclonal antibody was defined as a percentage of positively stained cells relative to the cell populations stained with all other antibodies except for the one tested (FMO control). A total of 150,000 events were processed in each measurement

Statistical analysis of the data was performed using the t-test for normally distributed values, and non-parametrical Mann-Whitney and Spearman raking tests, all performed with the help of STATISTICA AXA 10 (TIBCO Software, USA).

RESULTS

Few studies published so far have addressed the applicability of different commercially available monoclonal antibodies to the flow cytometry (FACS) of CM cells [19–21]. Here, we have elaborated an efficient protocol for characterizing the immune status of CMs using FACS with a multicolor panel of fluorescently labelled antibodies specific to the major subpopulations of lymphocytes and markers of T- and B-cell maturation and activation. Using this method, we characterize the immune status of naïve CMs with respect to the percentage of basic T- and B-lymphocyte subpopulations ($CD45^+$, $CD45^+CD3^-CD20^+$, $CD45^+CD3^+CD20^-$, $CD3^+CD4^+CD8^-$, $CD3^+CD4^-CD8^+$) and the level of expression of the maturation and activation markers (CD27, CD62L, CD69, CD45RO, CD107a) on these T- and B-lymphocytes. The gating strategy and staining patterns are shown in *Figs. 1* and 2 on the example of one naïve CM (ID 4540).

The proportions of peripheral blood cells of individual CMs labelled with receptor-specific antibodies are summarized in Table 1. CD45+ leukocytes accounted for 54.3±11.8% of total cells after RBC lysis. Within the $CD45^+$ population, 22.7±5.5% were B-cells ($CD45^+CD3^-$

Table 1. Proportions of reactive peripheral blood cells of naïve CMs

Parameter	Marmoset ID, parameter %										Total, M±σ, %
	Female						Male				
	2996	2998	0519	3016	2997	M±σ	2994	4540	4520	M±σ	
Age, months	29	29	23	48	25	30.8±10.0	30.0	25.0	25.0	26.7±2.9	29.3±8.0
*$CD45^+$	67.5	64.5	62.3	43.5	43.2	56.2±11.9	42.1	44.3	66.6	51.0±13.6	54.3±11.8
$CD45^+CD3^-CD20^+$	28.7	32.4	17.7	17.5	20.4	23.3±6.8	22.3	24.3	18.4	21.7±3.0	22.7±5.5
$CD45^+CD20^+CD27^+$	8.3	11.8	5.9	17	7.9	10.2±4.4	8.9	7.0	4.7	6.9±2.1	8.9±3.9
$CD45^+CD3^+CD20^-$	62.4	57.6	69.6	74.7	64.4	65.7±6.6	66.5	68.5	76.9	70.6±5.5	67.6±6.3
$CD45^+CD3^+CD27^+$	93.9	93.2	96.2	98.4	93.2	95.0±2.3	91.8	95.8	94.6	94.1±2.1	94.6±2.1
$CD3^+CD4^-CD8^+$	39.2	32.7	34.4	40	32.9	35.8±3.5	33.2	33.6	28.5	31.8±2.8	34.3±3.7
$CD3^+CD8^+CD62L^+$	72.7	81.2	89.3	86.7	51.8	76.3±15.1	76.4	65.2	72.0	71.2±5.6	74.4±12.1
$CD3^+CD8^+CD69^+$	0.9	1.1	1.6	1.9	0.3	1.2±0.6	1.2	1.8	1.0	1.3±0.4	1.2±0.5
$CD3^+CD8^+CD45RO^+$	2	2.4	1.8	1.8	0.8	1.8±0.6	2.0	0.8	0.7	1.2±0.7	1.8±0.7
$CD3^+CD8^+CD107a^+$	0.9	0.5	0.8	0.5	0	0.5±0.4	0.2	0.7	0.2	0.4±0.3	0.5±0.3
$CD3^+CD4^+CD8^-$	49.9	57.7	51.2	49.7	57.8	53.3±4.1	55.5	57.8	66.1	59.8±5.6	55.7±5.5
$CD3^+CD4^+CD62L^+$	47.3	56	73.8	66	43	57.2±12.8	49.1	48.6	47.8	48.5±0.7	54.0±10.7
$CD3^+CD4^+CD69^+$	1.1	2.3	3.8	4.2	1.7	2.6±1.3	2.0	4.0	2.7	2.9±1.0	2.7±1.2
$CD3^+CD4^+CD45RO^+$	2	1.7	2.3	2.4	1.1	1.9±0.5**	1.3	0.9	1.0	1.1±0.2**	1.6±0.6
$CD3^+CD4^+CD107a^+$	1.2	0.6	1.5	0.9	0.2	0.9±0.5	0.2	0.9	0.4	0.5±0.4	0.7±0.5

* — within lymphocyte population gated on a FSC-A/SSC-A plot and non-single cells excluded
** — values with statistically significant differences ($p < 0.05$)

$CD20^+$) and 67.6±6.3% were T-cells ($CD45^+CD3^+CD20^-$). The $CD3^+$ subpopulation was comprised of 55.7±5.5% T-helper cells ($CD3^+CD4^+CD8^-$) and 34.3±3.7% of cytotoxic T-cells ($CD3^+CD4^-CD8^+$). The proportions of B- and T-cells, including the $CD4^+$ and $CD8^+$ populations, found in this study corroborate earlier findings for naïve marmosets [20,22], as well as the reported values for a healthy human population [23,24].

Lymphocyte activation and maturation markers were expressed in the immune cell subpopulations specified above in the following proportions: CD62L (L-selectin; lymphoid system homing signal, cleaved following cell activation) on 54.0±10.7% of $CD3^+CD4^+$ cells and 74.4±12.1% of $CD3^+CD8^+$ cells; CD69 (early T-cell activation marker) on 2.7±1.2% of $CD3^+CD4^+$ cells and 1.2±0.5% of $CD3^+CD8^+$ cells; CD45RO (memory-activated T-cells) on 1.6±0.6% of $CD3^+CD4^+$ cells and 1.8±0.7% of $CD3^+CD8^+$ cells; CD107a (T-cell activation) on 0.7±0.5% of $CD3^+CD4^+$ cells and 0.5±0.3% of $CD3^+CD8^+$ cells; CD27 (TNF receptor superfamily member (TNFRSF7); and memory B-cells, mature T-cells) on 94.6±2.1% of T-cells ($CD20^-CD3^+$). The values lay in the range of the ones observed in the recently published unique study of the distribution of diverse immune cell populations/subpopulations by Neumann *et al.* [21].

Interestingly, however, we observed a lower, compared to the published data [21], proportion of $CD45^+CD20^+CD27^+$ memory B-cells (8.9±3.9%), indicating a low level of B-cell activation. We explained this by the fact that the mean age of the animals used in our study was lower compared to the study by Neumann *et al.* (29.3±8.0 months) (*Table 1*). Besides, the proportion of subpopulations of $CD62L^+CD4^+$ and $CD62L^+CD8^+$ T-cells determined in this report appeared to be lower than the respective values described by Yoshida *et al.* [25], which might indicate T-cell activation. The percentage of $CD20^+CD27^+$ cells (activated B-cells) correlated with the percentage of CD62L-positive (non-activated) $CD3^+CD4^+$, but not $CD3^+CD8^+$ T-cells

(Spearman Ranking test; r=0,902; p=0,006). No other signs of systemic immune activation were observed.

The composition of the lymphocyte subpopulations and the levels of activation markers of T- and B-cells did not differ for male and female subjects. The only statistically significant difference was found in the proportion of the reactive $CD3^+CD4^+CD45RO^+$ cells (1.9±0.5 in females vs 1.1±0.2 in males; t-value = 2.5658, df=6, p=0,0426; t-test). The observed levels of $CD3^+CD4^+CD45RO^+$ cells in both males and females were within the values previously reported for naïve healthy animals [20].

The animals were of different age; one CM was considerably older than the others in the group (ID 3016, Table 1). In view of this, we analyzed the age dependence of all immune parameters. The proportion of $CD45^+CD20^+CD27^+$ memory B-cells was found to highly correlate with animals' age (Spearman ranking test, $r = 0.923$, $p = 0.0011$). Furthermore, the correlation was still significant if this single older animal was removed from the analysis ($r = 0.798$; $p = 0.03$). This correlation supports our hypothesis that a lower percentage of B-cells in our study is observed due to the younger mean age of the animals used. An analysis of other parameters of the immune status and activation markers revealed no significant age-related differences ($p > 0.05$).

DISCUSSION

In this report, we define the basal characteristics of the status of the immune system of CMs, typical of naïve healthy animals of differing age and gender, which are necessary for identifying the changes induced by the disease, as well as by immune therapy and/or vaccination. We observed that young animals had a lower proportion of $CD45^+CD20^+CD27^+$ memory B-cells compared to the published data [21], which is indicative of the low level of B-cell activation. The relevance of these observations to other juvenile and sub-adult animals will be addressed in further studies. Aside from this, we observed no statistically significant age-related changes neither in the parameters of immune status nor in the markers of immune differentiation, which allowed us to assume that CMs older than two years are suitable for immune testing in mixed-age groups.

The proportion of subpopulations of CD62L positive $CD4^+$ and $CD8^+$ T-cells determined in this report was lower than the respective values described by Yoshida *et al.* [25]. L-selectin (CD62L) mediates T-cell entry into the lymph nodes. The L-selectin levels are down-regulated in T-cells transmigrating within the lymph nodes, while its levels on the T cells in non-lymphoid organs and blood remain unchanged [26]. During T-cell activation, L-selectin expression reduces to 10% of the initial level within several minutes by ectodomain shedding [27]. The decrease in the proportion of $CD62L^+$ T-cells indicates, therefore, a possible recent/on-going T-cell activation. Interestingly, expression of $CD27^+$ on the B-cells of CMs correlated with the expression of L-selectin/$CD62L^+$ by $CD4^+$ T-cells ($p < 0.01$): i.e., B-cell activation was associated with the absence of immune activation (no CD62L shedding) in $CD4^+$ T cells. Earlier reports described associations between the expression of surface activation markers of memory B-cells CD27 and CD21 [28]. Complement receptor type II CD21 is expressed on most of the mature B-cells; earlier papers demonstrated that shedding of CD21 by B-cells occurs simultaneously with shedding of CD62L by the naïve and memory lymphocytes, the latter required to recruit them to the sites of the infection [29]. Both processes appear to be driven by the same family of proteases [29]. These data help to define the mechanism of CD21-mediated correlation between the expression of the B-cell CD27 activation marker and CD62L on T-cells. The correlation between the expression of CD27 by B-cells designating their activation, and of CD62L by $CD4^+$ T-cells (actually, an inverse correlation with CD62L shedding, designating $CD4^+$ T cell activation), may reflect the concordant regulation of the differentiation of these immune cell subsets in non-human primates.

In conclusion, we have characterized basal parameters of the immune status of naïve healthy marmosets without markers of systemic immune activation. Knowledge of these parameters is crucial for documenting the changes induced in CMs by therapeutic and prophylactic interventions. The antibody panel and gating procedures elaborated here allowed for a reliable quantification of specific immune cell populations and assessment of their functional status. Therefore, they could be recommended for use in trials of novel immune interventions, such as vaccines against chronic viral infections and cancer, in CMs. ●

The study was supported by the Russian Science Foundation (grant no. 15-15-30039). The breeding plan and management of the colony of common marmosets was financed from the State Task topic no. 209 of the Chumakov Federal Scientific Center for Research and Development of Immune-and-Biological Products of Russian Academy of Sciences. Training of the personnel working with non-human primates and the associated mobility costs were supported by grants from the Swedish Institute TP 09272/2013 and PI 19806_2016 (INNOVIMMUNE). Stefan Petkov was supported by the EU Horizon2020 project VACTRAIN no. 692293.

REFERENCES

1. Moi M.L., Ami Y., Muhammad Azami N.A., Shirai K., Yoksan S., Suzaki Y., Kitaura K., Lim C.K., Saijo M., Suzuki R., et al. // J. Gen. Virol. 2017. V. 98. № 12. P. 2955–2967.
2. Orsi A., Rees D., Andreini I., Venturella S., Cinelli S., Oberto G. // Regul. Toxicol. Pharmacol. 2011. V. 59. № 1. P. 19–27.
3. Carrion R., Patterson J.L. // Curr. Opin. Virol. 2012. V. 2. № 3. P. 357–362.
4. Arrand J.R. // Immunotherapy and vaccination against Epstein-Barr virus-associated cancer. Cancer vaccines / Eds Stern P., Carroll M., Beverley P. Cambridge: Cambridge Univ. Press, 2000. P. 174–194.
5. Abbott D.H., Barnett D.K., Colman R.J., Yamamoto M.E., Schultz-Darken N.J. // Comp. Med. 2003. V. 53. № 4. P. 339–350.
6. Cadavid L.F., Shufflebotham C., Ruiz F.J., Yeager M., Hughes A.L., Watkins D.I. // Proc. Natl. Acad. Sci. USA. 1997. V. 94. № 26. P. 14536–14541.
7. van der Wiel M.K., Otting N., de Groot N.G., Doxiadis G.G.M., Bontrop R.E. // Immunogenetics. 2013. V. 65. № 12. P. 841–849.
8. Antunes S.G., de Groot N.G., Brok H., Doxiadis G., Menezes A.A., Otting N., Bontrop R.E. // Proc. Natl. Acad. Sci. USA. 1998. V. 95. № 20. P. 11745–11750.
9. Gough A.W., Barsoum N.J., Gracon S.I., Mitchell L., Sturgess J.M. // Lab. Anim. Sci. 1982. V. 32. № 1. P. 87–90.
10. Mätz-Rensing K., Jentsch K.D., Rensing S., Langenhuyzen S., Verschoor E., Niphuis H., Kaup F.J. // Vet. Pathol. 2003. V. 40. № 4. P. 405–411.
11. Moi M.L., Takasaki T., Omatsu T., Nakamura S., Katakai Y., Ami Y., Suzaki Y., Saijo M., Akari H., Kurane I. // J. Gen. Virol. 2014. V. 95. № 3. P. 591–600.
12. McIntosh G.H., Giesecke R., Wilson D.F., Goss A.N. // Vet. Pathol. 1985. V. 22. № 1. P. 86–88.
13. Haworth R., Jones S., Sanchez-Morgado J., Pilling A. // Vet. Rec. 2003. V. 153. № 11. P. 332–333.
14. Zöller M., Mätz-Rensing K., Fahrion A., Kaup F.-J. // Vet. Pathol. 2008. V. 45. № 1. P. 80–84.
15. Miller A.D., Kramer J.A., Lin K.C., Knight H., Martinot A., Mansfield K.G. // Vet. Pathol. 2010. V. 47. № 5. P. 969–976.
16. Laufs R., Steinke H., Gisela S., Petzold D. // J. Natl. Cancer Inst. 1974. V. 53. № 1. P. 195–199.
17. Wolfe L.G., Deinhardt F. // Primates Med. 1978. V. 10. № 1. P. 96–118.
18. Wright J., Falk L.A., Wolfe L.G., Ogden J., Deinhardt F. // J. Natl. Cancer Inst. 1977. V. 59. № 5. P. 1475–1478.
19. Neubert R., Foerster M., Nogueira A.C., Helge H. // Life Sci. 1995. V. 58. № 4. P. 317–324.
20. Brok H.P.M., Hornby R.J., Griffiths G.D., Scott L.A.M., Hart B.A. // Cytometry. 2001. V. 45. № 4. P. 294–303.
21. Neumann B., Shi T., Gan L.L., Klippert A., Daskalaki M., Stolte-Leeb N., Stahl-Hennig C. // J. Med. Primatol. 2016. V. 45. № 3. P. 139–146.
22. Nelson M., Loveday M. // J. Immunol. Res. 2014. ID 913632. P. 1–8.
23. Reichert T., DeBruyère M., Deneys V., Tötterman T., Lydyard P., Yuksel F., Chapel H., Jewell D., Van Hove L., Linden J., et al. // Clin. Immunol. Immunopathol. 1991. V. 60. № 2. P. 190–208.
24. Chng W.J., Tan G.B., Kuperan P. // Clin. Diagn. Lab. Immunol. 2004. V. 11. № 1. P. 168–173.
25. Yoshida T., Omatsu T., Saito A., Katakai Y., Iwasaki Y., Kurosawa T., Hamano M., Higashino A., Nakamura S., Takasaki T., et al. // Arch. Virol. 2013. V. 158. № 6. P. 1209–1220.
26. Klinger A., Gebert A., Bieber K., Kalies K., Ager A., Bell E.B., Westermann J. // Int. Immunol. 2009. V. 21. № 4. P. 443–455.
27. Galkina E., Tanousis K., Preece G., Tolaini M., Kioussis D., Florey O., Haskard D.O., Tedder T.F., Ager A. // J. Exp. Med. 2003. V. 198. № 9. P. 1323–1335.
28. Das A., Xu H., Wang X., Yau C.L., Veazey R.S., Pahar B. // PLoS One. 2011. V. 6. № 1. e16524.
29. Sengstake S., Boneberg E.-M., Illges H. // Int. Immunol. 2006. V. 18. № 7. P. 1171–1178.

Overexpression of Adenoviral E1A Sensitizes E1A+Ras-Transformed Cells to the Action of Histone Deacetylase Inhibitors

M. V. Igotti*, S. B. Svetlikova, V. A. Pospelov
Institute of Cytology, Russian Academy of Sciences, Tikhoretsky Ave., 4, St-Petersburg, 194064, Russia
*E-mail: marie.igotti@gmail.com
Received May 18, 2018; in final form October 23, 2018

ABSTRACT **The adenoviral E1A protein induces cell proliferation, transformation, and tumor formation in rodents, on the one hand. On the other hand, E1A expression increases cell sensitivity to a number of cytotoxic agents. Therefore, E1A is a candidate for use as a component of combination therapy for malignant tumors. The highest augmentation in the cytotoxic effect was achieved by a combined use of E1A expression and histone deacetylases (HDAC) inhibitors. However, HDAC inhibitors do not induce apoptosis in cells transformed with E1A and cHa-ras oncogenes. In this study, it was shown that HDAC inhibitors reduce the expression of adenoviral E1A. However, under unregulated E1A overexpression, these cells undergo apoptosis in the presence of HDAC inhibitors. Treatment with a HDAC inhibitor, sodium butyrate (NaBut), was shown to activate the anti-apoptotic factor NF-kB in control cells. However, NaBut was unable to modulate the NF-kB activity in E1A overexpressed cells. Therefore, it is fair to postulate that cells transformed with E1A and *cHa-ras* oncogenes avoid the apoptosis induced by HDAC inhibitors thanks to a NaBut-dependent decrease in E1A expression.**
KEYWORDS **apoptosis; histone deacetylase inhibitors; *E1A* and *cHa-ras* oncogenes, transformed cells.**
ABBREVIATIONS **HDAC – histone deacetylase; HDI – histone deacetylase inhibitor; mERas – mouse embryo fibroblasts transformed with E1A and cHa-ras oncogenes; NaBut – sodium butyrate.**

INTRODUCTION

The E1A gene of human adenovirus type 5 is an early response gene that is expressed in infected cells and provides the necessary conditions for virus replication [1]. At first, E1A was considered an oncogene due to its ability to immortalize rodent cells and transform them in cooperation with other oncogenes [2, 3]. It was found later that E1A exhibits antitumor activity [4]; it is sometimes considered a tumor suppressor for that reason.

The transforming activity of E1A is determined by its ability to deregulate the cell cycle by binding to and altering the activity of such cellular factors as pRb family proteins [5–7] and the cyclin-dependent kinase inhibitors p21Waf1 [8, 9] and p27Kip1 [10]. E1A also interacts with chromatin remodeling proteins, including histone acetyltransferase (p300/CBP) [11] and histone deacetylases [12]. This interaction changes the transcription of a number of the genes involved in cell cycle regulation. Adenoviral DNA and the E1A protein are found in the lung epithelium cells of patients with a chronic obstructive pulmonary disease [13]. However, as we have already mentioned, E1A possesses an antitumor activity and is the subject of clinical studies [14, 15]. Plenty of experimental data suggest that expression of adenoviral E1A protein increases the sensitivity of mammalian cancer cells to a number of cytotoxic agents used in antitumor therapy, such as etoposide, cisplatin, taxanes, etc. [16–19]. The combined effect of E1A gene therapy and HDIs leads to a more significant increase in the level of cancer cell death, accompanied by a minimal negative impact on normal cells, as compared to taxol or etoposide [19].

Adenoviral E1A promotes apoptotic cell death by modulating the expression of the genes regulating

apoptosis [17–19], the activation of p38 MAP kinase [17], and suppression of the anti-apoptotic factor NF-κB [20, 21]. E1A also stabilizes p53 via a modification of the ubiquitin proteasome pathway [16, 22]. As a result, the p53 protein level in cells expressing adenoviral E1A protein increases, leading to p53-dependent apoptosis [16].

The level of apoptosis in cells expressing E1A can be reduced by the complementary transforming *ras* oncogene, which activates the anti-apoptotic PI3K/Akt cascade and NF-κB via the stimulation of the Ras/Raf/MEK/ERK kinase cascade [23]. The anti-apoptotic functions of Ras are associated with its ability to stimulate the expression of the anti-apoptotic Bcl-2 and Bcl-XL proteins [23]. Thus, the action of the proapoptotic E1A protein and oncogenic Ras is balanced in mouse embryonic fibroblasts stably transformed by the vector encoding cHa-ras and the plasmid encoding the E1A protein of human adenovirus type 5 [24].

Histone deacetylase inhibitors (HDIs) inhibit tumor cell growth, thus causing cell cycle arrest, senescence, or apoptosis, without having a toxic effect on normal cells [25, 26]. Therefore, HDIs are considered to be promising antitumor agents.

We have previously shown that HDIs cause cell cycle arrest and senescence of cells transformed by *cHa-Ras* and *E1A* oncogenes [27–29] but do not induce their death. This feature distinguishes these cells from other tumor cells, where HDIs stimulate apoptotic death [25, 26]. Therefore, we studied the reasons behind the absence of apoptotic death of cells expressing E1A with activated Ras under the action of HDIs. It was found that the ability of cells transformed by E1A and *cHa-ras* to avoid death under the action of HDIs is due to the HDI-dependent decrease in E1A expression and activation of the NF-κB anti-apoptotic factor. Therefore, induction of apoptosis in E1A+Ras-transformed cells by HDIs is possible only under unregulated E1A expression.

MATERIALS AND METHODS

Cell lines

Our studies were performed using mouse embryonic fibroblasts that had been stably transformed with a vector encoding cHa-ras and with p1A plasmid that contained nucleotides 1–1634 of the genome of human adenovirus type 5 encoding the E1A protein [16, 24]. Cells were treated with NaBut (4 mM) for 24–72 h.

Cell distribution according to DNA content

The distribution of cells by DNA content was studied by flow cytometry. The cells were washed with a PBS solution (0.14 M NaCl, 2.7 mM KCl, 6.5 mM Na_2HPO_4, 1.5 mM KH_2PO_4, pH 7.2), permeabilized with saponin at a final concentration of 0.01% for 20 min, and repeatedly washed with the PBS solution to remove saponin. The cells were then incubated with RNase A (100 μg/mL) and propidium iodide (10 μg/mL, 15 min at 37°C) and analyzed on a Coulter Epicks XL flow cytometer (Bechman, USA).

Cell viability

Cell viability was measured by MTT assay. The cells were plated in 96-well plates at a density of 2×10^3 cells/well and cultured for 24 h in either the presence or absence of the respective inhibitors. Cell viability was determined spectrophotometrically by assessing their metabolic activity according to their ability to reduce 3-(4,5-dimethylthiazole-2-yl)-2,5-diphenyltetrazolium bromide (MTT) (Sigma) to insoluble purple formazan. The cells were incubated in a MTT solution in PBS at a final concentration of 0.5 mg/mL (1.5 h at 37°C in a CO_2 incubator). The culture medium was then removed, and the cells were suspended in dimethyl sulfoxide (DMSO). The optical density in each well was determined at a wavelength of 570 nm using a Multiscan-EX plate reader (Labsystems). DMSO was used as a blank control.

Protein immunoblotting

The cells were lysed in a buffer containing 1% NP-40, 0.5% sodium deoxycholate, 0.1% sodium dodecyl sulfate (SDS), protease, and phosphatase inhibitors. Proteins were separated by electrophoresis, transferred to a PVDF membrane (Millipore), and analyzed using the appropriate specific antibodies. Proteins on the membranes were detected using the enhanced chemiluminescence method (Thermo Sci., USA). Antibodies raised against E1A (M73) proteins (Santa Cruz Biotechnology, Inc., USA), Gapdh (14C10) (Cell Signalling, USA) and pan-Ras proteins (Oncogene Sci., USA) were used.

Gene transcription analysis

Cellular RNA was isolated using a Trizol reagent (Invitrogen, USA). The reverse transcription reaction was performed using 2 μg of RNA. The amplification reaction (PCR) was performed in the presence of 100 ng of the corresponding primers to cDNA of the mouse *e1a* and *gapdh* genes: 5'-TGTGATGGGTGTGAACCACG-3'/5'-CCAGTGAGCTTCCCGTTCAG-3'. Linear PCR amplification of DNA fragments was performed during 25–35 cycles. The specific reaction product was analyzed by electrophoresis in 2% agarose gel.

Caspase-3 activity

Caspase-3 activity was assayed *in vitro* based on the cleavage of the specific colorimetric substrate Ac-DEVD-pNA (Calbiochem). Cells were lysed for 20 min at +4°C in a buffer containing 50 mM Tris-HCl, pH 7.5; 120 mM NaCl; 1 mM EDTA; 1% NP-40, and protease inhibitors. Caspase activity was determined in 96-well plates in 40 μL of lysates mixed with 160 μL of a reaction buffer (20% glycerol; 0.5 mM EDTA; 5 mM DTT; 100 mM HEPES, pH 7.5) containing Ac-DEVD-pNA substrate. The efficiency of Ac-DEVD-pNA cleavage was determined spectrophotometrically based on the accumulation of *n*-nitroanilide at a wavelength of 405 nm using a Multiscan-EX spectrophotometer (Labsystems).

Temporary transfection and analysis of luciferase activity

Cells were transfected using the Lipofectamine-2000 reagent (Invitrogen), according to the manufacturer's protocol. A luciferase reporter vector carrying three copies of NF-κB-binding sequences (3 × κB-luc) was used for transfection. Renilla luciferase expression was used as an internal control. Cells were treated with 4 mM NaBut 24 h post-transfection and then processed according to the manufacturer's instructions for measuring luciferase activity after 48 h. Luciferase activity was determined using a TD-20/20 luminometer (Turner Designs). Each experiment was repeated at least 3 times.

RESULTS

Histone deacetylase inhibitor sodium butyrate inhibits the expression of adenoviral E1A

In order to clarify the reasons for the absence of the expected cytotoxic effect of HDIs in E1A-expressing cells, we analyzed the effect of a HDI, sodium butyrate (NaBut), on the expression of transforming oncogenes. The data presented in *Fig. 1* show that E1A expression is reduced in the presence of NaBut. In mouse embryo fibroblasts transformed with the E1A and *cHa-Ras* oncogenes (mERas line), transcription of the *e1a* gene (*Fig. 1A*) and the level of E1A protein (*Fig. 1B*) decreased as soon as during the first hours of exposure to NaBut. Is this effect specific to the particular cell line and HDIs employed? In order to answer this question, we analyzed the E1A expression in the transformed human cell lines and used alternative HDIs. We found that valproic acid (VA), trichostatin A (TSA) (data not shown), and vorinostat also reduced the amount of E1A in mERas transformants (*Fig. 1B, lower panel*). The results shown in *Fig. 1C* demonstrate that the decrease in E1A expression under the action of HDIs is not specific

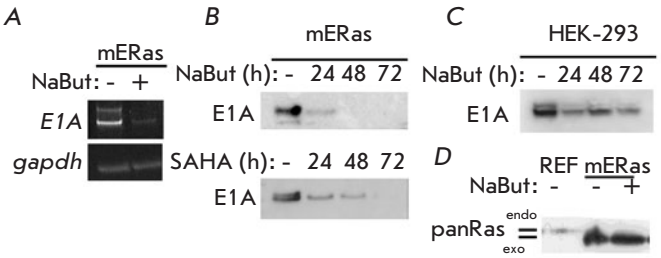

Fig. 1. Sodium butyrate downregulates E1A expression in cells expressing E1A. *A* – RT-PCR analysis of *E1A* transcription in mERas cells: either untreated (-) or treated (+) with 4 mM NaBut for 16 h; *B* – immunoblotting of proteins from mERas cells, either untreated (-) or treated with 4 mM NaBut (upper panel) or 2.5 μM SAHA (lower panel) for 24–72 h, with antibodies raised against E1A of human adenovirus type 5 (E1A5Ad); *C* – immunoblotting of proteins from HEK-293 cells with antibodies raised against E1A5Ad; *D* – immunoblotting of proteins from mERas cells with antibodies raised against pan-Ras

only to the mERas line. Immunoblotting demonstrated that the amount of E1A protein in the transformed human renal epithelial HEK-293 cells decreased in the presence of NaBut. The results of immunoblotting showed that the expression of the Ras protein did not change in the presence of NaBut (*Fig. 1D*). Thus, HDIs were found to suppress the expression of adenoviral E1A, whereas Ras expression was not modulated by HDIs.

The detected decrease in the E1A protein level in the presence of HDIs can shift the equilibrium between the activities of transforming proteins in mERas cells. Meanwhile, the action of oncogenic Ras becomes dominant. We considered that the low level of apoptosis in the E1A+Ras transformed cells treated with HDIs was associated with the HDIs-mediated decrease in pro-apoptotic E1A protein expression and activation of the anti-apoptotic Ras/Akt/NF-κB cascade.

Production of a E1A+Ras-transformed cell line with E1A expression unregulated by HDIs

The mERas cell line was obtained using a p1A plasmid carrying the nucleotides 1–1634 of human adenovirus type 5 encoding the E1A protein [16, 24]. In these cells, the native promoter regulates the expression of the *e1a* gene. In order to test the hypothesis that reduction in E1A expression is required to reduce the HDIs-induced apoptosis, we produced a MER-E1A cell line based on mERas cells. The MER-E1A cell line additionally expressed the E1A 12S protein under the

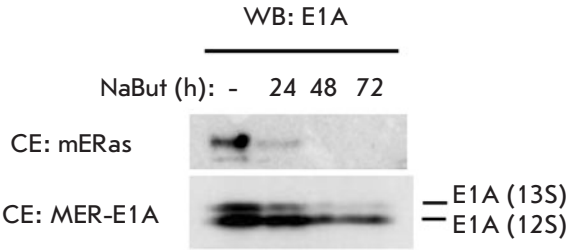

Fig. 2. Immunoblotting of proteins from mERas (upper panel) and MER-E1A (lower panel) cells treated with 4 mM NaBut for 24–72 h, with antibodies raised against E1A5Ad

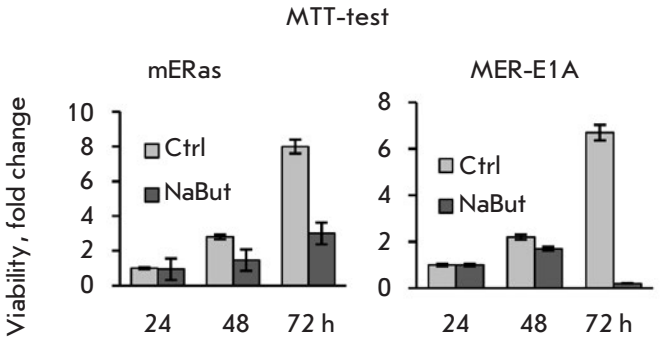

Fig. 3. Sodium butyrate suppresses the viability of mERas and MER-1A cells to different extents. Control mERas and MER-E1A cells stably expressing E1A were treated with NaBut for 24–72 h, and their viability was determined by MTT assay. Changes in viability (fold) were assessed with respect to the viability of untreated cells 24 h after plating

control of an unregulated cytomegalovirus (CMV) promoter. Regulation and activity of CMV and Ad5 viral promoters differ significantly: so, they can be used in target cells for different purposes. The high-activity CMV promoter is convenient for efficient transgene expression.

Figure 2 shows the immunoblotting results that demonstrate how NaBut affects the expression of the E1A protein in the original mERas cell line (upper panel) and in the new MER-E1A cell line with constitutive E1A expression under the control of the CMV promoter (lower panel). In the control mERas cells, E1A expression decreased to almost zero already during the first hours of exposure to NaBut and remained at a low level throughout the entire study (up to 72 h). However, in MER-E1A cells, the E1A 12S protein was expressed at a high level independently of NaBut.

Thus, we obtained a line of transformed rodent cells expressing the adenoviral E1A gene under the control of the CMV promoter in which E1A expression did not decrease in the presence of HDIs.

Sodium butyrate induces apoptosis only in E1A+Ras-transformed cells where the amount of E1A does not decrease in the presence of HDIs

Next, we compared the effect of HDIs on the proliferation of E1A+Ras-transformed cells where E1A is expressed under the control of an intrinsic promoter, and in cells where the CMV promoter regulates E1A expression. We evaluated the effect of NaBut on cell viability depending on E1A expression. The control mERas cells and MER-E1A cells with unregulated E1A expression were treated with NaBut for 24–72 h; their viability was determined using the MTT assay. *Figure 3A* demonstrates that the viability of control mERas cells treated with NaBut decreased more than that of the untreated ones. However, the amount of formazan, which characterizes cell viability, rose with an increase in the duration of exposure of mERas cells to NaBut. The increased amount of formazan attests to the fact that the cells did not divide but remained alive. Meanwhile, the number of viable MER-E1A cells decreased below the baseline, indicating cell death.

In order to test the hypothesis about the induction of death of cells with E1A expression not regulated by NaBut, we analyzed the distribution of cells by DNA content using a flow cytometer. Cell distribution after transient transfection is shown in *Fig. 4A*. One can see that NaBut did not increase the sub-diploid peak in cells transfected with the control empty pcDNA3 vector (*Fig. 4A*, upper panel). At the same time, the percentage of cells with a sub-diploid DNA content in cells transfected with CMV-E1A increased twofold already 48 h after the exposure to NaBut (*Fig. 4A*, bottom panel). The findings demonstrate that there is a significant difference in cell response to HDIs depending on how HDIs modulate E1A expression.

The corresponding results were obtained in stable clones with E1A overexpression under the control of the CMV promoter (MER-E1A). In the control mERas cells, NaBut did not increase the sub-diploid peak in the distribution histogram of DNA content, which is characteristic of dying cells, even after 72 h (*Fig. 4B*). Meanwhile, 35% of MER-E1A cells contained fragmented DNA 72 h after the exposure to NaBut.

Hence, it was shown that NaBut induced the death of only those Ras-transformed cells in which expression of E1A did not decrease in the presence of NaBut.

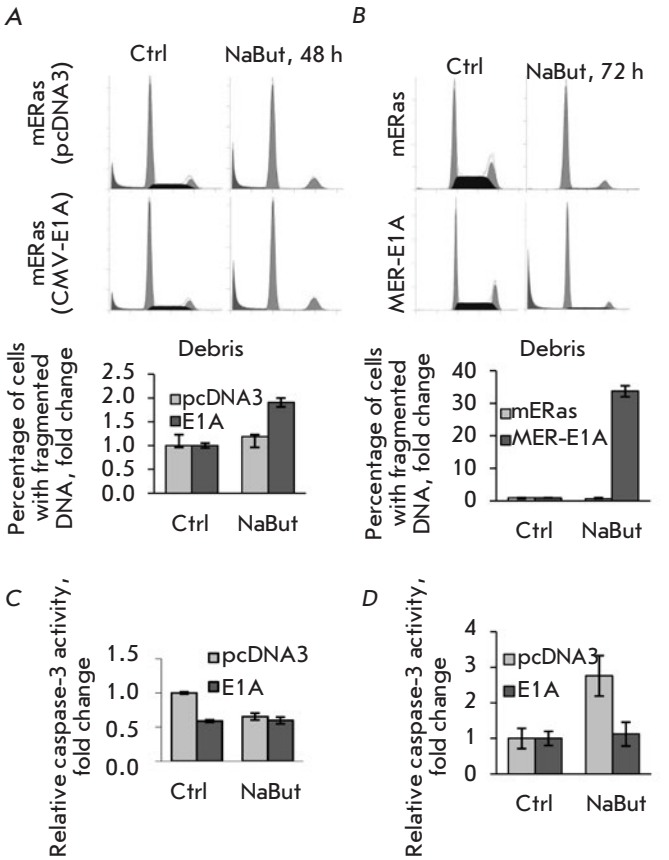

Fig. 4. Adenoviral E1A alters the effect of NaBut on transformed cells. *A* – FACS analysis of mERas cell distribution according to DNA content. The mERas cells were transfected with the control vector pcDNA3 (upper panel) or expression vector CMV-E1A (lower panel); after 24 h, the transfected cells were treated with NaBut for 48 h; *B* – distribution of stable clones according to DNA content. The mERas control cells or MER-1A cells stably expressing E1A were treated with NaBut for 72 h; *C* – the relative activity of caspase-3 in cells transfected with pcDNA3 (light gray bars) or CMV-E1A (dark bars), untreated (Ctrl) or treated with 4 mM NaBut for 24 h; *D* – the relative activity of luciferase transcribed from a NF-κB-regulated promoter. The mERas cells were co-transfected with a reporter 3*kB-luc vector and empty pcDNA3 vector (light gray bars) or with a CMV-E1A expression vector (dark bars) and treated with NaBut 24 h post-transfection for 24 h

We analyzed the activity of the caspase-3 mediating the transduction of the apoptotic signal. For this purpose, cells transfected with pcDNA3 or CMV-E1A were either left untreated or treated with NaBut for 24 h; the *in vitro* activity of caspase-3 in cell lysates was subsequently determined. NaBut reduced caspase-3 activity in control cells transfected with pcDNA3, identically to the case in the initial mERas cells [30]. Meanwhile, NaBut did not reduce caspase-3 activity in cells transfected with CMV-E1A (*Fig. 4C*). The differences in the regulation of caspase-3 activity by HDI depending on modulation of the E1A expression are consistent with our data demonstrating differences in the proliferative response of these cells to HDI.

NaBut does not increase NF-κB activity in cells with unregulated E1A expression

It was shown earlier that HDIs activate the anti-apoptotic factor NF-κB in cells transformed with E1A and *cHa-ras* [30]. This activation allowed transformants to avoid apoptosis when exposed to HDIs. Therefore, we compared the effect of HDIs on NF-κB activity in cells with regulated and unregulated E1A expression. For comparison, the initial mERas cells were co-transfected with a 3×κB-luc vector containing the luciferase gene under the control of a promoter regulated by NF-κB and either the CMV-E1A expression vector or empty pcDNA3 vector as a control. Twenty-four hours post-transfection, the cells were either left untreated or treated with NaBut for 24 h. Luciferase activity in lysates was measured. The NF-κB-dependent transcription in the control (pcDNA3) cells increased threefold in the presence of NaBut, whereas NF-κB activity in cells with unregulated high E1A expression (CMV-E1A) remained unchanged (*Fig. 4D*). We found that unregulated high expression of adenoviral E1A from the CMV promoter prevented HDI-dependent activation of the anti-apoptotic factor NF-κB. Therefore, inhibition of NF-κB activity by adenoviral E1A is one of the reasons for the induction of apoptosis by HDIs in these cells.

Cells with unregulated E1A expression do not accumulate senescence marker SA-β-Gal in the presence of NaBut

Cellular senescence and apoptosis are the alternative anti-proliferative programs induced by cytotoxic and stress factors. It was previously shown that HDIs induce senescence of cells transformed with *cHa-Ras* and E1A oncogenes [27–29]. The senescence program in these cells is presumably initiated due to the fact that HDIs downregulate E1A expression: so, the cellular senescence program induced by activated Ras starts to predominate [31]. In order to check the assumption that cellular senescence is not induced in E1A+Ras-transformed cells where E1A expression is not suppressed by HDIs, we analyzed the expression of the cellular senescence marker SA-β-Gal. The optical microscopy data (*Fig. 5*) show that there is SA-β-Gal in almost all control mERas transformants after treatment with NaBut for 72 h, thus indicating that cellular senes-

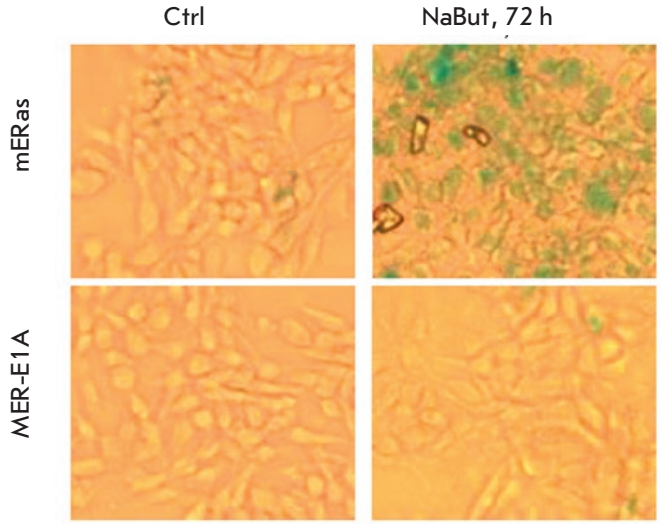

Fig. 5. Sodium butyrate failed to induce senescence in cells with unregulated E1A expression. SA-β Gal staining. The mERas and MER-E1A cells were treated with NaBut for 72 h; the cells were then fixed and stained for SA-βGal

cence was induced. In MER-E1A cells, the SA-β-Gal marker had not accumulated. After exposure to NaBut for 72 h, very few MER-E1A cells remained attached to the slides for further SA-β-Gal staining; most cells died and were floating. Hence, it is fair to conclude that NaBut induces cellular senescence in cells transformed with *E1A* and *Ras* if E1A expression decreases in the presence of NaBut. Meanwhile, the transformants with constitutive E1A expression die rather than senesce.

DISCUSSION

In cooperation with activated *Ras* or other oncogenes, adenoviral E1A immortalizes and transforms primary rodent cells [2, 3]. In this regard, E1A was earlier considered to be an oncoprotein, although it was not associated with any oncogenic activity. Later, E1A was found to exhibit antitumor activity [2, 17–19]. Overexpression of E1A causes arrest of proliferation and apoptosis of human tumor cells *in vitro* [4, 16]. Moreover, apoptosis plays a key role in the antitumor activity of E1A. A number of preclinical studies demonstrated that liposomal or adenoviral delivery of the E1A gene inhibits tumor growth and metastasis development in animals [17, 32]. Clinical trials of gene monotherapy and combination therapy with E1A for cancers of different localizations demonstrated that this approach is justified [14, 33, 34]. The efforts of many scientists have recently been focused on whether or not therapy using oncolytic viruses based on human adenovirus type 5 (Ad5) can be employed [35]. According to the ClinicalTrials.gov website of the National Institutes of Health, more than 180 clinical trials using adenoviruses in a particular form have already been conducted. The gene encoding E1A is the main target for the production of oncolytic adenoviruses with limited replicative ability. This choice is determined by the role played by this protein in the initiation of cell division in a resting cell via sequestration of the tumor suppressor pRb. Taking into account the potential significance of adenoviruses and adenoviral E1A in antitumor therapy, comprehensive research into the functioning and regulation of E1A, which leads to cell sensitization to cytostatics, is a relevant issue in molecular biology.

Many studies have demonstrated that combined use of HDIs and adenoviral E1A in tumor cells increases the cytotoxic effect [19, 36, 37]. HDIs did not cause the death of cells transformed with the *cHa-ras* and *E1A* oncogenes used in this study. However, sodium butyrate induced apoptosis in these cells when adenoviral *E1A* was expressed under the control of a HDI-unregulated promoter. In studies reporting that combined use of HDIs and E1A enhanced the cytotoxic effect, *E1A* expression was controlled not by a native promoter, but by the cytomegalovirus (CMV) promoter or by the catalytic subunit of telomerase (TERT) [19, 39–40]. The activity of these promoters was not suppressed by HDIs but stimulated by them [19, 38]. Consequently, our results are in line with the data on the efficiency of a combined use of HDIs and E1A for eliminating malignantly transformed cells under increased unregulated E1A expression. Our results are of higher priority as we have demonstrated that HDIs can suppress E1A expression on several levels. First, transcription of the E1A gene was reduced in the presence of NaBut (*Fig. 1A*). The regulation of E1A expression is currently understudied. No data on the role of acetyltransferases or deacetylases in the regulation of E1A transcription are available. Inhibition of histone deacetylases activates gene transcription via a relaxation of the chromatin structure. On the other hand, HDIs can inhibit or activate transcription by changing the acetylation level of transcription factors [41]. Hence, the demonstrated inhibition of E1A is probably mediated by a modulation of the activity of the transcription factors involved in the regulation of E1A expression by histone deacetylases. The enhancer region of the E1A promoter contains two binding sites for E2F transcription factors, along with other regulatory elements [42]. The absence of these sites completely suppresses E1A expression, thus indicating that the E2F-binding regions play an exceptionally important role in the regulation of *E1A* transcription. Earlier, we showed that NaBut suppresses the *trans*-activating ability of the E2F factor

[28, 43]. Therefore, it is fair to assume that the observed decrease in E1A expression is partially due to NaBut-dependent inhibition of the E2F factor. The activity of other viral promoters frequently used in genetic engineering (cytomegalovirus and polyomavirus (SV40)) is known to be stimulated by HDIs [38]. Although sharing a number of similar features, viral promoters differ significantly in terms of the mechanism of regulation of their activity. Thus, the CMV promoter is positively regulated by the E1A protein [44], whereas the E1A protein represses the native promoter of the E1A gene and HIV-LTR promoter [45, 46]. Therefore, it can be assumed that regulation of the activity of viral promoters by deacetylase inhibitors is also not universal.

Second, our data suggest that HDIs reduce the content of the E1A protein both in mERas cells and in a transformed human embryonic kidney (HEK) 293 cell line (*Fig. 1B*). Moreover, the content of the E1A protein decreases more intensively than *E1A* transcription does. This finding indicates that deacetylase inhibitors modulate the stability of the E1A protein. Like many cellular proteins, virus-encoded proteins also act as substrates for acetyltransferases and deacetylases. The E1A protein is able to bind to p300/CBP and can be acetylated by p300 and PCAF [47]. Acetylation alters the nature of the interaction between E1A and partner proteins [48] and determines its intracellular localization [47]. Thus, E1A acetylation prevents nuclear import and, accordingly, leads to E1A accumulation in the cytoplasm. However, inhibition of deacetylases by sodium butyrate in HEK-293 cells expressing E1A did not increase the amount of acetylated E1A and, consequently, did not cause accumulation of E1A in the cytoplasm [47]. These data suggest that E1A undergoes rapid degradation that follows protein acetylation. The E1A degradation can occur in proteasomes [48]. It was also shown that early-region 1A proteins of adenovirus type 2 and 12 (Ad2 and Ad12 E1A) were cleaved by caspases-3 and caspases-7 during induced apoptosis in human and mouse cells transformed by adenovirus [49]. The aforementioned data suggest that enhanced acetylation of the E1A protein induced by HDIs may be one of the factors responsible for E1A degradation.

Comparison of the responses of transformed cells with regulated and unregulated E1A expression to HDIs showed that apoptosis was induced only in cells with an increased unregulated E1A expression. In the control mERas cells with a reduced content of E1A, the cell senescence program was initiated (*Fig. 5*). We have shown that avoidance of apoptotic death by control mERas cells is associated with the downregulated expression of the pro-apoptotic E1A protein and activation of the anti-apoptotic NF-κB cascade. Meanwhile, the oncogenic Ras inducing senescence starts to play a predominant role. In turn, induction of apoptotic death in the presence of NaBut in cells with E1A overexpression is associated with a suppressed and unregulated activity of the anti-apoptotic NF-κB complex. Data on the repression of NF-κB activity by E1A oncoprotein have been reported [18, 20, 21]. Thus, E1A competitively binds and inactivates protein kinase A, which is expected to phosphorylate NF-κB and thus activate it [21]. E1A also suppresses IKK activity, thus reducing the degradation of IκB, the inhibitor regulating the NF-κB function [20]. Therefore, taking into account the aforementioned data and the findings that demonstrate that E1A content and activation of NF-κB decrease in a time-synchronized manner [30], it is fair to say that HDIs affect the NF-κB activity in cells transformed with E1A+Ras by modulating E1A expression.

CONCLUSIONS

Expression of adenoviral E1A increases the sensitivity of tumor cells to apoptosis-inducing agents [18]. Therefore, E1A is of great interest as a potential component of combination tumor therapy. The combined use of E1A and HDIs enhances the cytotoxic effect in many cancer cells, while having a minimal negative effect on normal cells [19]. However, HDIs do not induce apoptosis in a cell line transformed with *cHa-Ras* and E1A oncogenes in which E1A is expressed under the control of a native viral promoter. In the present study, we have shown that HDIs suppress the expression of adenoviral E1A. Apoptotic death of E1A/Ras-transformed cells can be induced by HDIs if E1A is expressed at a high unregulated level. In other words, the avoidance of apoptotic death by *Ras*-transformed cells expressing E1A is associated with downregulation of E1A expression in the presence of HDIs. In turn, the forced HDI-independent expression of E1A paves the way for apoptosis induction. ●

REFERENCES

1. Flint J., Shenk T. // Annu. Rev. Genet. 1989. V. 23. № 1. P. 141–161. http://www.ncbi.nlm.nih.gov/pubmed/2533472
2. Frisch S.M., Mymryk J.S. // Nat. Rev. Mol. Cell Biol. 2002. V. 3. № 6. P. 441–452. http://www.ncbi.nlm.nih.gov/pubmed/12042766
3. Ruley H.E. // Nature. 1983. V. 304. № 5927. P. 602–606. http://www.nature.com/doifinder/10.1038/304602a0
4. Frisch S.M. // Proc. Natl. Acad. Sci. USA. 1991. V. 88. № 20. P. 9077–9081. http://www.ncbi.nlm.nih.gov/pubmed/1833772
5. Pelka P., Ablack J.N.G., Fonseca G.J., Yousef A.F., Mymryk

J.S. // J. Virol. 2008. V. 82. № 15. P. 7252–7263. http://www.ncbi.nlm.nih.gov/pubmed/18385237
6. Chinnadurai G. // Trends Microbiol. 2011. V. 19. № 4. P. 174–183. http://www.ncbi.nlm.nih.gov/pubmed/21330137
7. Zamanian M., La Thangue N.B. // EMBO J. 1992. V. 11. № 7. P. 2603–10. http://www.ncbi.nlm.nih.gov/pubmed/1385776
8. Keblusek P., Dorsman J.C., Teunisse A.F., Teunissen H., van der Eb A.J., Zantema A. // J. Gen. Virol. 1999. V. 80. № 2. P. 381–390.
9. Bulavin D. V., Tararova N.D., Aksenov N.D., Pospelov V.A., Pospelova T. V. // Oncogene. 1999. V. 18. № 41. P. 5611–5619. http://www.ncbi.nlm.nih.gov/pubmed/10523840
10. Mal A., Poon R.Y.C., Howe P.H., Toyoshima H., Hunter T., Harter M.L. // Nature. 1996. V. 380. № 6571. P. 262–265. http://www.ncbi.nlm.nih.gov/pubmed/8637577
11. Ferrari R., Pellegrini M., Horwitz G.A., Xie W., Berk A.J., Kurdistani S.K. // Science. 2008. V. 321. № 5892. P. 1086–1088. http://www.ncbi.nlm.nih.gov/pubmed/18719284
12. Miura T.A., Cook J.L., Potter T.A., Ryan S., Routes J.M. // J. Cell. Biochem. 2007. V. 100. № 4. P. 929–940. http://www.ncbi.nlm.nih.gov/pubmed/17063489
13. Keicho N., Higashimoto Y., Bondy G.P., Elliott W.M., Hogg J.C., Hayashi S. // Am. J. Physiol. 1999. V. 277. № 3 Pt 1. P. L523–L532. http://www.ncbi.nlm.nih.gov/pubmed/10484459
14. Madhusudan S., Tamir A., Bates N., Flanagan E., Gore M.E., Barton D.P.J., Harper P., Seckl M., Thomas H., Lemoine N.R., et al. // Clin. Cancer Res. 2004. V. 10. № 9. P. 2986–2996. http://www.ncbi.nlm.nih.gov/pubmed/15131034
15. Yoo G.H., Hung M.C., Lopez-Berestein G., LaFollette S., Ensley J.F., Carey M., Batson E., Reynolds T.C., Murray J.L. // Clin. Cancer Res. 2001. V. 7. № 5. P. 1237–1245. http://www.ncbi.nlm.nih.gov/pubmed/11350889
16. Lowe S.W., Ruley H.E. // Genes Dev. 1993. V. 7. № 4. P. 535–545. http://www.ncbi.nlm.nih.gov/pubmed/8384579
17. Liao Y., Hung M.-C. // Cancer Res. 2004. V. 64. № 17. P. 5938–5942. http://www.ncbi.nlm.nih.gov/pubmed/15342371
18. Radke J.R., Siddiqui Z.K., Figueroa I., Cook J.L. // Cell Death Discov. 2016. V. 2. № 1. P. 16076. http://www.ncbi.nlm.nih.gov/pubmed/27833761
19. Yamaguchi H., Chen C.-T., Chou C.-K., Pal A., Bornmann W., Hortobagyi G.N., Hung M.-C. // Oncogene. 2010. V. 29. № 41. P. 5619–5629. http://www.nature.com/doifinder/10.1038/onc.2010.295
20. Shao R., Tsai E.M., Wei K., von Lindern R., Chen Y.H., Makino K., Hung M.C. // Cancer Res. 2001. V. 61. № 20. P. 7413–7416. http://www.ncbi.nlm.nih.gov/pubmed/11606372
21. Guan H., Jiao J., Ricciardi R.P. // J. Virol. 2008. V. 82. № 1. P. 40–48. http://www.ncbi.nlm.nih.gov/pubmed/17959673
22. Nakajima T., Morita K., Tsunoda H., Imajoh-Ohmi S., Tanaka H., Yasuda H., Oda K. // J. Biol. Chem. 1998. V. 273. № 32. P. 20036–20045. http://www.ncbi.nlm.nih.gov/pubmed/9685342
23. Pylayeva-Gupta Y., Grabocka E., Bar-Sagi D. // Nat. Rev. Cancer. 2011. V. 11. № 11. P. 761–774. http://www.ncbi.nlm.nih.gov/pubmed/21993244
24. Pospelova T.V., Medvedev A.V., Kukushkin A.N., Svetlikova S.B., van der Eb A.J., Dorsman J.C., Pospelov V.A. // Gene Expr. 1999. V. 8. № 1. P. 19–32. http://www.ncbi.nlm.nih.gov/pubmed/10543728
25. Bolden J.E., Shi W., Jankowski K., Kan C.-Y., Cluse L., Martin B.P., MacKenzie K.L., Smyth G.K., Johnstone R.W. // Cell Death Dis. 2013. V. 4. № 2. P. e519. http://www.ncbi.nlm.nih.gov/pubmed/23449455
26. Bolden J.E., Peart M.J., Johnstone R.W. // Nat. Rev. Drug Discov. 2006. V. 5. № 9. P. 769–784. http://www.ncbi.nlm.nih.gov/pubmed/16955068
27. Romanov V.S., Abramova M.V., Svetlikova S.B., Bykova T.V., Zubova S.G., Aksenov N.D., Fornace A.J., Pospelova T.V., Pospelov V.A. // Cell Cycle. 2010. V. 9. № 19. P. 3945–3955.
28. Abramova M.V., Pospelova T.V., Nikulenkov F.P., Hollander C.M., Fornace A.J., Pospelov V.A. // J. Biol. Chem. 2006. V. 281. № 30. P. 21040–21051.
29. Igotti Abramova M.V., Pojidaeva A.K., Filippova E.A., Gnedina O.O., Svetlikova S.B., Pospelov V.A. // Int. J. Biochem. Cell Biol. 2014. V. 51. № 6. P. 102-110.
30. Abramova M.V., Zatulovskiy E.A., Svetlikova S.B., Pospelov V.A. // Int. J. Biochem. Cell Biol. 2010. V. 42. № 11. P. 1847–1855.
31. Kilbey A., Terry A., Cameron E.R., Neil J.C. // Cell Cycle. 2008. V. 7. № 15. P. 2333–2340. http://www.ncbi.nlm.nih.gov/pubmed/18677118
32. Ueno N.T., Bartholomeusz C., Xia W., Anklesaria P., Bruckheimer E.M., Mebel E., Paul R., Li S., Yo G.H., Huang L., et al. // Cancer Res. 2002. V. 62. № 22. P. 6712–6716. http://www.ncbi.nlm.nih.gov/pubmed/12438271
33. Hortobagyi G.N., Ueno N.T., Xia W., Zhang S., Wolf J.K., Putnam J.B., Weiden P.L., Willey J.S., Carey M., Branham D.L., et al. // J. Clin. Oncol. 2001. V. 19. № 14. P. 3422–3433. http://www.ncbi.nlm.nih.gov/pubmed/11454891
34. Villaret D., Glisson B., Kenady D., Hanna E., Carey M., Gleich L., Yoo G.H., Futran N., Hung M.-C., Anklesaria P., et al. // Head Neck. 2002. V. 24. № 7. P. 661–669. http://www.ncbi.nlm.nih.gov/pubmed/12112540
35. Larson C., Oronsky B., Scicinski J., Fanger G.R., Stirn M., Oronsky A., Reid T.R. // Oncotarget. 2015. V. 6. № 24. P. 19976–19989. http://www.ncbi.nlm.nih.gov/pubmed/26280277
36. Hulin-Curtis S.L., Davies J.A., Jones R., Hudson E., Hanna L., Chester J.D., Parker A.L. // Oncotarget. 2018. V. 9. № 41. P. 26328–26341. http://www.ncbi.nlm.nih.gov/pubmed/29899862
37. Marchini A., Scott E., Rommelaere J. // Viruses. 2016. V. 8. № 1. P. 9. http://www.ncbi.nlm.nih.gov/pubmed/26751469
38. Lai M.-D., Chen C.-S., Yang C.-R., Yuan S.-Y., Tsai J.-J., Tu C.-F., Wang C.-C., Yen M.-C., Lin C.-C. // Cancer Gene Ther. 2010. V. 17. № 3. P. 203–211. http://www.ncbi.nlm.nih.gov/pubmed/19851354
39. Balakrishnan L., Milavetz B. // Virol. J. 2008. V. 5. P. 43. http://www.ncbi.nlm.nih.gov/pubmed/18353181
40. Takakura M., Kyo S., Sowa Y., Wang Z., Yatabe N., Maida Y., Tanaka M., Inoue M. // Nucl. Acids Res. 2001. V. 29. № 14. P. 3006–3011. http://www.ncbi.nlm.nih.gov/pubmed/11452025
41. Chueh A.C., Tse J.W.T., Tögel L., Mariadason J.M. // Antioxid. Redox Signal. 2015. V. 23. № 1. P. 66–84. http://www.ncbi.nlm.nih.gov/pubmed/24512308
42. Kirch H.C., Pützer B., Schwabe G., Gnauck H.K., Schulte Holthausen H. // Cell. Mol. Biol. Res. 1993. V. 39. № 8. P. 705–716. http://www.ncbi.nlm.nih.gov/pubmed/7951410
43. Abramova M.V., Zatulovskiy E.A., Svetlikova S.B., Kukushkin A.N., Pospelov V.A. // Biochem. Biophys. Res. Commun. 2010. V. 391. № 1. P. 142–146. http://www.ncbi.nlm.nih.gov/pubmed/19900401
44. Metcalf J.P., Monick M.M., Stinski M.F., Hunninghake

G.W. // Am. J. Respir. Cell Mol. Biol. 1994. V. 10. № 4. P. 448–452. http://www.ncbi.nlm.nih.gov/pubmed/8136160
45. Schaack J., Allen B., Orlicky D.J., Bennett M.L., Maxwell I.H., Smith R.L. // Virology. 2001. V. 291. № 1. P. 101–109. http://www.ncbi.nlm.nih.gov/pubmed/11878880
46. Song C.Z., Loewenstein P.M., Green M. // J. Virol. 1995. V. 69. № 5. P. 2907–2911. http://www.ncbi.nlm.nih.gov/pubmed/7707515
47. Madison D.L., Yaciuk P., Kwok R.P.S., Lundblad J.R. // J. Biol. Chem. 2002. V. 277. № 41. P. 38755–38763. http://www.ncbi.nlm.nih.gov/pubmed/12161448
48. Turnell A.S., Grand R.J., Gorbea C., Zhang X., Wang W., Mymryk J.S., Gallimore P.H. // EMBO J. 2000. V. 19. № 17. P. 4759–4773. http://www.ncbi.nlm.nih.gov/pubmed/10970867
49. Grand R.J.A., Schmeiser K., Gordon E.M., Zhang X., Gallimore P.H., Turnell A.S. // Virology. 2002. V. 301. № 2. P. 255–271. http://www.ncbi.nlm.nih.gov/pubmed/12359428

Variants of Mitochondrial Genome and Risk of Multiple Sclerosis Development in Russians

M. S. Kozin[1,2*], O. G. Kulakova[1,2], I. S. Kiselev[1,2], O. P. Balanovsky[3], A. N. Boyko[1], O. O. Favorova[1,2]

[1]Pirogov Russian National Research Medical University, Ostrovitjanova Str. 1, Moscow, 117997, Russia

[2]National Medical Research Center of Cardiology, 3rd Cherepkovskaya Str., 15a, Moscow, 121552, Russia

[3]Biobank of north Eurasia, Kotlyakovskaya Str., 3, Moscow, 115201, Russia.

*E-mail: kozinmax1992@gmail.com

Received September 10, 2018; in final form November 28, 2018

ABSTRACT **For the first time in the history of ethnic Russians, an association analysis the development of multiple sclerosis (MS) was performed for the mitochondrial haplogroups H, J, K, and U, as well as for the individual mitochondrial DNA (mtDNA) polymorphisms discriminating these haplogroups (m.1719G > A, m. 7028C > T, m.9055G > A, m.10398A > G, m.12308A > G). A total of 283 unrelated patients with the relapsing-remitting form of MS and 290 healthy controls were enrolled in the study. Association of haplogroup J with MS was observed ($P = 0.0055$, OR = 2.00 [95% CI 1.21–3.41]). After gender stratification, the association remained significant in women ($P = 0.0083$, OR = 2.20 [95% CI 1.19–4.03]). A multilocus analysis of the association between combinations of mtDNA haplogroups with variants of 38 nuclear immune-related genes and MS risk was carried out. MS-associated biallelic combinations of haplogroup J with the alleles *CCL5* rs2107538*A, *PVT1* rs2114358*G, *TNFSF14* rs1077667*C, and *IL4* rs2243250*C, which were not associated with MS individually, were identified. For the combination of haplogroup J and the *CCL5**A allele ($P = 0.00043$, OR = 5.47 [95% CI 1.85–16.15]), a epistatic (synergistic) interaction between the components was established using two statistical criteria: the P_{FLINT} value in the Fisher-like interaction numeric test and the synergy factor, SF ($P_{FLINT} = 0.025$, SF = 4.32 [95% CI 1.20–15.60]). The combination of haplogroup J and the *PVT1**G allele is characterized by $P_{FLINT} = 0.084$; SF = 3.05 [95% CI 1.00–9.31] and can also be epistatic. Thus, interaction between nuclear and mitochondrial genome components in the risk of developing MS was demonstrated for the first time.**

KEYWORDS **multiple sclerosis, mitochondrial genome, nuclear genome, genetic polymorphism, multilocus analysis.**

ABBREVIATIONS **FLINT – Fisher-like interaction numeric test; GWAS – genome-wide association study; SF – synergy factor; SNP – single nucleotide polymorphism; ATP – adenosine triphosphate; CI – confidence interval; mtDNA – mitochondrial DNA; NAD – nicotinamide adenine dinucleotide; OR – odds ratio; RFLP – restriction fragment length polymorphism; PCR – polymerase chain reaction; ETC – electron transport chain.**

INTRODUCTION

Multiple sclerosis (MS) is a neurodegenerative disease of the central nervous system; a chronic inflammatory process plays an important role in its pathogenesis. MS typically affects people of working age and, once it has appeared as isolated manifestations of neurological symptoms, it ultimately leads to severe disability [1]. According to the WHO, there are approximately 2.5 million people suffering from MS worldwide. Despite the significant progress achieved in our understanding of the nature of MS and the development of drugs that modify its course, the disease remains among the most socially disrupting conditions.

MS is a disease with a genetic component; the risk of developing it among family members depends on the genetic distance from the proband and reaches its highest values in the closest relatives of the latter [2] but does not obey Mendelian laws. This type of inheritance is typical of polygenic diseases, when there are many independent or interacting polymorphic variants of genes, each of which can only slightly determine disease susceptibility, with the effect often being specific

to individual populations (for example, ethnic groups). As a result of many years of research, over 200 independent nuclear loci have been identified using the conventional "candidate gene" approach and modern methods of genome-wide association studies (GWAS). Of these loci, only the region of the major histocompatibility complex class II on chromosome 6 strongly influences the risk of MS, while each of the remaining loci makes a small contribution to susceptibility to MS [3]. However, the combined variability of all identified nuclear loci can explain only approximately 38% of MS inheritance [4].

One of the possible causes underlying this phenomenon, which is called "missing heritability," may be the unaccounted for effect of mitochondrial genome variability on the risk of developing a polygenic disease. In the case of MS, this assumption agrees well with the data indicating that the disruption of mitochondrial function is one of the key factors leading to neurodegeneration in MS [5]. The main distinguishing features of the mitochondrial genome are known to be only maternal type of inheritance and the absence of recombination. These characteristics allowed researchers to combine different mtDNA variants into haplogroups: groups of related haplotypes present in people who share a common ancestor on the maternal line and inherited one or more nucleotide substitutions. The combination of such substitutions is specific to different haplogroups. In reality, one specific substitution is sufficient for assigning a sample to a haplogroup [6]. Inheritance from one parent leads to a fourfold increase in the effect of genetic drift compared to autosomal markers; as a result, haplogroup frequencies vary greatly in different populations.

To date, there have been approximately 20 studies devoted to the analysis of the association between MS and mitochondrial genome variants: both individual polymorphisms and haplogroups, with the samples being relatively small in some of the cases (see references in review [7]). Among these works, two studies were performed using the GWAS method, and the others involved the "candidate gene" approach. The data presented in these papers are often contradictory, which may be due to the ethnicity of the subjects. In this regard, conducting research on the association of mitochondrial genome variants with the risk of MS in ethnically homogeneous samples is a relevant issue.

The aim of our work is to study the association of the mitochondrial haplogroups H, J, K, and U, which are the most prevalent in European populations [8, 9], and the *MT-RNR2*, *COX1*, *ATP6*, *MT-ND3*, and *MT-TL2* polymorphisms [10] discriminating these haplogroups against the risk of MS in ethnic Russians. Having taken into account the interaction between the products of mitochondrial and nuclear genes, we also conducted a multilocus analysis of the association of the combinations of mtDNA haplogroups and polymorphic variants of a series of nuclear genes with previously determined frequencies in the sample with the risk of MS and investigated the nature of this effect.

EXPERIMENTAL

The study included 283 unrelated patients with MS (198 women and 85 men) who were diagnosed with a relapsing-remitting form of MS according to the international McDonald criteria [11]. The mean age of the MS patients at the time of blood collection was 38.0 ± 10.5 years, and the average age of the disease onset was 28.0 ± 9.1 years. All patients underwent treatment at Moscow Multiple Sclerosis Center or Moscow Interregional Department of Multiple Sclerosis at the State Budgetary Health Institution City Clinical Hospital № 24 of the Moscow City Health Department. The control group, which was comparable to the MS group in gender (197 women and 93 men) and age composition (mean age, 40.9 ± 12.9 years), included unrelated healthy individuals. All individuals included in the study were ethnic Russians (according to the survey data, all family members in two generations were Russians) and lived in the European part of Russia. Informed consent to conduct the study was obtained from all individuals. The study was approved by the ethical committee of Pirogov Russian National Research Medical University.

Genotyping assay

Total DNA was isolated from blood samples using commercial kits (QIAamp DNA BloodMidiKit).

Genotyping of single nucleotide polymorphisms (SNP) m.1719G > A, m.7028C > T, m.9055G > A, m.10398A > G, m.12308A > G mtDNA (*table 1*) was performed using polymerase chain-reaction-based (PCR) methods. For m.7028C > T, m.10398A > G and m.12308A > G SNPs, restriction fragment length polymorphism (PCR-RFLP) was performed according to the procedure described in [10], with the exception that the DdeI restriction enzyme was replaced with its isoschizomer, BstDEI. Polymorphism m.9055G > A was genotyped by PCR-RFLP using the primers 5'-TTAAGGCGACAGCGATTTCT-3', 5'-TACTGCAGGCCACCTACTCA-3' and the AspLEI restriction enzyme. Polymorphism m.1719G > A was genotyped by real-time PCR. Amplification of the studied region was carried out using the primers 5'-GCTAAACCTAGCCCCAAACC-3' and 5'-GCGCCAGGTTTCAATTTCTA-3'. SNP analysis was conducted using probes specific to the A (5' HEX-CCTTACTACCAGACAACCTTAAC-

Table 1. Mitochondrial polymorphisms analyzed in the study and used for the determination of haplogroups (H, J, K or U) in individuals

SNP	rs ID	Gene	Gene product	Haplogroup (allele)
m.1719G > A	rs3928305	*MT-RNR2*	16S ribosomal RNA	I, N1, X2 (1719A)
m.7028C > T	rs2015062	*COX1*	Cytochrome C oxidase subunit 1 (ETC IV)	H (7028C)
m.9055G > A	rs193303045	*ATP6*	ATP synthase subunit 6	K (9055A)
m.10398A > G	rs2853826	*MT-ND3*	NADH dehydrogenase subunit 4 (ETC complex I)	K, J, I (10398G)
m.12308A > G	rs2853498	*MT-TL2*	Leucine-specific tRNA	U, K (12308G)

CAAACC-3'BHQ1) and G (5' FAM-CCTTACTACCA-GACAACCTTAGCCAAACC-3'BHQ1) alleles.

Mitochondrial haplogroup (H, J, K or U) was determined based on the combination of the marker SNPs presented in *table 1*, according to [10]. Haplogroup H was defined as the extended haplotype G1719, C7028, G9055, A10398, A12308; haplotype G1719, T7028, G9055, G10398, A12308 was identified as haplogroup J; haplogroups K and U were defined as haplotype G1719, T7028, A9055, G10398, G12308 and haplotype G1719, T7028, G9055, A10398, G12308, respectively.

Statistical analysis

The search for individual mitochondrial SNPs and the mitochondrial haplogroups associated with MS, as well as combinations of haplogroups with the carriage of alleles/genotypes of a series of nuclear genes, which had been previously identified (unpublished data), was conducted using the APSampler software [12], based on Monte Carlo Markov chains and Bayesian nonparametric statistics [13]. The significance level of the identified associations was assessed using the validation tools included in the APSampler software and based on Fisher's exact test, evaluation of the corresponding odds ratio (OR), and a 95% confidence interval (CI). Associations were considered significant if the *P* value was less than 0.05, provided that the 95% CI of the OR did not cross 1.

Possible nonlinear interaction (epistasis) between alleles in the identified biallelic combinations was revealed using a previously proposed approach [14]. The method is based on the assessment of the nature of an interaction between the alleles (or genotypes) of two loci in their combined carriership using the two previously described statistical criteria: P_{FLINT} value of the exact three-way Fisher-like interaction numeric test (FLINT) [15] and based on the synergy factor (SF) values and 95% CI [16]. SF, P_{FLINT}, and 95% CI were assessed using tools included in the APSampler software. Interaction for biallelic combinations was considered epistatic for P_{FLINT} lower than 0.05, provided that the 95% CI of the SF did not cross 1.

RESULTS

Analysis of the frequencies of the mitochondrial genome variants m.1719G > A, m.7028C > T, m.9055G > A, m.10398A > G, and m.12308A > G was performed in MS patients and control individuals belonging to the Russian ethnic group. There were no significant differences in SNP frequencies when comparing the total samples of patients with MS and control individuals, nor when comparing patients with healthy men and healthy women separately (data not shown).

Mitochondrial haplogroup (H, J, K or U) was determined by genotyping of the above-indicated marker SNPs based on their combinations. The frequency of haplogroup J in patients with MS (15.9%) is almost 2 times higher than the frequency in the control group (8.6%) and significantly associated with the risk of MS ($P = 0.0055$; OR = 2.00 [95% CI 1.21–3.41]). No association with MS was found for haplogroups H, K, and U (*Fig. A*).

Due to the fact that MS is significantly more common in women than in men and the presence of gender differences in genetic risk factors for the disease [17], the association analysis of haplogroups H, J, K, U with MS was also performed separately for men and women . No significant associations with any of the studied haplogroups were found in men (*Fig. B*). On the contrary, association of haplogroup J with MS was revealed both in women and the total sample ($P = 0.0083$; OR = 2.20 [95% CI 1.19–4.03]) (*Fig. B*).

Current evidence suggests that mitochondria functioning is altered in chronic neuroinflammation specific to MS [7]. In order to assess the possible interaction of mitochondrial and nuclear genes, we carried out a multilocus analysis of the association of the carriership of combinations of each of the studied mtDNA haplogroups with polymorphic variants of the 37 nuclear genes involved in the immune system functioning with MS using the APSampler software.

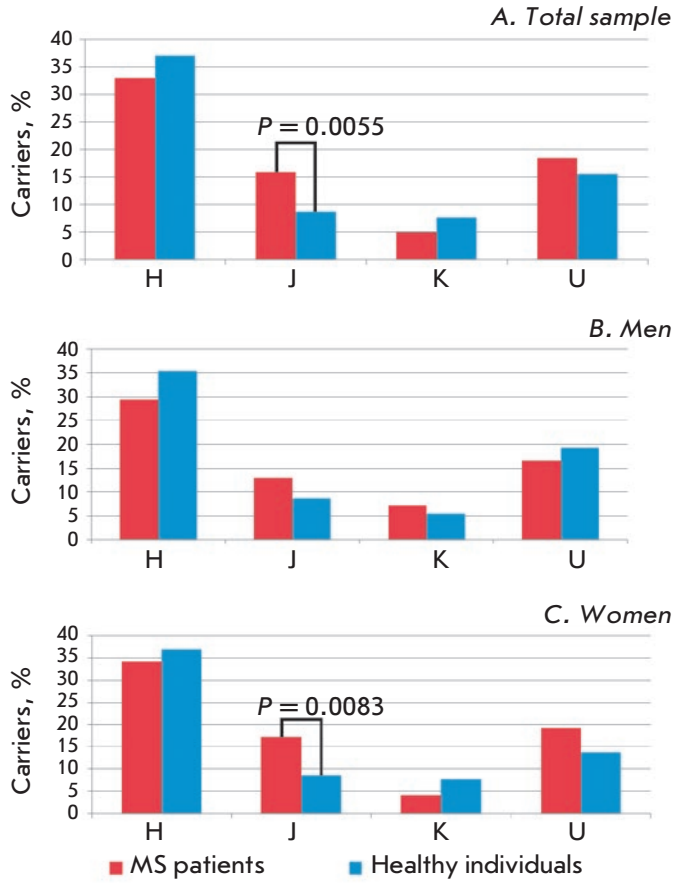

The frequencies of haplogroups H, J, K, and U in MS patients and healthy individuals.
A – total sample (283 patients with MS, 290 healthy individuals); B – men (85 patients with MS, 93 healthy individuals); C – women (198 patients with MS, 197 healthy individuals)

The studied genes include the major histocompatibility complex HLA-*DRB1* gene, the key gene determining susceptibility to MS, as well as *CD58*, *VCAM1*, *EVI5*, *EOMES*, *CD86*, *IL7RA*, *TCF7*, *IL22RA2*, *IRF5*, *PVT1*, *IL2RA*, *CD6*, *CXCR5*, *TNFRSF1A*, *CLEC16A*, *IRF8*, *STAT3*, *TYK2*, *TNFSF14*, and *CD4*, association with which MS has been shown using GWAS. These genes fall under the following criteria: at least two independent GWAS demonstrated association with MS; at the same time, a whole genome level of significance was reached ($P \leq 5 \times 10^{-8}$) in at least one study, while other studies showed a *P* value not exceeding 1×10^{-5} [18]. Of particular interest to us was *CLEC16A*, which is located in a relatively gene-rich region of chromosome 16 containing three linkage blocks. This area also includes *SOCS1*, one of the most important regulators of cytokine expression [19]. For this reason, we included two polymorphic sites located in the adjacent intergenic region of the chromosome, *CLEC16A-SOCS1* (rs1640923) and *SOCS1-TNP2* (rs243324), in the analysis. Products of the remaining genes under study are involved in the process of inflammation and/or described as associated with various autoimmune diseases, including MS. They include genes encoding the components of the cytokine/chemokine system, *IL4*, *IL6*, *IL17A*, *IFNB1*, *IFNG*, *TNF*, *TGFB1*, *CCL5*, *IFNAR*, *IFNAR2*, *CCR5*, as well as genes the products of which participate in the regulation of T lymphocyte activity: namely, the costimulatory molecule *CTLA4* and immunoproteasome subunit *PSMB9* required for processing of peptides prior to their presentation in MHC class I. Glypican 5 gene (*GPC5*) has been included in the study since its polymorphisms are known to be associated with the nature of the response of MS patients to immunomodulatory therapy with interferon-β [20]. Frequency of a minor allele was at least 0.05 for all studied polymorphic sites. Carrier frequencies of alleles and genotypes of nuclear genes in the analyzed sample had been determined by us earlier.

Combinations with the alleles of the nuclear genome significantly associated with the risk of MS were found only for haplogroup J (*table 2*). As a second component, these biallelic combinations included the alleles *CCL5* rs2107538*A, *PVT1* rs2114358*G, *TNFSF14* rs1077667*C and *IL4* rs2243250*C, which individually were not significantly associated with MS, and genotype *CLEC16A-SOCS1* rs1640923*A/A, which was significantly associated with MS ($P = 0.020$ and OR = 1.51 [95% CI 1.03–2.20]). All combinations were characterized by a high level of significance (*P* in the range of 0.00043 to 0.0011) exceeding the significance of association with MS for haplogroup J at least 5 times. At the same time, an increase in the OR was observed: OR was equal to 5.47 for the most significant combination (haplogroup J + *CCL5**A), which exceeds the OR showed for haplogroup J almost 3 times.

Increase in the significance level for the association with MS that is observed for combined carriership of haplogroup J and the alleles (or genotypes) of nuclear genes may occur as a result of summing up their mutually independent contributions or as a result of their positive epistatic (synergistic) interaction. In order to assess whether such interactions take place in the case of the identified combinations, we determined their SF and P_{FLINT} values. For the combination of haplogroup J with the allele rs2107538*A of *CCL5*, P_{FLINT} equals 0.025 and SF is equal to 4.32 [95% CI = 1.2–15.6] (*table 3*). Thus, it has been demonstrated that the increase in the risk of MS observed in combined carriership of haplogroup J with the *CCL5**A allele is associated with a synergistic epistatic interaction between these genetic

Table 2. Association of combinations between mitochondrial haplogroup J and carriage of alleles/genotypes of nuclear genes with MS (according to the results of a multilocus analysis)

Haplogroup, allele or genotype	Number of carriers, %		P	OR [95% CI]
	MS patients (N = 283)	Healthy donors (N = 290)		
Distinct genetic variants				
Haplogroup J	**45 (15.9)**	**25 (8.6)**	**0.0055**	**2.00[1.19–3.37]**
CCL5 rs2107538*A	110 (38.8)	105 (36.2)	0.44	1.04[0.74–1.46]
PVT1 rs2114358*G	169 (59.7)	170 (58.6)	0.43	1.04[0.75–1.46]
TNFSF14 rs1077667*C	266 (93.9)	261 (90.0)	0.064	1.72[0.90–3.27]
IL4 rs2243250*C	267 (94.3)	264 (91.0)	0.14	1.52[0.79–2.92]
***CLEC16A-SOCS1* rs1640923*A/A**	**221 (78.0)**	**203 (70.0)**	**0.020**	**1.51[1.03–2.20]**
Combinations of genetic variants				
Haplogroup J + *CCL5A**	**21 (7.4)**	**4 (1.4)**	**0.00043**	**5.47[1.85–16.15]**
Haplogroup J + *PVT1G**	**35 (12.4)**	**14 (4.8)**	**0.00093**	**2.78[1.46–5.29]**
Haplogroup J + *TNFSF14C**	**44 (15.5)**	**21 (7.2)**	**0.0013**	**2.35[1.35–4.07]**
Haplogroup J + *IL4C**	**44(15.5)**	**21 (7.2)**	**0.0013**	**2.35[1.35–4.07]**
Haplogroup J + *CLEC16A-SOCS1A/A**	**39 (13.7)**	**17 (5.9)**	**0.0011**	**2.56[1.41–4.63]**

Note. Significant associations are highlighted in bold

Table 3. Analysis of the nature of interactions between the components of combinations: carriership of mitochondrial haplogroup J and alleles/genotypes of nuclear genes

Combination of genetic variants	P_{FLINT}	SF [95% CI]
Haplogroup J + *CCL5**A	**0.025**	**4.32[1.20–15.60]**
Haplogroup J + *PVT1**G	0.084	**3.05[1.00–9.31]**
Haplogroup J + *TNFSF14**C	0.31	4.25[0.38–47.60]
Haplogroup J + *IL4**C	0.14	6.85[0.65–72.30]
Haplogroup J + *CLEC16A-SOCS1**A/A	0.34	2.24[0.63–7.97]

Note. Significance criteria are highlighted in bold

variants. Combination of haplogroup J with *PVT1**G is characterized by SF = 3.05 with CI not crossing 1. According to this criterion, it falls under the definition of epistatic interaction. However, the P_{FLINT} value (0.084) does not reach the level of significance and we cannot state that this combination is epistatic. SF values for 95% CI and P_{FLINT} obtained for the remaining combinations were shown to be not significant.

DISCUSSION

MS is a clinically and genetically heterogeneous disease [21]. For this reason, sampling criteria are of great importance for obtaining reliable results. We can state that the studied group of patients was fairly representative. All patients were diagnosed with the most common relapsing-remitting form of MS, which is characterized by periods of exacerbation and remission. The ratio of MS women and men and the average age of MS onset were close to that described in [22]. Gender ratio and the age of individuals in the control group did not differ significantly from those in the group of patients. Frequencies of the mitochondrial haplogroups in the control group were close to the frequencies determined earlier for the European part of Russia [8, 9].

This paper presents the first analysis of an association of MS with mitochondrial SNPs (m.1719G > A, m.7028C > T, m.9055G > A, m.10398A > G, m.12308A > G) and mtDNA haplogroups (H, J, K, U) in ethnic Russians. Of the SNPs included in the study, association of m.1719G > A, m.10398A > G, and m.9055G > A SNPs with MS was analyzed in three European populations (Hispanics, Norwegians, Germans); no significant association with MS was observed for any of these populations [23], which is consistent with our results. However, SNP m.9055G> A (haplogroup K) showed a significant association with the disease in caucasian Americans [24], which probably reflects their genetic differences from Europeans.

A significant association of haplogroup J with MS found in our study had been previously shown for some European ethnic groups [23, 25–27] (but not for all of the studied individuals), as well as for Americans of European descent [28] and Persians from Iran [29]. Thus, we replicated the previously obtained data on the association of haplogroup J with the risk of MS in

ethnic Russians. When stratifying our sample by gender, the association of haplogroup J with MS remained significant in women, but not in men, with the level of significance being lower in women than in the sample that was not divided by gender. It is possible that these results are due to the insufficient number of men in the sample. Previously published data on the relationship between haplogroup K and MS in the American [24] and Persian[30] populations were not reproduced for the Russian population in our study.

Increased risk of MS in individuals carrying haplogroup J is probably due to its specific impact on the functioning of mitochondria and cells in general. Indeed, the studies carried out using "cybrids," i.e. cells with an identical nuclear genome but different mitochondria, have showed that it is the carriage of haplogroup J that leads to significant changes in the cells. For instance, it was shown [31] that the global level of DNA methylation in the peripheral blood cells of haplogroup J carriers is higher than that for carriers of other haplogroups; it is also higher in cybrids containing this variant of mtDNA (J cybrids) compared to other cybrids. At the same time, ATP concentration and production of free radicals were shown to be reduced in J cybrids [31]. Polymorphism m.295C > T of the mtDNA control region (one of the SNPs determining haplogroup J) was shown to affect the processes of mtDNA transcription and replication. In particular, if the T allele is carried, binding of the mitochondrial transcription factor A (TFAM) to mtDNA is enhanced and the content of mtDNA in J cybrids becomes two time higher in comparison with H cybrids [32]. Unfortunately, the authors do not present data on microscopic examination of cells, and, therefore, it is unclear which of the previously described phenomena determines the increase in the amount of mtDNA: an increase in the number of mitochondria or an increase in the mtDNA copy number per mitochondria. However, one can assume that increase in the mtDNA content in carriers of haplogroup J is a compensatory response to a decrease in ATP production. One of the key features of MS is the increase in energy consumption for maintaining structural integrity and functioning of axons at the sites of demyelination, which can be compensated at the initial stages by an increase in the number of mitochondria and the size of stationary mitochondria, as well as by an increase in the speed of axonal mitochondrial transport [33]. One can assume that the carrier of haplogroup J has already run out of the compensatory reserve of neurons by the time of disease manifestation.

Using a multilocus analysis, we have demonstrated the involvement of a number of combinations of haplogroup J with the alleles *CCL5*, *PVT1*, *TNFSF14*, and *IL4* that are not individually associated with MS in the development of MS; these combinations are characterized by a greater significance of the association with the disease than haplogroup J only. Regardless of whether the observed cumulative effect occurs because of the summing up of the independent contributions of the two components of each of the combinations or due to the epistatic interactions between them [34], the obtained results allow us to suggest that not only the genes identified in combinations with haplogroup J, but also nuclear genes are involved in the formation of susceptibility to MS.

The products of the protein-encoding genes *CCL5*, *TNFSF14*, and *IL4*, which have been studied in combination with haplogroup J, share a similar role and participate in the functioning of the cytokine/chemokine system. CCL5 is a chemokine that acts as a chemoattractant of monocytes, memory T cells, and eosinophils. An increase in the concentration of CCL5 in the cerebrospinal fluid can serve as one of the markers of MS progression [35]. Proinflammatory cytokine TNFSF14, the fourteenth member of the superfamily of tumor necrosis factors, can function as a co-stimulator in lymphocyte cell activation, can stimulate T cell proliferation, and induce apoptosis of some types of tumor cells. IL4 is one of the key cytokines regulating differentiation of naive (Th0) T helpers into Th2 cells and differentiation of B cells into plasma cells. A multilocus analysis of mitochondrial and nuclear genome variants allowed us to replicate the data that were previously obtained for other populations on association of rs2107538 of the gene *CCL5* [36], rs1077667 of the gene *TNFSF14* [37], and rs2243250 of the gene *IL4* [38, 39] with the risk of MS in ethnic Russians.

Another gene that has been identified by us as a component in the combination of haplogroup J with MS, namely, *PVT1*, encodes long non-coding RNA presumably involved in cell cycle regulation [40] and contains a cluster of six miRNA genes [41]. The SNP rs2114358 included in our study is located in intron 5 of the gene *PVT1*, which also encodes miR-1206, and, as shown by *in silico* analysis, affects the structure of mature miR-1206 [42]. The GWAS method revealed association of MS with another polymorphism in *PVT1*, rs4410871 [37], which, like rs2114358, is part of the miRNA gene (*MIR1204*, located in intron 1 of the gene *PVT1*).

We have established the fact of synergistic interaction between carriage of haplogroup J and the allele rs2107538*A of the gene *CCL5*. Elucidation of the molecular mechanism of this interaction is a challenge for the future. However, chemokine CCL5 is known to play an essential role in the metabolism of glutamic acid in the central nervous system by modulating glutamatergic signal transduction [43], while the syn-

thesis of glutamate occurs with direct involvement of mitochondrial enzymes [44]. Moreover, it was found that glutamate homeostasis is disturbed at the sites of damage in MS [45]. Moreover, glutamate excitotoxicity, which develops in this case, is one of the mechanisms of neuronal damage [46]. These processes may underlie the observed synergistic effect of the combination of haplogroup J and allele *CCL5**A on the development of MS. Another biallelic combination that has been shown in the current study to be associated with the risk of MS, which includes haplogroup J and allele rs2114358*G of the gene *PVT1*, meets only one of the two criteria for nonlinear interaction between genetic variants. We would like to suggest that expanding the sample size will allow us to prove the synergistic nature of this combination.

Thus, we obtained data indicating epistatic interaction between haplogroup J and the gene *CCL5* and, apparently, the gene *PVT1*. Thus, interaction of the components of the nuclear and mitochondrial genomes in the formation of a risk of MS has been demonstrated for the first time. The obtained results certainly require reproduction on an independent sample. ●

This work was supported by the Russian Foundation for Basic Research (grant No. 17-04-01293).

REFERENCES

1. Karussis D. // J. Autoimmun. 2014. V. 48–49. P. 134–142.
2. Oksenberg J.R. // Expert Rev. Neurother. 2013. V. 13. № 12. P. 11–19.
3. Baranzini S.E., Oksenberg J.R. // Trends Genet. 2017. V. 33. № 12. P. 960–970.
4. Patsopoulos N.A., Baranzini S.E., Santaniello A., Shoostari P., Cotsapas C., Wong G., Beecham A.H., James T., Replogle J., Vlachos I., et al. // bioRxiv. https://doi.org/10.1101/143933.
5. Campbell G., Mahad D.J. // FEBS Lett. 2018. V. 592. № 7. P. 1113–1121.
6. Pakendorf B., Stoneking M. // Annu. Rev. Genomics Hum. Genet. 2005. V. 6. № 1. P. 165–183.
7. Kozin M.S., Kulakova O.G., Favorova O.O. // Biochemistry. 2018. V. 83. № 7. P. 1002–1021.
8. www.mitomap.org
9. Balanovsky O.P. Variability of the gene pool in space and time: synthesis of the data of the genogeography of mitochondrial DNA and Y-chromosome [in Russian]. M.: «Research Centre of Medical Genetics» RAMS, 2012.
10. Terrazzino S., Deantonio L., Cargnin S., Donis L., Pisani C., Masini L., Gambaro G., Canonico P.L., Genazzani A.A., Krengli M. // Clin. Oncol. 2016. V. 28. № 6. P. 365–372.
11. Polman C.H., Reingold S.C., Banwell B., Clanet M., Cohen J.A., Filippi M., Fujihara K., Havrdova E., Hutchinson M., Kappos L., et al. // Ann. Neurol. 2011. V. 69. № 2. P. 292–302.
12. http://apsampler.sourceforge.net
13. Favorov A.V., Andreewski T.V., Sudomoina M.A., Favorova O.O., Parmigiani G., Ochs M.F. // Genetics. 2005. V. 171. № 4. P. 2113–2121.
14. Barsova R.M., Lvovs D., Titov B.V., Matveeva N.A., Shakhnovich R.M., Sukhinina T.S., Kukava N.G., Ruda M.Y., Karamova I.M., Nasibullin T.R., et al. // PLoS One. 2015. V. 10. № 12. P. 1–16.
15. White D.R., Pesner R., Reitz K.P. // Cross-Cultural Res. 1983. V. 18. № 2. P. 103–122.
16. Cortina-Borja M., Smith A.D., Combarros O., Lehmann D.J. // BMC Res. Notes. 2009. V. 2. P. 1–7.
17. Bashinskaya V.V., Kulakova O.G., Kiselev I.S., Baulina N.M., Favorov A.V., Boyko A.N., Tsareva E.Y., Favorova O.O. // J. Neuroimmunol. 2015. V. 282. P. 85–91.
18. Bashinskaya V.V., Kulakova O.G., Boyko A.N., Favorov A.V., Favorova O.O. // Hum. Genet. 2015. V. 134. № 11–12. P. 1143–1162.
19. Zuvich R.L., Bush W.S., McCauley J.L., Beecham A.H., De Jager P.L.; Ivinson A.J., Compston A., Hafler D.A., Hauser S.L., Sawcer S.J., et al. // Hum. Mol. Genet. 2011. V. 20. № 17. P. 3517–3524.
20. Cénit M.D., Blanco-Kelly F., de las Heras V., Bartolomé M., de la Concha E.G., Urcelay E., Arroyo R., Martínez A. // Mult. Scler. 2009. V. 15. № 8. P. 913–917.
21. Gusev E.I., Zavalishin I.A., Boiko A.N. Multiple Sclerosis and Other Demyelinating Diseases [in Russian]. M.: Miklosh, 2004. 540c.
22. Kaminsky Z., Wang S.C., Petronis A. // Ann. Med. 2006. V. 38. № 8. P. 530–544.
23. Yu X., Koczan D., Sulonen A.M., Akkad D.A., Kroner A., Comabella M., Costa G., Corongiu D., Goertsches R., Camina-Tato M., et al. // PLoS One. 2008. V. 3. № 2. P. 1–7.
24. Vyshkina T., Sylvester A., Sadiq S., Bonilla E., Canter J.A., Perl A., Kalman B., Avenue I. // Clin. Immunol. 2009. V. 129. № 1. P. 31–35.
25. Tranah G.J., Santaniello A., Caillier S.J., Alfonso S.D., Hauser S.L., Oksenberg J.R. // Neurology. 2015. P. 325–330.
26. Mihailova S.M., Ivanova M.I., Quin L.M., Naumova E.J. // Eur. J. Neurol. 2007. V. 14. № 1. P. 44–47.
27. Otaegui D., Sáenz A., Martínez-Zabaleta M., Villoslada P., Fernández-Manchola I., Álvarez de Arcaya A., Emparanza J.I., López de Munain A. // Mult. Scler. 2004. V. 10. № 5. P. 532–535.
28. Kalman B., Li S., Chatterjee D., O'Connor J., Voehl M.R., Brown M.D., Alder H. // Acta Neurol. Scand. 1999. V. 99. № 1. P. 16–25.
29. Houshmand M., Sanati M.H., Babrzadeh F., Ardalan A., Teimori M., Vakilian M., Akuchekian M., Farhud D., Lotfi J. // Mult. Scler. 2005. V. 11. № 6. P. 728–730.
30. Hassani-Kumleh H., Houshmand M., Panahi M.S.S., Riazi G.H., Sanati M.H., Gharagozli K., Ghabaee M. // Cell. Mol. Neurobiol. 2006. V. 26. № 2. P. 119–125.
31. Bellizzi. D., D'Aquila. P., Giordano M., Passarino A.M. G. // Epigenomics. 2012. V. 4. № 1. P. 17–27.
32. Suissa S., Wang Z., Poole J., Wittkopp S., Feder J., Shutt T.E., Wallace D.C., Shadel G.S., Mishmar D. // PLoS Genet. 2009. V. 5. № 5. e1000474.
33. Kiryu-Seo S., Ohno N., Kidd G.J., Komuro H., Trapp B.D. // J. Neurosci. 2010. V. 30. № 19. P. 6658–6666.
34. Lvovs D., Favorova O.O., Favorov A.V. // Acta Naturae. 2012. T. 4. № 3. C. 62–75.
35. Tomioka R., Matsui M. // Intern. Med. 2014. V. 53. № 5. P. 361–365.

36. Gade-Andavolu R., Comings D.E., MacMurray J., Vuthoori R.K., Tourtellotte W.W., Nagra R.M., Cone L.A. // Mult. Scler. 2004. V. 10. № 5. P. 536–539.
37. International Multiple Sclerosis Genetics Consortium (IMSGC), Beecham A.H., Patsopoulos N.A., Xifara D.K., Davis M.F., Kemppinen A., Cotsapas C., Shah T.S., Spencer C., Booth D., Goris A., Oturai A., et al. // Nat. Genet. 2013. V. 45. № 11. P. 1353–1360.
38. Akkad D.A., Arning L., Ibrahim S.M., Epplen J.T. // Genes Immun. 2007. V. 8. № 8. P. 703–706.
39. Zhang Z., Wang L., Sun X., Zhang L., Lu L. // J. Neurol. Sci. 2016. V. 363. P. 107–113.
40. Colombo T., Farina L., Macino G., Paci P. // Biomed Res. Int. 2015. V. 2015. P. 17–21.
41. Huppi K., Pitt J.J., Wahlberg B.M., Caplen N.J. // Front. Genet. 2012. V. 3. № APR. P. 1–11.
42. Martin-Guerrero I., Gutierrez-Camino A., Lopez-Lopez E., Bilbao-Aldaiturriaga N., Pombar-Gomez M., Ardanaz M., Garcia-Orad A. // PLoS One. 2015. V. 10. № 3. P. 2–13.
43. Pittaluga A. // Front. Immunol. 2017. V. 8. № SEP. P. 1–13.
44. Miller K.E., Hoffman E.M., Sutharshan M., Schechter R. // Pharmacol Ther. 2011. V. 130. № 3. P. 283–309.
45. Werner P., Pitt D., Raine C.S. // Ann. Neurol. 2001. V. 50. № 2. P. 169–180.
46. Kostic M., Zivkovic N., Stojanovic I. // Rev. Neurosci. 2013. V. 24. № 1. P. 71–88.

The Mechanism of Fluorescence Quenching of Protein Photosensitizers Based on miniSOG During Internalization of the HER2 Receptor

E. O. Kuzichkina*, O. N. Shilova, S. M. Deyev
Shemyakin–Ovchinnikov Institute of Bioorganic Chemistry, Russian Academy of Sciences, Moscow, 117997, Russia
*E-mail: kuzichkinazhenya@mail.ru
Received August 04, 2018; in final form October 04, 2018

ABSTRACT **The protein photosensitizer miniSOG is a promising agent for photodynamic therapy. The genetically encoded phototoxins 4D5scFv-miniSOG and DARPin-miniSOG specifically bind to the HER2 receptor overexpressed on the surface of cancer cells and promote receptor-mediated internalization of HER2. We show that ingestion of proteins in a complex with the receptor reduces the fluorescent signal of the phototoxic module in endosomes. In order to clarify the mechanism of decrease in the fluorescence intensity of miniSOG-based proteins as they enter a cancer cell during internalization, we analyzed the influence of different factors, including low pH, proteolysis, cofactor reduction, and shielding, on changes in the fluorescence of photosensitizers. Shielding and absorption of miniSOG fluorescence by cell fluorophores, including cytochrome *c*, were found to contribute significantly to the changes in the fluorescent properties of miniSOG.**
KEYWORDS **targeted protein photosensitizers, internalization, miniSOG, HER2 receptor, fluorescence.**
ABBREVIATIONS **PDT – photodynamic therapy; HER2 – human epidermal growth factor receptor 2; scFv – single-chain variable antibody fragment; DARPin – designed ankyrin repeat protein; FITC – fluorescein isothiocyanate; FMN – flavin mononucleotide; IPTG – isopropylthio-β-D-galactopyranoside; PAG – polyacrylamide gel; SDS – sodium dodecyl sulfate; PBS – phosphate-buffered saline; GSH – glutathione.**

INTRODUCTION

The importance of a targeted delivery of anticancer agents in photodynamic therapy in modern theranostics is on the increase. This approach allows one to enhance the selective accumulation of a photosensitizer in the tumor and deliver it to the desired intracellular compartment [1, 2]. Monoclonal antibodies, antibody fragments, and other proteins capable of selective binding to tumor antigens can be used as targeting fragments.

The cell surface receptor HER2/neu, also known as ErbB2, is an important tumor marker and the best studied target for designing novel therapeutic agents, since it is overexpressed in many tumor types (including human breast cancer cells) and is associated with the aggressive tumor phenotype [3, 4].

The genetically encoded targeted phototoxins 4D5scFv-miniSOG [5] and DARPin-miniSOG [6] were designed and characterized at the Laboratory of Molecular Immunology of the Institute of Bioorganic Chemistry, Russian Academy of Sciences. A fragment of monoclonal antibody 4D5scFv and the artificial protein DARPin_9-29, capable of selective recognition of the extracellular domain of human epidermal growth factor receptor HER2/neu, were employed as targeting modules. In both cases, photoactivatable fluorescent flavoprotein miniSOG was used as a phototoxic module [7]. Both proteins exhibited a selective phototoxic effect in *in vitro* experiments: in HER2-positive human breast adenocarcinoma SK-BR-3 cells, IC_{50} was equal to 160 and 0.8 nM for 4D5scFv-miniSOG and DARPin-miniSOG, respectively. Furthermore, both of these proteins were capable of inducing receptor-mediated endocytosis [4–6]. However, the internalization rate of the DARPin-miniSOG–HER2 complex was higher than that of the 4D5scFv-miniSOG–HER2 complex [8]. The dissociation constants of the phototoxins and the

receptor measured by surface plasmon resonance are comparable. Therefore, a conclusion has been drawn that the internalization rate, which determines the residence time of the toxin on the membrane, makes the most significant contribution to the efficiency of these photosensitizers.

It is possible to rapidly assess the dynamics of internalization of these proteins due to the fact that miniSOG exhibits intrinsic fluorescence, with its intensity decreasing as phototoxins enter the endosomes. However, the mechanism of fluorescence quenching in miniSOG upon entering the cell has not been elucidated yet. Based on the processes taking place in the endosome, several hypotheses can be formulated to interpret this phenomenon. This fluorescence quenching of some fluorophores in the endosome can be related to protonation, as pH is decreased. For example, fluorescein isothiocyanate (FITC) responds to changes in acidity and is used to study the internalization of cell receptors [9]. The miniSOG chromophore is based on a flavin mononucleotide (FMN) that can also be protonated; so, this can be the reason for the fluorescence decline [9, 10]. The fluorescent properties of the miniSOG protein depend on its cofactor; therefore, it is less likely that proteolysis taking place in the endosome or lysosome is the cause of this phenomenon. Finally, the fluorescence intensity of phototoxins can be reduced as chromophores in the cytoplasm shield miniSOG and absorb its fluorescence.

This study focused on the causes of the reduction in the fluorescence intensity of the phototoxic proteins 4D5scFv-miniSOG and DARPin-miniSOG. Fluorescence quenching of miniSOG in the endosome makes this module a convenient tool for investigating internalization dynamics. However, it is important to understand the reasons for this phenomenon, since the fluorescent properties of miniSOG are closely related to its toxic properties. Furthermore, when designing systems for phototoxin delivery to therapeutic targets, researchers should take into account the physicochemical processes with the participation of miniSOG that take place in different cellular compartments.

MATERIALS AND METHODS

Cell lines and culture conditions

Chinese hamster ovary (CHO) cells and human breast adenocarcinoma SK-BR-3 cells overexpressing the cell surface receptor HER2 were cultured in the McCoy's 5A medium (Life Technologies, USA) supplemented with 10% fetal bovine serum (FBS) (HyClone, Belgium) and 2 mM *L*-glutamine (PanEco, Russia) in atmosphere of 5% CO_2 at 37°C.

Production of recombinant proteins 4D5scFv-miniSOG and DARPin-miniSOG

Proteins 4D5scFv-miniSOG and DARPin-miniSOG were produced in *Escherichia coli* strain BL21(DE3). The cells were transformed using a pET22b plasmid carrying the gene of the respective protein. The transformed bacteria were cultured in a LB liquid medium (1% tryptone, 0.5% yeast extract, and 1% NaCl) until the optical density OD_{600} reached 0.5. Expression was induced by 1 mM isopropyl β-*D*-1-thiogalactopyranoside (IPTG, Merck, Germany); the biomass was then grown at 25°C for 24 h. The resulting biomass was precipitated by centrifugation (10,000*g*) at 4°C for 10 min, re-suspended in 60 mL of 20 mM phosphate-buffered saline (3.2 mM NaH_2PO_4, 16.8 mM Na_2HPO_4, 0.3 M NaCl, pH 7.5), and subjected to ultrasonic lysis using a VCX120 sonicator (Sonic and Materials Inc., USA) in the pulsed mode (pulse for 30 s, cooling down for 30 s; 70% amplitude) for 5 min. In order to separate the soluble and insoluble fractions, the lysate was centrifuged (50,000*g*) at 10°C for 30 min. The precipitate was separated from the supernatant liquid, and the target proteins were isolated.

Proteins 4D5scFv-miniSOG and DARPin-miniSOG were isolated from the soluble fraction by metal-chelate affinity chromatography on a HisTrap FF 1 mL column (GE Healthcare, USA) loaded with Ni^{2+}-NTA-sepharose. The proteins were eluted via stepwise increase in imidazole concentration from 15 to 500 mM in 20 mM phosphate-buffered saline (pH 7.5) at an elution rate of 0.5 mL/min using a UV cell (RD2:250-280, Reach Devices, USA) detecting light absorption at 260 and 280 nm. After chromatography, the protein fractions were analyzed by sodium dodecyl sulfate polyacrylamide gel electrophoresis (SDS-PAGE) under denaturing conditions according to the Laemmli's protocol. Concentrations of the target proteins were determined by the biuret test in the presence of bicinchoninic acid using a Pierce BSA Protein Assay Kit (Thermo Scientific, USA), in compliance with the manufacturer's protocol.

Verification of the specificity of 4D5scFv-miniSOG and DARPin-miniSOG binding to the HER2 receptor

The presence of the HER2 receptor on cells and specificity of binding of the 4D5scFv-miniSOG and DARPin-miniSOG proteins to HER2 were analyzed using a BD Accuri C6 flow cytometer (Becton Dickinson, USA) with the following parameters: laser power, 20 mW; wavelength, 488 nm; and filters 533/30 BP (the FL1 channel) for detecting protein fluorescence and 585/40 BP (the FL3 channel) for detecting fluorescence of propidium iodide. The data were analyzed using the BD Accuri C6 software and processed using

the FlowJo program. HER2-positive SK-BR-3 cells and HER2-negative CHO cells were used in the experiment.

Samples consisting of ~10^5 cells were incubated with the proteins 4D5scFv-miniSOG, DARPin-miniSOG, and 4D5scFv conjugated to FITC (4D5scFv-FITC) or with FITC-conjugated beta-lactoglobulin (β-LG-FITC) (all proteins were taken at concentration of 2 μm) in PBS supplemented with 1% bovine serum albumin (Dia-M, Russia) on ice during 15 min. After staining, the cell suspension was washed twice with PBS supplemented with 1% bovine serum albumin. To eliminate non-living cells from the analysis, the sample was incubated with 2.5 μg/mL propidium iodide for 5 min prior to measurements. When performing fluorescence measurements, single-cell populations were isolated according to light scattering parameters (FSC-H/FSC-A). Among them, live cells not stained with propidium iodide were selected for the analysis. At least 10^4 fluorescent events were recorded for each sample.

Studying the internalization rate of DARPin-miniSOG and 4D5scFv-miniSOG

SK-BR-3 cells stained with DARPin-miniSOG and 4D5scFv-miniSOG were used to evaluate the rate of receptor-mediated internalization. The fluorescence of the samples was measured on a BD Accuri C6 flow cytometer (Becton Dickinson, USA) according to the procedure described above. The samples were subdivided into two groups. In the first one, the samples were incubated at 4°C after staining (receptor-mediated internalization does not occur under these conditions). The samples in the second group were incubated at 37°C. The readings were taken at several time points: 5, 10, 30, and 60 min. At least 10^4 events were recorded for each sample.

Studying the mechanism of quenching of miniSOG-based phototoxins in the endosome

The effects of pH and proteases on DARPin-miniSOG, 4D5scFv-miniSOG, and FMN were evaluated by measuring the intensity of the fluorescence induced by light with λ = 488 nm and detected at λ = 535 nm on an Infinite M1000 microplate reader (Tecan, Switzerland). The proteins at a concentration of 35 μm were incubated at 37°C in a buffer (100 mM Tris-HCl), with pH brought to the desired value, containing proteolytic enzymes at a concentration of 40 μM (trypsin, chymotrypsin, pepsin, and papain) (Sigma, USA) and reducing agents (dithiothreitol, glutathione (reduced form), ascorbic acid, NADH, $NaBH_4$ (Sigma, USA)) at concentrations of 10 mM. The readings were taken immediately after adding the protein and after incubation for 1 and 2 h.

A Trypan blue dye (PanEco, Russia) at a 0.1% concentration and cytochrome *c* at a 300 μM concentration (Sigma, USA) were used to evaluate the effect of the presence of other chromophores on the fluorescence intensity of FMN and DARPin-miniSOG as compared to that of DARPin-FITC. The fluorescence intensities of the samples were measured on an Infinite M1000 microplate reader (Tecan, Switzerland). Fluorescence was excited by light (λ = 488 nm) and detected in a wavelength range of 525–545 nm. The measurements were made immediately after the chromophores had been added.

RESULTS AND DISCUSSION

In order to ensure efficient performance by an antitumor agent in photodynamic therapy, it needs to be selectively delivered to the target. Thus, we used two target molecules specific to the HER2 surface receptor, a non-immunoglobulin protein (DARPin_9-29), and a single-chain variable fragment (scFv) of the 4D5 antibody, to deliver the cytotoxic module miniSOG. The phototoxic module miniSOG is a flavoprotein that can generate reactive oxygen species when exposed to blue light due to the bound FMN. In order to produce recombinant proteins, *E. coli* BL21(DE3) cells were transformed with the respective plasmids pET22b-4D5scFv-miniSOG and pDARPin-miniSOG. The proteins 4D5scFv-miniSOG and DARPin-miniSOG were isolated from the soluble fraction by Ni^{2+}-NTA metal-chelate affinity chromatography involving imidazole elution. In order to verify the activity of the resulting protein photosensitizers, the specificity of binding of the 4D5scFv-miniSOG and DARPin-miniSOG recombinant proteins to the HER2/neu receptor on the surface of human breast adenocarcinoma SK-BR-3 cells overexpressing HER2/neu was measured by flow cytofluorimetry. This procedure allowed for testing the selectivity of binding between the targeting module of DARPin and the receptor, as well as flavoprotein functionality, since the toxic module miniSOG exhibits intrinsic fluorescence and its binding to the cells can be detected directly [11].

The presence of the HER2/neu receptor on the cell surface was confirmed by the fact that the cells were stained with fluorescein isothiocyanate-labeled 4D5scFv (4D5scFv-FITC). FITC-labeled β-lactoglobulin (β-LG-FITC), which does not bind to HER2 on the cell surface, was used as a negative control. It was demonstrated that HER2-negative CHO cells do not generate a fluorescent signal after incubation with the protein 4D5scFv-FITC or β-LG-FITC and the target proteins 4D5scFv-miniSOG and DARPin-miniSOG (*Table*).

Fluorescence of cells after staining with various proteins. The mean values for the three experiments ± mean error are given

Sample	Fluorescence intensity measured in the FL1 channel	
	SK-BR-3 cells	CHO cells
Unstained cells	3700 ± 400	3700 ± 900
+ β-LG-FITC	5700 ± 600	3300 ± 400
+ 4D5scFv-FITC	$2.7\times10^4 \pm 7 \times 10^3$	3200 ± 500
+ 4D5scFv-miniSOG	$2.3\times10^4 \pm 3 \times 10^3$	4600 ± 400
+ DARPin-miniSOG	$1.71\times10^4 \pm 1.6 \times 10^3$	3000 ± 400

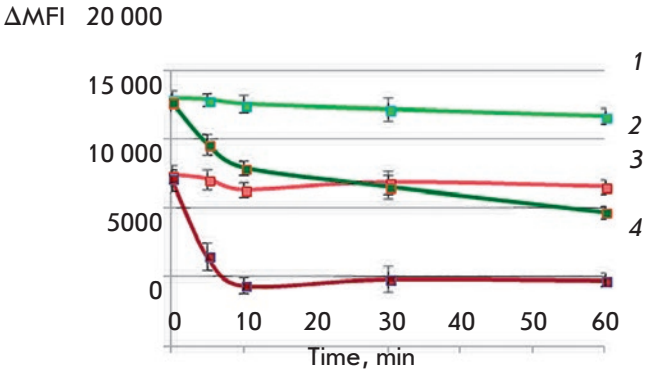

Fig. 1. Changes in the fluorescence intensity of phototoxic proteins during internalization in combination with HER2 (+37°C) and under conditions preventing internalization (+4°C). *1* – 4D5scFv-miniSOG, +4°C; *2* – DARPin-miniSOG, +4°C; *3* – 4D5scFv-miniSOG, +37°C; *4* – DARPin-miniSOG, +37°C. ΔMFI is the difference in fluorescence intensities between the stained cells and the unstained sample incubated under the same conditions

Hence, it has been demonstrated that the targeted recombinant proteins 4D5scFv-miniSOG and DARPin-miniSOG are capable of highly specific binding to the HER2/neu receptor on the surface of human breast adenocarcinoma SK-BR-3 cells.

It was revealed that receptor-mediated internalization of proteins did not take place after the DARPin-miniSOG and 4D5scFv-miniSOG proteins were bound to the receptor on the surface of SK-BR-3 cells at +4°C. However, the receptor–protein complex undergoes internalization at +37°C, as evidenced by the reduction in the fluorescence intensity ΔMFI (the difference between the average fluorescence intensities of stained and unstained cells) (*Fig. 1*). The DARPin-miniSOG recombinant protein as part of its complex with the receptor is internalized faster than 4D5scFv-miniSOG, since ΔMFI for DARPin-miniSOG decreases twofold as compared to its baseline during the first 10 min, while ΔMFI for 4D5scFv-miniSOG is 40 min. These findings are consistent with the published data: 4D5scFv-miniSOG has a higher cytotoxicity than DARPin-miniSOG [5, 6], because 4D5scFv-miniSOG resides on the membrane for a longer time. Since necrosis is the predominant death mechanism of cells irradiated in the presence of these phototoxins, membrane damage makes a crucial contribution to the toxicity of targeted proteins. However, the decline in the fluorescence intensity of miniSOG can be indicative of reactions involving chromophore, which is also expected to affect its efficiency as a phototoxin.

In order to elucidate the reasons for the decline in the fluorescence intensity and toxicity of miniSOG-based proteins observed during their internalization, we evaluated the effect of various factors on the fluorescent properties of miniSOG. A hypothesis has been put forward that quenching of DARPin-miniSOG fluorescence during internalization can be associated with changes in the pH of the environment, as the receptor–protein complex enters endosomes and lysosomes. *Figure 2* shows the dependence between the fluorescence intensity of the DARPin-miniSOG and 4D5scFv-miniSOG proteins and the flavin cofactor (FMN) on the pH of the solution at +37°C. A reliable and significant decline in fluorescent intensity (over twofold) was observed at pH 3 and a less pronounced decline was detected at pH 4. Meanwhile, the minimal pH in the endosomes and lysosomes is 4.8 [12]. Therefore, quenching of miniSOG fluorescence during its internalization cannot be attributed to its response to endosomal acidification. Furthermore, variation in the temperature in a range from +4° to +37°C is not the reason for the decline in the fluorescence intensity of FMN and DARPin-miniSOG.

In order to test the hypothesis regarding the possible effect of proteolysis in the endosome on the fluorescence intensity of DARPin-miniSOG and 4D5scFv-miniSOG, we simulated the conditions of proteolytic cleavage by such enzymes as trypsin, papain, and chymotrypsin that is similar to endosomal cathepsin G [13], and pepsin. The activity of the latter enzyme was comparable to those of the lysosomal cathepsins D and E at pH values optimal for them. FMN was used as a control. A significant decline in the fluorescence intensity of FMN, DARPin-miniSOG, and 4D5scFv-miniSOG was observed only when the target proteins were treated with pepsin (*Fig. 3*). However, the data presented above (*Fig. 2*) provide

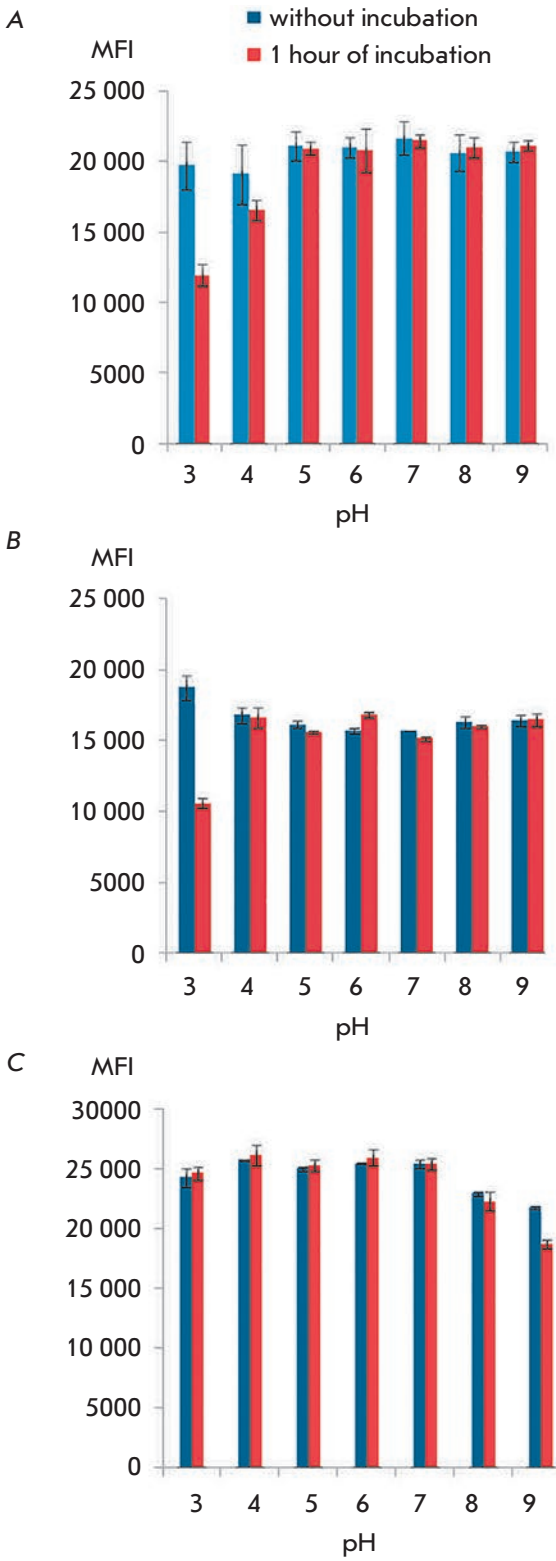

Fig. 2. Dependence of the intensity of the fluorescent signals of 4D5scFv-miniSOG (*A*) DARPin–miniSOG (*B*) and FMN (*C*) on the pH of the medium at 37°C for 1 h. The fluorescence intensity was recorded in a wavelength range of 525–545 nm on an M1000 Pro microplate reader (Tecan, Switzerland). Here and in *Figs. 3–5*, MFI is the fluorescence intensity; M ± m, $n = 3$

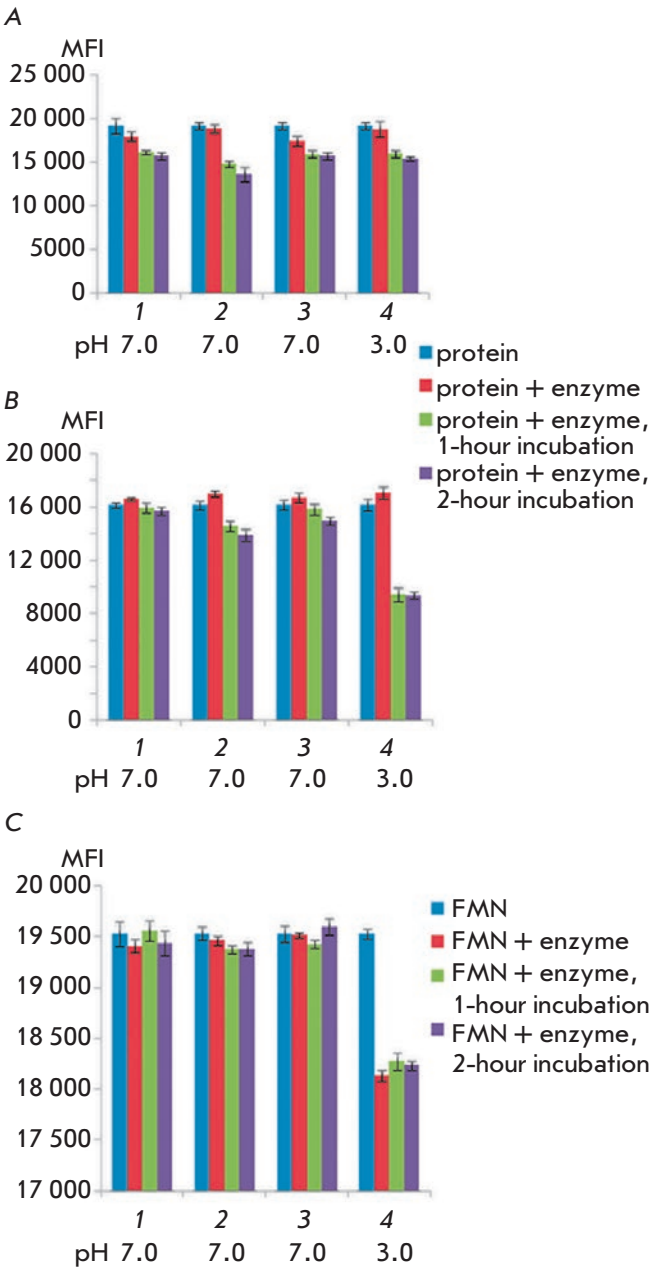

Fig. 3. Dependence of the fluorescence intensity of 4D5scFv-miniSOG (*A*), DARPin–miniSOG, (*B*) and FMN (*C*) on treatment with specific proteases at 37°C for 1 h. *1* – trypsin; *2* – chymotrypsin; *3* – papain; and *4* – pepsin. The fluorescence was recorded in a wavelength range of 525–545 nm

grounds for inferring that a low pH is the reason for fluorescence quenching. This hypothesis is also supported by the fact that the fluorescence intensity decreased in the reaction mixture that contained FMN (insensitive to proteolysis), instead of phototoxic pro-

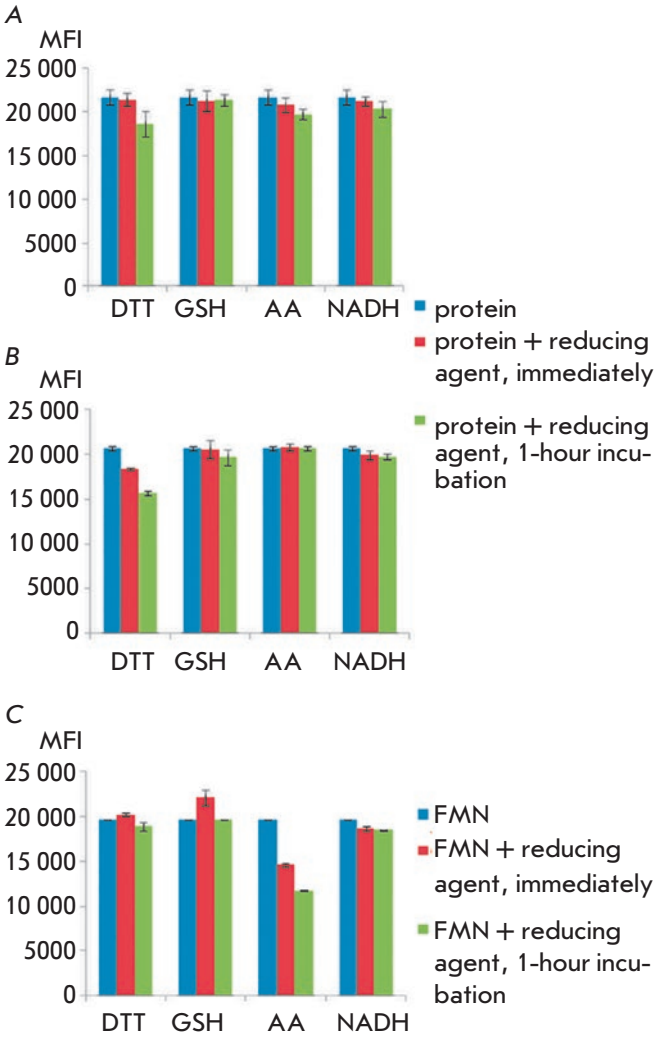

Fig. 4. Dependence of the intensity of the fluorescent signal of 4D5scFv-miniSOG (*A*), DARPin–miniSOG (*B*), and FMN (*C*) on the effects of intracellular reducing agents at 37°C for 1 h. DTT – dithiothreitol; AA – ascorbic acid. The fluorescence was recorded in a wavelength range of 525–545 nm

teins. Treatment with other proteases did not reduce the fluorescence intensity twofold or more, while such a reduction was observed upon internalization (*Fig. 1*). Cleavage of DARPin-miniSOG and 4D5scFv-miniSOG under the experimental conditions was confirmed by PAGE (15% PAG), using the Laemmli protocol. Phototoxic proteins were fully cleaved after 1-hour incubation.

Another reason for the decline in the fluorescence intensity of miniSOG during receptor-mediated internalization could be based on the fact that the flavin mononucleotide cofactor was reduced by the reactive molecules in the cell. Reduction of FMN is known to decrease its intensity [15]. In case a significant percentage of the oxidized form of the cofactor is ingested by the protein during production of miniSOG in bacteria or the cofactor is easily oxidized upon storage, its reduction can be responsible for quenching of the fluorophore in the cell. The effects of the following reducing agents on DARPin-miniSOG and 4D5scFv-miniSOG were studied: dithiothreitol, glutathione (in its reduced form, GSH), ascorbic acid, NADH, sodium borohydride ($NaBH_4$) (*Figs. 4A,B*), and FMN in the absence of the protein component (*Fig. 4C*). It was found that unbound FMN can be reduced by $NaBH_4$ and ascorbic acid, which leads to an almost twofold decrease in the fluorescence intensity. Meanwhile, reduction of the flavin mononucleotide cofactor within DARPin-miniSOG occurs only at high $NaBH_4$ concentrations (starting from 10 mM). Since the more physiologically relevant reducing agents did not exhibit this effect, a conclusion was drawn that reduction of the cofactor does not significantly contribute to the changes in the fluorescence intensity of miniSOG in the cell. Furthermore, the effect of intracellular reducing agents on the fluorescence intensity of DARPin-miniSOG and 4D5scFv-miniSOG after protease treatment at a pH optimal for these enzymes has been evaluated. This treatment also did not affect the fluorescent properties of the miniSOG-based proteins.

An alternative hypothesis explaining the decline in the fluorescence intensity of miniSOG in the cell is shielding of a protein molecule and quenching of its fluorescence by intrinsic chromophores. The Trypan blue dye was tested as a model molecule capable of *in vitro* quenching of miniSOG fluorescence. The dye contributed to complete fluorescence quenching of both DARPin-miniSOG and 4D5scFv-miniSOG. Hemoproteins, such as cytochrome *c*, can act as native agents that absorb miniSOG radiation inside the cell. It has been demonstrated that when fluorescence is excited in the presence of cytochrome, fluorescence intensity decreases twofold both for FMN and for the target proteins. This effect was not observed for DARPin conjugated to FITC, the conventional fluorescent dye (*Fig. 5*).

It is worth mentioning that FITC fluorescence in endosomes and lysosomes also varies depending on the pH of the environment. This dye is currently used as a sensor for measuring the pH of endosomes in cells [9, 10]. Like FITC, the cytotoxic module miniSOG can be employed to detect HER2 internalization, but the reasons for the decline in fluorescence intensity in these two cases are different.

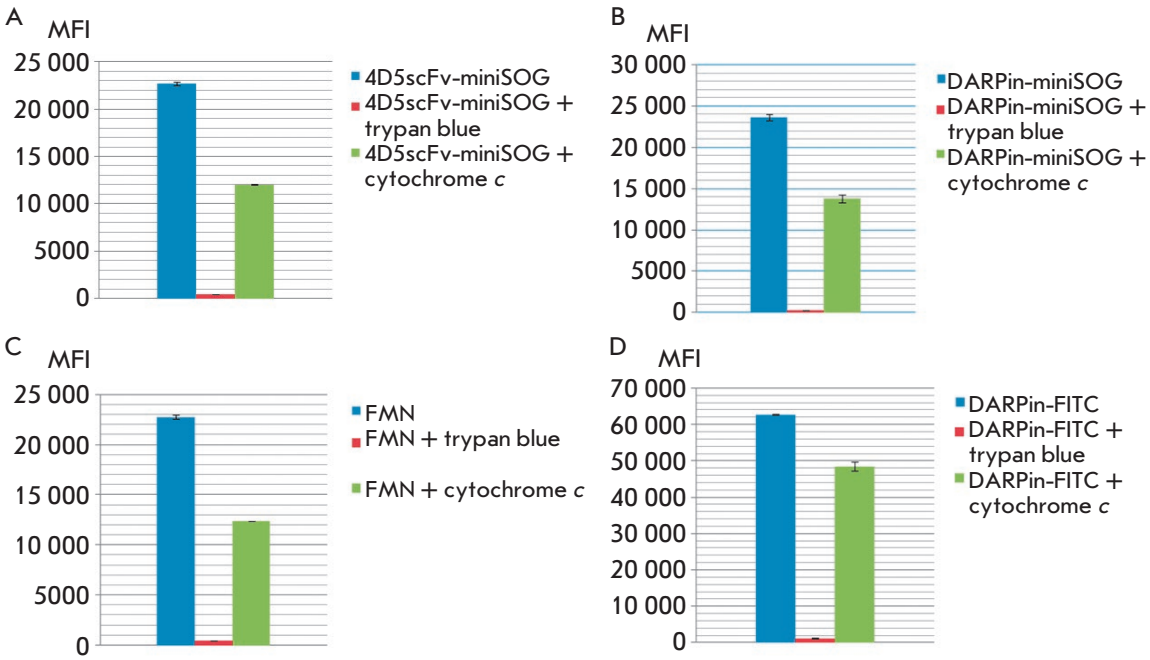

Fig. 5. Effect of the presence of different chromophores on the fluorescence intensity of 4D5scFv-miniSOG (*A*), DARPin–miniSOG (*B*) FMN (*C*), and DARPin-FITC (*D*). The fluorescence was recorded in a wavelength range of 525–545 nm

CONCLUSIONS

The key reason for the decline in the fluorescence intensity of miniSOG-based phototoxins is their shielding and absorption of miniSOG fluorescence by intrinsic cellular fluorophores. The stability of miniSOG inside the cell makes it a promising component for designing theranostic agents, as its spectral properties make it possible to use it together with NanoLuc luciferase, which solves the problem of miniSOG shielding [16]. We have discovered that the cytotoxic module miniSOG within the recombinant proteins 4D5scFv-miniSOG and DARPin-miniSOG can be used to detect HER2 internalization in the same manner as FITC, but the reasons for quenching of the fluorescent signals are different.

Understanding the mechanism of fluorescence quenching in the photosensitizer allows one to adequately interpret the data on the dynamics of internalization of theranostic agents in a complex with the HER2 receptor. This is of utmost importance for a rational design of targeted phototoxic agents, since their efficiency was earlier found to depend on their localization and accumulation in tumor cells [17]. ●

This work was supported by the Russian Foundation for Basic Research KOMFI grant no. 17-00-00121 (designing target-specific recombinant proteins) and the Russian Science Foundation grant no. 14-24-00106 (tumor cell studies). The studies were performed using the facilities of the Common Use Center of the Institute of Bioorganic Chemistry supported by the Ministry of Education and Science of the Russian Federation (Agreement ID RFMEFI62117X0018).

REFERENCES

1. Kuimova M.K., Bhatti M., Deonarain M., Yahioglu G., Levitt J.A., Stamati I., Suhling K., Phillips D. // Photochem. Photobiol. Sci. 2007. V. 6. № 9. P. 933–939.
2. Wu D., Yotnda P. // J. Vis. Exp. 2011. № 57. P. 3357.
3. Green D.R., Llambi F. // Cold Spring Harbor Perspectives in Biology. 2015. V. 7. № 12. P. a006080.
4. Shilova O.N., Proshkina G.M., Lebedenko E.N., Deyev S.M. // Acta Naturae. 2015. V. 7. № 3. P. 126–132.
5. Mironova K.E., Proshkina G.M., Ryabova A.V., Stremovskiy O.A., Lukyanov S.A., Petrov R.V., Deyev S.M. // Theranostics. 2013. V. 3. № 11. P. 831–840.
6. Proshkina G.M., Shilova O.N., Ryabova A.V., Stremovskiy O.A., Deyev S.M. // Biochimie. 2015. V. 118. P. 116–122.
7. Shu X., Lev-Ram V., Deerinck T.J., Qi Y., Ramko E.B., Davidson M.W., Jin Y., Ellisman M.H., Tsien R.Y. // PLoS Biol. 2011. V. 9. № 4. P. 1–10.
8. Shilova O.N., Proshkina G.M., Ryabova A.V., Deyev S.M., Petrov R.V. // Doklady Biochemistry and Biophysics. 2017. V. 475. № 1. P. 256–258.
9. Brabec M., Schober D., Wagner E., Bayer N., Murphy R.F., Blaas D., Fuchs R. // J. Virology. 2005. V. 79. № 2. P. 1008–1016.
10. Jin T., Sasaki A., Kinjo M., Miyazaki J. // Chem. Commun. 2011. V. 46. № 14. P. 2408–2410.
11. Shilova O.N., Shilov E.S., Deyev S.M. // Cytometry. Part A. 2017. V. 91. № 9. P. 917–925.
12. Geisow M.J., Evans W.H. // Exp. Cell Res. 1984. V. 150. №

1. P. 36–46.
13. Thomas M.P., Whangbo J., McCrossan G., Deutsch A.J., Martinod K., Walch M., Lieberman J. // J. Immunol. 2014. V. 192. № 11. P. 5390–5397.
14. Stoka V., Turk V., Turk B. // Ageing Res. Rev. 2016. V. 32. P. 22–37.
15. Benson R.C., Meyer R.A., Zaruba M.E., McKhann G.M. // J. Histochem. Cytochem. 1979. V. 27. № 1. P. 44–48.
16. Shramova E.I., Proshkina G.M., Chumakov S.P., Khodarovich Y.M., Deyev S.M. // Acta Naturae. 2016. V. 8. № 4. P. 118–123.
17. Shramova E.I., Proshkina G.M., Deyev S.M., Petrov R.V. // Doklady Biochemistry and Biophysics. 2017. V. 474. № 1. P. 228–230.

The TLR4 Agonist Immunomax Affects the Phenotype of Mouse Lung Macrophages during Respiratory Syncytial Virus Infection

A. A. Nikonova[1,2*], A. V. Pichugin[1], M. M. Chulkina[1], E. S. Lebedeva[1], A. R. Gaisina[1], I. P. Shilovskiy[1], R. I. Ataullakhanov[1], M. R. Khaitov[1], R. M. Khaitov[1]

[1]NRC Institute of Immunology FMBA of Russia, Kashirskoe shosse, 24, Moscow, 115478, Russia

[2]Mechnikov Research Institute for Vaccines and Sera, Maliy Kazenniy Lane, 5A, Moscow, 105064, Russia

*E-mail: aa.nikonova@nrcii.ru

Received October 06, 2018; in final form November 08, 2018

ABSTRACT **In the study, the effect of the TLR4 agonist Immunomax was investigated *in vitro* and *in vivo*. In particular, Immunomax was shown to polarize mouse bone marrow macrophages from the M0 and M2 states into the M1 state (*ARG1* and *iNOS* mRNA expression levels were used to identify the mouse M1 and M2 phenotypes). Next, we investigated the prophylactic antiviral effect of Immunomax in both a model of mouse respiratory syncytial virus (RSV) infection and a model of RSV-induced bronchial asthma (BA) exacerbation. In the experiment with RSV-induced BA exacerbation, Immunomax-treated mice were characterized by a significant decrease of the viral load in lung homogenates, an increased amount of M1 macrophages in the lung, a tendency toward Th2-dependent ovalbumin-specific IgG1 antibodies decrease in blood serum, a significant increase in RSV-activated $CD4^+$ T cells secreting IFNγ (Th1 cells), and a simultaneous significant decrease in the amount of $CD4^+$ cells secreting IL-4 (Th2 cells) in the mouse spleen, which were detected by ELISPOT 1.5 months after experiment. These findings suggest that treatment with the TLR4 agonist Immunomax polarizes the immune response towards antiviral Th1 and may be used for short-term antiviral prophylaxis to prevent acute respiratory viral infections in asthmatics.**

KEYWORDS **bronchial asthma, macrophages, PRR, respiratory syncytial virus, TLR4 agonists.**

ABBREVIATIONS **BA – bronchial asthma; ARVI – acute respiratory viral infection; IL – interleukin; RSV – respiratory syncytial virus; TLR – Toll-like receptor; Mф – macrophage; IFN – interferon; i.n. – intranasal administration; i.p. – intraperitoneal administration; BAL – bronchoalveolar lavage; RT-PCR – real-time PCR; aMP – alveolar MP.**

INTRODUCTION

Bronchial astma (BA) is a disease associated with a chronic inflammation of the respiratory tract. Inflammation underlying bronchial hyperreactivity develops under the influence of type 2 T-helpers (Th2-response). Over the past 15–20 years, the prevalence of BA in the Russian Federation population has increased more than 3-fold and amounted to 902.8 per 100,000 (2007). In most cases, BA exacerbations in children and adults are associated with acute respiratory viral infections (ARVIs). Some viral species, such as the respiratory syncytial virus (RSV), rhinoviruses, metapneumovirus, influenza, parainfluenza viruses, and coronaviruses, are detected in the fluids of the respiratory tract during BA exacerbation [1]. In this regard, the development of new medical products of ARVI prevention is an important health care issue.

Alveolar Mфs (aMфs) are the most abundant cell population of bronchoalveolar lavage (BAL); their distinctive feature is the ability to acquire various phenotypes based on microenvironmental signals (classically activated M1, alternatively activated M2). The regulatory role of various Mф phenotypes *in vivo* has been substantially studied; however, there is data indicating that Mфs may be involved in the pathogenesis of BA [2, 3].

Amongst pathogen pattern recognition receptors (PRRs), the most studied are Toll-like receptors (TLRs), activation of which is necessary for triggering mechanisms of the innate immune response to infection. For

this reason, TLR agonists are believed to be potential immunotherapeutic agents or vaccine adjuvants for the treatment of infectious diseases. Immunomax, a TLR4-agonist isolated from potato sprouts [4], is effective against a number of viral (papillomavirus, herpes virus) and bacterial pathogens and likewise exhibits potential antitumor activity [5]. Earlier, the immunomodulator Immunomax was reported to activate monocytes, Mφs, NKs, and dendritic cells [6].

In this study, we investigated the role of M2 Mφs in BA exacerbation induced by viral infections, as well as the possibility of influencing the Mφ polarization from M2 to M1 using TLR agonists in order to increase the effectiveness of immune defense against RSV under an allergic immune response.

EXPERIMENTAL

Polarization of mouse macrophages by Immunomax *in vitro*

Macrophages (Mφs) derived from mouse bone marrow were placed in 24-well plates at a concentration of 10^5 cells per well and cultured in a medium containing the granulocyte-macrophage colony-stimulating factor (GM-CSF) for 7 days. After the 7 days, the cells were treated for 24 hour with IL-4 to obtain M2 Mφs, Immunomax to obtain M1, or the medium alone to produce M0. Twenty-four hours after treatment with IL-4, the medium was replaced with a new one containing Immunomax for repolarization of M2 into M1; in addition, Immunomax was added to M0 for repolarization to M1. The experiment scheme is shown in *Fig. 1A*. Twenty-four hours after treatment, cell lysates were collected, frozen at −80 ˚C, and stored until the analysis. Next, the samples were analyzed by RT-PCR to determine mouse *iNOS* and the *ARG1* mRNA levels.

In vivo experiments

We assessed the prophylactic effect of Immunomax *in vivo* in two experimental models: RSV infection in mice and virus-induced BA exacerbation in mice. The experiment schemes are presented in *Figs. 2A* and *2B*, respectively. The RSV strain A2 was chosen as a viral agent. Female BALB/c mice weighing 18–20 g received from Stolbovaya (Russia) were used in the experiments.

For the experiments, four groups of animals were formed (N = 17) (*Fig. 2*). Eight mice in each group were used for histological examination and PCR analysis. A number of mice (N = 4) were used to analyze the phenotypes of lung macrophage populations (by means of complex cell analysis of bronchial lavage and multiparameter flow cytometry of lung cell infiltrate). Four mice from each group were used to determine the amount of RSV-specific $CD4^+$ T cells secreting IFN-γ and IL-4 by the ELISPOT method 1.5 months after infection.

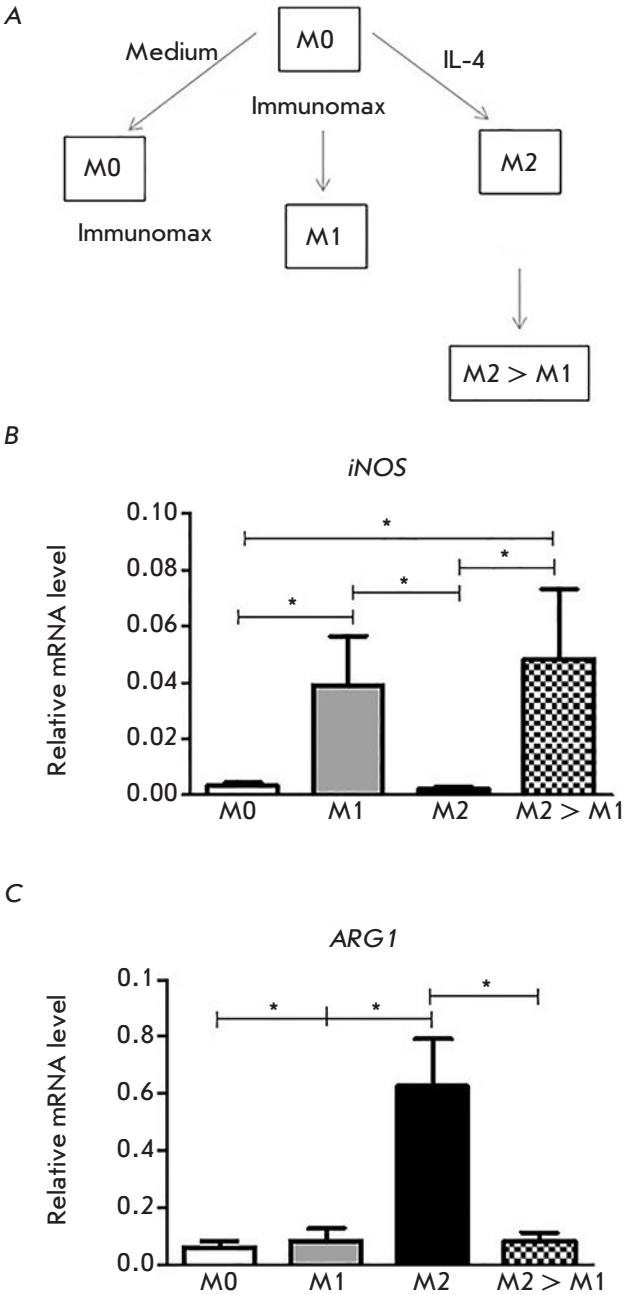

Fig. 1. A TLR4 agonist Immunomax polarizes *in vitro* mouse macrophages towards the M1 phenotype. (*A*) Design of the experiment; *iNOS* (*B*) and *ARG1* (*C*) mRNA expression measured by RT-PCR

Based on the study by Misharin *et al.* [7], we selected the following combination of antibodies to identify myeloid cell populations: CD11b Brilliant Violet 510™, CD45 AlexaFluor®, Ly-6C PE, CD11cPE/Dazzle™ 594,

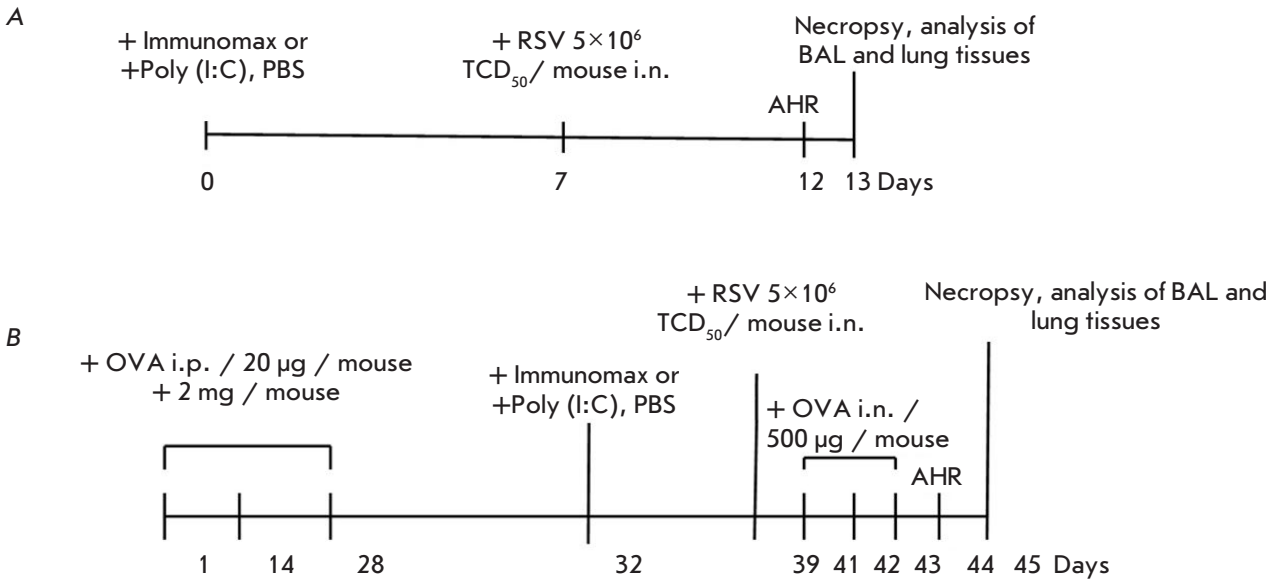

Fig.2. Experimental protocol of animal sensitization, challenge, RSV infection, and TLR agonist treatment. (*A*) The mouse model of RSV infection; (*B*) the mouse model of RSV-induced BA exacerbation. PBS – phosphate-buffered saline, i.n. – intranasal introduction, AHR – airway hyperresponsiveness, OVA – ovalbumin, i.p – intraperitoneal injection, BAL – bronchoalveolar lavage. The following experimental animal groups were used (RSV infection model): (1) RSV+Immunomax (*N*=17); (2) RSV+Poly (I:C) (*N*=17); (3) RSV (*N*=17); (4) intact mice (*N*=17). The RSV-induced BA exacerbation model: (1) BA/RSV+Immunomax (*N*=17); (2) BA/RSV+Poly (I:C) (*N*=17); (3) BA/RSV (*N*=17); (4) intact mice (*N*=17)

CD49bPerCP/Cy5.5, Ly-6GPE/Cy7, F4/80APC, and IA/I-EAPC/Cy7. FACSAria II flow cytometer was used to sort cells. The expression of *iNOS* and *ARG1* mRNAs in sorted Mφs was evaluated by RT-PCR.

To evaluate the antiviral effect of TLR agonists, the RSV RNA level in the lysates of cells isolated from lung homogenates was determine by RT-PCR .

RSV-specific $CD4^+$ T cells secreting IFN-γ and IL-4 were identified using the commercial Mouse IL-4 ELISPOT Set and Mouse IFN-γ ELISPOT Kit (BD Biosciences, USA), according to the manufacturers' instructions.

The statistical analysis was performed with the GraphPad Prism version 4.0 software. Data was considered statistically significant at $P < 0.05$.

RESULTS AND DISCUSSION

We studied the ability of Immunomax, a TLR4 agonist, to polarize mouse macrophages from M0 and M2 into M1. The Mφ phenotype was identified based on the expression of mRNA of the *iNOS* and *ARG1* genes – markers of the M1 and M2 phenotypes, respectively [8]. Our findings confirm the ability of Immunomax to repolarize cells to the M1 state. In particular, Immunomax-treated M0s were characterized by increased *iNOS* expression and reduced *ARG1* expression. We observed the same effect in Immunomax-treated M2 cells (an increase in the *iNOS* mRNA level and a decrease in the *ARG1* mRNA level (*Fig. 1B, C*)).

At the next stage, we studied *in vivo* the prophylactic effect of Immunomax in both experiments of mouse RSV infection and experiments of RSV-induced BA exacerbation (*Fig. 2*). In these experiments, we evaluated a number of parameters, such as the lung function, BAL cell composition, histological alteration, and level of serum ovalbumin-specific antibodies of different classes (IgE, IgG1, and IgG2). There were no statistically significant differences in the values of these parameters in the animals of the experimental groups (data not shown).

However, it should be noted that in the experiment with BA + RSV, we established a tendency of the ovalbumin-specific IgG1 antibody level in the serum of Immunomax-treated mice to decrease (data not shown). Th2-dependent IgG1 antibodies are classic carriers of antibody properties, the level of which may increase in allergic diseases. A decrease in the level of IgG1 antibodies under the influence of Immunomax, which was observed in this study, seems to indicate the development of Th1-type immune responses. Interestingly, these responses were observed at the systemic level, despite intranasal administration of the agent.

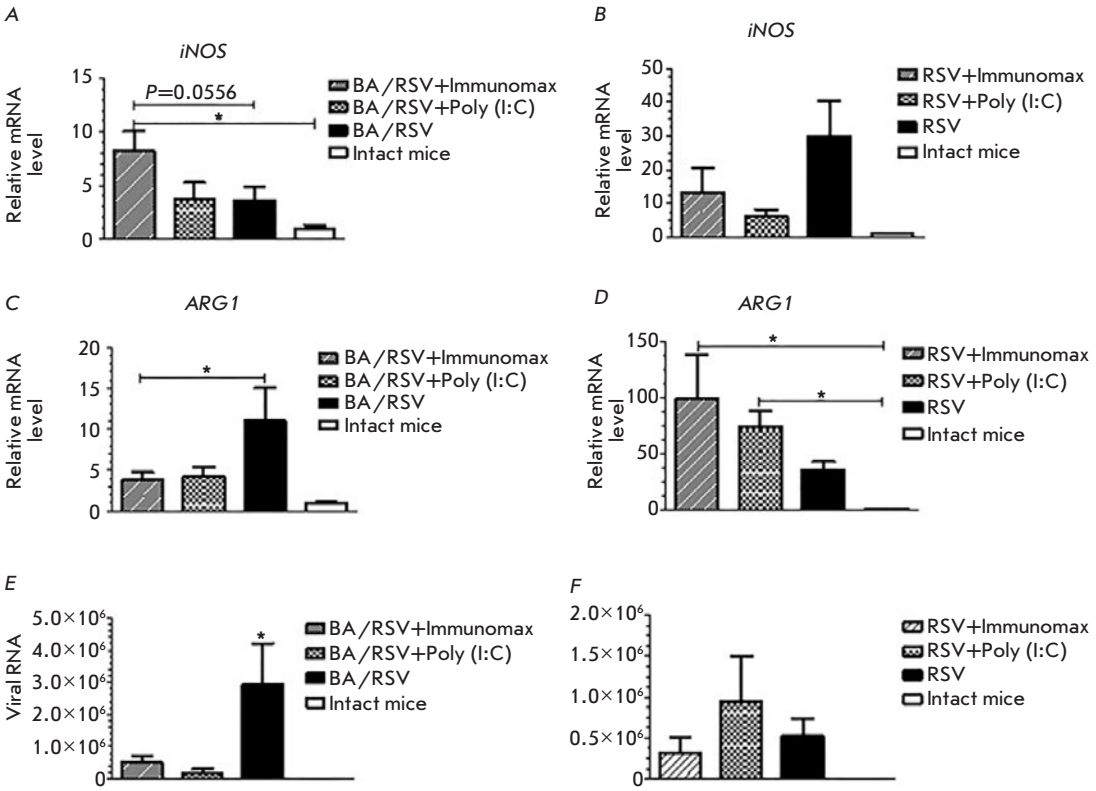

Fig.3. *iNOS* (*A*, *B*) and *ARG1* (*C*, *D*) mRNA expression in mouse alveolar macrophages and (E, F) viral load in lung tissue (RSV RNA copies per 1 g of lung tissue) measured by RT-PCR. (*A*, *C*, *E*) the RSV-induced BA exacerbation model; (*B*, *D*, *F*) the mouse model of RSV infection

Of particular interest was the phenotype of mouse pulmonary Mφs in different experimental conditions, because we supposed that intranasally administered Immunomax would act on these cells, polarizing them into the M1 state. To test this hypothesis, we isolated Mφs from the lungs by sorting cells with a FACSAria II flow cytometer and evaluated the expression of *iNOS* and *ARG1* mRNAs. An analysis of the RT-PCR data revealed an increase in the *iNOS* level (*Fig. 3A*) and a significant decrease in the *ARG1* level (*Fig. 3C*) in Mφs of Immunomax-treated mice with RSV- induced BA exacerbation. This indicates polarization of Mφs into the antiviral M1 state. However, in the mouse RSV infection experiment, this tendency was not revealed (*Fig. 3B,D*).

Assessment of the viral load revealed a statistically significant decrease in the viral RNA level in the lungs of Immunomax-treated mice compared to that in untreated animals (*Fig. 3E*). There was also a reduction in the viral load in a group treated with a TLR3 agonist, Poly (I:C). These data were obtained in the experiment with virus-induced BA exacerbation. We also found a decrease in the viral load in RSV-infected mice treated with the studied agent (*Fig. 3F*).

Figure 4 presents the results of identification of RSV-specific Th1 and Th2 cell differentiation using

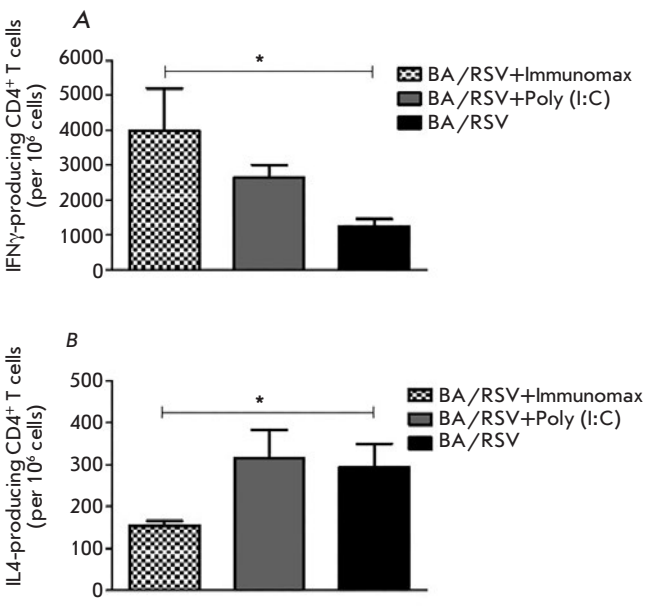

Fig.4. Amount of IFNγ (A) and IL-4 (B) producing CD4+ T cells in the spleen of mice with RSV-induced BA exacerbation (mice were maintained up to 1.5 months after the experiment), determined by ELISPOT (cells were stimulated by UV-inactivated RSV)

the ELISPOT method. In the experiment with the model of RSV-induced BA exacerbations, we observed a significant increase in RSV-activated $CD4^+$ T cells secreting IFN-γ (Th1 cells) (*Fig. 4A*) and simultaneously a significant decrease in $CD4^+$ cells secreting IL-4 (Th2 cells) (*Fig. 4B*) in the spleen of Immunomax-treated mice. In Immunomax-treated mice with RSV infection, there was an increase in the level of activated $CD4^+$ T cells secreting IFN-γ (Th1 cells), while no $CD4^+$ cells secreting IL-4 (Th2 cells) were detected (data not shown).

Therefore, *in vitro* and *in vivo* experiments demonstrated that the TLR4 agonist Immunomax is able to re-polarize the Th2 response to the antiviral Th1 state. The effect of Immunomax was observed on the model of RSV-induced BA exacerbation where a pronounced Th2 response was initially induced in mice by sensitization with a model allergen ovalbumin. The basal concept in the treatment of allergic diseases is an inversion of the immune Th2 response towards Th1. This approach is especially important for BA patients, because abundant data has indicated a more severe course of ARVIs in asthmatics [9]. This is believed to be related to the dominant Th2 response that is probably associated with the prevalence of activated M2 Mφs in the lungs of patients [3]. In this regard, our findings indicate that treatment with Immunomax, a TLR4 agonist, affects the phenotype of pulmonary Mφs, polarizing the immune response towards Th1, and, therefore, that it may be used for the prophylaxis of RSV infection in asthmatics. ●

This study was supported by a grant from the Russian Science Foundation (project No. 16-14-10188).

REFERENCES

1. Tsarev S.V., Khaitov M.R. // Rus Med J. 2009. №. 2. P. 136–113.
2. Nikonova A.A. Khaitov M.R., Khaitov R. M. // Medical immunology. 2017. V. 9. № 6. P. 657–672.
3. Melgert B.N., ten Hacken N.H., Rutgers B., Timens W., Postma D.S., Hylkema M.N. // J. Allergy Clin. Immunol. 2011. V. 127. № 3. P. 831–833.
3. Ataullakhanov R.I., Pichugin A.V., Melnikova T. M., Khaitov R.M. Patent, RU2013151824A, Russia, A61P 37/02, 2013.
4. Ghochikyan A., Pichugin A., Bagaev A., Davtyan A., Hovakimyan A., Tukhvatulin A., Davtyan H., Shcheblyakov D., Logunov D., Chulkina M., et al. // J. Transl. Med. 2014. V. 29. № 12. P. 322.
5. Bagaev A., Pichugin A., Nelson E.L., Agadjanyan M.G., Ghochikyan A., Ataullakhanov R.I. // J. Immunol. 2018. V. 200. № 8. P. 2656–2669.
6. Misharin A.V., Morales-Nebreda L., Mutlu G.M., Budinger G.R., Perlman H. // Am. J. Respir. Cell Mol. Biol. 2013. V. 49. № 4. P. 503–510.
7. Murray P.J., Wynn T.A. // J. Leukoc. Biol. 2011. V. 89. № 4. P. 557–563.
8. Corne J.M., Marshall C., Smith S., Schreiber J., Sanderson G., Holgate S.T., Johnston S.L. // Lancet. 2002. V. 359. № 9309. P. 831–834.

Identification of Novel Interaction Partners of AIF Protein on the Outer Mitochondrial Membrane

N. P. Fadeeva[1], N. V. Antipova[1], V. O. Shender[1], K. S. Anufrieva[1], G. A. Stepanov[2], S. Bastola[3], M. I. Shakhparonov[1], M. S. Pavlyukov[1*]

[1]Shemyakin-Ovchinnikov Institute of Bioorganic Chemistry of the Russian Academy of Sciences, Miklukho-Maklaya Str., 16/10, Moscow, 117997, Russia

[2]Institute of Chemical Biology and Fundamental Medicine, Siberian Branch, Russian Academy of Sciences, Akad. Lavrentiev Ave., 8, Novosibirsk, 630090, Russia

[3]Department of Neurosurgery, University of Alabama at Birmingham, AL 35294, USA

*E-mail: marat.pav@mail.ru

Received September 06, 2017; in final form September 24, 2018

ABSTRACT **In response to the wide variety of external and internal signals, mammalian cells undergo apoptosis, programmed cell death. Dysregulation of apoptosis is involved in multiple human diseases, including cancer, autoimmunity, and ischemic injuries. Two types of apoptosis have been described: the caspase-dependent one, leading to digestion of cellular proteins, and caspase-independent apoptosis, resulting in DNA fragmentation. The latter type of apoptosis is executed by AIF protein and is believed to have appeared first during evolution. The key step in the caspase-independent apoptosis program is the dissociation of AIF from the outer mitochondrial membrane (OMM). However, the molecular mechanism of interaction between AIF and OMM remains poorly understood. In this study, we demonstrated that AIF can bind to OMM via mortalin protein. We confirmed interaction between AIF and mortalin both *in vitro* and *in vivo* and mapped the amino acid sequences that are important for the binding of these proteins. Next, we showed that apoptosis induction by chemotherapy leads to downregulation of AIF–mortalin interaction and dissociation of AIF from the OMM. Finally, a bioinformatic analysis demonstrated that a high level of mortalin expression correlates with a worse survival prognosis for glioma patients. Altogether, our data revealed that mortalin plays an important role in the regulation of the caspase-independent apoptotic pathway and allowed us to speculate that inhibition of AIF–mortalin interaction may induce a dissociation of AIF from the OMM and subsequent apoptosis of cancer cells.**

KEYWORDS **AIF, caspase independent apoptosis, glioma, heat-shock proteins.**

ABBREVIATIONS **AIF – apotosis inducing factor; Hsp – heat-shock proteins; OMM – outer mitochondrial membrane; BiFC – bimolecular fluorescence complementation; YFP – yellow fluorescent protein; PLA – *in situ* proximity ligation assay.**

INTRODUCTION

Dysregulation of apoptosis is known to be involved in the development of many human diseases. On the one hand, inhibition of apoptosis can promote a malignant transformation of cells [1] and initiation of autoimmune processes [2]. On the other hand, hyperactivation of apoptosis causes the death of normal cells in patients with ischemic injuries (infarction and stroke) [3]. Caspases (cysteine proteases that cleave cellular proteins) have, for a long time, been regarded as the main apoptosis effectors. However, there currently is a growing pool of data attesting to the important role of the caspase-independent apoptotic pathway, with the apoptosis-inducing factor (AIF) playing the major role in this process [4].

Many types of tumors are known to be resistant to the caspase-dependent pathway of cell death; however, all of them are sensitive to AIF-mediated apoptosis [4, 5]. This sensitivity is attributed to the fact that not only is AIF involved in apoptosis, but it is also essential for the functioning of mitochondria. Therefore, any tumor cell contains a significant amount of AIF protein, making it a promising target for the development of anti-tumor drugs [6]. On the

other hand, AIF plays a crucial role in ischemic injuries to healthy cells. Recent studies have shown that the death of muscle and nerve cells in infarctions [7] and strokes [8] occurs only via caspase-independent AIF-mediated apoptosis, while inhibition of AIF before simulation of an infarction model efficiently prevents cell death, making it possible to completely restore the cardiac function two weeks after the simulated infarction [7].

The AIF protein encoded by the *aifm1* gene is a NAD-binding flavoprotein that normally localizes on the mitochondrial membrane. This protein is synthesized as a 67 kDa pre-propeptide consisting of 613 amino-acid residues (fAIF). Its N-terminus carries the sequence of mitochondrial localization (1–30 a.a.) and the hydrophobic transmembrane segment (66–84 a.a.), followed by two nuclear import sequences, and the FAD- and NAD-binding domains [9, 10]. A comparative analysis of the genomes of different organisms demonstrated that AIF is highly conserved; its close homologs were found in all metazoan organisms, including plants [11]. Interestingly, a loss of this protein causes death at the early stages ontogenesis [12].

AIF synthesized in the cytoplasm is integrated into the inner mitochondrial membrane, subsequently loses its N-terminal segment dueto mitochondrial peptidase activity, and gives rise to 62 kDa mitochondrial AIF (Δ1–54) [10]. During induction of apoptosis, this protein is dissociated from the mitochondrial membrane and transported into the nucleus. In the nucleus, AIF interacts with histone H2AX and inactive CypA endonuclease. The resulting three-component complex cleaves genomic DNA into fragments ~50 kbp long, causing cell death [13].

The kinetics of AIF dissociation from the mitochondrial membrane is very peculiar. According to some findings, this process takes place 12–18 h after induction of apoptosis and results from the activation of the conventional caspase-dependent apoptotic pathway [14]. However, AIF translocation was observed in other studies as soon as 10–20 min after the induction of apoptosis, much earlier than activation of the caspase-dependent pathway takes place [15]. Such contradictory results are attributed to the fact that two pools of AIF exist inside the cell. One fraction of AIF (~70%) is anchored to the inner mitochondrial membrane through the AIF transmembrane segment. Dissociation of these molecules starts when the integrity of the OMM is disrupted, and AIF is cleaved between the amino acids 96 and 120, which results in the formation of soluble Δ1–102 (57 kDa) or Δ1–118 (55 kDa) AIF fragments [10]. On the other hand, approximately 30% of AIF localizes on the cytoplasmic surface of the outer mitochondrial membrane (OMM). Binding between these molecules and the membrane is much weaker; so, alteration of AIF conformation caused by its interaction with poly-ADP-ribose synthesized in response to DNA damage is enough to trigger AIF dissociation [8, 16].

It is assumed that the highly mobile fraction of AIF anchored to the OMM is responsible for the caspase-independent apoptotic pathway in malignant and normal cells. However, it remains unclear how AIF and OMM interact and why dissociation of this protein takes place. In order to answer this question, we have identified proteins capable of forming a complex with AIF on the OMM and studied how induction of apoptosis alters the interaction between AIF and these proteins.

MATERIALS AND METHODS

Purification of outer mitochondrial membrane proteins

OMM was purified as described previously [17] with slight modifications. Livers from four mice that were starved for 18 hours were washed with buffer A (70 mM sucrose, 210 mM d-mannitol, 0.1 mM EDTA, 1 mM Tris-HCl, pH 7.2), cut into 2- to 4-mm pieces and homogenized with Dounce homogenizer in a 10x volume of buffer A on ice. Next, the solution was centrifuged for 10 min at 500g. Supernatant was collected and centrifuged for 10 min at 9000g. Supernatant was decanted, and the surface of the pallet was carefully washed three times with a small amount of buffer A. Next, pellet was re-suspended in 35 ml of buffer D (20 mM Na-phosphate, 0.02% BSA, pH 7.2) and incubated 20 min on ice. The solution was centrifuged for 20 min at 35000g. Supernatant was decanted, and the pellet was re-suspended in 35 ml of buffer D and centrifuged for 15 min at 1900g. Next, the supernatant was carefully removed and centrifuged for 20 min at 35000g. The yellow-brownish pellet obtained after centrifugation represented a purified OMM fraction. The OMM proteins were solubilized in PBS containing 1% TritonX100, 0.1% Na-deoxycholate and 0.5 mM DTT.

Plasmid Construction

The DNA fragment encoding Mortalin was amplified from U87MG cDNA by the PCR technique using the primer pair Mort_for (AAAA AGA TCT ATG ATA AGT GCC AGC CGA GC) and Mort_rev (ACCA GTC GAC CTG TTT TCT CCT TTT GAT) and cloned into the BglIII/SalI sites of the pET28a+ plasmid (Novagen) to generate the pET28-Mort_FULL plasmid. The DNA fragment encoding the N-terminal domain of Mortalin was amplified from pET28-Mort_FULL plasmid by the PCR technique using the primer pair Mort_for and Mort_I_rev (AATA GTC GAC TCA

GCC GGC CAA CAC ACC TC) and cloned into the BglIII/SalI sites of the pET28a+ plasmid to generate the pET28-Mort_I plasmid. The DNA fragment encoding the C-terminal domain of Mortalin was amplified from the pET28-Mort_FULL plasmid by the PCR technique using the primer pair Mort_II_for (GGGT AGA TCT ACG GAT GTG CTG CTC) and Mort_rev and cloned into the BglIII/SalI sites of the pET28a+ plasmid to generate the pET28-Mort_II plasmid. For overexpression of full-length AIF fused to Halo-tag, we created the pET-HALO plasmid. The DNA fragment encoding Halo-tag was amplified from the pF-C20K HaloTag T7 SP6 Flexi plasmid (Promega) by the PCR technique using the primer pair Halo_for (ACTA ACC GGT CGC CAC CAT GGG ATC CGA AAT CGG TAC TGG) and Halo_rev (AATT AGA TCT ACC GGA AAT CTC CAG AGT A) and cloned into the NcoI/BamHI sites of the pET28a+ plasmid to generate the pET-HALO plasmid. Next, the DNA fragment encoding AIF was amplified from the pEBB-AIF-YC plasmid [18] by the PCR technique using the primer pair AIF_for (AATA GAA TTC GCT AGC TCT GGT GCA TCA GGG G) and AIF_rev (CTGT GTC GAC TCA GTC TTC ATG AAT GTT GA) and cloned into the EcoRI/SalI sites of the pET-HALO plasmid to generate the pET-HALO-AIF plasmid. For overexpression of AIF fused to His-tag, we digested the pET-HALO-AIF plasmid with EcoRI/SalI restriction endonucleases and the resulting DNA fragments were cloned into the corresponding sites of the pet28a+ plasmid to generate the pET28-AIF_FULL plasmid. The DNA fragment encoding apoAIF was amplified from the pEBB-AIF-YC plasmid by the PCR technique using the primer pair apoAIF_for (TAGA GAA TTC GGG CTG ACA CCA GAA CAG A) and AIF_rev and cloned into the EcoRI/SalI sites of the pet28a+ plasmid to generate the pET28-apoAIF plasmid. For overexpression of Mortalin fused to the N-terminal part of YFP, we created the pTagYN-N plasmid. The DNA fragment encoding the N-terminal part of YFP was amplified from the pEBB-XIAP-YN plasmid [18] by the PCR technique using the primer pair YN_for (AAAA GTC GAC ATG GTG AGC AAG GGC GAG GAG C) and YN_rev (AAAT GCGG CCGC TCA GGA TCC GCT CAC G) and cloned into the SalI/NotI sites of the pTagCFP-N (Evrogen) plasmid to generate the pTagYN-N plasmid. Next, the pET28-Mort_FULL plasmid was digested with BglII /SalI restriction endonucleases and the resulting DNA fragments were cloned into the corresponding sites of the pTagYN-N plasmid to generate the pTagYN-Mort plasmid. In all cases, the absence of unwanted mutations in the inserts and vector-insert boundaries was verified by sequencing.

Induction of recombinant protein synthesis in E.coli

BL21(DE3) Codone+ RIL E.coli cells transformed with plasmids and bacteria from a single colony were transferred into 17 ml of a LB medium containing a corresponding antibiotic. After overnight incubation at 37°C, the medium with bacteria was transferred into 200 ml of a fresh LB medium with a corresponding antibiotic. Bacteria were incubated at 37°C on a shaker until OD_{600} reached 0,7. Next, IPTG was added to a final concentration 1mM and bacteria were incubated on the shaker for an additional 18 hours at room temperature.

Purification of His-tag fusion proteins

After IPTG induction, 200 ml of the medium with bacteria was centrifuged for 15 min, 5,000 g at 4°C and the pellet was re-suspended in 12 ml of lysis buffer B (pH 8.0, 100 mM NaH_2PO_4, 10 mM Tris-HCl, 8 M Urea) and incubated for 1.5 hours at room temperature. Next, the solution was centrifuged for 15 min, 18,000 g at 4°C and supernatant was incubated with 2 ml of Ni-NTA resin for 1 hour under constant agitation. Next, the suspension was transferred to a column and washed with 10 ml of buffer B and 10 ml of buffer C (same as buffer B but pH 6.3). Next, the bounded proteins were eluted with buffer D (buffer C with 250 mM of imidazole) and dialyzed overnight against PBS with 1mM DTT. The purity of the obtained proteins was assessed by electrophoresis and subsequent Coomassie Blue staining.

Purification of Halo-tag fusion proteins

After IPTG induction, 200 ml of medium with bacteria was centrifuged for 15 min, 5,000 g at 4°C and the pellet was re-suspended in 6 ml of lysis buffer F (pH 7.9, 50 mM HEPES, 100 mM NaCl, 0.5 mM DTT, 0.5 mM EDTA, 0.005% Igepal and protease inhibitor cocktail). The suspension was sonicated 10 times for 1 min with 2 min resting time between sonications. Some 1.5 ml of the obtained lysate was incubated with 50 µl of Magne HaloTagBeads (Promega) for 1 hour under constant agitation. Next, beads were washed 4 times with buffer F and, after that, equal aliquots of the beads were used for protein interaction assay.

Recombinant protein pull-down assay

To obtain a protein complex, 50 µl of the magnetic beads with immobilized Halo-tagged protein was incubated with a His-tagged protein solution. The suspension was incubated overnight at 4°C under constant agitation. Next, the beads were washed 3 times with PBS and the proteins were eluted with SLB buffer (100 mM Tris-HCl pH 6.8, 4% SDS, 5% β- mercaptoethanol, 20% glycerol and 0.02% bromophenol blue).

Cell lysate protein pull-down assay

To obtain a protein complex, 50 μl of the magnetic beads with immobilized His-tagged protein was incubated with the lysate prepared from U87MG cells. The suspension was incubated overnight at 4°C under constant agitation. Next, the beads were washed once with mammalian cell lysis buffer (50 mM HEPES pH 7.5, 140 mM NaCl, 1 mM EDTA, 10% glycerol, 1% NP40, 0.1% sodium deoxycholate) and 3 times with PBS. After washing, the proteins were eluted with PBS containing 250 mM of imidazole.

Immunoblotting

Immunoblotting was performed as described previously [19]. The following antibodies were used: anti-AIF 1 : 500 (ab32516, Abcam), anti-Mortalin 1 : 250 (sc133137, Santa Cruz), HRP- conjugated secondary antibodies against γ-chain of rabbit IgG 1 : 5000 (Sigma) and HRP- conjugated secondary antibodies against mouse IgG (Sigma).

Cell Culture

Cells were grown in air enriched with 5% (v/v) CO_2 at 37°C in Dulbecco's modified Eagle's medium (DMEM) supplemented with 10% (v/v) fetal bovine serum (FBS), 2mM L-glutamine, and a penicillin (100 units/ml) streptomycin (100μg/ml) mixture. The cells were transfected with a Lipofectamine LTX reagent (Thermo Fisher Scientific; USA) according to the manufacturer's protocol. Apoptosis was induced by addition of various concentrations of cisplatin (Sigma) or staurosporine (Sigma). Cell viability assay was performed using a Alamar Blue reagent (Thermo Fisher Scientific; USA) according to the manufacturer's protocol. Briefly, the cells were plated into a 96-well plate (6,000 cells per well). On the next day, cisplatin or staurosporine was added at different concentrations and, 4 days later, cell viability was determined by a Alamar Blue reagent.

BiFC protein interaction assay

U87MG cells were plated in the wells of a Lab-Tek II chamber and cotransfected with the pEBB-AIF-YC and pTagYN-N, pTagYN-Mort or pEBB-XIAP-YN plasmids. The next day, the cells were examined with a Leica DM IRE2 confocal microscope. At least 50 cells were analyzed for each plasmid pair.

PLA assay

U87MG cells were plated in the wells of a Lab-Tek II chamber and treated with staurosporine for 24 hours. Next, the cells were washed 3 times with phosphate buffered saline (PBS) and fixed with 4% PFA in PBS for 15 min at room temperature. The cells were washed 2 times with PBS and permeabilized with 0.2% Triton-X100 in PBS for 15 min. All subsequent procedures were performed using a Duolink In Situ Orange Starter Kit (Duolink) according to the manufacturer's protocol.

RESULTS

It was demonstrated earlier that AIF interacts with the OMM surface without being integrated into the lipid bilayer [20]. Taking into account the specificity of AIF binding to the OMM and the fact that this interaction is inhibited by high concentrations of NaCl, we hypothesized that AIF is localized on the OMM surface by binding to a certain adapter protein anchored to the OMM. In order to identify this protein, we studied the interaction between recombinant AIF and proteins isolated from the outer membrane of mouse liver mitochondria by ultracentrifugation. Next, the fraction of solubilized OMM proteins was passed through the sorbent with immobilized control protein or full-length AIF (fAIF). The bound proteins were identified by MALDI-TOF mass spectrometry. One of the proteins capable of interacting with AIF but not with the control recombinant protein was identified as mortalin (*Fig. 1*), a member of the family of heat shock proteins (Hsp) associated with the outer surface of the OMM [21].

Mortalin protein carries two functional domains. They are the ATP-binding domain (1–443 a.a.) at its N-terminus and the peptide-binding domain (444–581 a.a.) at its C-terminus [22]. In order to determine which domain is involved in the interaction with AIF, we tested the binding of fAIF to the N- and C-terminal fragments of mortalin (1–443 a.a. and 433-666, a.a. respectively, *Fig. 2A*). With this aim in mind, we constructed plasmid vectors encoding mortalin fragments which carried a hexahistidine tag at their C-terminus, and a plasmid encoding fAIF with the Halo Tag at its N-terminus. The respective recombinant proteins were isolated from bacterial cells (*Fig. 2B*). Purified mortalin fragments were added to magnetic beads with immobilized fAIF. Following incubation and subsequent washing, solvent-bound proteins were eluted and separated by polyacrylamide gel electrophoresis (*Fig. 2C*). The Mort II fragment interacts with fAIF *in vitro*, while Mort I is incapable of such interaction.

Once the mortalin fragment capable of binding to AIF had been identified, we decided to establish what AIF region is needed for this interaction. For this purpose, we constructed plasmids encoding full-length AIF (fAIF) and processed AIF (apoAIF, amino acids 103 to 613, *Fig. 2A*). Processed AIF emerges upon induction of apoptosis and migrates from the

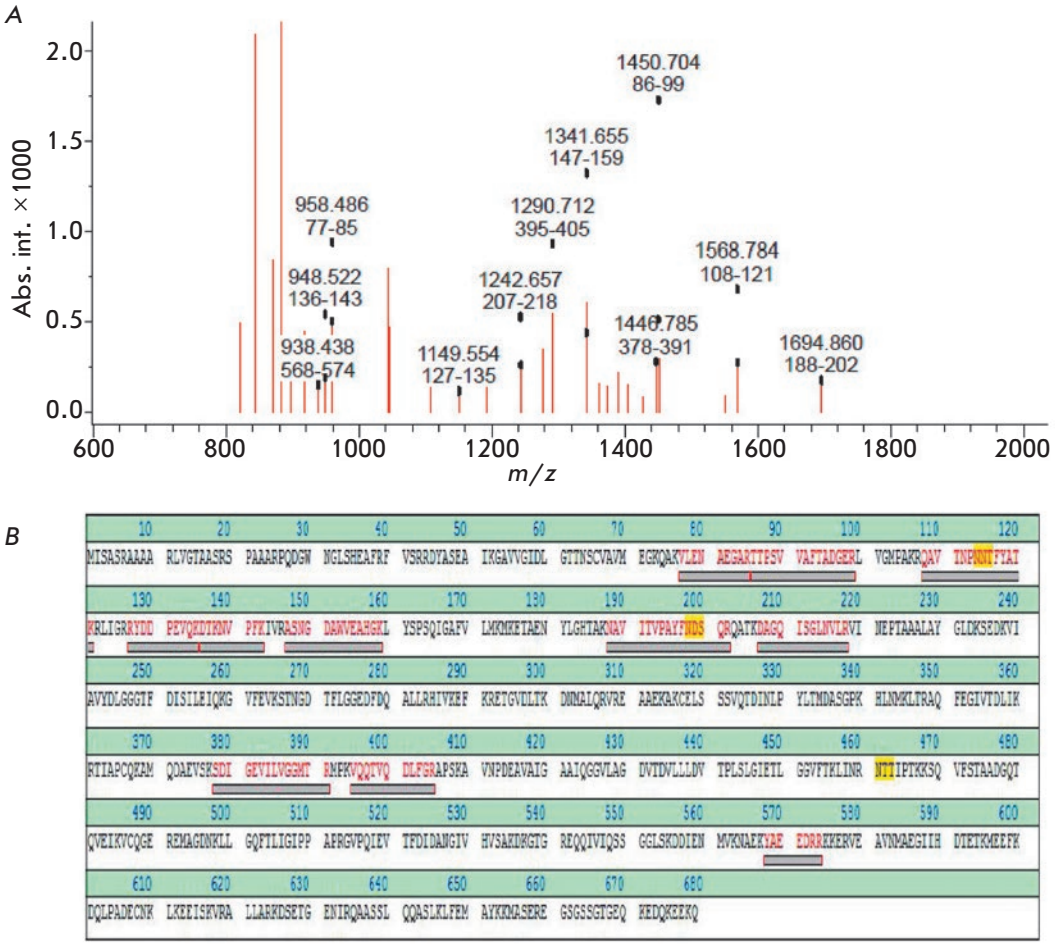

Fig. 1. Identification of OMM protein that interacts with full length AIF. A – Mass spectra of OMM proteins that binds to immobilized AIF. Mortalin-related peptides are indicated. B – amino acid sequence of mortalin, peptides that were identified by MALDI-TOF mass spectrometry are highlighted

mitochondrial membrane into the cell nucleus after dissociation. Both proteins carried the N-terminal hexahistidine tag. The isolated recombinant AIF fragments were immobilized on magnetic beads. Next, a fraction of solubilized OMM proteins containing mortalin was added to the beads. After incubation and subsequent washing, the bound proteins were eluted and subjected to electrophoresis. Mortalin was detected by Western blot analysis with anti-mortalin primary antibodies. According to the immunodetection data (*Fig. 2D*), endogenous mortalin interacts with full-length recombinant fAIF *in vitro* and does not interact with apoAIF, which is consistent with earlier published findings demonstrating that apoAIF cannot be localized on the OMM [20].

Next, we used the biomolecular fluorescence complementation (BiFC) assay to confirm that AIF can interact with mortalin not only *in vitro* but also *in vivo* inside a living cell. This method relies on the fact that YFP protein retains its fluorescence properties even after it has divided into two parts, in case both parts are located close enough to one another. For this very reason, we constructed plasmids encoding mortalin bound to the N-terminal fragment of YFP (Mort-YN) and fAIF carrying the C-terminal fragment of YFP (YC-AIF) (*Fig. 3A*). These plasmids were used to co-transfect U87MG human glioblastoma cells. Furthermore, cells co-transfected with the plasmids encoding YC-AIF and XIAP protein with the N-terminal portion of YFP (YN-XIAP) served as the positive control. It has been demonstrated earlier that AIF interacts with XIAP in mitochondria [18]. Cells co-transfected with the plasmids encoding YC-AIF and the unbound N-terminal portion of YFP (YN) served as the negative control. Confocal microscopy images of cells co-expressing different pairs of proteins were obtained 24 h post-transfection. *Figure 3A* shows the bright fluorescence of YFP in cells co-expressing YC-AIF and Mort-YN, as well as in cells co-expressing YC-AIF and YN-XIAP. These findings

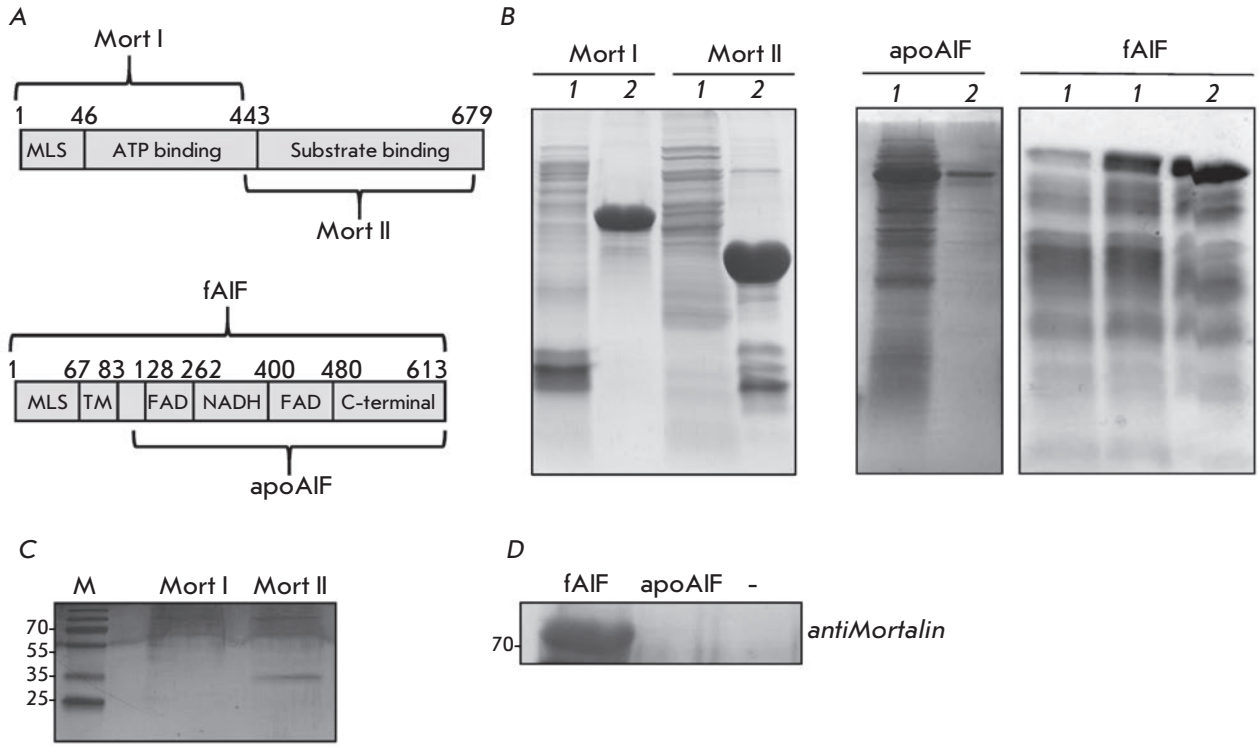

Fig. 2. AIF interacts with mortalin *in vitro*. A – schematic representation of mortalin and AIF proteins. The recombinant fragments that were used in this study are indicated. B – electrophoresis of recombinant mortalin and AIF fragments that were purified from E. coli (1 – before optimization of expression and purification conditions; 2 – after optimization). C – electrophoresis demonstrating interaction of mortalin fragments with full-length AIF that was immobilized on magnetic beads. D – Western blotting for endogenous mortalin that was eluted from magnetic beads with immobilized fragments of AIF

confirm the hypothesis that AIF and mortalin interact with one another *in vivo*.

After obtaining the results demonstrating that AIF can interact with mortalin both *in vitro* and *in vivo*, we investigated alterations in the intensity of this interaction during apoptosis. For this reason, we first treated U87MG cells with cisplatin [$Pt(NH_3)_2Cl_2$], a drug widely used in the chemotherapy of many types of tumors. In order to determine the cisplatin concentration that causes apoptosis in most cells, we evaluated the effect of various amounts of this compound on cell viability by staining cells with a Alamar blue dye. As shown in *Fig. 3B*, 60 μM cisplatin was enough to induce apoptosis in the majority of the cells. Therefore, the cells were treated with 60 μM cisplatin for 24 h and lysed. The lysate was incubated with magnetic beads with immobilized recombinant mortalin. Lysate of normal cells not treated with cisplatin was used as a control. After the incubation and subsequent washing, the bound proteins were eluted and subjected to polyacrylamide gel electrophoresis. AIF was detected by Western blotting with primary antibodies specific to this protein. *Figure 3C* demonstrates that recombinant mortalin interacts with endogenous full-length AIF in normal cells, while the intensity of this interaction decreases noticeably once apoptosis is induced.

To further confirm our data, we performed proximity ligation assay (PLA) for mortalin and AIF using staurosporine, a widely known apoptosis inducer. During PLA, the fixed and permeabilized cells are incubated with two primary antibodies specific to the investigated proteins and a pair of oligonucleotide-conjugated secondary antibodies. If the oligonucleotides conjugated to different antibodies turn out to lie in appreciably close proximity to each other as happens during interaction of the target proteins, ad-

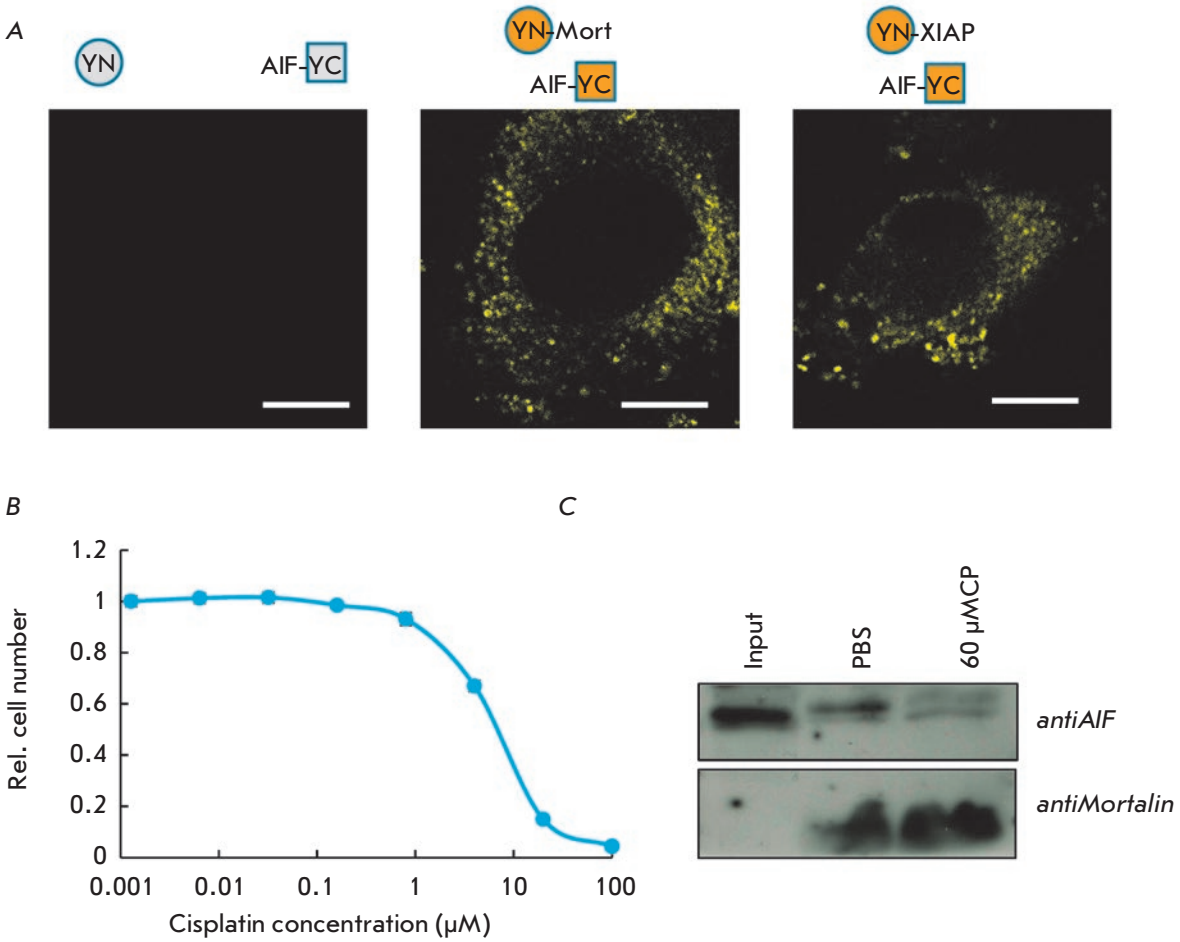

Fig. 3. AIF interacts with mortalin in living cells. A – YFP fluorescence in U87-MG cells coexpressing YC-AIF and YN (left panel), YN-Mort (middle panel) or YN-XIAP (right panel). B – Survival of U87-MG cells treated with different concentrations of cisplatin. C – Western blotting for endogenous AIF that was eluted from magnetic beads with immobilized recombinant mortalin. U87-MG cells treated or untreated with 60 μM of cisplatin were lysed and cell lysate was incubated with magnetic beads with immobilized mortalin. Bounded proteins were eluted and separated in gel. Recombinant mortalin was detected as a loading control

dition of DNA polymerase induces rolling circle DNA amplification on these nucleotides. Next, the cells are incubated with a fluorescently labeled oligonucleotide probe, which is annealed at the amplification sites of the respective DNA. Intracellular protein–protein interactions are eventually visualized as single-point fluorescent regions, with their number being proportional to the binding intensity of the analyzed proteins [23]. Similarly to the previous experiment, we measured the concentration of staurosporine causing apoptosis in most cells (*Fig. 4A*). Next, we used PLA to study the alterations in the intensity of interaction between endogenous AIF and mortalin after induction of apoptosis (*Figs. 4B* and *4C*). Our findings indicate that in apoptotic cells the intensity of mortalin–AIF interactions is significantly reduced ($p < 0.05$), which agrees well with the data obtained in the previous experiment.

According to the results described above, it is fair to assume that the elevated mortalin level in cancer cells may increase the intensity of the binding between AIF and the OMM, thus being responsible for the increased apoptosis resistance of cells and, therefore, a more aggressive tumor phenotype. We tested a possible association between mortalin expression and the survival rate of patients using the open-access Rembrandt

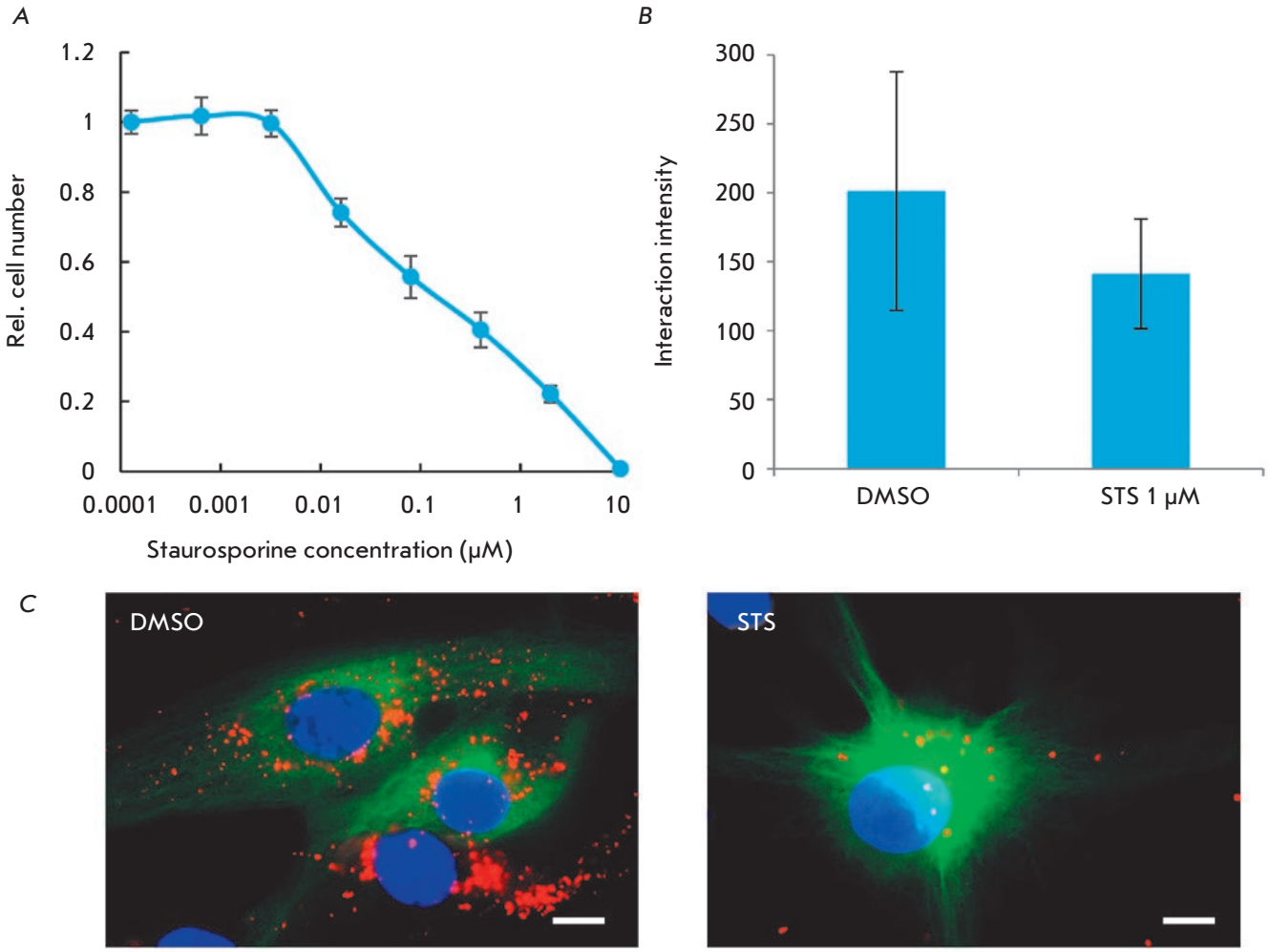

Fig. 4. AIF interacts with mortalin in fixed cells. A – Survival of U87-MG cells treated with different concentrations of staurosporine. B – Effect of staurosporine on Mortalin-AIF interaction intensity determined by PLA assay in U87-MG cells ($p < 0,05$). C – Visualization of Mortalin-AIF interaction by PLA assay in U87-MG cells treated with 1 μM staurosporine (STS) or DMSO as a control

database containing data on gene expression and the survival rates of patients with brain tumors. An analysis of this database (*Fig. 5*) demonstrated that a higher level of mortalin expression statistically significantly correlates with poor survival of glioma patients.

DISCUSSION

The caspase-independent apoptotic pathway consists of two stages. First, AIF is dissociated from the mitochondrial membrane. Next, cytoplasmic AIF is imported into the cell nucleus and activates DNA fragmentation. It is interesting that the second stage of this process (translocation of AIF into the nucleus) is inhibited by the Hsp70 protein, which is present in the cytoplasm and binds to the 150–228 a.a. of AIF [24]. We have demonstrated for the first time that another member of the family of heat shock proteins, mortalin, which binds to the 1–102 a.a. of AIF, is involved in the AIF–OMM interaction. Hence, it is fair to hypothesize that heat shock proteins are important inhibitors of the caspase-independent apoptotic pathway. Mortalin protein can anchor AIF to the OMM and impede apoptosis induction. However, if AIF is dissociated from the OMM, Hsp70 protein inhibits AIF translocation into the nucleus. This hypothesis agrees well with the recently published reports indicating that mortalin can

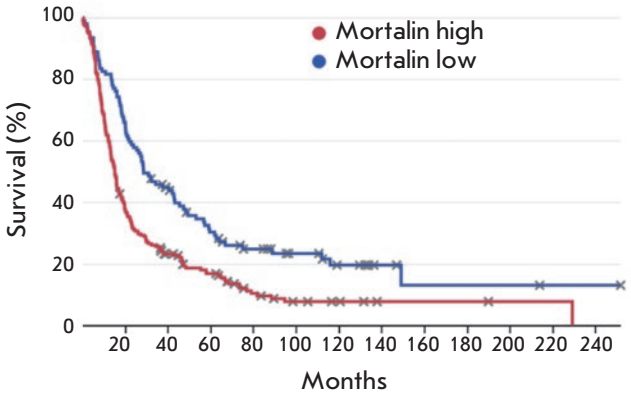

Fig. 5. Kaplan-Meier survival curve for patients with glioma divided into two groups based on mortalin expression level. Results were obtained by bioinformatic analysis of the Rembrandt database. p = 0,00002 (log-rank t-test)

hinder apoptosis by anchoring HIF1a, another essential protein that regulates cellular response to stress, to the outer surface of the OMM [21]. As proof for our findings, we demonstrated that elevated mortalin expression correlates with an aggressive phenotype of cancer and, therefore, is a poor prognostic factor for patients with brain tumors.

CONCLUSIONS

Although many studies have focused on the caspase-independent apoptotic pathway, the first and most important stage of this process (namely, AIF dissociation from the outer mitochondrial membrane) is still a riddle to be solved. Our findings demonstrate that mortalin protein is involved in the binding between AIF and the OMM. Additional experiments are needed to evaluate the contribution of this interaction to the localization of AIF to the OMM. However, our findings and the data published earlier provide grounds for assuming that when a cell is exposed to DNA-damaging agents, poly-ADP-ribose is produced in the nucleus and further translocated into the cytoplasm, where it binds to AIF [8, 16]. This interaction alters the conformation of AIF and makes it lose its ability to bind to mortalin, through which AIF is anchored to the OMM. As a result, AIF is dissociated from the OMM and translocated into the nucleus, where it causes a cascade of events, eventually leading to cell death. However, further research is needed to confirm the interaction between endogenous AIF and mortalin and to prove that specific inhibition of binding between these proteins will cause dissociation of AIF from the OMM and eventual cell death. ●

This work was supported by the Russian Foundation for Basic Research grants № 16-34-60136, 17-29-06056 and 18-29-01027.

REFERENCES

1. Reed J.C. // J Clin Oncol. 1999. V. 17. P. 2941–2953.
2. Kühtreiber W.M., Hayashi T., Dale E.A., Faustman D.L. // J. Mol. Endocrinol. 2003. V. 31. P. 373–399.
3. Cao G., Xing J., Xiao X., Liou A.K., Gao Y., Yin X.M., Clark R.S., Graham S.H., Chen J. // J. Neurosci. 2007. V. 27. P. 9278–9293.
4. Liu T., Biddle D., Hanks A.N., Brouha B., Yan H., Lee R.M., Leachman S.A., Grossman D. // J. Invest. Dermatol. 2006. V. 126. P. 2247–2256.
5. Mahmud H., Dälken B., Wels W.S. // Mol. Cancer Ther. 2009. V. 8. P. 1526–1535.
6. Galluzzi L., Joza N., Tasdemir E., Maiuri M.C., Hengartner M., Abrams J.M., Tavernarakis N., Penninger J., Madeo F., Kroemer G. // Cell Death Differ. 2008. V. 15. P. 1113–1123.
7. Choudhury S., Bae S., Ke Q., Lee J.Y., Kim J., Kang P.M. // Basic Res. Cardiol. 2011. V. 106. P. 397–407.
8. Wang Y., Kim N.S., Haince J.F., Kang H.C., David K.K., Andrabi S.A., Poirier G.G., Dawson V.L., Dawson T.M. // Sci. Signal. 2011. V. 4. № 167. P. ra20.
9. Cho B.B., Toledo-Pereyra L.H. // J. Invest. Surg. 2008. V. 21. P. 141–147.
10. Norberg E., Orrenius S., Zhivotovsky B. // Biochem. Biophys. Res. Commun. 2010. V. 396. P. 95–100.
11. Lorenzo H.K., Susin S.A., Penninger J., Kroemer G. // Cell Death Differ. 1999. V. 6. P. 516–524.
12. Brown D., Yu B.D., Joza N., Bénit P., Meneses J., Firpo M., Rustin P., Penninger J.M., Martin G.R. // Proc. Natl. Acad. Sci. U S A. 2006. V. 103. P. 9918–9923.
13. Baritaud M., Boujrad H., Lorenzo H.K., Krantic S., Susin S.A. // Cell Cycle. 2010. V. 9. P. 3166–3173.
14. Arnoult D., Parone P., Martinou J.C., Antonsson B., Estaquier J., Ameisen J.C. // J. Cell. Biol. 2002. V. 159. P. 923–929.
15. Yu S.W., Wang H., Poitras M.F., Coombs C., Bowers W.J., Federoff H.J., Poirier G.G., Dawson T.M., Dawson V.L. // Science. 2002. V. 297. P. 259–263.
16. Yu S.W., Wang H., Dawson T.M., Dawson V.L. // Neurobiol. Dis. 2003. V. 14. P. 303–317.
17. Parsons D.F., Williams G.R., Chance B. // Ann. N.Y. Acad. Sci. 1966. V. 137 P. 643–666.
18. Wilkinson J.C., Wilkinson A.S., Galbán S., Csomos R.A., Duckett C.S. // Mol. Cell. Biol. 2008. V. 28 P. 237–247.
19. Pavlyukov M.S., Antipova N.V., Balashova M.V., Vinogra-

dova T.V., Kopantzev E.P., Shakhparonov M.I. // J. Biol. Chem. 2011. V. 286. P. 23296–23307.
20. Yu S.W., Wang Y., Frydenlund D.S., Ottersen O.P., Dawson V.L., Dawson T.M. // ASN Neuro. 2009. V. 1(5). pii: e00021.
21. Mylonis I., Kourti M., Samiotaki M., Panayotou G., Simos G. // J. Cell. Sci. 2017. V. 130. P. 466–479.
22. Londono C., Osorio C., Gama V., Alzate O. // Biomolecules. 2012. V. 2. P. 1431–64.
23. Maszczak-Seneczko D., Sosicka P., Olczak T., Olczak M. // Methods Mol. Biol. 2016. V. 1496. P. 133–143.
24. Gurbuxani S., Schmitt E., Cande C., Parcellier A., Hammann A., Daugas E., Kouranti I., Spahr C., Pance A., Kroemer G., et al. // Oncogene. 2003. V. 22. P. 6669–6678.

Zinc Finger Protein CG9890 - New Component of ENY2-Containing Complexes of Drosophila

N. A. Fursova, J. V. Nikolenko, N. V. Soshnikova, M. Y. Mazina, N. E. Vorobyova, A. N. Krasnov*
*E-mail: krasnov@genebiology.ru
Institute of Gene Biology Russian Academy of Sciences, Vavilova Str., 34/5, Moscow, 119334, Russia

Received May 18, 2018; in final form September 28, 2018

ABSTRACT **In previous studies, we showed that the insulator protein Su(Hw) containing zinc finger domains interacts with the ENY2 protein and recruits the ENY2-containing complexes on Su(Hw)-dependent insulators, participating in the regulation of transcription and in the positioning of replication origins. Here, we found interaction between ENY2 and CG9890 protein, which also contains zinc finger domains. The interaction between ENY2 and CG9890 was confirmed. It was established that CG9890 protein is localized in the nucleus and interacts with the SAGA, ORC, dSWI/SNF, TFIID, and THO protein complexes.**

KEYWORDS **ENY2, CG9890, drosophila, immunoprecipitation, zinc fingers.**

ABBREVIATIONS **ENY2 – enhancer of yellow 2; C2H2 – zinc fingers of C2H2 type; SAGA – histone acetyltransferase complex; SWI/SNF – chromatin remodeler; AMEX – mRNA export complex; ORC – origin recognition complex.**

INTRODUCTION

In eukaryotes, the regulation of gene expression is a complex multi-factor process that can occur at several successive stages of transcription (initiation and elongation), mRNA processing, export of mRNP from the nucleus, and translation and folding of proteins [1]. The local chromatin structure, position of the gene relative to functional nuclear compartments and long-range interactions of regulatory elements represent an additional level of regulation of genetic processes in the context of the complex organization of the eukaryotic genome in the three-dimensional space of the nucleus [2–4]. The ENY2 protein is a multifunctional factor that is involved in various stages of gene expression [5–15]. Various cellular functions of ENY2 are defined by the activities of the protein complexes in which it is included. For example, ENY2 is a subunit of the SAGA deubiquitinating module, an important transcription coactivator in Drosophila [13, 16]. This complex possesses histone acetyltransferase activity. The modification introduced by it is recognized by the bromodomains of chromatin remodeling complexes of the SWI/SNF family, through which they are attracted to SAGA-regulated genes [17]. As a result of the active remodeling of the chromatin structure, local nucleosomes are removed or destabilized, which creates favorable conditions for the binding of RNA polymerase to the various transcription factors necessary for the regulation of transcription [18, 19]. In addition, ENY2 was found present in the AMEX complex, which interacts with nuclear pore complexes (NPC) and participates in the export of mRNA from the nucleus [14]. Being a shared component of these two complexes, ENY2 is responsible for the localization of part of the SAGA-regulated genes at the nuclear pore and thereby participates in the creation of local, transcriptionally active regions at the periphery of the nucleus. ENY2-dependent positioning of certain genetic loci near the NPC provides for a high rate of export of newly synthesized RNA, which is mandatory for responding to stress or hormonal signal. The engagement of the complexes involved in creating regions of locally open chromatin by the ENY2 protein plays an important role in providing for the barrier activity of Su(Hw)-dependent insulators [15]. In addition, Su(Hw) is the first protein of higher eukaryotes for which the role in the positioning of replication origins in the Drosophila genome has been demonstrated [20, 21]. The attraction of the SAGA and dSWI/SNF complexes to the binding sites of this protein leads to the formation of regions with low local nucleosome density, which contributes to the binding of the ORC complex responsible for the assembly of the pre-initiation replication complex. Apparently, ENY2-containing complexes are involved

not only in the regulation of gene expression, but are also important for transcription synchronization and replication during the cell cycle.

EXPERIMENTAL

Cell lines and transfection

The cell line *Drosophila melanogaster* S2 was used in the study. Cell transfection was performed using an Effectene Transfection Reagent (Qiagen), according to the manufacturer's protocol. The genetic construct used for transfection encoded the CG9890 protein, labeled with a 3×FLAG epitope.

Antibodies

The following antibodies were used: polyclonal rabbit antibodies to GCN5, Xmas-2, OSA, N-terminus of TBP, Thoc5, ORC2, ORC3, PB, Moira produced in our laboratory, and rabbit antibodies to ADA2b kindly provided by L. Tora α-CG9890 polyclonal antibodies were obtained from serum of a rabbit immunized with full-length CG9890 protein expressed in *Escherichia coli*. All rabbit antibodies were purified. The concentration of all antibodies obtained in the laboratory was about 1 mg/ml. We also used murine antibodies against lamin Dm0 (Developmental Studies Hybridoma Bank, University of Iowa, Department of Biological Sciences), antibodies to FLAG epitope (Sigma), as well as antibodies to FLAG epitope conjugated with horseradish peroxidase. Commercial antibodies were diluted 1 : 500, and the dilution of antibodies obtained in the laboratory was modified to obtain the optimal signal on a Western blot. Goat or donkey antibodies to rabbit and mouse immunoglobulins were used as secondary antibodies, recognizing both full-length immunoglobulins and those specific only to the light chains of the antibodies (dilution 1 : 5000). Secondary antibodies were conjugated with horseradish peroxidase. In addition, secondary Cy3 and AlexaFluor™ 488 antibodies were used for fluorescence microscopy (dilution 1 : 500).

Immunofluorescence microscopy of the D. melanogaster S2 cell line

The cells of a S2 line attached to coverslips were washed twice with 1×PBS, fixed with 3.7% PFA (pH 7.5) for 10 minutes, and washed with 1×PBS two times for 5 minutes, each. They were subsequently treated with a 0.2% Triton X-100 solution in 1×PBS for 5 min, washed with 1×PBS 2 times for 5 min, then incubated for 10 min in 3% non-fat dry milk diluted in 1×PBS. Primary antibodies were diluted in 3% milk/PBS, and the specimens were incubated with antibodies (1 h, room temperature, humid chamber). We used mouse antibodies against lamin Dm0 (Developmental Studies Hybridoma Bank, University of Iowa, Department of Biological Sciences) at a dilution of 1 : 5000, and polyclonal rabbit antibodies against CG9890 (dilution 1 : 1000). The specimen was washed 3 times for 5 minutes in 1×PBS and incubated with secondary antibodies for 1 h at room temperature in a humid chamber covered with foil. The following secondary antibodies were used: anti-rabbit IgG (H+L) antibodies conjugated to Cy3 (Amersham) and anti-mouse IgG antibodies conjugated to AlexaFluor 488 (Molecular Probes) at a dilution of 1 : 500. The foil-sealed specimen was washed 3 times for 5 minutes in 1×PBS and incubated with DAPI (dilution 1: 1000 dilution, Sigma) for 10 s. The specimen was washed for 5 min in 1×PBS. After drying, the cover glass was enclosed in a Tris-glycerol buffer (Vectashield) on a slide. The edges of the coverslip were lacquered to prevent the specimen from drying out and immersion getting inside of it. The specimen was examined immediately after preparation using a Leica light microscope. Lenses ×100 with immersion were used. Image processing was performed using the ImageJ software.

Immunoprecipitation

Cells were centrifuged for 5 min at 500*g* at +4°C to isolate the nuclei. The precipitate was washed with 1 ml of LB cyto 3 buffer (3 mM $MgCl_2$, 20 mM HEPES NaOH, pH 8.0) with addition of sodium butyrate (deacetylase inhibitor) to a final concentration of 20 mM. Repeated centrifugation was carried out under the same conditions, and the cell sediment was carefully re-suspended in 200 μl of LB cyto 3 buffer with the addition of sodium butyrate to a final concentration of 10 mM and a protease inhibitor (Protease Inhibitor Cocktail (PIC), Roche). The mixture was then incubated on ice for 15 minutes. After the centrifugation, the supernatant was discarded and only the nuclear fraction was subsequently used.

The nuclei sediment was dissolved in 500 μl MN III buffer (20 mM HEPES KOH, 3 mM $MgCl_2$, 0.1% NP40, 0.1 M KCl, pH 8.0) with addition of sodium butyrate to a final concentration of 20 mM (deacetylase inhibitor) and protease inhibitor (PIC, Roche). DNA was fragmented by treating the cells with ultrasound (2 times for 10 s, 1 minute break, average power of the device) on ice. After the re-suspension, the cells were incubated for 30 min with 2 units of DNase I on ice and centrifuged at 16,000 *g* for 20 min at +4°C.

Polyclonal antibodies to the CG9890 protein were used for coimmunoprecipitation, and serum immunoglobulins of an unimmunized rabbit were used as negative controls. Antibodies were immobilized on Mab-sepharose.

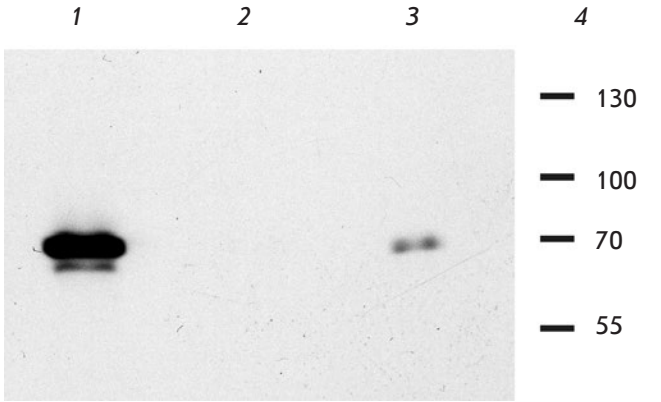

Fig. 1. Verification of the interaction between the ENY2 and CG9890 proteins. Western blot analysis of coimmunoprecipitation of ENY2 with the 3xFLAG-tagged CG9890 protein from transformed S2 cells. Affinity-purified rabbit antibodies against ENY2 and IgG from rabbit pre-immune serum (as negative control) were used in immunoprecipitation. Antibodies to 3xFLAG epitope (Sigma)were used in western blotting. *1* – input cell lysate, *2* – immunoprecipitation using non-specific antibodies, *3* – immunoprecipitation using anti-ENY2 antibodies, *4* – molecular weight marker

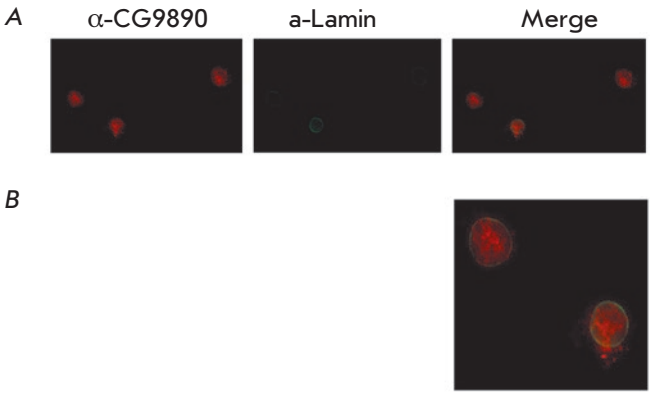

Fig. 2. Immunostaining of *Drosophila* S2 cells transfected with 3×FLAG CG9890. *A* – Affinity-purified rabbit antibodies against CG9890 (first panel) and mouse monoclonal antibodies against Lamin (second panel) were used for staining. Cy3, conjugated anti-rabbit, and Alexa 488 Fluor-conjugated anti-mouse antibodies were used as secondary antibodies. The third panel shows a merged image of the previous panels. *B* – A magnified image of part of the third panel

The lysate of S2 cells (200 ml) was incubated with 15 μl of 50% Mab-sepharose with antibodies immobilized on it for 3 hours on a shaker at +4 °C. Sepharose was washed with MN III buffer (3 times 10 min each) at +4 °C. Results were analyzed by Western blot.

RESULTS AND DISCUSSION

Analysis of the interaction of ENY2 with CG9890 proteins.

Earlier, in order to identify new protein partners of ENY2, the Drosophila cDNA library was screened in a two-hybrid yeast system. We have identified more than 10 interacting proteins, some of which have been studied [11–15, 20–22]. The screening revealed the interaction of ENY2 with a still uncharacterized protein, CG9890, which is the subject of this article. As predicted by the bioinformatics analysis of the amino acid sequence of CG9890, it belongs to the family of proteins bearing the zinc finger domain C2H2, the most common DNA binding motif in eukaryotes [23]. Proteins of this family are involved in various cellular functions, which is made possible by potential involvement of the zinc finger domain in specific recognition of not only DNA, but also RNA and proteins [24–26]. A genetic construct was created for the expression of the CG9890 protein labeled with a 3×FLAG epitope to confirm the interaction of ENY2 with CG9890 proteins. A *D. melanogaster* cell line S2 expressing this fusion protein was created and immunoprecipitated from a cell lysate using antibodies to the ENY2 protein and nonspecific antibodies as a negative control. The results of immunoprecipitation were analyzed using Western blotting and detected using antibodies to 3×FLAG epitope (Sigma). As seen in *Fig. 1*, antibodies to the ENY2 protein precipitate the 3×FLAG_CG9890 protein (lane *3*), while nonspecific antibodies do not (lane *2*). Therefore, interaction of the ENY2 and CG9890 proteins was confirmed.

For further study of CG9890, polyclonal antibodies to this protein were obtained and were affinity-purified on a column containing recombinant protein CG9890. Western blot analysis of the antibodies' specificity showed that these antibodies recognize a band in the region of 60 kDa, which is close to a calculated mass of the protein of 53 kDa (data not shown).

Study of the intracellular localization of the CG9890 protein

The intracellular localization of the CG9890 protein was determined using immunostaining of the Drosophila S2 cell line by the polyclonal antibodies that we have described. The results of the experiment are shown in *Fig. 2*. The analysis of a series of microphotographs showed that the CG9890 protein is localized predominantly in the cell nucleus, although some of it is present in the cytoplasm.

Analysis of interactions of the CG9890 protein with subunits of ENY2-containing complexes

Since interaction between the ENY2 and CG9890 proteins had been confirmed, it was suggested that CG9890 must be involved in some ENY2-dependent processes and that its interaction with individual ENY2 partners may determine the mechanism underlying its functioning in the cell. To test this hypothesis, it was decided to investigate which subunits of ENY2-containing complexes the CG9890 protein interacts with. For this purpose, an experiment was conducted on the immunoprecipitation of proteins from the lysate of S2 cells of *D. melanogaster* with α-CG9890 polyclonal antibodies, followed by Western blot analysis, and the results are presented in *Fig. 3*.

As a result of the experiments, interaction of the CG9890 protein with proteins that are part of various ENY2-containing complexes was revealed. In particular, it was shown to interact with the ORC2 and ORC3 subunits of the ORC complex, which is involved in the positioning of replication origins. We also identified interactions with such proteins involved in transcription regulation as TBP (subunit of the TFIID complex, functional partner ENY2), GCN5 (subunit of the histone acetyltransferase SAGA complex containing ENY2), and Thoc5 (subunit of the ENY2-containing THO complex involved in the formation of mRNP and transcription elongation). The fact of CG9890 interaction with the complexes involved in transcription is consistent with the data on the nuclear localization of this protein. We also identified interaction of CG9890 with the Polybromo (PB) protein, a subunit of the chromatin remodeling dSWI/SNF complex, which is necessary in the creation of an open chromatin region when the promoter is activated. Interaction with the Xmas-2 protein (AMEX complex) could not be demonstrated (data not shown). Thus, CG9890 interacts with the transcriptional complexes involved in the initiation and elongation of transcription, but not with the AMEX complex associated with the export of mRNA from the nucleus to the cytoplasm, which indicates involvement of CG9890 in the first stages of the transcription cycle.

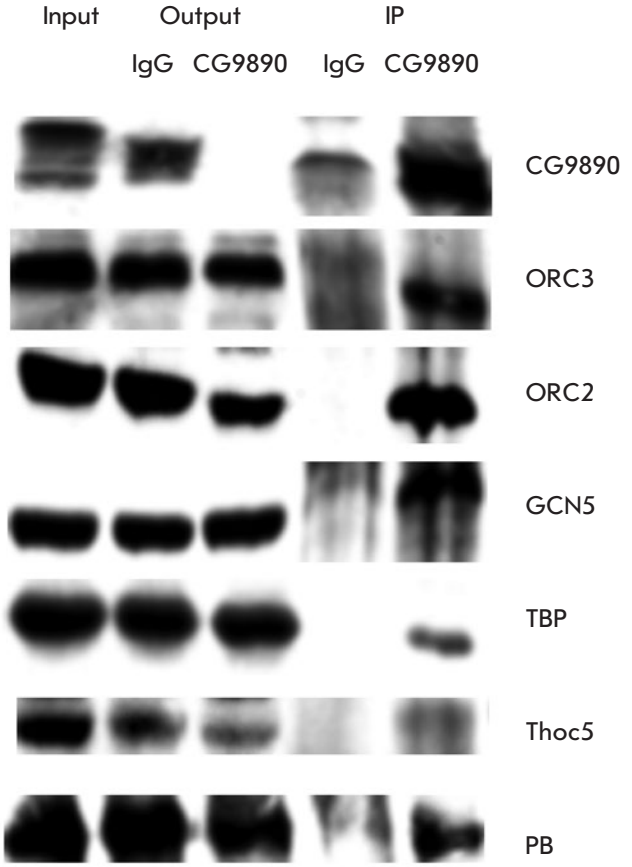

Fig. 3. Co-immunoprecipitation of CG9890 with subunits of ENY2-containing complexes. Affinity-purified rabbit antibodies against CG9890 and IgG from rabbit pre-immune serum (as negative control) were used in immunoprecipitation. Input – 2.5% of input cell lysate; Output–unbound fraction of lysate after incubation with nonspecific antibodies (IgG) or antibodies against CG9890; IP – 10% of elution fraction from the immunosorbent (IgG or CG9890). The presence of the subunits of ENY2-containing complexes was detected by western blot analysis using corresponding antibodies (shown on the right)

CONCLUSION

In previous studies, we discovered that insulator protein Su(Hw) containing zinc finger domains interacts with ENY2 protein and recruits the ENY2-containing complexes on Su(Hw)-dependent insulators, participating in the regulation of transcription and in the positioning of the replication origins. Here, we established interaction of ENY2 with another protein, CG9890, which, like Su(Hw), contains zinc finger domains. By analogy with Su(Hw), we assume that CG9890 is a DNA-binding protein that attracts ENY2-containing complexes to its binding sites, therefore arranging the regulatory elements of the genome necessary for the functioning of the cell. We have shown that the CG9890 protein is localized in the cell nucleus. Interaction of ENY2 and CG9890 was confirmed. Biochemical methods were used to identify the binding between the CG9890 protein and the ENY2-containing SAGA, ORC, dSWI/SNF, TFIID, and THOC complexes. Interaction with the Xmas-2 protein (AMEX complex) could not be shown. Thus, CG9890 interacts with the complexes in-

volved in the initiation and elongation of transcription, but not with the AMEX complex involved in the export of mRNA from the nucleus to the cytoplasm, which indicates the 'contribution' of CG9890 to the first stages of the transcription cycle. In addition, CG9890 interacts with the ORC complex, which is necessary for the positioning of the replication start points. ●

This work was supported by the Russian Foundation for Basic Research, grant No. 17-04-02193.

REFERENCES

1. Orphanides G., Reinberg D. // Cell. 2002. V. 108. № 4. P. 439–451.
2. Maksimenko O., Georgiev P. // Front. Genet. 2014. V. 5. P. 28.
3. van Bemmel J.G., Pagie L., Braunschweig U., Brugman W., Meuleman W., Kerkhoven R.M., van Steensel B. // PLoS One. 2010. V. 5. № 11. P. e15013.
4. Rando O.J., Chang H.Y. // Annu. Rev. Biochem. 2009. V. 78. P. 245–271.
5. Mardanov P.V., Krasnov A.N., Kurshakova M.M., Nabirochkina E.N., Georgieva S.G. // Genetika. 2005. V. 41. № 4. P. 536–541.
6. Krasnov A.N., Kurshakova M.M., Ramensky V.E., Mardanov P.V., Nabirochkina E.N., Georgieva S.G. // Nucl. Acids Res. 2005. V. 33. № 20. P. 6654–6661.
7. Georgieva S.G., Nabirochkina E.N., Pustovoitov M.V., Krasnov A.N., Soldatov A.V. // Genetika. 2001. V. 37. № 1. P. 18–23.
8. Orlova A.V., Kopytova D.V., Krasnov A.N., Nabirochkina E.N., Ilyin Y.V., Georgieva S.G., Shidlovskii Y.V. // Dokl. Biochem. Biophys. 2010. V. 434. P. 227–231.
9. Kopytova D.V., Orlova A.V., Krasnov A.N., Gurskiy D.Y., Nikolenko J.V., Nabirochkina E.N., Shidlovskii Y.V., Georgieva S.G. // Genes Dev. 2010. V. 24. № 1. P. 86–96.
10. Kopytova D.V., Krasnov A.N., Orlova A.V., Gurskiy D.Y., Nabirochkina E.N., Georgieva S.G., Shidlovskii Y.V. // Cell Cycle. 2010. V. 9. № 3. P. 479–481.
11. Kurshakova M.M., Kopytova D.V., Nabirochkina E.N., Soshnikova N.V., Georgieva S.G., Krasnov A.N. // Genetika. 2009. V. 45. № 3. P. 330–335.
12. Kurshakova M.M., Kopytova D.V., Nabirochkina E.N., NikolenkoIu V., ShidlovskiiIu V., Georgieva S.G., Krasnov A.N. // Genetika. 2009. V. 45. № 10. P. 1332–1340.
13. Zhao Y., Lang G., Ito S., Bonnet J., Metzger E., Sawatsubashi S., Suzuki E., Le Guezennec X., Stunnenberg H.G., Krasnov A., et al. // Mol. Cell. 2008. V. 29. № 1. P. 92–101.
14. Kurshakova M.M., Krasnov A.N., Kopytova D.V., Shidlovskii Y.V., Nikolenko J.V., Nabirochkina E.N., Spehner D., Schultz P., Tora L., Georgieva S.G. // EMBO J. 2007. V. 26. № 24. P. 4956–4965.
15. Kurshakova M., Maksimenko O., Golovnin A., Pulina M., Georgieva S., Georgiev P., Krasnov A. // Mol. Cell. 2007. V. 27. № 2. P. 332–338.
16. Helmlinger D., Tora L. // Trends Biochem. Sci. 2017. V. 42. № 11. P. 850–861.
17. Baker S.P., Grant P.A. // Oncogene. 2007. V. 26. № 37. P. 5329–5340.
18. Mazina M.Y., Nikolenko Y.V., Krasnov A.N., Vorobyeva N.E. // Genetika. 2016. V. 52. № 2. P. 164–169.
19. Krasnov A.N., Mazina M.Y., Nikolenko J.V., Vorobyeva N.E. // Cell Biosci. 2016. V. 6. P. 15.
20. Vorobyeva N.E., Mazina M.U., Golovnin A.K., Kopytova D.V., Gurskiy D.Y., Nabirochkina E.N., Georgieva S.G., Georgiev P.G., Krasnov A.N. // Nucl. Acids Res. 2013. V. 41. № 11. P. 5717–5730.
21. Mazina M., Vorob'eva N.E., Krasnov A.N. // Tsitologiia. 2013. V. 55. № 4. P. 218–224.
22. Krasnov A.N., Vorobyova N.E., Mazina M.Y. // Dokl. Biochem. Biophys. 2018. V. 479. № 1. P. 80–82.
23. Razin S.V., Borunova V.V., Maksimenko O.G., Kantidze O.L. // Biochemistry (Mosc.). 2012. V. 77. № 3. P. 217–226.
24. Brayer K.J., Segal D.J. // Cell Biochem. Biophys. 2008. V. 50. № 3. P. 111–131.
25. Brown R.S. // Curr. Opin. Struct. Biol. 2005. V. 15. № 1. P. 94–98.
26. Fedotova A.A., Bonchuk A.N., Mogila V.A., Georgiev P.G. // Acta Naturae. 2017. V. 9. № 2. P. 47–58.

Tag7-Mts1 Complex Induces Lymphocytes Migration via CCR5 and CXCR3 Receptors

T. N. Sharapova, E. A. Romanova, L. P. Sashchenko, D. V. Yashin*
Institute of Gene Biology of the Russian Academy of Sciences, Vavilova Str., 34/5, Moscow, 119334, Russia
*E-mail: yashin_co@mail.ru
Received August 02, 2018; in final form October 02, 2018

ABSTRACT **The discovery of new chemokines that induce the migration of lymphocytes to the infection site is important for the targeted search for therapeutic agents in immunotherapy. We recently showed that Tag7 (PGLYRP1), an innate immunity protein, forms a stable complex with the Ca^{2+} -binding protein Mts1 (S100A4), which is able to induce lymphocyte movement, although the individual Tag7 and Mts1 do not have this activity. The purpose of this study is to identify receptors that induce the migration of lymphocytes along the concentration gradient of the Tag7-Mts1 complex, and the components of this complex capable of interacting with these receptors. The study investigated the migration of human PBMC under the action of the Tag7-Mts1complex. PBMC of healthy donors were isolated using a standard Ficoll-Hypaque gradient centrifugation procedure. It has been established that the movement of PBMC along the concentration gradient of the Tag7-Mts1 complex is induced by the classical chemotactic receptors CCR5 and CXCR3. It has been shown that only Mts1 is able to bind to the extracellular domain of CCR5, however, this binding is not enough to induce cell movement. A comparative analysis of the primary and 3D structures of the three proteins revealed the homology of the amino acid sequence fragments of the Tag7-Mts1 protein complex with different sites of the CCR5 receptor ligand - MIP1α protein. In conclusion, it should be noted that the Tag7-Mts1 complex can be considered as a new ligand of the classical chemotactic receptors CCR5 and CXCR3.**
KEYWORDS **Chemotaxis, chemokine, chemoreceptor, Tag7-Mts1 complex.**
ABBREVIATIONS **PBMC – peripheral blood mononuclear cells; HLA – human lymphocyte antigen; CCR5 and CXCR3 – chemoreceptors; TNFR1 – tumor necrosis factor receptor; TNFα – tumor necrosis factor; Tag7 (PGLYRP1) – an innate immunity protein; Mts1 (S100A4) – Ca^{2+} -binding protein; MIP1α – macrophage inflammatory protein, chemokine; NK – natural killers; PMSF – *p*-phenylmethylsulfonyl fluoride.**

INTRODUCTION

At least two stages are required for the development of the immune response: activation of effector lymphocytes capable of killing foreign cells, and their delivery to the affected area. Therefore, in order to understand the processes of immune protection, one should understand both cytotoxic and chemotactic mechanisms [1]. The search for new stimulators of cytotoxicity and chemotoxicity is also important.

Cytokines that cause lymphocyte migration are called chemokines. One of the peculiarities of chemokines structure is characteristic disulfide bonds. Depending on the relative position of the first two N-terminal cysteine residues, chemokines are divided into four classes (CC, C, CXC, CX_3C) [2]. Induction of chemotaxis occurs through interaction with specific chemotactic receptors. These receptors belong to a large group of transmembrane G-protein-coupled receptors [3]. The interaction of the chemokine with the receptor causes the dissociation of the β-, γ-subunits of the G-protein, which leads to the activation of the protein kinase cascade and an increase in the concentration of Ca^{2+} ions [4, 5].

The second structural feature of chemokines is their small molecular weight (from 8–10 kDa) [6]; however, there are stimulators of lymphocytes migration with both higher and lower molecular weight [7]. Recently, we have shown that the migration of lymphocytes can be caused by a complex of two proteins: Tag7 and Mts1 [8].

Mts1 (S100A4) belongs to the family of Ca^{2+}-binding proteins. It is known to be involved in the process of tumor cells metastasis [9–12]. At the same time, its gene is actively expressed in cells of the immune system involved in antitumor activity. Previously we have demonstrated that Mts1 on the surface of CD4+ lymphocytes is involved in the recognition of HLA-negative tumor cells and promotes their lysis [13].

Tag7 protein (PGLYRP1), whose gene was discovered at our institute, is a protein of the innate immunity system that participates both in antibacterial and antitumor activity [14–16]. Like cytokines, Tag7 can activate lymphocyte cytotoxicity. In combination with the main heat shock protein, Tag7 has a cytotoxic effect on TNFR1-bearing tumor cells and inhibits tumor growth [17, 18]. It can interact with the Mts1 protein with the formation of a stable chemoattractant complex, causing the migration of lymphocytes. Taken separately, neither Mts1 nor Tag7 possess such activity [8]. Therefore, it is interesting to find out why chemotactic activity appears only after the formation of the complex.

The purpose of this study is to identify receptors that induce the migration of cells along the concentration gradient of Tag7-Mts1 and the protein of this two-component complex capable of interacting with these receptors.

EXPERIMENTAL

Proteins

Recombinant proteins Mts1 (S100A4) and Tag7 (PGLYRP1) were expressed in *Escherichia coli* M15 strain [pREP4] (Qiagen, USA) carrying pQE-30 plasmid (Qiagen, USA). cDNAs of Tag7 or Mts1 protein were previously cloned into pQE-30 plasmid. Mts1 was purified on Ni-NTA-agarose (Qiagen, USA) according to the manufacturer's protocol. Tag7 was isolated and purified as described in [19].

Comparison of the primary and spatial structures of proteins was performed using https://blast.ncbi.nlm.nih.gov/ and https://ncbi.nlm.nih.gov/ database.

Cell cultures

We used peripheral blood mononuclear cells (PBMCs) obtained from the leukomass of healthy donors by sequential Ficoll-Hypaque gradient centrifugation (GE Healthcare, Sweden) as described in [20].

Flow cytofluorometry

Cells were fixed in 4% formaldehyde (Sigma) and incubated with antibodies to CCR5 and CXCR3 (Abcam, United Kingdom) overnight, and then with anti-rabbit IgG-PE (Beckman coulter, USA) in the dark at 40 °C for 2 hours. At least 10^4 cells were analyzed in each sample. The measurements were performed on a Cytomics FC 500 MPL flow cytometer (Beckman coulter, USA), data were processed in EXPO32 software (Applied Cytometry Systems, Sheffield, UK).

Analysis of chemotactic activity

A Boyden chamber (Costar Corning Inc., USA) was used to measure the chemotactic activity. 200×10^3 PBMC cells were added to its upper part and a chemoattractant at a concentration of 10^{-9} M in RPMI 1640 medium (Gibco, USA) was added to the lower part. MTT test (Sigma, United States) was used to measure the number of cells that passed through the membrane after 1.5 h. In the case of preincubation, antibodies (at a dilution of 1:1000) or proteins (Tag7, Mts1 at a concentration of 10^{-8} M) were added to PBMC and incubated for 1 hour at 37 °C, 5% CO_2, and then washed twice with the medium. Unless stated otherwise, all diagrams are based on at least three independent experiments. Bilateral ANOVA was used for statistical processing.

Chemoreceptor detection

PBMC cells (~ 250 mln) were suspended in 1.5 ml of solubilization buffer: 50 mM Tris, pH 7.5 with PMSF (Sigma, USA) (1 mM) and a protease inhibitor cocktail (Calbiochem, Germany) at a concentration specified by the manufacturer, and Triton X-100 detergent (Sigma, USA) (1% by volume). After incubation for 30 minutes on ice on a shaker, the resulting suspension was diluted 10 times by adding solubilizing buffer free from detergents, and centrifuged at 185,000 *g* (Beckman L7 Ultracentrifuge, USA) for 1 h at 4 °C. The supernatant was collected and applied to a Br-CN-Sepharose column with conjugated Mts1. Bound proteins were separated using 12% SDS-PAGE, transferred to a nitrocellulose membrane and detected by Western blot with specific antibodies to CCR5 and CXCR3 (1:1000) and secondary anti-rabbit antibodies (1:10,000), conjugated with horseradish peroxidase, and stained with the ECL Plus kit (Amersham, UK) according to the manufacturer's recommendations.

RESULTS

CCR5 and CXCR3 chemotactic receptors induce the movement of lymphocytes along the concentration gradient of the Tag7–Mts1 complex

At the first stage of the study, we identified the receptors involved in the transmission of the chemotactic signal from the new chemokine described by us, the Tag7–Mts1 complex. Earlier, we had demonstrated that this complex can direct the movement of T-lymphocytes and NK-cells [8]. Therefore, we evaluated the presence of chemotactic receptors CCR5 and CXCR3 on PBMCs, which are most densely present on the surface of T-lymphocytes and NK cells.

Using flow cytofluorometry and highly specific antibodies, we showed that the studied PBMC populations contain 54.8% of the cells that carry CCR5 receptor on their surface and that the cells expressing CXCR3 constitute 58.1% of the total PBMC population: i.e., both receptors are present on PBMCs *(Fig. 1A)*.

We further examined whether these receptors are involved in the induction of lymphocyte migration along the concentration gradient of the Tag7–Mts1 complex. For this purpose, PBMCs were incubated with antibodies to CCR5 or CXCR3 and the movement of these cells under the action of the Tag7–Mts1 complex was investigated *(Fig. 1B)*. Unlike Tag7 and Mts1 proteins separately, the Tag7–Mts1 complex causes the movement of PBMCs. Preincubation with CCR5 antibodies almost completely abolishes chemotaxis. However, CXCR3 antibodies reduced the migration of PBMCs by no more than 20%. Therefore, both studied receptors can induce cell movement along the concentration gradient of the Tag7–Mts1 complex but they display different affinity for this complex. The stronger inhibition of cell movement by antibodies to CCR5 suggests that the spatial structure of the functional regions of the Tag7–Mts1 complex involved in interaction with CCR5 is more similar to the spatial structure of the CC-chemokines regions, ligands of the CCR5 receptor which are responsible for interaction in the complex.

Mts1 can bind to chemotactic receptors

Next, we determined which of the proteins of the two-component complex can interact with the receptors. We preincubated the PBMC with Tag7 or Mts1 and examined the migration of such cells under the action of the Tag7–Mts1 complex. The results of five independent experiments without averaging are presented on *Fig. 2A*. In four cases preincubation with Tag7 has virtually no effect on cell motility, whereas preincubation with Mts1 dramatically reduces the movement of PBMCs. The observed abnormalities may depend on the immune status of the donor. The similarity of observed effects in four cases suggests that Mts1 can bind to the receptor.

To test this assumption, we studied the possibility of binding of CCR5 and CXCR3 to Mts1 using affinity chromatography. Solubilized PBMC membrane proteins were applied to a column with Mts1 immobilized on Br-CN-sepharose, and the specifically bound material was analyzed using 12% SDS-PAGE followed by Western blot *(Fig. 2B)*. Antibodies to CCR5 revealed a 41 kDa protein, and antibodies to CXCR3, a 70 kDa protein corresponding in molecular weight to these receptors. We can see weaker binding of CXCR3 to Mts1, which confirms the assumption of higher affinity of the chemoattractant Tag7–Mts1 complex to the CCR5 receptor.

Thus, Mts1 can bind to the CCR5 receptor, but this is not enough to induce cell movement. However, by interacting with CCR5, it prevents the binding of a two-component chemoattractant with it and inhibits the movement of cells along the concentration gradient of the Tag7–Mts1 complex.

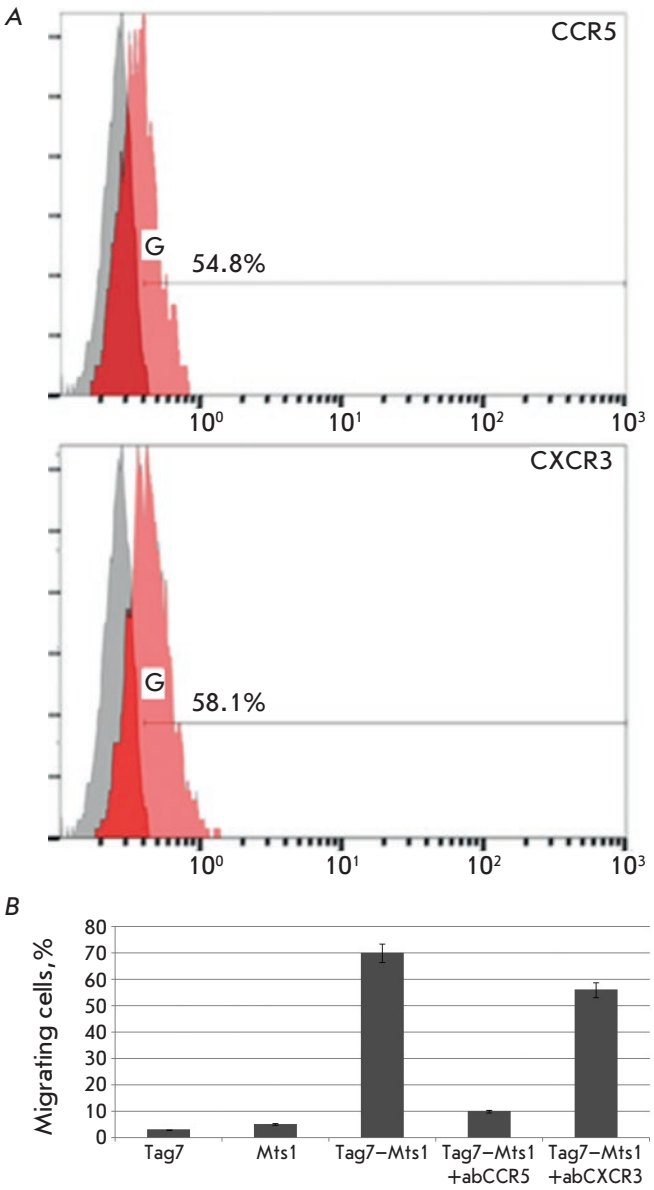

Fig. 1. The chemotaxis of PBMC under the action of Tag7-Mts1 is achieved through interaction with CCR5 and CXCR3 receptors. *(A)* Expression of CCR5 and CXCR3 on the surface of mononuclear cells. The number of events is plotted on the abscissa axis, and the average fluorescence intensity is plotted on the ordinate axis. Gray peak – isotypic control by secondary antibodies. *(B)* Antibodies to CCR5 and CXCR3 receptors block the chemotactic activity of PBMCs

The primary and spatial structures of Tag7 and Mts1 fragments have partial homology with the structures of MIP1α fragments

As already mentioned, none of the proteins in the Tag7–Mts1 complex has a standard chemokine structure referred to as a "Greek key." Therefore, we com-

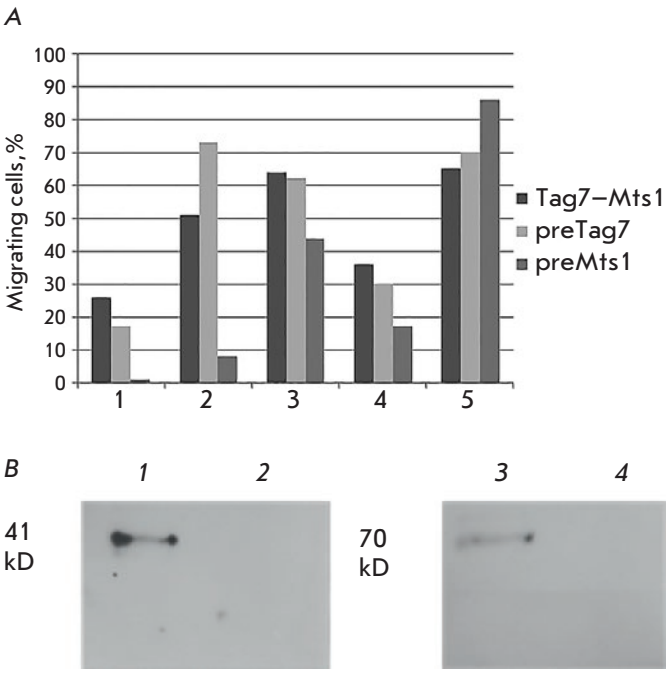

Fig. 2. Mts1 can bind to CCR5 and inhibit chemotaxis activity. *(A)* Mts1 is able to block the PBMC chemotaxis. The abscissa axis presents the results of chemotaxis from 5 different donors. *(B)* Mts1 binds to CCR5 and CXCR3 receptors. The proteins (*1*, *3*) interacting with Mts1 and unbound material (*2*, *4*) were stained with specific antibodies to CCR5 (*1* and *2*) and CXCR3 (*3* and *4*)

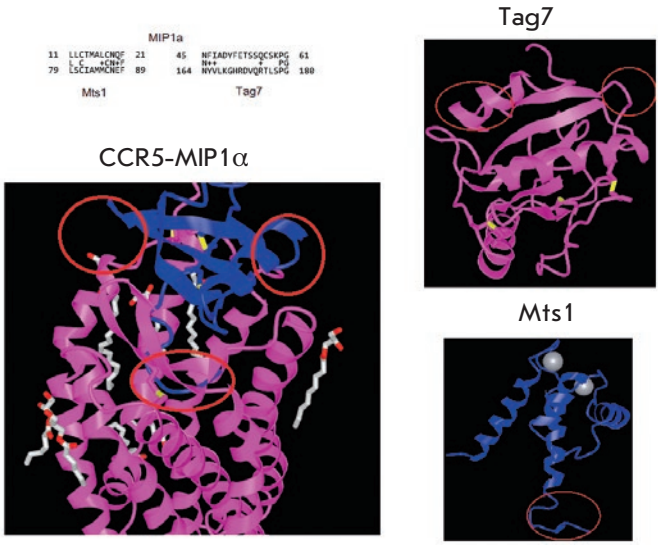

Fig. 3. Homologous amino acid sequences and 3D structures of the Mts1, Tag7 and MIP1α proteins. In the upper left corner there is a superposition of homologous fragments of the amino acid sequences of the proteins MIP1α (above), Mts1 and Tag7 (below). On 3D models of the MIP1a complex (blue, left) with CCR5 (pink, left), and Tag7 proteins (pink, right) and Mts1 (blue, right) red areas show homology sequences of amino acid sequences

pared the primary and spatial structures of Mts1 and Tag7 proteins and MIP1α, the known functional ligand of the CCR5 receptor.

A comparative analysis of the amino acid sequences of the three proteins revealed the homology of the Mts1 and Tag7 molecules fragments with some regions of MIP1α. The result of comparing fragments of amino acid sequences is presented in *Fig. 3* (top left). In the C-terminal part, Mts1 has an 11-membered fragment (amino acid residues 79–89), 65% homologous to an 11-membered N-terminal fragment of MIP1α (amino acid residues 11–21). Tag7 has a 17-membered fragment (amino acid residues 164–180) in the central part of the molecule, which is homologous to the MIP1α fragment (amino acid residues 45–61), also located in the middle of the polypeptide chain.

Figure 3 shows the spatial structures of the MIP1α complex with CCR5 [21] and the spatial structures of Tag7 [19] and Mts1 [22]; the coordinates of the spatial structures in PDB ID: 5UIW, 1YCK, 3C1V, respectively. The comparison of the spatial structures of the Mts1 and Tag7 proteins with the structure of MIP1α make it obvious that the C-terminal region of Mts1 (amino acid residues 79–89) is an α-helix protruding from the central globular part of the molecule. In the chemokine MIP1α, the N-terminal region (amino acid residues 11–21) also protrudes far from the central part of the molecule. Both sites have five hydrophobic amino acids. Tag7 fragments (amino acid residues 164–180) and MIP1α (amino acid residues 45–61) are β-sheets located on the surface of the molecules in both proteins. Homologous amino acids (residues 164–166 and 179–180) are located in the region that is involved in direct interaction with the CCR5 receptor in MIP1α (residues 45–47 and 60–61).

None of the proteins in the Tag7–Mts1 complex possesses the spatial structure of a chemokine, however, both Mts1 and Tag7 contain regions homologous in their amino acid and spatial structures to the MIP1α chemokine sites important for activation of the CCR5 receptor. It may be the reason why Tag7 and Mts1 taken individually do not possess chemoattractant activity, and only the stable two-component complex of these proteins can initiate the migration of lymphocytes.

DISCUSSION

The presented data allow us to make two conclusions. CCR5 and CXCR3 chemotactic receptors are involved

in the induction of PBMCs migration along the concentration gradient of the Tag7–Mts1 complex. One of the components of this complex, Mts1 protein, can bind to both receptors.

Different binding specificities of the Tag7–Mts1 complex with these receptors should be noted. The studied complex rather weakly interacts with the CXCR3 receptor: no more than 20% of CXCR3-containing PBMCs migrate along the Tag7–Mts1 concentration gradient. At the same time, almost all populations of PBMC carrying CCR5 can move under the influence of this chemoattractant.

CCR5 is present, as a rule, on memory cells, macrophages and dendritic cells. Recently, it has been shown to be present on the cell surface of NK cell subpopulations [23]. Based on a set of cells carrying CCR5, it can be assumed that the Tag7–Mts1 complex can attract cells of the immune system mainly in the early stages of the immune response.

We have demonstrated that preincubation of cells with Tag7 protein does not inhibit cell migration under the action of the Tag7–Mts1 complex. The interaction between Tag7 and the chemotactic receptor is probably much weaker than that of the Tag7–Mts1 complex. Tag7 also does not contain a hydrophobic fragment in the polypeptide chain capable of binding to the transmembrane active center of the receptor.

In contrast, Mts1 can bind to CCR5 receptor and inhibit the movement of PBMCs, although no similarities are found in the amino acid and spatial structures of the central region of the Mts1 and MIP1α molecules. The mechanism of such binding requires further study [19, 21, 22].

We have recently obtained similar results in a study of interaction of the Tag7–Hsp70 cytotoxic complex with the receptor of the well-known TNFα cytokine, TNFR1. Tag7 bound to TNFR1 and inhibited the cytotoxic effect of TNFα [24] but did not have the homology of the primary and three-dimensional structures with TNFα.

A detailed study of the mechanism of interaction of CCR5 with the ligand allowed us to propose a hypothetical pattern of contacts between this receptor and ligands [25]. According to this scheme, the interaction of the chemokine receptor with the ligand is a two-step process. In the first stage, the central part of the chemokine molecule interacts with the receptor binding center, located on the extracellular domain. Then, the interaction of the N-terminal of the chemokine with the second binding site located in the bundle of transmembrane helices is required for the activation of the receptor.

Notably, Mts1 itself cannot induce cell migration, although it has a hydrophobic fragment (amino acid residues 79–89) homologous to the MIP1α fragment (amino acid residues 11–21), which induces a change in the conformation of the receptor. Considering the differences in the spatial structure of Mts1 and in the structure of a classical chemokine, it can be assumed that after binding to the extracellular domain in the first stage of the interaction of Mts1 with the CCR5 receptor, the C-terminal fragment of Mts1 cannot penetrate into the cell membrane [22]. Interaction with Tag7 may change the conformation of Mts1, providing access of the C-terminal region to the active center in the transmembrane bundle. Such a hypothetical scheme can explain why only the Tag7–Mts1 complex can cause migration of PBMCs.

Apparently, the two-stage interaction of ligands with receptors is a common property of receptors of different nature. First, the ligand is fixed on the surface of the receptor, then it is activated. Earlier, we studied the interaction of the Tag7–Hsp70 two-component complex with the TNFR1 receptor and identified the functional activity of each protein. We have demonstrated that Tag7 can bind to TNFR1 but is not capable of causing aggregation of its cytoplasmic domains, which is necessary for the induction of cytolysis. Hsp70, which can aggregate in solution, binds to Tag7 and trimerizes the receptor.

It is possible that Mts1 can bind to other receptors on the surface of T-lymphocytes and NK cells and, in combination with Tag7, induce the migration of these cells. However, this issue requires further study.

CONCLUSION

In conclusion, it should be noted that as a result of the studies performed, the chemotactic complex Tag7–Mts1 can be considered a new ligand of the chemotactic receptors CCR5 and CXCR3, which are present on the cells of the immune system. Although none of the proteins of this ligand has the structural motive of a classic chemokine, Tag7–Mts1 can induce the migration of PBMCs with the involvement of classical chemokine receptors and shows greater affinity for CCR5. It has also been shown that Mts1, one of the proteins of the two-component complex, can bind to the extracellular domain of CCR5; however, additional interaction of Tag7 with its extracellular region is required for receptor activation. Understanding the processes underlying the interaction of a nonclassical chemokine with a classical chemotactic receptor will help understand the mechanisms of migration of immune system cells to the affected area and the search for new chemokines. ●

This work was supported by the grant of the Russian Science Foundation No. 15-14-00031-P.

REFERENCES

1. Bryant V.L., Slade C.A. // Immunol. Cell Biol. 2015. V. 93. № 4. P. 364–371.
2. Zlotnik A., Yoshie O. // Immunity. 2000. V. 12. № 2. P. 121–127.
3. Miller A.F., Falke J.J. // Adv. Protein Chem. 2004. V. 68. P. 393–444.
4. Bachelerie F., Ben-Baruch A., Burkhardt A.M., Combadiere C., Farber J.M., Graham G.J., Horuk R., Sparre-Ulrich A.H., Locati M., Luster A.D., et al. // Pharmacol Rev. 2014. V. 66. № 1. P. 1–79.
5. Jin T. // Curr. Opin. Cell Biol. 2013. V. 25. № 5. P. 532–537.
6. Palomino D.C.T., Marti L.C.// Einstein (Sao Paulo). 2015. V. 13. № 3. P. 469–473.
7. Rossi D., Zlotnik A. //Annu. Rev. Immunol. 2000. V. 18. P. 217–242.
8. Dukhanina E.A., Lukyanova T.I., Romanova E.A., Guerriero V., Gnuchev N.V., Georgiev G.P., Yashin D.V., Sashchenko L.P. // Cell Cycle. 2015. V. 14. № 22. P. 3635–3643.
9. Ambartsumian N.S., Grigorian M.S., Larsen I.F., Karlstrøm O., Sidenius N., Rygaard J., Georgiev G., Lukanidin E. // Oncogene. 1996. V. 13. № 8. P. 1621–1630.
10. Garrett S.C., Varney K.M., Weber D.J., Bresnick A.R. // J. Biol. Chem. 2006. V. 281. № 2. P. 677–680.
11. Grigorian M.S., Tulchinsky E.M., Zain S., Ebralidze A.K., Kramerov D.A., Kriajevska M.V., Georgiev G.P., Lukanidin E.M. // Gene. 1993. V. 135. № 1–2. P. 229–238.
12. Tarabykina S., Griffiths T.R.L., Tulchinsky E., Mellon J.K., Bronstein I.B., Kriajevska M. // Curr. Cancer Drug Targets. 2007. V. 7. № 3. P. 217–228.
13. Dukhanina E.A., Kabanova O.D., Lukyanova T.I., Shatalov Y.V., Yashin D.V., Romanova E.A., Gnuchev N.V., Galkin A.V., Georgiev G.P., Sashchenko L.P. // Proc. Natl. Acad. Sci. USA. 2009. V. 106. № 33. P. 13963–13967.
14. Kustikova O.S., Kiselev S.L., Borodulina O.R., Senin V.M., Afanas'eva A.V., Kabishev A.A. // Genetika. 1996. V. 32. № 5. P. 621–628.
15. Michel T., Reichhart J.M., Hoffmann J.A., Royet J. // Nature. 2001. V. 414. № 6865. P. 756–759.
16. Larin S.S., Korobko E.V., Kustikova O.S., Borodulina O.R., Raikhlin N.T., Brisgalov I.P., Georgiev G.P., Kiselev S.L. // J. Gene Med. 2004. V. 6. № 7. P. 798–808.
17. Sashchenko L.P., Dukhanina E.A., Yashin D.V., Shatalov Y.V., Romanova E.A., Korobko E.V., Demin A.V., Lukyanova T.I., Kabanova O.D., Khaidukov S.V., et al. // J. Biol. Chem. 2004. V. 279. № 3. P. 2117–2124.
18. Dukhanina EA, Yashin DV, Lukjanova TI, Romanova EA, Kabanova OD, Shatalov YV, Sashchenko LP, Gnuchev NV. // Dokl Biol Sci. 2007. V. 414 № 2. P. 246–248.
19. Guan R., Wang Q., Sundberg E.J., Mariuzza R.A. // J. Mol. Biol. 2005. V. 347. № 4. P. 683–691.
20. Sashchenko L.P., Gnuchev N.V., Lukjanova T.I., Redchenko I.V., Kabanova O.D., Lukanidin E.M., Blishchenko E.Y., Satpaev D.K., Khaidukov S.V., Chertov O.Y. // Immunol. Lett. 1993. V. 37. № 2–3. P. 153–157.
21. Ren M., Guo Q., Guo L., Lenz M., Qian F., Koenen R.R., Xu H., Schilling A.B., Weber C., Ye R.D., et al. // EMBO J. 2010. V. 29. № 23. P. 3952–3966.
22. Gingras A.R., Basran J., Prescott A., Kriajevska M., Bagshaw C.R., Barsukov I.L. // FEBS Lett. 2008. V. 582. P. 1651–1656.
23. González-Martin A., Mira E., Mañes S. // Anticancer Agents Med. Chem. 2012. V. 12. № 9. P. 1045–1057.
24. Yashin D.V., Ivanova O.K., Soshnikova N.V., Sheludchenkov A.A., Romanova E.A., Dukhanina E.A., Tonevitsky A.G., Gnuchev N.V., Gabibov A.G., Georgiev G.P., et al. // J. Biol. Chem. 2015. V. 290. № 35. P. 21724–21731.
25. Blanpain C., Doranz B.J., Bondue A., Govaerts C., Leener A.D., Vassart G., Doms R.W., Proudfoot A., Parmentier M.J. // Biol. Chem. 2003. V. 278. № 7. P. 5179–5187.

The Preferable Binding Pose of Canonical Butyrylcholinesterase Substrates Is Unproductive for Echothiophate

A. S. Zlobin[1,2†], A. O. Zalevsky[1,2,3†*], Yu. A. Mokrushina[2], O. V. Kartseva[2], A. V. Golovin[1,3,4], I. V. Smirnov[2,5]

[1]Faculty of Bioengineering and Bioinformatics, Lomonosov Moscow State University, Leninskie gori, 1, bldg. 73, Moscow, 119991, Russia

[2]Shemyakin-Ovchinnikov Institute of Bioorganic Chemistry RAS, Miklukho-Maklaya Str., 16/10, Moscow, 117997, Russia

[3]Institute of Molecular Medicine, I.M. Sechenov First Moscow State Medical University, Trubetskaya Str., 8, bldg. 2, Moscow, 119992, Russia

[4]National Research University HSE, Myasnitskaya Str., 20, Moscow, 101000, Russia

[5]Chemical Faculty of Lomonosov Moscow State University, Leninskie gori, 1, bldg. 3, Moscow, 119991, Russia

[†]These authors contributed equally to the study.

[*]E-mail: aozalevsky@fbb.msu.ru

Received August 28, 2018; in final form December 10, 2018

ABSTRACT **In this paper, we, for the first time, describe the interaction between the butyrylcholinesterase enzyme and echothiophate, a popular model compound and an analogue of the chemical warfare agents VX and VR, at the atomistic level. Competition between the two echothiophate conformations in the active site was found using molecular modeling techniques. The first one is close to the mode of binding of the substrates of choline series (butyrylcholine and butyrylthiocholine) and is inhibitory, since it is unable to react with the enzyme. The second one is characterized by a significantly worse estimated binding affinity and is reactive. Thus, echothiophate combines the features of two types of inhibitors: competitive and suicidal. This observation will help clarify the kinetic reaction scheme in order to accurately assess the kinetic constants, which is especially important when designing new butyrylcholinesterase variants capable of full-cycle hydrolysis of organophosphorus compounds.**

KEYWORDS **butyrylcholinesterase, echothiophate, organophosphates, QM/MM, metadynamics.**

ABBREVIATIONS **BChE – butyrylcholinesterase; ECH – echothiophate; RMSD – root-mean-square deviation; QM/MM – hybrid, quantum mechanics/molecular mechanics modeling; PAS – peripheral anion site.**

INTRODUCTION

Butyrylcholinesterase (BChE) is an enzyme with broad substrate specificity: hence its significant importance as a basis for developing antidotes against organophosphorus poisons, such as the VX and VR nerve agents [1, 2]. Meanwhile, the kinetic scheme of the reaction catalyzed by cholinesterases is extremely complex, in particular, due to the presence of an additional peripheral anionic binding site (PAS). Close examination of the PAS for butyrylthiocholine, the characteristic BChE substrate, increases the total number of states of this enzyme in its kinetic scheme to eight [3]. If the substrate can irreversibly inactivate the enzyme due to the formation of a stable phosphorylated complex, the kinetic scheme can be even more complicated. Echothiophate is one of such substrates that both carry a choline moiety and have an inactivation potential. Echothiophate is a less toxic analogue of V-series chemical warfare agents and is used as a model organophosphorus compound to study the reactivity of butyrylcholinesterase and its inactivation-resistant modifications. In our study, the interaction between echothiophate and BChE was studied in order to evaluate whether the kinetic schemes earlier proposed for butyrylthiocholine can be used for it.

We decided to use molecular modeling methods, as they provide an atomistic insight into the ongoing events. Furthermore, they have previously proved effective in understanding the reaction mechanisms between BChE and some substrates [4] and even in

rational modification of BChE and its transformation to the cocaine hydrolyzing enzyme [5].

MATERIALS AND METHODS

Modeling of molecular docking was performed using the Autodock Vina software package [6]. The BChE structure with PDB ID 1XLW covalently conjugated to the product of phosphorylation by echothiophate, diethyl phosphate residue (DEP), was selected for docking analysis. DEP was removed, while the lacking residues V377-D378-D379-Q380 and C66 were recreated according to the structure of PDB ID 2XMD, since these structures are appreciably close to each other (the root mean square deviation (RMSD) calculated for all heavy atoms was 0.4 Å). The echothiophate structure was built using the Avogadro molecular editor [7]. The AutoDock Tools software was used to prepare the inbound files and process the results of docking [8]. The docking cell was centered so as to cover the entire binding pocket. All cell dimensions were 20 Å. For the sake of scanning efficiency, the exhaustiveness parameter was set to 64 and 20 independent replicas were performed. The enzyme remained rigid during docking, while the ligand had all degrees of freedom.

The starting configurations of BChE and the ligand were taken from the molecular docking procedure. Modeling of the metadynamics and data processing were carried out according to the procedure described in [9]. The Oγ(Ser198)-P(ECH) distance was used as a collective variable. The metadynamics potential, with a hill height of 2 kJ/mol and the adaptive width calculated using the diffusion criterion according to the previous 220 steps, was applied every 220 steps of molecular modeling. Three independent replicas were performed for each starting echothiophate binding pose.

RESULTS AND DISCUSSION

The molecular docking studies were applied to search for the echothiophate binding position within the structure of human butyrylcholinesterase (PBD ID 1XLW). The echothiophate positions in the active site potentially capable of participating in the reaction (the ES state in the kinetic scheme [3]) were of specific interest to us. Therefore, we selected the main two metrics for the analysis of docking: (1) the distance between the oxygen atom of catalytic residue Ser198 and the phosphorus atom of echothiophate and (2) the distance between the center of mass of the oxyanion hole formed by backbone nitrogen atoms of the Gly116, Gly117, and Ala199 residues and the phosphoryl oxygen atom of echothiophate. The second metric was chosen because coordination of oxygen in the oxyanion hole is crucial for binding and positioning in the known mechanisms of the reaction [3]. Filtering by these criteria allowed us to single out the three best clusters of poses: run6_2, run2_15, and run11_16 (*Fig. 1*). According to the AutoDock Vina scoring function, the binding affinity of run6_2 pose is ~0.4 kcal/mol, better than that for the other two poses. Interestingly, the same arrangement of the choline moiety as in run6_2 is observed in the case of acetylthiocholine hydrolysis [4] and is presumably typical of ligands of a similar chemical nature. The interaction between the positive charge of the cationic choline group with the aromatic π system of Trp82 plays a key role in this case [10], while the Glu197 residue involved in catalysis has a smaller effect [10]. At the same time, this arrangement of the ligand leads to the leaving group - thiocholine - being located not on the line of nucleophilic attack.

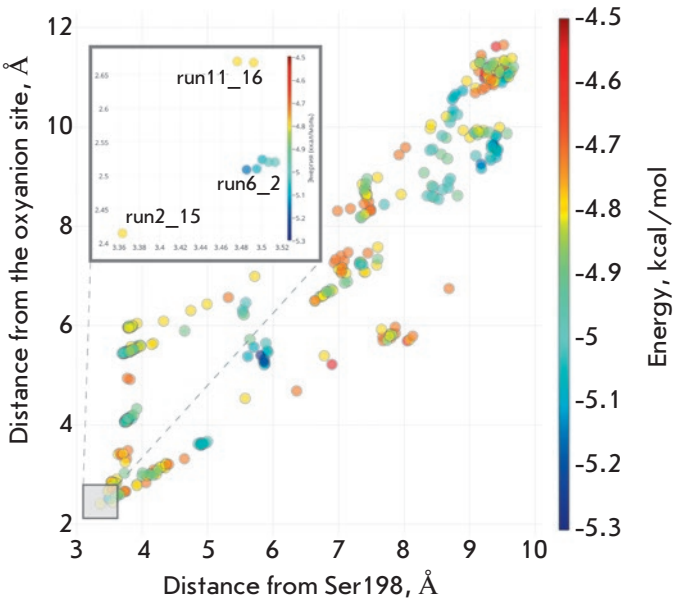

Fig. 1. The results of docking of echothiophate into the binding pocket of BChE. The inset shows the best results from the lower left segment

In contrast, in the run11_16 position, the thiocholine leaving group is in line with the attacking Oγ Ser198 (*Fig. 2*) and the arrangement of ethyl groups is similar to that of the covalent conjugate in the 1XLW crystal structure [11]. The choline moiety, in turn, can electrostatically interact with the negatively charged Asp70 and the aromatic π system of Tyr332 within the peripheral anionic site (PAS) [10]. Previously, it was suggested that this position is the one most likely for echothiophate hydrolysis; the importance of the contact with the Asp70 residue was confirmed by a series of Asp70Gly and Asp70Lys mutants [12]. In this case,

binding of the second substrate molecule in PAS is impossible. The run2_15 position is intermediate: the position of phosphate matches that in run6_2, while the choline tail occupies an intermediate position between run6_2 and run11_16 (*Fig. 2*).

We utilized hybrid quantum mechanics/molecular mechanics (QM/MM) modeling to estimate the reactivity of all three positions. In combination with metadynamics, the method designed to enhance sampling efficiency, this made it possible to estimate the energy barriers of the reactions [9].

The values obtained for run6_2, run2_15, and run11_16 are 15.9 ± 0.7, 15.9 ± 1.9, and 5.7 ± 0.4 kcal/mol, respectively (*Fig. 3*). These values are within the limits characteristic of enzymatic reactions in general, and are similar to those obtained in cases when the BChE reaction is studied with other substrates and using other computational methods [5].

However, the reaction barrier for the system run1_16 where the starting position of the ligand is such that the leaving group — thiocholine — is in line with the attacking oxygen Oγ Ser198 is noticeably lower, which makes the probability of a reaction from this position ~10^7 times higher.

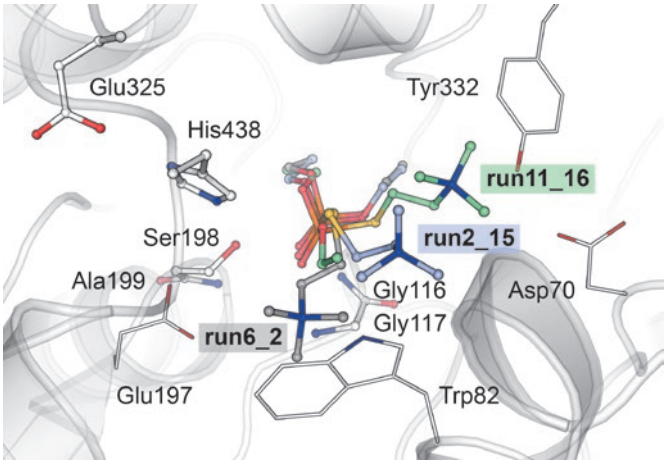

Fig. 2. Three options for the starting position of the ligand. The residues included in the quantum system are indicated in the ball-and-stick model. Thin lines indicate the residues that bind the choline fragment. The carbon atoms of echothiophate in the binding variant run6_2 are shown in gray; run2_15, in blue; and run11_16, in green. The display of hydrogen atoms is omitted

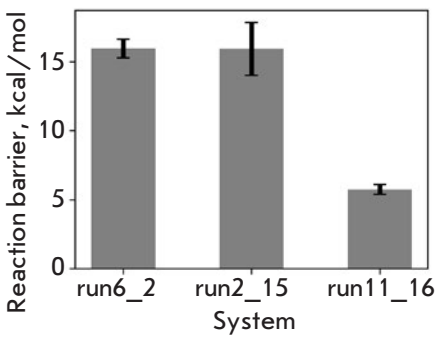

Fig. 3. The estimated values of the reaction barriers for different starting positions. The average value and its error from three independent replicates are shown

CONCLUSIONS

We have used molecular modeling methods to reveal that there are two possible competing binding poses of echothiophate in the active site of butyrylcholinesterase. The first binding pose (the reactive one) had been predicted earlier. The second binding pose is inhibitory; it is close to choline substrates in terms of the binding mode and has a better binding affinity. Consideration of both of these binding poses will make it possible to refine the kinetic scheme of the reaction between echothiophate and butyrylcholinesterase, which is especially important in order to properly assess the kinetic constants when designing butyrylcholinesterase variants with phosphatase activity. ●

This study was supported by the Russian Science Foundation (grant no. 14-50-00131). All computations were carried out using the equipment of the shared research facilities of HPC computing resources at Lomonosov Moscow State University supported by the project RFMEFI62117X0011.

REFERENCES

1. Ilyushin D.G., Smirnov I.V., Belogurov A.A., Jr., Dyachenko I.A., Zharmukhamedova T.I., Novozhilova T.I., Bychikhin E.A., Serebryakova M.V., Kharybin O.N., Murashev A.N., et al. // Proc. Natl. Acad. Sci. USA. 2013. V. 110. P. 1243–1248.
2. Terekhov S.S., Smirnov I.V., Shamborant O.G., Bobik T.V., Ilyushin D.G., Murashev A.N., Dyachenko I.A., Palikov V.A., Knorre V.D., Belogurov A.A., et al. // Acta Naturae. 2015. V. 7. P. 136–141.
3. Bevc S., Konc J., Stojan J., Hodošček M., Penca M., Prapro-

tnik M., Janežič D. // PLoS One. 2011. V. 6. e22265.
4. Chen X., Fang L., Liu J., Zhan C.-G. // Biochemistry. 2012. V. 51. P. 1297–1305.
5. Zheng F., Xue L., Hou S., Liu J., Zhan M., Yang W., Zhan C.-G. // Nature Comm. 2014. V. 5. P. 3457.
6. Trott O., Olson A.J. // J. Comp. Chem. 2010. V. 31. P. 455–461.
7. Hanwell M.D., Curtis D.E., Lonie D.C., Vandermeersch T., Zurek E., Hutchison G.R. // J. Cheminform. 2012. V. 4. P. 17.
8. Morris G.M., Huey R., Lindstrom W., Sanner M.F., Belew R.K., Goodsell D.S., Olson A.J. // J. Comp. Chem. 2009. V. 30. P. 2785–2791.
9. Zlobin A., Mokrushina Y., Terekhov S., Zalevsky A., Bobik T., Stepanova A., Aliseychik M., Kartseva O., Panteleev S., Golovin A., et al. // Front. Pharmacol. 2018. V. 9. P. 834.
10. Nachon F., Ehret-Sabatier L., Loew D., Colas C., van Dorsselaer A., Goeldner M. // Biochemistry. 1998. V. 37. P. 10507–10513.
11. Nachon F., Asojo O.A., Borgstahl G.E.O., Masson P., Lockridge O. // Biochemistry. 2005. V. 44. P. 1154–1162.
12. Masson P., Froment M.T., Bartels C.F., Lockridge O. // Biochem. J. 1997. V. 325 (Pt 1). P. 53–61.

Mouse Model for Assessing the Subchronic Toxicity of Organophosphate Pesticides

V. A. Palikov[1], S. S. Terekhov[2], Yu. A. Palikova[1], O. N. Khokhlova[1], V. A. Kazakov[1], I. A. Dyachenko[1], S. V. Panteleev[2], Yu. A. Mokrushina[2], V. D. Knorre[2], O. G. Shamborant[2], I. V. Smirnov[2,3], A. G. Gabibov[2]

[1]Branch of the Institute of Bioorganic Chemistry, Academicians M.M. Shemyakin and Yu.A. Ovchinnikova RAS, Nauki Ave., 6, Pushchino, Moscow region, 142290, Russia

[2]Institute of Bioorganic Chemistry, Academicians M.M. Shemyakin and Yu.A. Ovchinnikova RAS, Miklukho-Maklaya Str., 16/10, Moscow, 117997, Russia

[3]Faculty of Chemistry, Moscow State University M.V. Lomonosov, Leninskie gori, 1, bldg. 3, Moscow, 119991, Russia

*E-mail: gabibov@ibch.ru

Received December 06, 2018; in final form December 10, 2018

ABSTRACT **The development of antidotes to organophosphate poisons is an important aspect of modern pharmacology. Recombinant acetylcholinesterase and butyrylcholinesterase are effective DNA-encoded acceptors of organophosphate poisons and, in particular, pesticides. Here, we present the results of a study on the effectiveness of recombinant butyrylcholinesterase (BChE) in modeling organophosphate poisoning caused by oral administration of paraoxon at a dose of 2 mg / kg. The study showed a high activity of BChE as a protective agent for subchronic anticholinesterase poisoning in an *in vivo* model. The administration of BChE in a dose of 20 mg / kg allows one to avoid mortality, and also contributed to rapid recovery after model poisoning.**

KEYWORDS **butyrylcholinesterase, *in vivo* model, organophosphorus toxins, bioscavenger.**

INTRODUCTION

The modern therapy of acute and severe chronic poisoning with organophosphorus agents (OPs) involves resuscitation, mechanical ventilation, treatment with a muscarinic antagonist (typically, atropine), in combination with the administration of large amounts of liquid and an acetylcholinesterase activator (e.g., pralidoxime) [1]. However, such treatment often causes severe adverse events: nausea, vomiting, and partial or total disability as it is impossible to avoid the risk of irreversible neuronal damage.

Application of biological antidotes, biomolecules that bind to OPs and inactivate them, is one of the promising approaches to the treatment of organophosphate poisoning [2–5]. Such an enzyme as human butyrylcholinesterase (hBChE) and antibodies capable of binding to OPs or hydrolyzing them are regarded today as potential bioscavengers [6, 7]. hBChE is a natural biological antidote (a suicidal inactivator) for organophosphate poisoning. Due to its unique similarity to human acetylcholinesterase (hAChE) and the large volume of the cavity in its active site, hBChE inactivates a broad range of OPs and is often even more efficient than hAChE [8]. Furthermore, application of hBChE allows one to avoid the long-term adverse effects of OP poisoning, including irreversible brain damage [9].

Organophosphorus agents form the largest group of chemical pesticides used for plant protection. Since most people eat fresh fruits and vegetables, they automatically belong to the group of people susceptible to an increased risk of pesticide poisoning. Paraoxon, an active metabolite of the parathion pesticide, is considered one of the most potent agents that can inhibit hAChE [10]. Paraoxon and insecticides similar to paraoxon penetrate an organism through skin contact or the gastrointestinal tract [11], which leads to acute or chronic poisoning in humans and animals. Furthermore, most OP-based insecticides are lipophilic agents that are prone to accumulation in adipose tissues, which significantly increases the potential for a chronic effect on the human organism. Hence, the development of *in vivo* models making it possible to evaluate the subchronic toxicity of organophosphorus pesticides is of substantial interest, since it allows one to identify the

long-term effects of exposure to OPs on animal's physiological and behavioral characteristics.

MATERIALS AND METHODS

Toxicity of rhBChE was studied in 36 BALB/c mice. The mice were allocated into three groups (two study groups and one control group), with six males and six females per group. Formation of these groups allows one to obtain a representative sample and statistically significant data. Prior to study initiation, the groups of animals in cages were placed in a separate room and left there for 7 days for adaptation. The signs of abnormalities in animals' health were monitored during this period. Healthy animals with an individual weight corresponding to the mean weight for the respective sex with 10% accuracy were randomly selected to be used in the experiment. The main guidelines for animal housing and care complied with the regulations listed in the Guide for Care and Use of Laboratory Animals (ILAR publication, 1996, National Academy Press).

The animals in the study group received a subcutaneous injection of a carboxylesterase inhibitor, cresylbenzodioxaphosphorin oxide (CBDP), at a dose of 1.5 mg/kg. Fifteen minutes later, the mice were given an intravenous injection of either rhBChE at a dose of 20 mg/kg or normal saline and subsequently received an oral dose of paraoxon (2 mg/kg). The agents were administered on study days 1, 3, and 5. An integrated testing was conducted after the third administration, on study day 6. An animal's body weight, food, and water intake were measured daily. Performance tests, such as grip strength test, assessment of respiratory parameters, and locomotor and exploratory activity in the animals were carried out to evaluate antidote effectiveness.

Recording respiratory parameters

The status of the respiratory system was assessed using the PowerLab 8/35 software. Such parameters as the respiratory rate (breaths per minute), tidal volume (mL), and the peak expiratory flow (mL/s) were evaluated through this test. The test was performed on study day 6 (after the third administration of agents).

Recording locomotor and exploratory activity

Total locomotor and exploratory activity was recorded during integrated testing of the animals after clinical examination. Behavioral activity was analyzed using the open-field test on a TSE Multi-Conditioning System Extended Advanced multiple-purpose platform. The test was performed on study day 6 (after the third administration of the agents). Test duration was 3 min. An animal was placed into the "open field" of an actometer, and such parameters as the distance travelled (cm), immobility time (s), and the number of rearings was recorded.

Recording muscle strength, which represents the function of peripheral nerves in the grip strength test

The animal's muscle strength was measured using a grip strength meter (Columbus Instruments). The force applied to the dynamometer grid by the animal's front paws (kg) was recorded. The measurements were carried out during the integrated testing of the animal, after the procedure of recording locomotor activity, on study day 6 (after the third administration of the agent). Descriptive statistics were used for all the quantitative data obtained throughout the study. The Kruskal–Wallis one-way analysis of variance and/or the Mann–Whitney test were used to determine intergroup differences and to compare the study groups to the control one. Statistical analysis was carried out using the Statistica for Windows 7.1 software. The differences were regarded as statistically significant at $P < 0.05$. The results were presented as the value ± standard deviation ($P \leq 0.0005$).

RESULTS AND DISCUSSION

A biological model taking into account the difference between the "esterase" statuses of humans and mice has been elaborated to evaluate the effectiveness of butyrylcholinesterase as a therapeutic agent used to prevent organophosphate poisoning. The blood level of BChE in humans is twice as high as that in mice (5 and 2.6 mg/L, respectively), while the blood level of hAChE is 25-fold lower (0.008 and 0.2 mg/L, respectively). Furthermore, the conventionally used laboratory animals (rodents: mice, rats, and guinea pigs) have another evolutionarily important protection mechanism against OP poisoning. This mechanism is related to the presence of the carboxylesterase ES1 gene encoding an enzyme that irreversibly inactivates a broad range of OPs. Human blood plasma does not contain this enzyme, so the data can be misinterpreted when assessing the toxicity of OPs. There are two main esterases in human blood plasma: butyrylcholinesterase (hBChE, 5 mg/L) and PON1 (50 mg/L). In order to maximally reduce the background activity of endogenous carboxylesterase in mouse blood plasma, we used a specific inhibitor, cresylbenzodioxaphosphorin oxide (CBDP), at a dose of 1.5 mg/kg, which fully inhibited the activity of this enzyme. CBDP had been administered subcutaneously before the animal received an organophosphorus agent. Paraoxon was chosen as a model OP, since this agent and its analogues are natural metabolites of the overwhelming majority of the currently used organophosphorus pesticides. Chronic poisoning was simulated by oral administration of paraoxon, mimicking pesticide

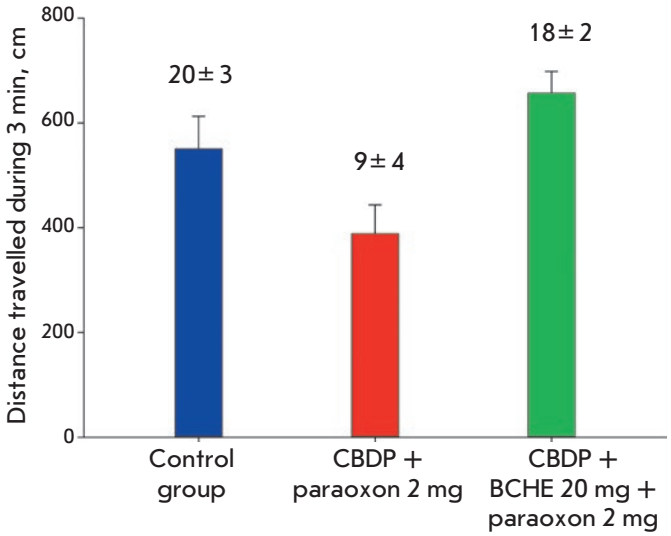

Fig. 1. Analysis of locomotor and exploratory activity. The distance travelled by the animal (cm) was evaluated. The numbers above the respective bars correspond to the number of rearings. The error bars illustrate the standard deviation in a group

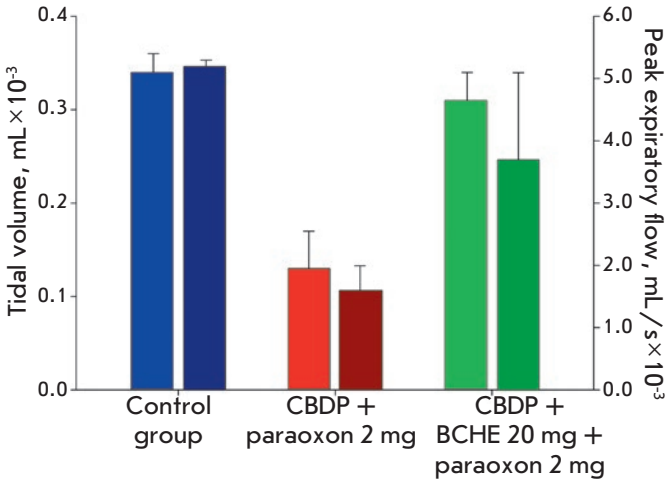

Fig. 2. Analysis of respiratory parameters. The tidal volume (left columns) and the peak expiratory flow (right columns) were estimated. Testing was performed on study day 6 (after the 3rd injection of agents). The error bars illustrate the standard deviation in a group

penetration into the organism during food consumption.

We demonstrated that locomotor activity fell in mice that received the OP without therapy with rhBChE. The distance travelled by the mice changed 1.5-fold; their exploratory activity decreased more than twofold (*Fig. 1*). In turn, administration of rhBChE completely restored the motor function and exploratory activity. The significant reduction in motor function and exploratory activity in our model was associated with strong suppression of respiratory center activity (*Fig. 2*). The key characteristics of respiratory function, such as tidal volume and the peak expiratory flow, in the group of animals that received OP dropped threefold compared to those in the control group. Meanwhile, treatment with rhBChE helped recover normal respiration. A comparable effect was observed for grip strength (*Fig. 3*). Paraoxon significantly reduced muscle strength. Grip strength in animals that received the OP was 2.5-fold lower than that in the control group. Identically to the effects described earlier, treatment with rhBChE made it possible to maintain muscle activity and prevented the physiological manifestations of chronic exposure to paraoxon.

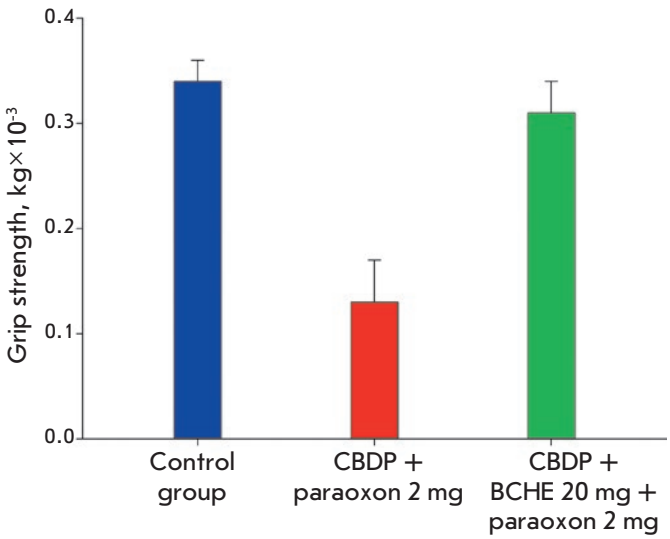

Fig. 3. Analysis of muscle strength in the grip strength test. The force applied to the dynamometer grid from the animal's front paws was recorded (kg). Error bars illustrate the standard deviation in a group

CONCLUSIONS

Hence, we have elaborated a biological model that allows one to evaluate the subchronic toxicity of a paraoxon pesticide administered orally. This model is of significant interest in studying the chronic effects of exposure to OPs. It was demonstrated that key physiological characteristics, such as locomotor and exploratory activity, respiration, and muscle activity, were the parameters sensitive to OPs in our *in vivo* model. The rhBChE used as a protective agent exhib-

ited high activity. Intravenous administration of this biological product at a dose of 20 mg/kg both prevented animal mortality and contributed to rapid recovery from poisoning. We found that the key physiological characteristics of animals treated with rhBChE did not differ from those in the control group not exposed to the toxic activity of paraoxon. This demonstrates that the biological product has a high protective effect not only for the earlier described acute toxicity model, but also for the developed biological model of subchronic toxicity.

The reduction in motor function, exploratory activity, respiratory parameters, and muscle strength reported for this biological model may be indicative of a loss of neuronal associations. A detailed evaluation of neurophysiological characteristics and the irreversibility of the effect of OPs for the elaborated biological model of subchronic toxicity is of significant interest and will be performed in further studies. ●

This work was supported by the Russian Science Foundation (grant no. 16-14-00191). The performance tests were partially supported by the Small Enterprise Assistance Funds for R&D, UMNIK program 10278GU/2015 (for P.A. Palikov).

REFERENCES

1. Eddleston M., Buckley N.A., Eyer P., Dawson A.H. // Lancet (London, England). 2008. V. 371. P. 597–607.
2. Ilyushin D.G., Smirnov I.V., Belogurov A.A., Jr., Dyachenko I.A., Zharmukhamedova T.I., Novozhilova T.I., Bychikhin E.A., Serebryakova M.V., Kharybin O.N., Murashev A.N., et al. // Proc. Natl. Acad. Sci. USA. 2013. V. 110. P. 1243–1248.
3. Masson P., Lockridge O. // Arch. Biochem. Biophys. 2010. V. 494. P. 107–120.
4. Nachon F., Brazzolotto X., Trovaslet M., Masson P. // Chem.-Biol. Interactions. 2013. V. 206. P. 536–544.
5. Terekhov S.S., Smirnov I.V., Shamborant O.G., Bobik T.V., Ilyushin D.G., Murashev A.N., Dyachenko I.A., Palikov V.A., Knorre V.D., Belogurov A.A., et al. // Acta Naturae. 2015. V. 7. P. 136–141.
6 Smirnov I., Belogurov A., Friboulet A., Masson P., Gabibov A., Renard P.-Y. // Chem.-Biol. Interactions. 2013. V. 203. P. 196–201.
7. Smirnov I., Carletti E., Kurkova I., Nachon F., Nicolet Y., Mitkevich V.A., Débat H., Avalle B., Belogurov A.A., Jr., Kuznetsov N., et al. // Proc. Natl. Acad. Sci. USA. 2011. V. 108. P. 15954–15959.
8. Shenouda J., Green P., Sultatos L. // Toxicol. Appl. Pharmacol. 2009. V. 241. P. 135–142.
9. Rosenberg Y.J., Laube B., Mao L., Jiang X., Hernandez-Abanto S., Lee K.D., Adams R. // Chem.-Biol. Interactions. 2013. V. 203. P. 167–171.
10. Salerno A., Devers T., Bolzinger M.-A., Pelletier J., Josse D., Briançon S. // Chem.-Biol. Interactions. 2017. V. 267. P. 57–66.
11. Roberts D.M., Aaron C.K. // BMJ (Clinical research ed.). 2007. V. 334. P. 629–634.

Effect of Temperature, pH and Plasmids on *In Vitro* Biofilm Formation in *Escherichia coli*

A. Mathlouthi[1,2#], E. Pennacchietti[1#], D. De Biase[1*]

[1]Department of Medico-Surgical Sciences and Biotechnologies, Sapienza University of Rome, Laboratory affiliated to the Istituto Pasteur Italia – Fondazione Cenci Bolognetti, Corso della Repubblica 79, 04100 Latina, Italy

[2]Université de Carthage, Faculté des Sciences de Bizerte, Département des Sciences de la Vie, Laboratoire de Biosurveillance de l'Environnement (LR01/ES14), Unité d'Ecotoxicologie, Route de Tunis, 7021 Zarzouna, Tunisie

[#]AM and EP equally contributed to this work.

*E-mail: daniela.debiase@uniroma1.it

Received August 29, 2018; in final form November 10, 2018

ABSTRACT **Acid resistance (AR) in *Escherichia coli* is an important trait that protects this microorganism from the deleterious effect of low-pH environments. Reports on biofilm formation in *E. coli* K12 showed that the genes participating in AR were differentially expressed. Herein, we investigated the relationship between AR genes, in particular those coding for specific transcriptional regulators, and their biofilm-forming ability at the phenotypic level. The latter was measured in 96-well plates by staining the bacteria attached to the well, following 24-hour growth under static conditions, with crystal violet. The growth conditions were as follows: Luria Bertani (LB) medium at neutral and acidic pH, at 37°C or 25°C. We observed that the three major transcriptional regulators of the AR genes (*gadX*, *gadE*, *gadW*) only marginally affected biofilm formation in *E. coli*. However, a striking and novel finding was the different abilities of all the tested *E. coli* strains to form a biofilm depending on the temperature and pH of the medium: LB, pH 7.4, strongly supported biofilm formation at 25°C, with biofilm being hardly detectable at 37°C. On the contrary, LB, pH 5.5, best supported biofilm formation at 37°C. Moreover, we observed that when *E. coli* carried a plasmid, the presence of the plasmid itself affected the ability to develop a biofilm, typically by increasing its formation. This phenomenon varies from plasmid to plasmid, depends on growth conditions, and, to the best of our knowledge, remains largely uninvestigated.**

KEYWORDS ***Escherichia coli*, biofilm, growth conditions, transcriptional regulators, plasmids.**

ABBREVIATIONS **LB – Luria Bertani; AR – acid resistance; ATR – acid tolerance response; AFI – acid fitness island; H-NS – histone-like nucleoid structuring protein; MES – 2-(N-morpholino)ethanesulfonic acid; OD – optical density; SD – standard deviation.**

INTRODUCTION

In the last two decades, several reports have greatly contributed to our current understanding of the molecular mechanisms that underlie the acid tolerance response (ATR) and acid resistance (AR) in many neutralophilic bacteria. The literature on this topic has recently been reviewed [1].

Concerning AR, this is defined as the astonishing ability of bacteria in the stationary phase of growth to withstand exposure to extreme acid stress (pH $\leqslant$ 2.5) for at least 2 hours (such as the one encountered in the gastric compartment) and recover their growth after a return to neutral pH [2]. In this regard, AR is considered to be a key factor during colonization of a host and the infectious process carried out by the gram-negative bacterium *Escherichia coli*, as well as by other bacteria, including pathogenic ones [3–5]. Four AR systems (AR1-4) have been identified in *E. coli*, the most potent of them being AR2, which relies only on the availability of amino acid *L*-glutamate in the minimal salt medium in which the acid challenge is carried out [3, 6, 7]. In this system, amino acid *L*-glutamate is the substrate of the cytosolic enzyme glutamate decarboxylase (two isoforms, GadA and GadB, are expressed in *E. coli*); *L*-glutamate is imported from the medium by the inner membrane antiporter GadC, which couples the import of *L*-glutamate with export of γ-aminobutyrate (GABA), the decarboxylation product. In fact, during the decarboxylation, the α-carboxylic group of *L*-glutamate is released as carbon dioxide (CO_2) and is replaced with a proton irreversibly incorporated in the GABA molecule. Therefore, the system works by con-

suming proton intracellularly (through GadA/B activity) and by exporting positive charges through GadC [1, 6].

The regulation of the AR2 system in *E. coli* is extremely complex: it involves several global regulators, such as RpoS (the sigma factor of RNA polymerase of the stationary phase, which positively affects expression of the system) and H-NS (histone-like nucleoid structuring protein, which represses the relevant genes), small RNAs, and several specific transcriptional regulators, such as GadE, GadX and GadW [3, 6]. These specific regulators are encoded by the relevant genes located in the AFI (Acid Fitness Island), the *E. coli* genome region that carries 14 genes involved in the AR at various levels, including the gene coding for GadA [6]. The coordinated transcriptional control of expression of the AFI and AR2 genes (including *gadB* and *gadC*, which are not in the AFI), as well as the involvement of the global and specific transcriptional regulators, was shown in several transcriptional studies, mostly using microarrays [3]. As expected, some studies showed that *gadBC* and the AFI genes were upregulated under all those conditions, which are compatible with the timely activation of AR, such as inorganic and organic acid stress, respiratory stress/anaerobiosis (typical of the gut environment), whereas downregulation was observed under alkaline stress and in an *rpoS* mutant. Notably, in a temporal study of biofilm formation, *gadB*, *gadC*, and the AFI genes were found to be downregulated and the same trend was observed in a study of a protein involved in AR, YmgB [8].

It is well known that biofilm formation is a very complex process which is affected by many factors, such as the strain under investigation and the nature of the surface on which the biofilm develops. In this report, we used the reference laboratory strain *E. coli* K12 MG1655 and its Δ*gadE*, Δ*gadX*, and Δ*gadW* isogenic derivatives to perform a comparative phenotypic study focusing on the effect of these mutations on the ability of *E. coli* MG1655 to form a biofilm at acidic *vs* neutral pH and under temperatures that closely resemble those of the host (37°C) and non-host/ambient (25°C) environment. In addition, we assessed the effect of empty plasmids, i.e. the ones not carrying a gene *in trans*, on biofilm formation and concluded that, when using a plasmid, caution is waranted regarding the plasmid-specific effect on biofilm formation, depending on the experimental conditions under analysis.

EXPERIMENTAL PROCEDURES

Materials

The ingredients for bacterial growth were from Difco. Crystal violet was from Merck. Acetone, absolute ethanol and polystyrene 96-well plates (untreated) were from VWR. Ampicillin was from Roche Applied Science. Kanamycin was from Fluka, and chloramphenicol was from Sigma-Aldrich.

Table 1. Bacterial strains and plasmids used in this study

Bacterial strains	Relevant genotype/information
MG1655	F^- λ^- *rph*$^{-1}$
MG1655/pBBR	F^- λ^- *rph*$^{-1}$ carrying plasmid pBBR1MCS
MG1655/pBS	F^- λ^- *rph*$^{-1}$ carrying plasmid pBS
MG1655Δ*gadE*	MG1655 *gadE*::Kan^R
MG1655Δ*gadX*	MG1655 *gadX*::Kan^R
MG1655Δ*gadW*	MG1655 *gadW*::Kan^R
Plasmids	
pBBR1MCS	Expression plasmid (4707 bp): *lac*, T3 and T7 promoters, CAT/Cam^R
pBS	(pBluescriptSK) multicopy phagemid vector; ColE1 replicon, *lacZα bla*

Bacterial strains, plasmids and growth conditions

The bacterial strains and plasmids used in this work are listed in *Table 1*. *E. coli* K12 MG1655 and Δ*gadE*, Δ*gadX*, Δ*gadW* isogenic derivatives ([9] and referenced therein) were grown at 37°C or 25°C in one of the following media: LB (Luria Bertani) broth, pH 7.4; LB-MES, pH 5.5 (LB buffered with 100 mM of 2-(N-morpholino)-ethanesulfonic acid, MES, at pH 5.5). When required, the ampicillin, kanamycin, and chloramphenicol antibiotics were added at concentrations of 100, 25, and 34 μg/ml, respectively.

Conditions for biofilm formation

The experiments were performed in triplicates, starting from independent bacterial colonies picked from a freshly streaked plate from a bacterial stock at -80°C. Each bacterial culture was prepared by transferring a single colony into 2 ml of LB pH 7.4 and allowing the bacteria to grow overnight (16–18 hours) at 37°C under orbital shaking (120 rpm). On the following day, each culture was diluted 1 : 10 into a fresh LB medium and the optical density (OD) at 600 nm was measured. Each culture was then brought to the same OD_{600} = 2.0 and diluted 1 : 100 in independent wells by transferring 2 μl of each culture into 198 μl of either LB, pH 7.4 or LB-MES, pH 5.5. The starting OD (time 0) was checked using a Tecan Sunrise

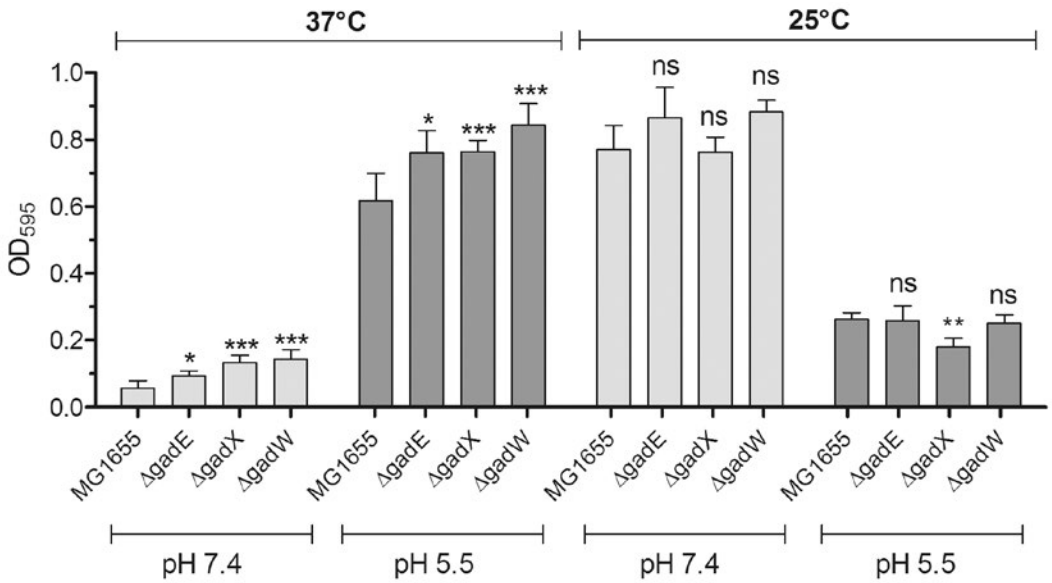

Fig. 1. Biofilm formation in *E. coli* MG1655 at different pH values and temperatures. Statistical significance: *, $P \leq 0.05$; **, $P \leq 0.01$; ***, $P \leq 0.001$; n.s., not significant

microplate reader at 595 nm. The plates were then transferred to thermostatic static incubators at 25˚C and 37˚C, respectively. The external wells in each plate contained sterile water or LB to avoid evaporation, and some wells contained only the growth medium (bk), which was read at time 0 and 24 h. Following growth under static conditions for 24 hours, the final OD_{595} (time 24 h) was read and planktonic bacteria were removed. Each well was rinsed with sterile water three times, and then 200 µl of 0.1% crystal violet was added and allowed to stain the biofilm for 15 min. After removal of the crystal violet and three subsequent washes with sterile water to remove the excess of stain, the stained biofilm was solubilized by adding 200 µl of an acetone:ethanol (20:80, v/v) solution. 125 µl/200 µl were transferred from each well in a clean 96-wells plate. Readings were again performed at 595 nm using a microplate reader.

Analysis of biofilm formation

The readings obtained after staining with crystal violet were subtracted from those of the wells containing only the medium (bk at 24 h); the readings were previously checked to be identical to the readings of the medium at time 0 in order to verify that there was no contamination. The net readings were then analyzed using the Prism 4.0 GraphPad software. The data for the biofilms obtained using the mutant strains *vs* the wild-type strains were analyzed by two-way ANOVA using the Bonferroni test (as available in the GraphPad Prism software suite, version v5.0a). The data were expressed as the means of 3 to 8 independent experiments with standard deviations (SD). Differences were considered statistically significant at $P < 0.05$.

RESULTS AND DISCUSSION

Effect of temperature and pH of the medium on biofilm formation

We analyzed the ability of *E. coli* MG1655 and its Δ*gadE*, Δ*gadX*, and Δ*gadW* isogenic derivatives to form biofilms following growth of bacteria in LB at neutral and acidic pHs at two temperatures, 37˚C and 25˚C. Strikingly, we noticed that the temperature had a significant effect on biofilm formation for the strain under analysis (*Fig. 1*). In particular, in LB at pH 7.4, biofilm formation was pronounced at 25˚C and hardly detectable at 37˚C. However, pH of the medium also had an effect, because in LB at pH 5.5 MG1655 formed much more biofilm at 37˚C than at 25˚C. This phenomenon was only slightly affected by the mutations in the genes coding for the major transcriptional regulators of the AR2 system. This implies that none of these regulators is strongly involved in the transcriptional repression of the genes participating in biofilm formation, at least under our growth conditions. This is in line with the report showing that GadX only marginally affects biofilm biomass in the *E. coli* strain BW25113 [10].

Such striking inversion of the ability to produce biofilms was an unexpected finding. A possible explanation may reside in the pH 5.5, which is more typical of the distal gut. Therefore, the combination of two cues –mildly acidic pH and 37˚C –could better approximate the host gut environment, thereby triggering biofilm formation, at least on an inert surface such as polystyrene. The slight increase in biofilm formation observed at 37˚C when testing the mutants, regardless of the pH of the medium, could very likely

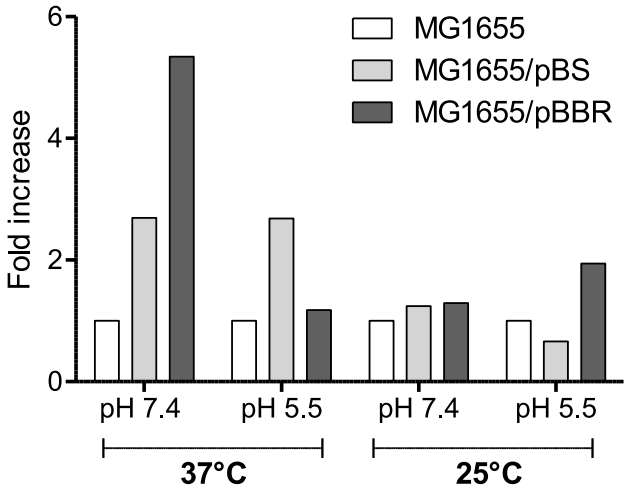

Fig. 2. Biofilm formation in *E. coli* MG1655 in the presence of plasmids. The change is reported as fold change increase/decrease with respect to the biofilm formed by the reference strain, i.e. *E. coli*, MG1655 under the indicated condition, which was set to 1.0. The SD of the reported values never exceeded 20% of the indicated value

be related to an effect of the regulators on the biofilm structure rather than on the biomass, as noticed by other researchers [10], which may also be related to the observed repression of the AR2 and AFI genes in a temporal study of biofilm formation [11].

Effect of plasmids on biofilm formation

Another interesting finding derived from the observation of the effect of empty plasmids in bacteria tested for their biofilm-forming ability. In order not to add too many variables, we transformed *E. coli* MG1655 with either a high-copy number plasmid (pBS, in *Table 1*) or a medium-copy number plasmid (pBBR1MCS, in *Table 1*). Biofilm formation was assayed under the same conditions as those shown in *Fig. 1*. The results are shown in *Fig. 2* as fold increase with respect to *E. coli* MG1655 not carrying a plasmid. These data clearly show that both plasmids sometimes exerted a negligible and sometimes a substantial effect on biofilm formation. This phenomenon depended on the medium pH and the temperature and could not be predicted *a priori*.

CONCLUSIONS

Our results clearly show that pH is an important driving force in dictating the formation of biofilms, to the same extent as temperature. Moreover, care should be taken when interpreting results on *E. coli* strains carrying plasmids that contain a gene complementing a mutation. In fact, we have shown that empty plasmids affect biofilm formation. To the best of our knowledge, this aspect is less investigated than the plasmid transfer within a biofilm [12]. ●

This work was in part funded to Daniela De Biase by the Pasteur Institute (Institut Pasteur, Paris; PTR 540).

REFERENCES

1. Lund P.A., Tramonti A., De Biase D. // FEMS Microbiol. Rev. 2014. V. 38. № 6. P. 1091–1125.
2. Lin J., Lee I.S., Frey J., Slonczewski J.L., Foster J.W. // J. Bacteriol. 1995. V. 177. № 14. P. 4097–4104.
3. De Biase D., Lund P.A. // Adv. Appl. Microbiol. 2015. V. 92. P. 49–88.
4. Occhialini A., Jimenez de Bagues M.P., Saadeh B., Bastianelli D., Hanna N., De Biase D., Kohler S. // J. Infect. Dis. 2012. V. 206. № 9. P. 1424–1432.
5. Cotter P.D., Gahan C.G., Hill C. // Mol. Microbiol. 2001. V. 40. № 2. P. 465–475.
6. De Biase D., Pennacchietti E. // Mol. Microbiol. 2012. V. 86. № 4. P. 770–768.
7. Lin J., Smith M.P., Chapin K.C., Baik H.S., Bennett G.N., Foster J.W. // Appl. Environ. Microbiol. 1996. V. 62. № 9. P. 3094–3100.
8. Lee J., Page R., Garcia-Contreras R., Palermino J.M., Zhang X.S., Doshi O., Wood T.K., Peti W. // J. Mol. Biol. 2007. V. 373. № 1. P. 11–26.
9. Tramonti A., De Canio M., De Biase D. // Mol. Microbiol. 2008. V. 70. № 4. P. 965–982.
10. Hodges A.P., Dai D., Xiang Z., Woolf P., Xi C. // PLoS One. 2010. V. 5. № 3. P. e9513.
11. Domka J., Lee J., Bansal T., Wood T.K. // Environ. Microbiol. 2007. V. 9. № 2. P. 332–346.
12. Stalder T., Top E. // NPJ Biofilms Microbiomes. 2016. V. 2. P. 16022.

GENERAL RULES

Acta Naturae publishes experimental articles and reviews, as well as articles on topical issues, short reviews, and reports on the subjects of basic and applied life sciences and biotechnology.

The journal is published by the Park Media publishing house in both Russian and English.

The journal *Acta Naturae* is on the list of the leading periodicals of the Higher Attestation Commission of the Russian Ministry of Education and Science. The journal Acta Naturae is indexed in PubMed, Web of Science, Scopus and RCSI databases.

The editors of *Acta Naturae* ask of the authors that they follow certain guidelines listed below. Articles which fail to conform to these guidelines will be rejected without review. The editors will not consider articles whose results have already been published or are being considered by other publications.

The maximum length of a review, together with tables and references, cannot exceed 60,000 characters with spaces (approximately 30 pages, A4 format, 1.5 spacing, Times New Roman font, size 12) and cannot contain more than 16 figures.

Experimental articles should not exceed 30,000 symbols (approximately 15 pages in A4 format, including tables and references). They should contain no more than ten figures.

A short report must include the study's rationale, experimental material, and conclusions. A short report should not exceed 12,000 symbols (8 pages in A4 format including no more than 12 references). It should contain no more than four figures.

The manuscript and the accompanying documents should be sent to the Editorial Board in electronic form:
1) text in Word 2003 for Windows format;
2) the figures in TIFF format;
3) the text of the article and figures in one pdf file;
4) the article's title, the names and initials of the authors, the full name of the organizations, the abstract, keywords, abbreviations, figure captions, and Russian references should be translated to English;
5) the cover letter stating that the submitted manuscript has not been published elsewhere and is not under consideration for publication;
6) the license agreement (the agreement form can be downloaded from the website www.actanaturae.ru).

MANUSCRIPT FORMATTING

The manuscript should be formatted in the following manner:

- Article title. Bold font. The title should not be too long or too short and must be informative. The title should not exceed 100 characters. It should reflect the major result, the essence, and uniqueness of the work, names and initials of the authors.
- The corresponding author, who will also be working with the proofs, should be marked with a footnote *.
- Full name of the scientific organization and its departmental affiliation. If there are two or more scientific organizations involved, they should be linked by digital superscripts with the authors' names.
- Abstract. The structure of the abstract should be very clear and must reflect the following: it should introduce the reader to the main issue and describe the experimental approach, the possibility of practical use, and the possibility of further research in the field. The average length of an abstract is 20 lines (1,500 characters).
- Keywords (3 – 6). These should include the field of research, methods, experimental subject, and the specifics of the work. List of abbreviations.
- INTRODUCTION
- EXPERIMENTAL PROCEDURES
- RESULTS AND DISCUSSION
- CONCLUSION

  The organizations that funded the work should be listed at the end of this section with grant numbers in parenthesis.
- REFERENCES

  The in-text references should be in brackets, such as [1].

RECOMMENDATIONS ON THE TYPING AND FORMATTING OF THE TEXT

- We recommend the use of Microsoft Word 2003 for Windows text editing software.
- The Times New Roman font should be used. Standard font size is 12.
- The space between the lines is 1.5.
- Using more than one whole space between words is not recommended.
- We do not accept articles with automatic referencing; automatic word hyphenation; or automatic prohibition of hyphenation, listing, automatic indentation, etc.
- We recommend that tables be created using Word software options (Table → Insert Table) or MS Excel. Tables that were created manually (using lots of spaces without boxes) cannot be accepted.
- Initials and last names should always be separated by a whole space; for example, A. A. Ivanov.
- Throughout the text, all dates should appear in the "day.month.year" format, for example 02.05.1991, 26.12.1874, etc.
- There should be no periods after the title of the article, the authors' names, headings and subheadings, figure captions, units (s – second, g – gram, min – minute, h – hour, d – day, deg – degree).
- Periods should be used after footnotes (including those in tables), table comments, abstracts, and abbreviations (mon. – months, y. – years, m. temp. – melting temperature); however, they should not be used in subscripted indexes (T_m – melting temperature; $T_{p.t}$ – temperature of phase transition). One exception is mln – million, which should be used without a period.
- Decimal numbers should always contain a period and not a comma (0.25 and not 0,25).
- The hyphen ("-") is surrounded by two whole spaces, while the "minus," "interval," or "chemical bond" symbols do not require a space.
- The only symbol used for multiplication is "×"; the "×" symbol can only be used if it has a number to its

right. The "·" symbol is used for denoting complex compounds in chemical formulas and also noncovalent complexes (such as DNA·RNA, etc.).
- Formulas must use the letter of the Latin and Greek alphabets.
- Latin genera and species' names should be in italics, while the taxa of higher orders should be in regular font.
- Gene names (except for yeast genes) should be italicized, while names of proteins should be in regular font.
- Names of nucleotides (A, T, G, C, U), amino acids (Arg, Ile, Val, etc.), and phosphonucleotides (ATP, AMP, etc.) should be written with Latin letters in regular font.
- Numeration of bases in nucleic acids and amino acid residues should not be hyphenated (T34, Ala89).
- When choosing units of measurement, SI units are to be used.
- Molecular mass should be in Daltons (Da, KDa, MDa).
- The number of nucleotide pairs should be abbreviated (bp, kbp).
- The number of amino acids should be abbreviated to aa.
- Biochemical terms, such as the names of enzymes, should conform to IUPAC standards.
- The number of term and name abbreviations in the text should be kept to a minimum.
- Repeating the same data in the text, tables, and graphs is not allowed.

GUIDENESS FOR ILLUSTRATIONS

- Figures should be supplied in separate files. Only TIFF is accepted.
- Figures should have a resolution of no less than 300 dpi for color and half-tone images and no less than 500 dpi.
- Files should not have any additional layers.

REVIEW AND PREPARATION OF THE MANUSCRIPT FOR PRINT AND PUBLICATION

Articles are published on a first-come, first-served basis. The members of the editorial board have the right to recommend the expedited publishing of articles which are deemed to be a priority and have received good reviews.

Articles which have been received by the editorial board are assessed by the board members and then sent for external review, if needed. The choice of reviewers is up to the editorial board. The manuscript is sent on to reviewers who are experts in this field of research, and the editorial board makes its decisions based on the reviews of these experts. The article may be accepted as is, sent back for improvements, or rejected.

The editorial board can decide to reject an article if it does not conform to the guidelines set above.

The return of an article to the authors for improvement does not mean that the article has been accepted for publication. After the revised text has been received, a decision is made by the editorial board. The author must return the improved text, together with the responses to all comments. The date of acceptance is the day on which the final version of the article was received by the publisher.

A revised manuscript must be sent back to the publisher a week after the authors have received the comments; if not, the article is considered a resubmission.

E-mail is used at all the stages of communication between the author, editors, publishers, and reviewers, so it is of vital importance that the authors monitor the address that they list in the article and inform the publisher of any changes in due time.

After the layout for the relevant issue of the journal is ready, the publisher sends out PDF files to the authors for a final review.

Changes other than simple corrections in the text, figures, or tables are not allowed at the final review stage. If this is necessary, the issue is resolved by the editorial board.

FORMAT OF REFERENCES

The journal uses a numeric reference system, which means that references are denoted as numbers in the text (in brackets) which refer to the number in the reference list.

For books: the last name and initials of the author, full title of the book, location of publisher, publisher, year in which the work was published, and the volume or issue and the number of pages in the book.

For periodicals: the last name and initials of the author, title of the journal, year in which the work was published, volume, issue, first and last page of the article. Must specify the name of the first 10 authors. Ross M.T., Grafham D.V., Coffey A.J., Scherer S., McLay K., Muzny D., Platzer M., Howell G.R., Burrows C., Bird C.P., et al. // Nature. 2005. V. 434. № 7031. P. 325–337.

References to books which have Russian translations should be accompanied with references to the original material listing the required data.

References to doctoral thesis abstracts must include the last name and initials of the author, the title of the thesis, the location in which the work was performed, and the year of completion.

References to patents must include the last names and initials of the authors, the type of the patent document (the author's rights or patent), the patent number, the name of the country that issued the document, the international invention classification index, and the year of patent issue.

The list of references should be on a separate page. The tables should be on a separate page, and figure captions should also be on a separate page.

The following e-mail addresses can be used to contact the editorial staff: vera.knorre@gmail.com, actanaturae@gmail.com, tel.: (495) 727-38-60, (495) 930-87-07